University of Southampton

Faculty of Engineering and Physical Sciences

School of Chemistry

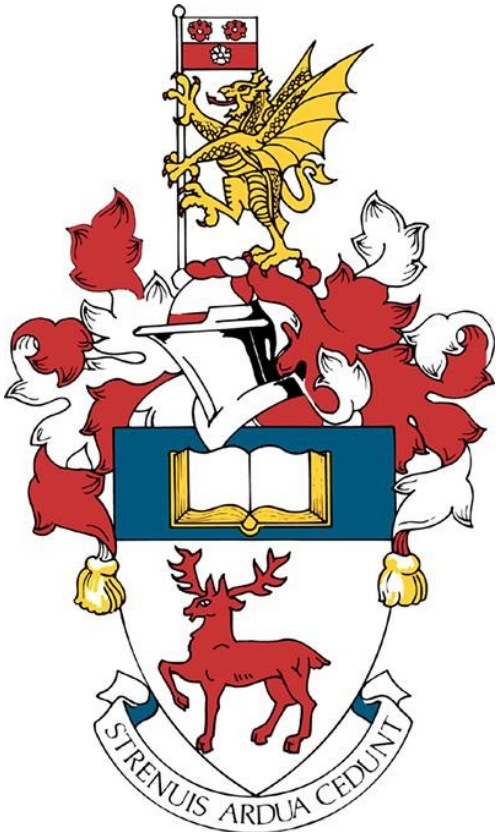

Mapping the β-Catenin Interactome: CRISPR-Based Functional Proteomics, Proximity Labelling, and Small Molecule Screening for Wnt-Targeted Cancer Therapy

by

Steve Shaju John

ORCiD ID: 0009-0005-9463-2491

Thesis for the degree of Doctor Of Philosophy

June 2025

University of Southampton

Abstract

Faculty of Engineering and Physical Sciences

School of Chemistry

Doctor of Philosophy

Mapping the β-Catenin Interactome: CRISPR-Based Functional Proteomics, Proximity Labelling, and Small Molecule Screening for Wnt-Targeted Cancer Therapy

By

Steve Shaju John

The Wnt signaling pathway is critical for embryonic development and the homeostasis of adult tissues, with β-catenin acting as a key transcriptional co-activator in canonical Wnt signaling. Dysregulated β-catenin activity, often due to mutations or stabilization, is a hallmark of Wnt-driven cancers, particularly colorectal cancer (CRC). Despite its central role, direct therapeutic targeting of β-catenin has proven challenging, with limited success in clinical applications. In this study, we sought to further characterize the β-catenin interactome and identify novel protein-protein interactions (PPIs) and small-molecule modulators. First, we generated a CRISPR/Cas9-mediated CTNNB1 knockout (KO) in U2OS cells to examine proteomic changes associated with β-catenin loss, confirming its pivotal role in cancer-associated signaling networks. Next, we employed a proximity-dependent biotinylation approach (MiniTurbo) fused to β-catenin in U2OS cells, coupled with affinity purification mass spectrometry (AP-MS) to map the β-catenin interactome. This approach identified 112 high-confidence β-catenin interactors, verified by BIOGRID and INTACT databases, and revealed 39 novel candidate interactors, suggesting previously uncharacterized roles in β-catenin signaling regulation. To explore potential therapeutic interventions, we screened small-molecule inhibitors and identified a carnosic acid derivative (MAM4-141) as a Wnt signaling modulator. Whole-cell proteomic profiling in SW480 colorectal cancer cells, combined with interactome analysis using the MiniTurbo system, demonstrated cell toxicity and revealed potential effects on β-catenin-associated pathways, providing initial insights into its mechanism of action. These findings establish a robust β-catenin interactome platform and highlight MAM4-141 as a promising candidate for further investigation in Wnt-targeted therapies.

Table of Contents

Table of Contents i
Table of Tables v
Table of Figures vii
Research Thesis: Declaration of Authorship ix
Acknowledgements xi
Definitions and Abbreviations xiii
Chapter 1 Introduction 15
1.1 History of Wnt signaling 15
1.2 Canonical Wnt signaling 17
1.3 Main Wnt signal transduction 17
1.4 Wnt signaling in cancer 20
1.4.1 Wnt signaling in Cancer Stem Cells 22
1.4.2 Wnt signaling in Metastasis 22
1.4.3 Oncogenic hotspot mutations in β catenin 22
1.5 β-catenin structural insights 23
1.6 β-catenin protein-protein interactions in the Wnt-signaling pathway 25
1.7 Wnt signaling-small molecule modulators 26
1.7.1 Indirect targeting of β-catenin 28
1.7.2 Direct targeting of β-catenin and the associated challenges 28
1.8 Main Aims 33
Chapter 2 Materials and Methods 35
2.1 Reagents and Antibodies 35
2.2 Cell Culture 36
2.3 Cell lysate preparation 37
2.4 SDS PAGE and Western Blotting 37
2.4.1 Western Blot Quantitation 38
2.5 TOPFlash 38
2.6 Quantitative PCR 39
2.6.1 Primer design 39
2.6.2 RNA extraction 39
2.6.3 cDNA synthesis and qPCR 39
2.7 Viability assay 40
2.8 Wound healing assay (scratch assay) 41
2.9 Clonogenic assays 41
2.9.1 2D crystal violet assay 41
2.9.2 Soft agar colony formation assay 41
2.10 Immunocytochemistry 43
2.11 Nuclear fractionation (nuclear enrichment) 43
2.12 General molecular cloning for generation of MiniTurbo expressing stable cell line 45
2.12.1 Primer Design 45
2.12.2 Polymerase Chain Reaction (PCR) 45
2.12.3 Agarose gel electrophoresis and DNA purification 46

2.12.4 Restriction enzyme digest and Ligation 46
2.12.5 Bacterial transformation and DNA plasmid extraction 46
2.13 Implementation of Mini Turbo affinity purification-mass spectrometry 47
2.13.1 Cell culture preparation for AP-MS 47
2.13.2 Affinity purification of Biotinylation proteins coupled to mass spectrometry 48
2.14 Generation of knockout cell lines using CRISPR/Cas9 gene editing 49
2.14.1 Guide RNA selection for CTNNB1 49
2.14.2 Lentiviral transfection and transduction 50
2.15 Proteomic sample preparation 51
2.15.1 Cell culture preparation 51
2.15.2 Proteomic sample preparation-off the bead digestion 51
2.16 Statistical analysis 52
Chapter 3 CRISPR-Cas9-mediated CTNNB1 knockout and proteomic profiling 53
3.1 Introduction 53
3.2 Results 55
3.2.1 Phenotype of CTNNB1 KO cells 55
3.2.2 Functional enrichment analyses of the impact of CTNNB1 deficiency in U2OS cells 61
3.3 Discussion 64
Chapter 4 Mapping the B-catenin interactome via proximity dependent biotinylation 67
4.1 Introduction 67
4.1.1 Current knowledge on previous attempts to characterize the β-catenin interactome. 67
4.1.2 Introduction to MiniTurbo and other Proximity labelling methods 68
4.2 Results 71
4.2.1 The design and implementation of CTNNB1-MiniTurbo vector 71
4.2.2 Verification of MiniTurbo construct in U2OS cells 75
4.2.3 Proteomic functional enrichment analysis confirms β-catenin associated terms 80
4.2.4 Interactome analysis and database comparisons reveals network of novel candidates for β-catenin direct binding 83
4.3 Discussion 88
Chapter 5 Investigating the impact of small molecule modulators on the β-catenin interactome 91
5.1 Introduction 91
5.2 Results 92
5.2.1 Influence of CA on β-catenin levels in HCT116 and SW480 cell lines 92
5.2.2 HEK293T as a model cell line for induced Wnt activity for compounds CA and MSAB 95
5.2.3 Working with CA derivatives in cell lines and proteomics 99
5.2.3.1 Proteomic analysis reveals down regulation of key carcinogenic signaling proteins with MAM4-141 treatment in SW480 cells 111

5.2.3.2 Interactome analysis reveals β-catenin selective proximity with junctional proteins when treated with MAM4-141 in U2OS cells 113

5.3 Discussion 115

Chapter 6 Overall Discussion 117

6.1 Insights and Reproducibility 117
6.2 Multi-Omic Integration and Functional Analysis 117
6.3 MiniTurbo and Proximity Biotinylation for β-Catenin Interactome Mapping 118
6.4 Expanding Beyond a Single Bait Protein 118
6.5 Future work and research directions 119

Appendix 120

List of References 301

Table of Tables

Table 1.1. **Summary description of examples of downstream effects of Wnt signaling in cancer.** 21
Table 1.2 **Examples of small molecules that propose to target β-catenin interactions.** 31
Table 1.3 **Drug candidates associated with β-catenin interactions in clinical trials.** 32
Table 2.1 **Table of Antibodies** 35
Table 2.2 **Table of Reagents** 36
Table 2.3 **Constituents of 10% SDS-PAGE gel with respective volumes** 37
Table 2.4 **qPCR primer sequences** 39
Table 2.5 **qPCR cycle conditions for StepOne plus instrumentation** 40
Table 2.6 **Primer sequences and characteristics used for MiniTurbo Cloning** 45
Table 2.7 **PCR conditions with qPCRBIO kit** 45
Table 3.1 **Results from COMPARTMENT analysis.** 61
Table 4.1. **Detailed comparison of proximity labelling methods.** 70

Table of Figures

Figure 1.1 **Timeline of significant discoveries in Wnt signaling[1, 3, 9, 14, 17, 20-33]** 16
Figure 1.2 **Schematic representation of the canonical Wnt signalling pathway.** 18
Figure 1.3 **Structure of β-catenin.** 24
Figure 1.4 **Targeting the Wnt pathway-small molecule modulators.** 27
Figure 1.5 **Cartoon illustration of PROTAC design and mechanism of action.** 30
Figure 2.1 **Illustration of cell counting grid and calculation** 40
Figure 2.2 **Colony quantification process with Image J.** 42
Figure 2.3 **Stages of Cell Fractionation process.** 44
Figure 2.4 **Schematic of MiniTurbo AP-MS pipeline** 47
Figure 2.5 **An overview of the sgRNA designs.** 49
Figure 3.1 **Western blot images of U2OS CRISPR CTNNB1 KO validation.** 55
Figure 3.2 **Immunofluorescence of U2OS WT and CTNNB1 CRISPR KO cells.** 57
Figure 3.3 **Representative image of U2OS cell colony formation in soft agar.** 58
Figure 3.4 **Wound healing assay on WT and CTNNB1 KO U2OS cells.** 60
Figure 3.5 **Proteomic analysis of CTNNB1 KO in U2OS cells.** 63
Figure 4.1 **Cartoon diagram of MiniTurbo mechanism of action.** 68
Figure 4.2 **Plasmid maps of pre- and -post SLiCE cloning.** 72
Figure 4.3 **Cloning verification by restriction enzyme digest.** 73
Figure 4.4 **Plasmid map showing successful sequence alignment in two independent constructs** 74
Figure 4.5 **Verification of MiniTurbo system in U2OS cells.** 77
Figure 4.6 **Functional enrichment analysis shows significant β-catenin associations.** 82
Figure 4.7 **Qualitative interactome analysis of B-catenin by proximity dependent biotinylation.** 85
Figure 4.8 **Quantitative analysis of β-catenin using SAINT.** 87
Figure 5.1 **CA treatment on HCT116 cells.** 93
Figure 5.2. **CA treatment on SW480 cells.** 94
Figure 5.3 **HEK293T cells respond to CA treatment.** 96
Figure 5.4 **HEK293T cells respond to MSAB treatment.** 97
Figure 5.5. ***CA induces changes in the expression of Wnt target genes.*** 98
Figure 5.6 **CA and derivative structures with molar mass** 99
Figure 5.7 **HCT116 cells with 24-hour MAM4-141 and MAM7-139 treatment.** 101
Figure 5.8 **SW480 cells with 24-hour MAM4-141 and MAM7-139 treatment.** 102
Figure 5.9 **U2OS and MDAMB231 cells treated with MAM4-141 for 24 hours.** 103
Figure 5.10 **MCF10A cells treated with MAM4-141 and MAM7-139 for 24 hours.** 104
Figure 5.11 **ARPE-19 cells treated with MAM4-141 and MAM7-139 for 24 hours.** 105
Figure 5.12 **IC_{50} calculations of MAM4-141 and MAM7-139.** 106
Figure 5.13. **Crystal violet assay of HCT116 cells with treatment of MAM7-139 and MAM4-141.** 108
Figure 5.14 **Crystal violet assay of SW480 cells treated with MAM7-139 and MAM4-141.** 109
Figure 5.15 **Soft agar analysis of MAM7-139 and MAM4-141.** 110
Figure 5.16 **Proteomic analysis of MAM4-141 treatment in SW480 cells** 112
Figure 5.17 **β-catenin interactome analysis with MAM4-141 treatment by proximity-dependent biotinylation.** 114

Research Thesis: Declaration of Authorship

Print name: STEVE SHAJU JOHN

Title of thesis: Mapping the β-Catenin Interactome: CRISPR-Based Functional Proteomics, Proximity Labelling, and Small Molecule Screening for Wnt-Targeted Cancer Therapy

I declare that this thesis and the work presented in it are my own and has been generated by me as the result of my own original research.

I confirm that:

1. This work was done wholly or mainly while in candidature for a research degree at this University;
2. Where any part of this thesis has previously been submitted for a degree or any other qualification at this University or any other institution, this has been clearly stated;
3. Where I have consulted the published work of others, this is always clearly attributed;
4. Where I have quoted from the work of others, the source is always given. With the exception of such quotations, this thesis is entirely my own work;
5. I have acknowledged all main sources of help;
6. Where the thesis is based on work done by myself jointly with others, I have made clear exactly what was done by others and what I have contributed myself;
7. None of this work has been published before submission

Signature .....

Date: 17/06/2025

Acknowledgements

I want to take this opportunity to show my gratitude for the last 6 years that encompassed my PhD journey. First and foremost, I want to thank and give all the glory to God because if it was not for His mercy and grace, I would not be here. He is the reason I am standing here today. Thank you, Jesus, for leading me through from start to finish through every high and low, you never gave up on me. Thank you, Lord.

To my supervisors Dr Matt Baud and Professor Rob Ewing:
I don't have the words to say thank you for taking me on as your student and for not giving up on me. I know I gave you both a hard time and not made your lives easy, I'm truly sorry for that but through it all you always showed kindness and support which I will never forget. I have a great degree of respect for you both and for how hard you work. Thank you for all that you have done and are doing for me and the University.

To Professor Nullin Divecha:
Nal, thank you so much for being such a great mentor and friend to me. Your constant excitement for science is something I will always cherish. You have always checked in on me and showed great concern, it's a joy to know you.

To my friends and academic colleagues:
Bhav, Charlotte, Matt, Maggie, Luis, Andy, Michael and more…Thank you for making work a fun place to be around. You guys have guided, listened, and joked with me through the years. I appreciate you all. Tom W, Ollie, John, Zac, and Geoff. thank you for being great friends and checking up on me throughout my studies. Marcin, thank you for your encouragement to keep going over the years, your scientific curiosity isa great inspiration to me.

To my dearest family:

Appa and Amma, thank you for being such wonderful parents to me, from the time I was crawling up until now, you have been a source of strength to me. Thank you for raising, nurturing, and loving me throughout my school journey and up to my PhD. I literally and figuratively would not be here without you both. Thank you and may God bless you both. Reuben you're an awesome brother, thank you for all the love and banter you provide!

Papa and Mummy, my second set of parents. Words cannot describe how thankful and grateful I am for the love and support you have shown me these last 6 years. I wouldn't have been able to do my lab work and writing if it wasn't for all the practical help, you graciously provided. I am greatly indebted to you for all the sacrifices you have made to help me complete my PhD. Thank you so much and may God bless you.

Now, I would like to thank and honour the most important woman in my life, my darling wife, Ash. Dear, thank you for being there with me right from the beginning of this journey until now. You've sacrificed so much for me every single day. The unwavering support, love and understanding you've shown has been a great comfort to me over these years. Thank you, Ms. Panda, for having my back, I love you.

Finally, Ezra, my darling boy, you are my pride and joy. You and Mummy have been a great motivation to me when times were tough. You might be only two and a half at this time of writing but even you learnt how to say the word "thesis". It is the greatest honour in life to be your dad and I thank God for giving you to me. This thesis I dedicate to you, my son. I love you.

Definitions and Abbreviations

AML .....Acute myeloid leukaemia

AP-MS .....Affinity Purification-Mass Spectrometry

APC .....Adenomatous Polyposis Coli

Bait .....Tagged protein of interest for AP-MS experiment

BCL9.....B cell Lymphoma 9

CA .....Carnosic Acid

CIN .....Chromosomal instability

CBP .....CREB binding protein

CID .....β-catenin inhibitory domain

CK1α .....Casein Kinase 1 alpha

Co-IP .....Co-immunoprecipitation

CRC .....Colorectal Cancer

CRISPR .....Clustered regularly interspaced palindromic repeats

DCTN1.....Dynactin Subunit 1

DKK .....Dickkopf

DSB .....Double strand break

DSF.....Differential Scanning Fluorimetry

DTT .....Dithiothreitol

DVL .....Dishevelled

EGTA .....Ethylene glycol-bis(β-aminoethyl ether)-N,N,N′,N′-tetraacetic acid

FA .....Formaldehyde

FZD .....Frizzled

GO .....Gene Ontology

GSK3β..... Glycogen Synthase Kinase 3 Beta

HCC ..... Hepatocellular Carcinoma

ICAT..... Inhibitor of β-catenin and TCF

ITC ..... Isothermal Calorimetry

KCl ..... Potassium Chloride

KO ..... Knockout

LEF..... Lymphoid enhancing factor

$MgCl_2$..... Magnesium Chloride

MSAB ..... 3-[[(4-methylphenyl)sulfonyl]amino]-benzoic acid, methyl ester

NHEJ..... Non-homologous end joining

PBS ..... Phosphate Buffered Saline

POI ..... Protein of interest

Prey/Hit..... Potential interacting partners

PMSF ..... Phenylmethylsulphonyl fluoride

PSM..... Peptide-spectrum match

RNF43..... Ring finger protein 43

sgRNA..... single guide RNA

SLiCE..... Seamless Ligation Cloning Extract Cloning

TBL1-TBLR1 ..... Transducin β-like protein 1- Transducin β-like related protein 1

TCF4 ..... T cell factor 4

TLE..... Transducin-like enhancer split

TOP1MT ..... Mitochondrial Topoisomerase I

WT..... Wildtype

ZNRF3..... Zinc and ring finger 3

Chapter 1 Introduction

1.1 History of Wnt signaling

The first mammalian Wnt gene, Int1, was discovered over 37 years ago from an investigation into the retroviral oncogenic properties in animal models which fuelled a search for its involvement in human cancer. The interest at the time was to discover the link between onset of cancer and retroviruses that seemed to confer cancer progression upon insertion. It was difficult to elucidate the function of wnt1 as it was hard to extract and purify it in sufficient quantities for biochemical analyses. However, this question was beginning to be answered when the wingless gene, was shown to be the drosophila homolog to wnt1, highly conserved in evolution[1, 2]. Hence, mutant experiments showed that the wingless(wnt1) gene was implicated in animal development[3] since the mutated Wnt gene lead to drosophila not developing full wing tissue, hence the name "wingless"[4]. Further elucidation pointed to its role in segment polarity and axial development[3].

Further investigations into the interaction partners of Wingless (Wnt1) led to the discovery of some of the key signalling components, including Armadillo, the drosophila homologue of B-catenin as a central component[5]. Alongside drosophila as a model organism for Wnt study, the *Xenopus laevis* shed more light on the role of Wnt1 in development as affecting the embryonic axis formation[6]. It can't go unmentioned that by the early 1990s the nomenclature became rather difficult to keep up with due to the mammalian and drosophila studies holding different names. So, it was changed to "Wnt" as a portmanteau of Int1 and Wingless[7].

As interest surrounding the phenotypic effects of Wnt continued to grow, a technique to insert a homozygous mutation into embryonic stem cells in mice was developed by Mario Capecchi and Oliver Smithies[8]. This technique was prototyped with Wnt mutant mice which showed an underdeveloped cerebellum and ataxia[8], further confirming Wnt's role in embryonic development. Around the same time, Tsukamoto *et al*'s experiments established Wnt as a bona fide proto-oncogene[9]. They did this by reproducing the oncogenic effect in mice without having to introduce the lentivirus and rather just expressing the Wnt1 transgene with the MMTV promoter[9]. This made Wnt one of the first examples of a gene involved in both development and cancer induction.

Over the last few decades, cancer research has gained significant attention. However, in the early days of Wnt discovery it had proved extremely difficult to find any link between Wnt and human cancers, since no mutation was present in the Wnt gene that directly linked with cancer. It was only with the study of colon cancers[10] and especially the hereditary syndrome Familial Adenomatous Polyposis that helped connect the dots. This syndrome had an associated gene in the 5q21 region of the human chromosome called Adenomatous Polyposis Coli, named after the symptoms seen in the colon. This gene was cloned[11-13] and studies two years later proposed that it interacted with β-catenin[14, 15] and thus connected it to the Wnt pathway. However, the role of this interaction in oncogenesis and how APC is "crucial for cell expansion in the early stages of colorectal carcinogenesis"[16] was only uncovered a few years later with the knowledge of APC being part of the "destruction complex" to target β-catenin for proteasomal degradation in the absence of Wnt stimulation[17-19]. **Figure 1.1** highlights some of the seminal discoveries over the last few decades of Wnt signalling.

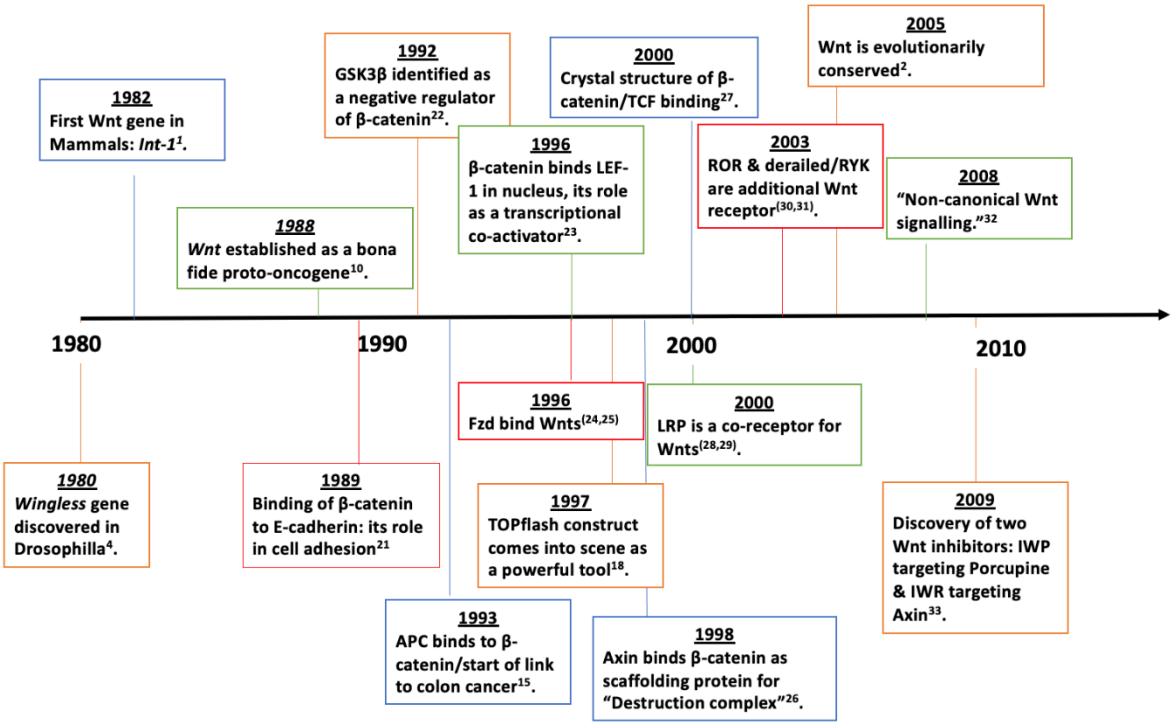

Figure 1.1 ***Timeline of significant discoveries in Wnt signaling[1, 3, 9, 14, 17, 20-33]***

1.2 Canonical Wnt signaling

One of the fascinating and distinguishing factors of Wnt signals compared to other growth factors is its ability to induce cell proliferation while producing a structured framework for tissue formation and hence have been referred to as directional growth factors[34-38]. It is heavily integrated in cell development and tissue maintenance[39-41]. It is able to achieve this morphogenetic outcome through an array of signal transduction processes triggered by Wnt. There are 3 pathways triggered by Wnt that are well documented. The 'canonical Wnt/β-catenin pathway', the 'non-canonical planar cell polarity pathway' and the 'non-canonical Wnt/Calcium pathway'. The latter two do not involve β-catenin and help regulate cytoskeleton and intracellular calcium release respectively. The canonical Wnt/β-catenin signaling pathway will be discussed here since addressing all the pathways is beyond the scope of this review.

The 40kDa Wnt protein ligand is part of a family of 19 genes in the human genome is a cell-proliferation inducing morphogen[42]. It is post-translationally modified by the palmitoyl transferase porcupine[43], which promotes the addition of palmitoleic acid on a highly conserved serine 77 residue[44]. Palmitoylated Ser77 then acts as a recognition motif for interacting with the Frizzled receptor[45]. The lipidated-form of Wnt is recognized by the trans-membrane protein, Wntless/Evi, which aids Wnt packaging and exocytosis[46] but the exact mechanisms involved in Wnt exocytosis remain elusive. Following exocytosis, the Wnt protein acts as a localized intercellular signal and binds to the 7-transmembrane receptor, Frizzled (Fzd), in the N-terminal extracellular cysteine- rich domain where the Palmitoyl group gets embedded into a hydrophobic pocket and tethers Wnt to Fzd[45] to initiate the downstream signalling events.

1.3 Main Wnt signal transduction

Under unstimulated conditions, the small dynamic pool of β-catenin is bound by a multiprotein "destruction" complex[26, 47] consisting of tumour suppressors Adenomatous Polyposis Coli(APC)[14, 19] and Axin[26] acting as scaffolding proteins, along with serine/threonine kinases Casein kinase 1(CK1α/β/δ)[48] and Glycogen Synthase Kinase 3 (GSK3)[22]. CK1 initially phosphorylates β-catenin at the Ser45 position[48] and then GSK3 sequentially phosphorylates at Thr41, Ser33, and Ser37[49]. These phosphate tags induce the docking of E3 RING ligase β-TrCP to the β-catenin-destruction complex[50]. β-TrCP then polyubiquitinates β-catenin marking it for degradation by the 26S proteasome[51](**Figure 1.2**).

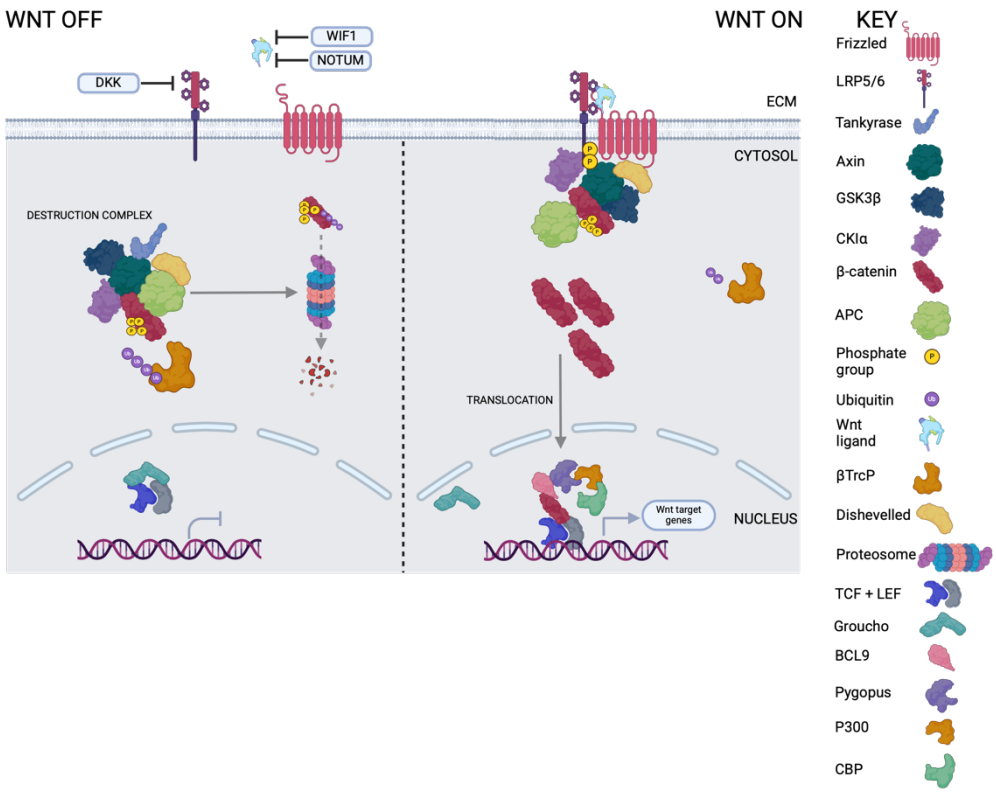

Figure 1.2 Schematic representation of the canonical Wnt signalling pathway.
In the absence of Wnt, β-catenin, while being held by Axin and APC, is phosphorylated by serine/threonine kinases GSK3β and CK1 and poly-ubiquitylated by β-TrCP E3 ligase targeting it to the 26S-proteasome for degradation. In the presence of Wnt, it binds to frizzled-LRP receptor complex and causing perturbation of the destruction complex, and subsequent accumulation of unphosphorylated β-catenin and translocation to the nucleus. In the nucleus β-catenin binds and interacts with co-transcription factors to initiate transcription of Wnt target genes such as c-myc and axin-2. Created in Biorender.com

The Wnt binding event to Frizzled[24, 25] triggers its cooperation with lipoprotein related protein 5/6 (LRP5/6) to form a dimer receptor complex[28, 29]. The conformational change enables Axin to translocate to the LRP tail following multiple phosphorylation events, some of which is by GSK3β. This is paralleled by Dishevelled binding to the Fzd tail[52] and subsequently forming a bridge link between a homologous binding domain DIX between Axin and Dishevelled[53]. This is thought to help stabilise the LRP5/6-Fzd dimer. The movement of the scaffolding protein, Axin, to the surface receptor[54] disrupts the destruction complex and no longer keeps β-catenin in complex.

Consequently, β-catenin is not phosphorylated, β-TrCP doesn't bind and ubiquitylate β-catenin. This leads to the accumulation of β-catenin in the cytoplasm and subsequent translocation to the nucleus. Here it forms a transcription complex with T-cell factor/Lymphoid enhancing factor (TCF/LEF)[26, 27] by displacing the repressive Transducin-like enhancer of split (TLE)/Groucho complex[55]. It is important to note that there are multiple transcriptional co-factors that aid to enhance the transcriptional efficiency and frequency of Wnt genes.

These include adaptor protein B cell lymphoma 9(BCL9)[56, 57] which links Pygopus(Pygo)[58] to β-catenin guiding it to TCF/LEF, where other transcriptional co-activators[59, 60] CREB Binding Protein (CBP) and P300 acetylate histones to help initiate transcription of Wnt target genes such as AXIN2[61], CCND1[62] and MYC[63].

Examples of the downstream signaling of activated Wnt signalling transduces include cell proliferation, cell differentiation, cell migration, stem cell maintenance, tissue regeneration. Wnt signaling is associated with cell proliferation because it increases the expression of a number of genes involved in cell cycle, such as cyclin D1[64]. Kielman *et al*[65] demonstrated that the interplay between APC and intracellular levels of B-catenin effected the level of embryonic stem cell differentiation into the 3 germ layers. Varying degrees of mutations in APC result in constitutive activation of Wnt/B-catenin signaling causing defective cell differentiation in tissue homeostasis and contributing to tumour formation[62]. Non-canonical Wnt signaling plays a crucial role in regulating cell polarity and cytoskeletal dynamics for guiding neural crest cell migration by activating small GTPases like Cdc42, RHoA, and Rac1 which directly control cytoskeletal dynamics, leading to cell polarisation and migration[66].

Under normal conditions, Wnt signalling is kept under tight control to ensure homeostasis using negative feedback checkpoints mechanisms. At the plasma membrane, the single pass transmembrane E3 ligases ring finger protein 43 (RNF43) and zinc and ring finger 3 (Znrf3) E3 are products of activated Wnt signaling which ubiquitinate Fzd receptors and subsequently induce its endocytosis and lysosomal degradation, regulating Wnt recognition[67, 68]. At the same level, the co-receptor LRP6 is down-regulated from the cell surface by the binding of antagonist Dickkopf (DKK)[69]. Furthermore, within APC, there is a conserved β- catenin inhibitory domain (CID) located between the 2nd and 3rd 20-mer repeats[70, 71] which is reported to be crucial in negatively regulating β-catenin and is within the mutation site that results in APC truncation in colorectal cancer (CRC) incidences. Moreover, regulation is also found within the nucleus as Inhibitor of β-catenin and TCF (ICAT) down-regulates the level of transcription of Wnt target genes[72].

1.4 Wnt signaling in cancer

Wnt signaling plays a critical role in several cancers, driving tumorigenesis, therapy resistance, and metastasis through β-catenin and associated pathways. In colorectal cancer (CRC), APC mutations are the primary driver of β-catenin overactivation, resulting in constitutive activation of Wnt signaling. *APC* gene mutations account for 80-90% of CRC cases. The loss-of-function mutation results in a truncated and non-functional APC protein that is no longer able to effectively bind β-catenin in the destruction complex[73], thus, preventing β-catenin degradation, leading to continuous Wnt activation. In addition, chromosomal instability (CIN) is heightened with dysregulated Wnt signaling and is a hallmark of CRC. In tumors harboring RNF43 mutations, cells become highly dependent on Wnt ligand secretion, making them vulnerable to Wnt-targeting therapies[74]. Wnt signaling in CRC contributes to tumor maintenance and drug resistance, complicating treatment outcomes.

Moreover, in leukemias such as acute myeloid leukemia (AML), chronic lymphocytic leukemia (CLL), and T-cell acute lymphoblastic leukemia (T-ALL), Wnt signaling plays a pivotal role in the survival and proliferation of leukemia-initiating cells (LICs)[75]. Inactivation of β-catenin has been shown to eliminate leukemia stem cells, providing a potential therapeutic strategy to prevent relapse and disease progression.

Wnt/β-catenin signaling also influences melanoma progression, which delays oncogene-induced senescence and promotes early tumor initiation. However, the role of β-catenin in melanoma metastasis remains controversial, with studies suggesting both pro-metastatic and anti-metastatic effects depending on the tumor context[76]. In a similar vein, researchers conducting melanoma studies have contrastingly argued that suppression or loss of β-catenin expression may be associated with tumour progression[77-79]. This highlights the complexity of directly inhibiting β-catenin and requires further study to selectively target it in the optimal cellular context.

Furthermore, in breast cancer, over 50% of cases exhibit Wnt pathway activation, which correlates with poor prognosis and increased tumor aggressiveness[80]. Canonical Wnt signaling promotes tumor heterogeneity and stemness, driving the growth of treatment-resistant cancer cell populations and contributing to disease progression[81]. These downstream effects of Wnt signaling that are evident across these different cancers are described in more detail in **Table 1.1**.

Table 1.1. Summary description of examples of downstream effects of Wnt signaling in cancer. *Table information adapted from Zhao et al[82]*

Downstream Effect	Description	Key Molecular Players
Cell Proliferation and Survival	Promotes cancer cell proliferation and inhibits apoptosis. β-catenin translocates to the nucleus and activates genes involved in cell cycle regulation like **c-Myc** and **cyclin D1**.	**β-catenin, c-Myc, Cyclin D1, APC, GSK-3β**
Cancer Stemness	Maintains cancer stem cell (CSC) population, essential for tumor initiation, progression, and therapy resistance. Wnt signaling is critical for CSC self-renewal.	**β-catenin, Wnt3a, LGR5, Axin, APC**
Epithelial-Mesenchymal Transition (EMT) & Metastasis	Enhances invasion and metastasis by promoting EMT, characterized by loss of E-cadherin and gain of mesenchymal markers such as **N-cadherin** and **vimentin**.	**β-catenin, Snail, Twist, E-cadherin, LEF1**
Resistance to Therapy	Contributes to resistance to chemotherapy and radiotherapy. Cells with high Wnt activity evade apoptosis and exhibit survival advantages under treatment stress.	**β-catenin, TCF7L2, GSK-3β**
Interaction with Other Pathways	Crosstalk with **TGF-β**, **Notch**, and **PI3K/Akt** pathways enhances tumor progression and promotes cancer cell survival.	**TGF-β, Notch, PI3K, Akt**
Microenvironment Modulation	Wnt signaling affects the tumor microenvironment by promoting angiogenesis, immune evasion, and chronic inflammation, which supports tumor growth and metastasis.	**VEGF, MMPs, MyD88, IL-17A**
Regulation of Metabolism and Autophagy	Alters metabolic processes such as glycolysis and lipid metabolism to meet high proliferative demands. Regulates autophagy, which can either promote or suppress cancer progression.	**GSK-3, β-catenin, AMPK, LC3**
Inflammation and Immune Response	Wnt signaling promotes chronic inflammation, contributing to cancer progression. It suppresses anti-tumor immune responses and promotes an immunosuppressive microenvironment.	**β-catenin, MyD88, IL-17A, Lect2**

1.4.1 Wnt signaling in Cancer Stem Cells

Wnt signaling plays a critical role in cancer stem cells (CSCs), which are responsible for self-renewal, metastasis, and therapy resistance. Key regulators of CSC behaviour include Lgr5, a Wnt target gene, and Rac1, which is involved in Wnt-induced dedifferentiation[83].
In CRC, Lgr5+ cells are the primary source of tumour growth, and Wnt inhibition has been shown to reduce CSC populations and prevent metastasis[84]. Wnt signaling also upregulates NFκB, enhancing the survival and plasticity of CSCs, making them resistant to both chemotherapy and radiotherapy[81]

1.4.2 Wnt signaling in Metastasis

Epithelial-mesenchymal transition (EMT), a key driver of metastasis, is also regulated by Wnt signaling through β-catenin, Snail, and Fzd2. Yang and colleagues[85] have reported that EMT allows cancer cells to acquire invasive and migratory properties, which are crucial for metastatic dissemination. Recent studies show that exosomes transport Wnt ligands, facilitating tumor progression and promoting communication between cancer cells and the tumour microenvironment[86]. Circulating tumor cells (CTCs), known to have high Wnt activity, are associated with increased metastatic potential, and Wnt inhibition has been shown to reduce their survival and metastatic colonization[87].

1.4.3 Oncogenic hotspot mutations in β catenin

From an oncogenic point of view, genome scale analysis of 276 samples by cancer genome atlas research[88] have found that 16% harboured hypermutations including hotspot mutation sites in exon 3 of CTNNB1. This forms the N-terminal region of β-catenin and somewhat unsurprisingly the majority of somatic mutations in CRC involve the phosphorylation and β-TrCP recognition sites: D32, S33, G34, S37, T41, and S45[89]. Due to the flexible nature of this region, there are questions as to the impact of these mutations on structure and stability as they avoid ubiquitylation and proteasomal degradation in tumorigenesis. In 2019, the Catalogue of Somatic mutations in cancer recorded over 100 independent tumours that harbour these 2 mutations in the armadillo repeats 5 and 6: K335I, N387K. A majority of which are associated with liver, colon, and kidney tumours[89]. Research by Liu and colleagues[90] have suggested that reduced binding of β-catenin to APC is a mechanism associated with the observed increase in Wnt signalling and oncogenicity in mice models.

However, in hepatocellular and endometrial tumours, a gain-of-function mutation in β-catenin is predominantly observed involving deletions or substitutions of the serine/threonine residues mentioned earlier that are part of the phospho-degron sequence (DpSGϕXpS) within the β-catenin N-terminus[18].

Consequently, there is insufficient phosphorylation and β-TrCP recognition making it less prone to degradation and a constitutive presence of β-catenin in the nucleus. This results in increased Wnt transcriptional output of oncogenes, such as *MYC*, leading to uncontrolled cell proliferation and tumour formation[91]. Thus, a more robust understanding of the β-catenin structure and protein interactions in the light of these mutations would offer further insight for therapeutic manipulation.

1.5 β-catenin structural insights

β-catenin, an 85 kDa oncogenic transcriptional co-activator takes centre stage in the Wnt signalling pathway. It has two distinct and important roles. It is heavily involved in forming intercellular adherence junctions with E-cadherin[92] and β-catenin[93]. Structurally, β-catenin is comprised of a folded and conserved Armadillo repeat domain (ARD) flanked by unstructured N-terminal and C- terminal domains. The N-terminal domain contains the binding site for β-catenin for structural functions[94]. Also found here is the phospho-degron sequence ((DpSGϕXpS) where kinases GSK3β and CK1 phosphorylate promoting subsequent recognition by β-TrCP E3 ligase[95, 96]. The ARD(residues 141-664) consists of 12 armadillo repeats, each approximately 42 residues long, forming a tri-α-helical repeating motif. In unison these 12 repeats form a long groove portraying a super-helical structure[97]. The 3rd helix in each repeat forms the “floor” of the groove. The surface of the ARD holds a highly positive charge[97], while the N- and C-terminal region displays a negative charge.

There is some controversy surrounding the effect of unstructured termini on ligand interactions where the potential backfolding of unstructured termini on the ARD acts to competitively inhibit β-catenin interactions. Authors have Isothermal Calorimetry (ITC) data proposing that the termini have no effect on strong binders like E-cadherin but do suggest an effect on weaker binders such as Axin and unphosphorylated APC[98, 99], perhaps supporting the notion of transient electrostatic interactions due to its absence in structural data. The 12 ARD repeats harbour the binding sites for many of the key interaction partners of β-catenin. (see **Figure 1.3**), including Axin, APC and the nuclear partners TCF, BCL-9.

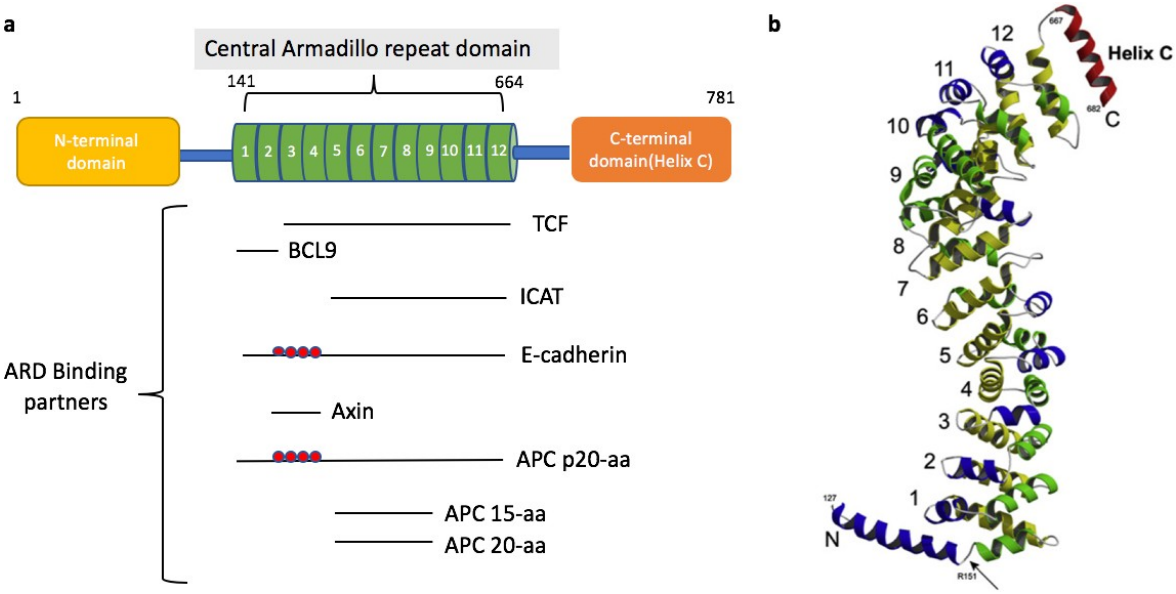

Figure 1.3 Structure of β-catenin.
a) Domain description of β-catenin with the regions of binding from some known interaction partners below b) Crystal structure of full length β-catenin from Danio Rerio in cartoon representation. PDB: 2Z6G. Produced by[100]. Figure adapted from[101].

The groove formed in the ARD accommodates the binding of several proteins in an exclusive manner, with steric hindrance providing an additional level of control through preventing simultaneous binding[98, 101]conserving spatial and temporal regulation of the Wnt pathway. There is a remarkable conserved binding motif DxθθxΦx2-7E that is present in some of these binding partners that strengthen the interaction with β-catenin. Positively charged residues K435 and K312 within the core of the ARD (repeats 5-9), referred to as "charged buttons" are binding hotspots[27, 100] that form salt bridges with key aspartate and glutamate residues in the consensus sequence, respectively. In APC for example, these are residues D1486 and E1494, and within TCF it is D16 and E17. The formation of these salt bridges drastically increases the affinity of the APC-β-catenin and TCF-β-catenin interaction respectively. The D16A mutation in TCF4 decreased the binding affinity by two orders of magnitude.[27, 99, 102] One must note, there are some irregularities in the β-catenin structure, especially in the ARD. For example, the first 2 helices of the first armadillo repeat are more flexible than the rest and form a kinked helix[45(27)]. It remains elusive whether these differences have some functional implications.

1.6 β-catenin protein-protein interactions in the Wnt-signaling pathway

There are some key interactions that define the Wnt-signalling network and its output. This ranges from the level of the Frizzled/LRP5/Dishevelled to the transcription complex leading to gene transcription. However, the protein of great interest is β-catenin, with its array of diverse PPIs ranging from the destruction complex in the cytoplasm to the multiple interactions with the transcription complex binding partners[103].

In the absence of Wnt stimulation the small population of cytoplasmic β-catenin is bound by two proteins; scaffold protein Axin[26] and tumour suppressor APC[14]. The interaction of β-catenin with Axin is via a single α-helical stretch of 17 amino acid residues that binds in the groove between the 3rd and 4th armadillo repeats[104] with ITC data demonstrating a binding affinity of 1.3μM to full-length β-catenin[99]. Interestingly, the GSK-3β binding site on Axin is in close proximity to where β-catenin binds[104] forming a hydrophobic helical ridge between residues 388-399, possibly aiding in the phosphorylation events.

In contrast, the β-catenin-APC interaction involves much broader and varied contacts spanning much of the ARD. This includes 3x15-aa and 7x20-aa repeats[105]. The 15-aa is not regulated by phosphorylation but the 20aa repeats that span the groove of the ARD can be phosphorylated in the 3rd repeat which greatly increases the affinity of APC for β-catenin[90, 105]. Quantitative analysis by Choi *et al* [99] supports this as the 3rd unphosphorylated 20-mer repeat had a K_d of 3.1μM while the phosphorylated 3rd repeat showed more than a 300-fold increase in affinity with a K_d value of 10nM[99].

There are two models that suggest a functional explanation for this difference in binding contacts. One model[101] suggests that β-catenin interacts with Axin and APC via the 15aa repeats. Then upon phosphorylation of β-catenin and APC's 3rd 20aa repeat, APC increases its affinity for β-catenin and competes with Axin[106] and displaces it, detaching β-catenin from the destruction complex making way for a new molecule of β-catenin. An alternative model[107] suggests that in the absence of Wnt, β-catenin only binds APC after the 3rd repeat is phosphorylated, and thus β-catenin is released slowly. However, upon Wnt stimulation when levels of β-catenin are higher, APC is binding β-catenin even at low affinity and released soon after phosphorylation to help with β-catenin turnover and is proposed to provide negative feedback to the Wnt signal[107]. It remains unconfirmed which model is more accurate or whether it is an integrated mechanism.

Following β-catenin translocation into the nucleus, it is recruited to the promotor region by a complex of proteins to augment transcription of Wnt target genes[108]. BCL9, one of the transcriptional co-activators binds in the groove created by helices 2 and 3 of the first repeat of the ARD via an α-helix and caps the N-terminus of the ARD[109] with a moderate affinity (0.5μM). This small binding surface and lower affinity are favourable properties for therapeutic intervention.

Established by crystallography studies[27], TCF4 is suggested to have three prominent binding modules that run anti-parallel to the β-catenin groove comprised of a β-hairpin module (res. 2-15), an extended region (res. 16-29) and an α-helix (res. 40-51). The β-hairpin and α-helix bind to the repeats 9 & 10 and 3 & 4, respectively[27]. The extended region contains the critical salt bridge mentioned earlier which fastens the binding [110]. Thus, it is not surprising, with the presence of multiple binding contacts that TCF4 binds with high affinity (~30nM)[102], making it a difficult therapeutic target.

1.7 Wnt signaling-small molecule modulators

The purposeful regulation of the Wnt signalling pathway has been attractive for a long time because of its involvement with many cancers[111], especially β-catenin. The design and synthesis of small molecules gained great interest because of its greater potential to exhibit more favourable biochemical, biophysical and pharmacological properties than higher molecular weight peptidic compounds[112]. However, there are still considerable hurdles that need to be addressed. For example, though a compound may show promising binding in silico, gaining efficient intracellular access can become a limiting factor due to charged moieties on the compound. Over the last 10 to 15 years, there have been numerous attempts at Wnt pathway modulation, as highlighted in **Figure 1.4**.

Targeting the Wnt pathway with small molecular weight molecules has positive expected outcomes theoretically with respect to cancer therapy. Firstly, in Wnt-dependent cancers i.e. cancers that constitutively rely on Wnt signaling to proliferate, migrate and evade immune checkpoints, such as CRC and HCC, small-molecule inhibitors reduce β-catenin nuclear translocation, thereby suppressing transcription of oncogenic target genes such as *MYC* and *CCND1* (Cyclin D1) [113]. This would reduce tumour growth, proliferation arrest, and increased apoptosis. Another expected outcome of targeting the Wnt pathway in this manner would be the prevention of Metastasis. Wnt signaling drives epithelial-mesenchymal transition (EMT), facilitating cancer cell migration and invasion. Targeting the pathway disrupts EMT and limits metastasis. This would result in reduced invasiveness and prevention of metastatic spread[39].

Moreover, Wnt signaling also regulates angiogenesis by modulating VEGF expression. Inhibitors targeting Wnt can suppress the formation of new blood vessels in tumours. The expected outcome is reduced vascularization, limiting nutrient supply to tumours and inhibiting growth[114]. The practical challenge to achieve this can be the undesired off-target effects on healthy cells. While transient inhibition may be relatively safe, chronic, or broad-spectrum Wnt suppression can lead to complications such as impaired tissue homeostasis and regeneration. This is because Wnt signaling is essential for tissue renewal in organs like the intestine, skin, liver and bone marrow and long-term Wnt inhibition could impair tissue regeneration and maintenance, resulting in intestinal atrophy, skin thinning or bone marrow suppression[115].

Furthermore, Wnt signaling promotes osteoblast differentiation and bone formation. Chronic Wnt inhibition could result in osteopenia or osteoporosis, increasing risk of fracture[116]. Balancing the therapeutic effects and safety. The goal is to reduce oncogenic Wnt signaling while preserving normal tissue functions.

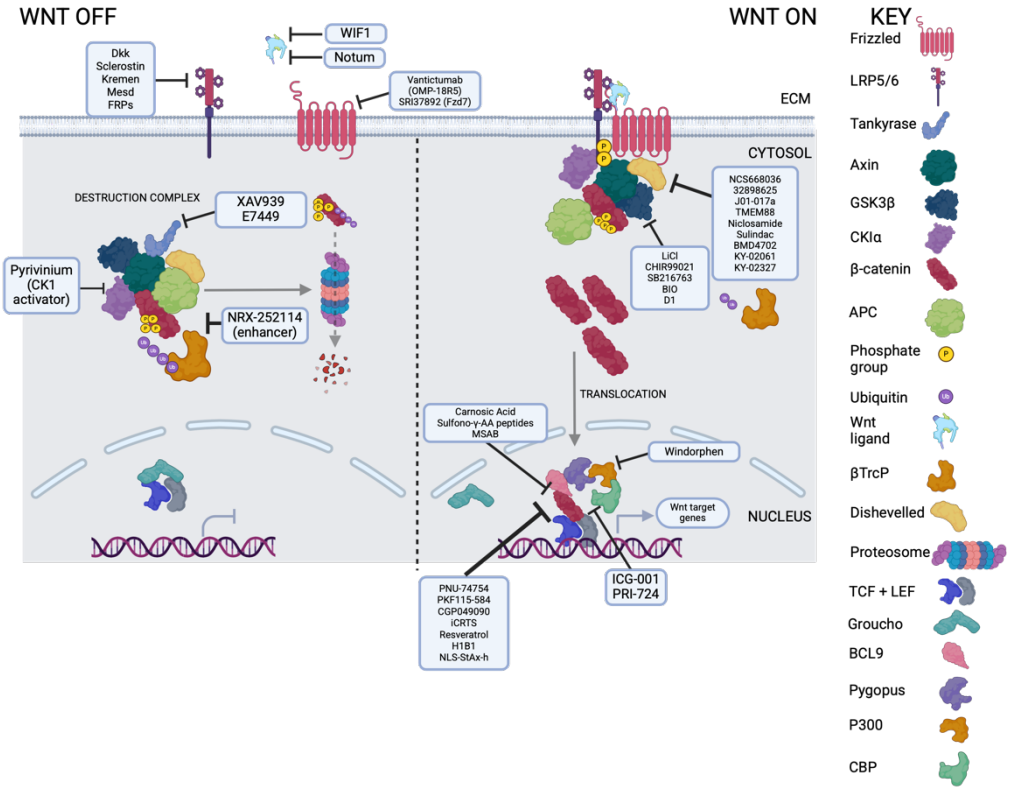

Figure 1.4 Targeting the Wnt pathway-small molecule modulators.
Figure adapted from[112]

1.7.1 Indirect targeting of β-catenin

Focussing on β-catenin, few examples of indirect modulators include tankyrase inhibitors IWR-1[33] and XAV939[117] which stabilise Axin and promote β-catenin degradation. The CK1α activator, pyrivinium[118] enhances the S45 priming phosphorylation of β-catenin that triggers the phosphorylation cascade and consequent degradation. An example within the nucleus includes, ICG-001 which binds CBP and subsequently interferes with and inhibits the β-catenin-CBP PPI to downregulate transcription[119]. Many more examples are illustrated in **Figure 1.4**.
Although indirect targeting seems to demonstrate target effect, there is an increased risk of potential off-target effects and due to the spectrum of β-catenin interactors, it seems desirable to directly target it. However, this has proven to be a difficult challenge.

1.7.2 Direct targeting of β-catenin and the associated challenges

One of the small molecules that gained some attention was Carnosic acid (CA), a natural compound derived from Rosemary. De la Roche *et al*[120] argued that this compound interacts with H1 an "intrinsically labile alpha-helix" within the first 4 repeats of the ARD domain which overlaps the BCL9 binding site and disrupts the interaction. In conjunction, they hypothesized that CA binding exacerbates the aggregation propensity of β-catenin reducing the stability of the protein, making it recognisable by Ubiquitin-Proteasome System for ubiquitination and proteasomal degradation, attributing a second mode of action for CA. This is supported by Western blot analysis in the presence/absence of the proteasome inhibitor MG132[120]. To add to the β-catenin:BCL9 targeting, recent work by Sang and colleagues[121] employed a peptidomimetic strategy for interrupting this interaction. The sulfono-γ-AA peptides mimic the BCL9 alpha helix that targets the N-terminus of the ARD. This molecule has shown excellent stability, being virtually resistant to enzymatic cleavage which greatly increases its biological potential[121].

The β-catenin:TCF4/LEF interaction is of critical importance for transcriptional output and disrupting it holds therapeutic potential. However, there are several obstacles to overcome as this interaction has a large binding interface (~4800Å^2)[27], very strong binding (~30nM)[102] and has overlapping binding sites with key interactors; cadherins, Axin and APC[109]. StAx[122] is a stapled peptide that has been designed to directly target β-catenin and interfere with this interaction. Prominent challenges with this peptide included efficient cell permeability, targeting specificity and susceptibility to proteolytic cleavage[122].

In response to this, Dietrich *et al* developed an enhanced modified version NLS-StAx-h[123] which contains a nuclear localisation sequence harbouring positively charged lysine residues that enhances cell permeability and nuclear targeting as well as homo-arginines which increase the hydrophobicity. The enhanced properties resulting from the combination of cationic and hydrophobic residues resulted in drastically enhanced inhibition of the β-catenin:TCF nuclear complex and downstream transcription by NLS-StAx-h[123] . Further examples of reported modulators of the β-catenin:TCF interaction include; PKF115-584[124, 125], CGP049090[125], Resveratrol[126] and H1-B1[127]. See **Table 1.2**for chemical structures and target information of some β-catenin interactors discussed here.

PROteolysis TArgeting Chimeras (PROTACs)[128] are heterobifunctional molecules consisting of two ligands; an "anchor" to bind to an E3 ubiquitin ligase and a "warhead" to bind to a protein of interest (POI), connected by a chemical linker. The warhead binds the POI while the anchor binds an E3 ubiquitin ligase, thus bringing them in close enough proximity to allow for the poly ubiquitylation of the POI and subsequent degradation by the 26S proteasome[128].(**Figure 1.5**) Many pharmaceutical companies are utilizing this approach to find suitable drug modalities. Unfortunately, success has been slim due to the majority of these molecules not possessing the desired physio-chemical properties required for efficient binding as well as transient entry into the cells. In response to this, Simonetta *et al*[129] assessed the drawbacks of PROTAC and adapted the strategy for proteolysis-based drug discovery by designing a single molecule that has functional groups to act as a PROTAC without the need for a linker. This immediately decreases the physical size of the drug moiety.

They investigated the β-catenin-TrCP E3 ligase complex and targeted the pocket at the binding interface left by the absence of the phosphate group on mutation hotspot Ser37[129]. They developed a molecule to mimic the effect the anionic moiety of the phosphate group to enhance β-catenin- TrCP E3 ligase interaction. Following high-throughput screens and structure optimization, NRX- 252114 (See **Table 1.2** below for structure) showed over 1500-fold cooperativity, surpassing the affinity of WT double phosphorylated β-catenin peptide[129], thus illustrating the potency in modulating target structures for optimisation. However, one of the drawbacks was that in the in vitro cellular system, they couldn't induce degradation of the target β-catenin protein and this highlights one of the main challenges facing drug development, the translation of biophysical analysis to cellular effect.

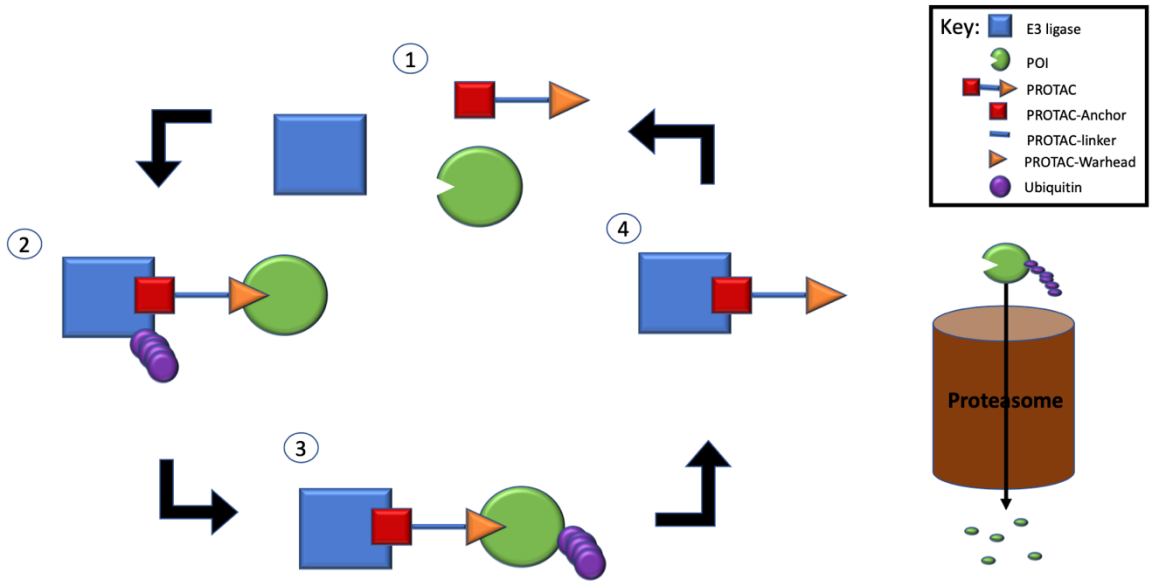

Figure 1.5 Cartoon illustration of PROTAC design and mechanism of action.
(1) PROTAC primed to bind E3 ligase and protein of interest (2) PROTAC has bound to E3 ligase via anchor region and to POI via Warhead ligand. (3) E3 ligase in close enough proximity to polyubiquitinate POI. (4) Polyubiquitinated POI targeted to proteasome for degradation.

Finally, a molecule that has shown potential as a potent Wnt inhibitor as documented by Huang *et al* is MSAB[130]. A compound that is readily cell permeable and has been shown via NMR analysis to interact directly with β-catenin between a.a. 301-670 of the ARD, however this remains ambiguous as biophysical data from Differential Scanning Fluorimetry (DSF) and ITC experiments by McCoy *et al*[131] does not support this. MSAB has shown specificity towards inhibiting the Wnt-dependent proliferation of colorectal cancer cell lines (HCT-116, SW480) with high efficacy[130]. Within these cell lines, MSAB has induced β-catenin ubiquitination and proteasomal degradation. The mechanism of action, precise binding mode and affinities are yet to be determined.

Table 1.2 ***Examples of small molecules that propose to target β-catenin interactions.***

Name of compound	Proposed target and effect	Structure	Proposed Affinity (K_D)
Carnosic acid	-R1-R4 of ARD. Inhibits BCL-9 binding -Down-regulates Wnt target gene transcription and β-catenin degradation	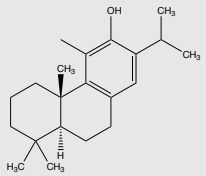	5-20μM
Sulfono-γ-AA peptide	-Mimics BCL-9 helix Inhibits BCL-9 binding -Down-regulates Wnt target gene transcription	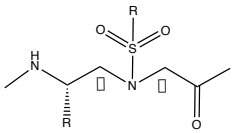	0.16μM
CGP049090	-Exact binding site unknown. Inhibits β-catenin: TCF interaction -Down-regulates Wnt target gene transcription	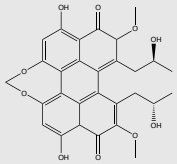	N/A
NRX-252114	-Binds in S37 groove. Enhances β-catenin:β-TrCP interaction -Promotes β-TrCP ubiquitylation of β-catenin and enhances its degradation	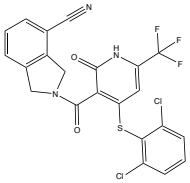	0.4nM
H1-B1	Exact binding site unknown. Inhibits β-catenin: TCF interaction. -Down-regulates Wnt target gene transcription -Caused apoptosis of β-catenin dependent cancer cells	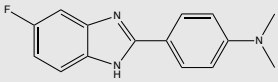	N/A
NLS-StAx-h	-Exact binding site unknown. Inhibits β-catenin: TCF interaction. -Down-regulates Wnt target gene transcription -Inhibits proliferation & migration of CRC cells	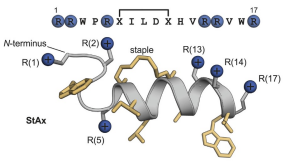	0.12μM
MSAB	-Exact binding site unknown. -Down-regulates Wnt target gene transcription and induces β-catenin degradation -Inhibits proliferation & migration of CRC cells	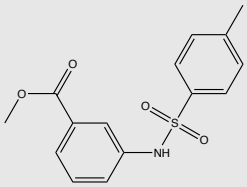	N/A

Currently, there are only 3 drug candidates in clinical trials that target β-catenin PPI and two drug candidates (PRI-724[132],E7386[133]) target the β-catenin-CBP PPI. E7386 is an orally active derivative of the active form of PRI-724. They are both being tested as single agents and in combination therapy against both solid tumours (CRC & pancreatic) and AML. (See Table 1.2). Tegavivint (BC2059-β-cat pharmaceuticals) is the only other compound in clinical trials that works by inhibiting a β-catenin interaction. It binds to the protein transducin β-like protein 1 (TBL1) and its highly related family member (TBLR1)[134]. TBL1-TBLR1 crucially interacts with β-catenin during Wnt activation to recruit it to the promoter region of the Wnt target genes to help drive transcription[135]. Tegavivint disrupts that interaction and results in degradation of nuclear β-catenin[134]. It is being trialled in patients with progressive, unresectable desmoid tumour, initial phase study shows good tolerance and may warrant further investigation[136].

Although this is evidence that progress is being made in targeting β-catenin interactions for therapy, as the 'outcome' column in table 1.2 shows, some studies were withdrawn or terminated and phase I results for some cohorts are still unknown, further highlighting the lack of late stage and marketed candidates and the difficulty of targeting β-catenin directly. This warrants the need for further characterisation of the β-catenin interactome to attempt to find novel interactions that improve our understanding of the signalling landscape which in turn may provide more candidates to take from pre-clinical analysis to the clinic.

Table 1.3 Drug candidates associated with β-catenin interactions in clinical trials.
Figure adapted from[137]

DRUG	TARGET	CANCER	TRIAL STATUS	PHASE	TRIAL NUMBER	OUTCOME	REFERENCES
PRI-724	Binds CBP and inhibits CBP: β-Catenin interaction	Pancreatic cancer	Completed	I	NCT01764477	Awaiting publication of results	121
		-Acute myeloid leukemia -Chronic myeloid leukemia	Completed	I, II	NCT01606579	Awaiting publication of results	
		Colorectal cancer	Withdrawn	II	NCT02413853	Combination trial with bevacizumab withdrawn due to study drug supply issues	
		Advanced solid tumors	Terminated	I	NCT01302405	Terminated due to low patient enrolment	
E7386	Binds CBP and inhibits CBP: β-Catenin interaction	Colorectal neoplasms	Recruiting	I	NCT03833700	In process	122
		Advanced neoplasms	Recruiting	I	NCT03264664	In process	
		Hepatic neoplasms	Recruiting	I	NCT04008797	In process	
Tegavivint (BC2059)	Binds TBL1/TBLR1 and inhibits TBL1/TBLR1: β-Catenin interaction	Desmoid Tumour	Completed	I	NCT03459469	-Well tolerated with low risk of adverse effects. No serious toxicity associated with Wnt inhibition. Warrants further investigation.	123, 125

1.8 Main Aims

The primary goal of this project is to deepen our understanding of the Wnt signaling pathway, with a particular focus on the β-catenin interactome, through the integration of advanced bioengineering techniques and small molecule screening platforms. By employing cutting-edge approaches such as CRISPR-Cas9 gene editing, proximity labeling with MiniTurbo, and high-resolution mass spectrometry, this project aims to uncover novel β-catenin protein-protein interactions (PPIs) and assess how small molecule modulators influence the β-catenin interactome. The outcomes of this work have the potential to provide valuable insights into the therapeutic relevance of Wnt signaling modulation in cancer. The project objectives can be broadly categorized as follows:

1. **CRISPR-Cas9-mediated CTNNB1 knockout and proteomic profiling**
   I. Implement CRISPR-Cas9 technology to generate a CTNNB1 (β-catenin) knockout model in U2OS cells.
   II. Perform whole-cell proteomics using liquid chromatography-tandem mass spectrometry (LC-MS/MS) to analyze changes in the proteomic landscape caused by the knockout of CTNNB1.
   III. Identify proteins and pathways that are significantly altered in the absence of β-catenin, providing insights into the functional dependencies of β-catenin in the Wnt signaling pathway and beyond.
2. **Mapping the β-catenin interactome via proximity dependent Biotinylation**
   i. Develop a proximity-dependent biotinylation platform using the MiniTurbo system, a biotin ligase engineered for rapid and sensitive labeling of proteins in the β-catenin interactome.
   ii. Couple MiniTurbo biotinylation with affinity purification-mass spectrometry (AP-MS) to identify novel β-catenin protein-protein interactions (PPIs) in U2OS cells.
   iii. Establish a robust pipeline to distinguish high-confidence interactors from background noise, thereby enhancing the specificity of the β-catenin interactome dataset.
3. **Investigating the impact of small molecule modulators on the β-catenin interactome**
   i. Conduct cell-based assays to profile both known small molecule modulators of Wnt signaling and novel derivatives to assess their impact on β-catenin interactions.
   ii. Use the MiniTurbo system to identify how small molecule treatments alter β-catenin's interactome and functional networks in living cells.
   iii. Leverage advanced proteomic platforms, including LC-MS/MS and AP-MS, to map how these small molecules modulate β-catenin-dependent signaling and its protein partners.

Chapter 2 Materials and Methods

2.1 Reagents and Antibodies

Table 2.1 Table of Antibodies

Name	Company(Cat No.)	Recommended Dilution	Antibody preparation and treatment (Western Blot)
β-actin (Mouse)	Protein Tech (66009-1-Ig)	WB: 1:10000-30000	5% milk in TBST, overnight 4°C
β-catenin (Mouse)	CST (2698S)	WB: 1:1000 IF: 1:200	2.5% milk in PBST, overnight 4°C
HA (mouse)	ThermoFisher (26183)	IF: 1:100	N/A
HA (Rabbit)	CST (3724S)	WB: 1:3000	5% w/v BSA in TBST Overnight 4°C
γ-catenin (Rabbit)	CST (2309S)	WB 1:10000	5% w/v BSA in TBST Overnight 4°C
Non-phospho (Active) β-catenin (Ser33/37/Thr41) (Rabbit)	CST (8814S)	WB: 1:1000 IF: 1:200	2.5% milk in PBST, overnight 4°C
Streptavidin (Rabbit)-Secondary	ThermoFisher (S32354)	WB: 1:5000 IF: 1:1000	5% milk in TBST Overnight 4°C
Goat Anti-Rabbit IgG Secondary Alexa Fluor™ 488	Invitrogen (A-11008)	IF: 1:500	PBS-0.2% BSA , 45 minutes at room temperature
Goat Anti-Mouse IgG Secondary Alexa Fluor™ 488	Invitrogen (A-11001)	IF: 1:2000	PBS-0.2% BSA , 45 minutes at room temperature
Goat Anti-Rabbit IgG Secondary Alexa Fluor™ 594	Invitrogen (A-11012)	IF: 1:1000	PBS-0.2% BSA , 45 minutes at room temperature
Goat Anti-Mouse IgG Secondary Alexa Fluor™ 594	Invitrogen (A-11005)	IF: 1:2000	PBS-0.2% BSA , 45 minutes at room temperature

Table 2.2 Table of Reagents

Reagent Name	Reagent Constituents
RIPA Buffer	50mM Tris-HCl pH8, 150mM NaCl, 0.1% SDS, 0.5% Deoxycholic acid, 1% NP-40
TBST Wash buffer	2mM tris-HCL pH7.5, 15mM NaCl, 0.1% tween20
Towbin's Transfer Buffer	2.5mM Tris-BASE pH8.6, 19.2mM glycine
Hypotonic Buffer (Nuclear fractionation)	20 mM Tris-HCl (pH 7.4), 10 mM KCl, 2 mM MgCl2, 1 mM EGTA, 0.5 mM DTT, 0.5 mM PMSF
Fractionation Wash buffer	PBS, 0.1% SDS
10x SLiCE Buffer	500 mM Tris–Cl (pH 7.5 at 25 °C), 100 mM MgCl2, 10 mM ATP, 10 mM DTT, store at −20 °C

2.2 Cell Culture

Colorectal cancer cell line HCT-116 was grown and cultured using McCoy-5a media (Life Technologies, Cat no. 16600-108, Carlsbad, CA). Colorectal cancer cell line SW480 was cultured in DMEM media (Life technologies, Cat no. 11965092) to accommodate for 5% CO_2 incubators. The following cell lines were also cultured in DMEM media: HEK293T, U2OS (kindly gifted by Prof Divecha Lab, University of Southampton), MDA-MD-231 (kindly gifted by Dr Wang Lab, University of Southampton). ARPE-19 cell line was cultured in RPMI (Life Technologies, Cat no. 61870036. MCF10A cells and custom prepared media (Media Recipe) were kindly gifted by Dr Elias (University of Southampton). All other media were supplemented with 10% fetal bovine serum (Life Technologies, Cat no. 10438-026) and 1% Penicillin-Streptomycin (Life Technologies, Cat no. 15140-148) in 37°C incubator set at 5% CO_2. Cells were washed with PBS and sub-cultured using TrypLE express 1X (ThermoFisher, Cat no. 12563011).

2.3 Cell lysate preparation

For the purpose of Western blot analysis and DNA/RNA extraction for qPCR following drug application. Cells were harvested together and lysed using RIPA buffer mixed with protease and phosphatase inhibitor cocktail (Fisher Scientific, Cat no. 78440), sonicated (4% power, 3 seconds total, 2 seconds on and 1 second off) and spun down at *12600 x* g for 10 minutes. The Bicinchoninic acid (BCA) assay is one of the most common procedures for determining protein concentration and is more accurate than using the dye-binding Bradford assay. The BCA/copper complex formed resulted in a strong linear absorbance at 562nm as sample protein concentration increased. This was read on a POLAR®star Omega microplate reader (BMG Labtech). The protein concentrations were interpolated from a standard BSA curve. Pierce™ BCA protein assay kit (ThermoFisher, Cat no. 23225) was used.

2.4 SDS PAGE and Western Blotting

Western blotting is a well-established method for analysing protein expression levels[138]. It was utilised in this project to study the effect of small compounds on levels of β-catenin. Quantified amount of protein lysate samples (5-10 μg) were combined with NuPAGE™ LDS Sample Buffer (ThermoFisher, Cat no. NP0008) and 0.25M DTT and run on a 10% acrylamide gel comprised of resolving gel and stacking gel in the composition highlighted in **Table *2.3*** with 1x NuPAGE™ MOPS SDS running buffer (ThermoFisher, Cat no. NP0001). The gel was run for 15 minutes at 120 volts until samples reached the resolving gel, then increased to 160 volts for approximately 45 minutes at room temperature. Proteins on the acrylamide gel were transferred (Trans-blot® Cell, Bio-Rad, Cat no. 170-3910) to a nitrocellulose membrane for 2 hours at 60V at 4°C, blocked, and incubated with primary and secondary antibodies according to manufacturer's instructions (**Table 2.1**) and imaged on LI-COR Odyssey® CLx and analysed with LI-COR Image Studio Lite V5.2 software.

Table 2.3 Constituents of 10% SDS-PAGE gel with respective volumes

10% Gel		
	Resolving Gel (10%)	**Stacking Gel (5%)**
1M Bis-Tris Buffer pH 6.5	2 ml	0.667 ml
40% Acrylamide	1.5 ml	0.25 ml
H_2O	2.5 ml	1.083 ml
10% Ammonium persulfate	24 μl	8 μl
Tetramethylethylenediamine (TEMED)	12 μl	4 μl
Total	**6ml**	**2 ml**

2.4.1 Western Blot Quantitation

To retrieve quantitative image information from the immunoblot membrane, the protein bands were subjected to densitometry measurements using LI-COR Image Studio Lite V5.2 software which give an arbitrary value that is relative to the control protein bands (β-actin). Region of interest tool enabled a lasso to be drawn around the bands for the proteins of interest and β-actin retrieving densitometry values. This was used to calculate a percentage value relative to the control band to help visualise graphically the changes in protein levels. T-test analyses were conducted to determine significance between levels of protein expression.

2.5 TOPFlash

TOPFlash is a plasmid containing TCF binding sites upstream of a modified Luciferase reporter gene driven by a thymidine kinase minimal promoter[17]. This system was designed to give an expressional output of Wnt signalling activity when β-catenin has been activated. Renilla luciferase is a background reporter gene. The plasmids were obtained from Addgene as bacterial stabs (Addgene, Plasmid #12456). Colonies were grown and the plasmids were extracted using a QIAGEN® DNA miniprep kit (Cat no. 12123). HEK293T cells were plated at a density of $1x10^5$ cells in a 24-well plate. Four hours post seeding, cells were transfected with 300 ng of plasmid DNA at a 20:1 ratio of firefly luciferase to renilla luciferase using polyethylenimine(71) at 3:1 ratio with DNA. Following 24 hours of seeding, the cells were stimulated with 50 ng/ml of Wnt3a ligand (BioTechne, R&D systems, Cat no. 5036-WN) for a period of 24 hours and treated for a further 24 hours with specified compound of interest.

The Promega Dual Luciferase Reporter assay kit (Promega, Cat no. E1910) was used to measure the TOPflash activity. The cells were washed with cold PBS and lysed with 100μl of Passive Lysis buffer (Cat no. E1910) for 15 minutes at room temperature avoiding the need for scraping the cells for lysis. The Promega Dual luciferase® assay was performed using its protocol (Cat no. E1910) 5 μl of cell lysate was then transferred in triplicates to a 96-well plate and inserted into the Promega Glomax® multi detection plate reader which has a dual injector system automated to release 25μl of luciferase assay reagent (Cat no. E1910) and 25 μl STOP and GLO reagent (Cat no. E1910) respectively. The background signal was subtracted from the raw firefly luciferase data and then normalised using the renilla luciferase luminescence signal. The statistical significance was measured using the ANOVA test on PrismPad 9.0.

2.6 Quantitative PCR

2.6.1 Primer design

Table 2.4 qPCR primer sequences

Gene	Forward Primer	Reverse Primer
36B4	GCAATGTTGCCAGTGTCTGT	GCCTTGACCTTTTCAGCAAG
AXIN2	ACTGCCCACACGATAAGGAG	CTGGCTATGTCTTTGGACCA
MYC	GCTGCTTAGACGCTGGATTT	CACCGAGTCGTAGTCGAGGT
CCND1	CCATCCAGTGGAGGTTTGTC	AGCGTATCGTAGGAGTGGGA
JUP	TCTTCAAGTCGGGTGGCATC	CCTGGTACAGGAGCAGGTTG
CTNNB1	GTCGAGGACGGTCGGACT	GAGTAGCCATTGTCCACGCT
BMP4	ATCAAACTAGCATGGCTCGC	TGGCTGTCAAGAATCATGGA

2.6.2 RNA extraction

For retrieving RNA material from cultured cells[139], the Monarch® RNA Total Miniprep kit (New England Biolabs Cat No. T2010S) was utilised. To minimise the occurrence of contamination and RNA degradation, thorough aseptic preparation was followed including frequent changes of gloves and the use of RnaseZap™ (ThermoFisher Cat No. AM9782) along with RNAse-free filter tips. Protocol was carried out at room temperature to prevent precipitation from forming in the samples after the addition of lysis buffer. Nanodrop 2000 spectrophotometer was utilised to conduct a quality check on RNA purity and calculate RNA concentration. Following use, the RNA was aliquoted and frozen on dry ice and then stored at -80°C.

2.6.3 cDNA synthesis and qPCR

Quantitative PCR was developed to study the changes in DNA and RNA expression[140]. In this study, alterations in Wnt target gene expression after treatment of small compounds was investigated. The UltraScript® cDNA synthesis kit (PCRBIOSYSTEMS, Cat no PB30.11-10) was used to synthesise first strand cDNA from purified RNA. Following the manufacturer's instructions a master mix containing cDNA synthesis mix, reverse transcriptase, and the recommended amount of purified RNA (400 ng) was prepared to a total volume of 20 µl. The samples were placed in a T100 thermal cycler (Bio-Rad, Cat no. 1861096) with the following recommended running programme:

A. Incubate at 35°C for 5 minutes
B. Incubate at 42°C for 30 minutes
C. Incubate at 85°C for 10 minutes

D. Infinite hold at 12°C

The resulting cDNA samples were kept on ice and the master mix for qPCR was prepared. The mix for each gene consisted of qPCRBIO SyGreen® blue mix (PCRBIOSYSTEMS, Cat no. PB20.15-01), along with 400 nM forward and reverse primer (**Table 2.4**) and 25 ng cDNA. The StepOne® Plus instrumentation for the qPCR reaction was programmed as described in **Table 2.5** below. The housekeeping gene, 36B4, was used to normalise the expression levels of the target genes and the comparative C_T methods was used to perform gene expression analysis.

Table 2.5 qPCR cycle conditions for StepOne plus instrumentation

Cycles	Temperature	Time	Notes
1	-95°C	-2min	Polymerase activation, 2 minutes for cDNA and 3 minutes for genomic
40	-95°C -60°C	-15 seconds -30 seconds	-Denaturation -Anneal/Extension, do not exceed 30 seconds, do not use temperatures below 60°C
Melt analysis	-Step 1: 95°C -Step 2: 60°C -Step 3: 95°C(+0.3°C from 60°C)	-15 seconds -1min -15 seconds	-Optimal melt profile analysis

2.7 Viability assay

To determine cell viability[141] following any form of treatment, the Neubauer® haemocytometer (Brand ™ Cat No. 717810)was utilised. The cells were trypsinised and collected, pelleted, and then given media replacement. The cells were then pipetted thoroughly and 20µl was aspirated to be mixed with 20µl of Trypan blue dye. This diazo dye is negatively charged and doesn't interact with cells unless there is membrane damage and hence exclusively labels dead cells leaving viable cells reflecting white light under the microscope. The viable cells were counted using the formula in below to approximate number of cells per millilitre.

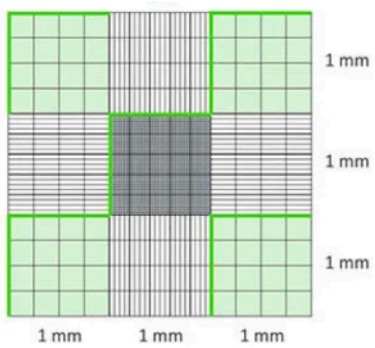

$$\text{cells/ml} = \frac{(\text{Sum of cells in green grids} * 10^4)}{2}$$

Figure 2.1 Illustration of cell counting grid and calculation

2.8 Wound healing assay (scratch assay)

This method was developed by Liang and colleagues[142] and is a straightforward technique to measure cell migration, cell-cell interaction, cell proliferation and changes in the cell cycle. A scratch was created in the cell monolayer using a p200 pipette tip. Cell images were taken at the time the scratch was made and then at regular intervals (12hr/24hr/48hr) to observe cell migration and wound closure using the light microscope. Images were then analysed to quantify relative cell migration in the presence of a compound or cell condition using Image J software. The drawing tool was utilised to mark the edges of where the cell surface had been scratched, obtaining the starting reference distance between the two edges using the ruler tool on Image J. This gap was measured until the gap closed or for the intended time points.

2.9 Clonogenic assays

2.9.1 2D crystal violet assay

This assay tested the ability of each cell to undergo continuous cell division under the influence of chemotherapeutic agents. The method used here was adapted from Puck *et al*[143] and Franken *et* al[144]. HCT116 and SW480 cells were cultured as mentioned in section 2.2 and seeded at sufficient low density to measure growth from single cells. Plates were incubated for a minimum of 7 days to allow for colony formation. Colonies were defined to consist of at least 50 cells. After 7 days the media was aspirated, and the cells were washed with PBS and fixed with 4% formaldehyde (FA) for 15 minutes. The wells were washed with dH_2O and stained with 0.1% crystal violet for 20 minutes. The cells were washed 3 times and air-dried for 24 hours. Images were taken using the Odyssey imager and analysed in Image J software to quantify the colonies using a minimum threshold ROI to count colonies and discard artefacts (see **Figure 2.2** below). This method eliminated the risk of human counting error. It also increased reproducibility between conditions due to the transferrable outline of the plate wells.

2.9.2 Soft agar colony formation assay

Anchorage-independent cell growth is a hallmark of tumourigenic cells. This method enabled the study of tumourigenic cell growth under varying cell conditions, including small molecule application. This method was adapted from Macpherson[145] and Shin and colleagues[146]. NuSieve™ agarose was made up as a 2x stock in serum free DMEM media. Following optimisation for U2OS and HCT116 cell lines, 0.35%-0.5% agarose was selected. 12 well plates were used, consisting of two layers. The bottom layer was 0.5% agarose, and the top layer was 0.35%, the cells grew on the top layer.

The bottom layer was prepared using a 1:1 ratio of the 2x agarose (serum free) and 20% FBS containing DMEM to achieve a 1x agarose with 10% final FBS. The agarose was warmed to 42°C in a water bath to keep it in liquid form. Once mixed, 1ml agar was carefully pipetted into the 12 wells and allowed to set. The top layer was prepared in the following manner: the required number of cells for triplicates were collected in a volume less than 100ul and transferred to a total volume of 0.8ml of DMEM with 20% FBS. 0.8ml of the 2x top layer agarose was added to the cell mixture for a total volume of 1.6ml. From this mix, 0.5ml was pipetted carefully on top of the bottom agarose layer in triplicates. Once the plate was ready, the plate was placed in the fridge for 15 minutes and subsequently transferred to a 37°C/5% CO_2 incubator. Plate was checked after 7 days for media change (if required). Images were collected after 14 days using the wide lens Leica M205 stereo microscope and analysed for colony formation using ImageJ. This approach proved to be less subjective than counting colonies manually, reducing human error. Region of interest parameters were fixed across plates enabling more fair comparison between cell condition and treatments as shown below in **Figure 2.2**

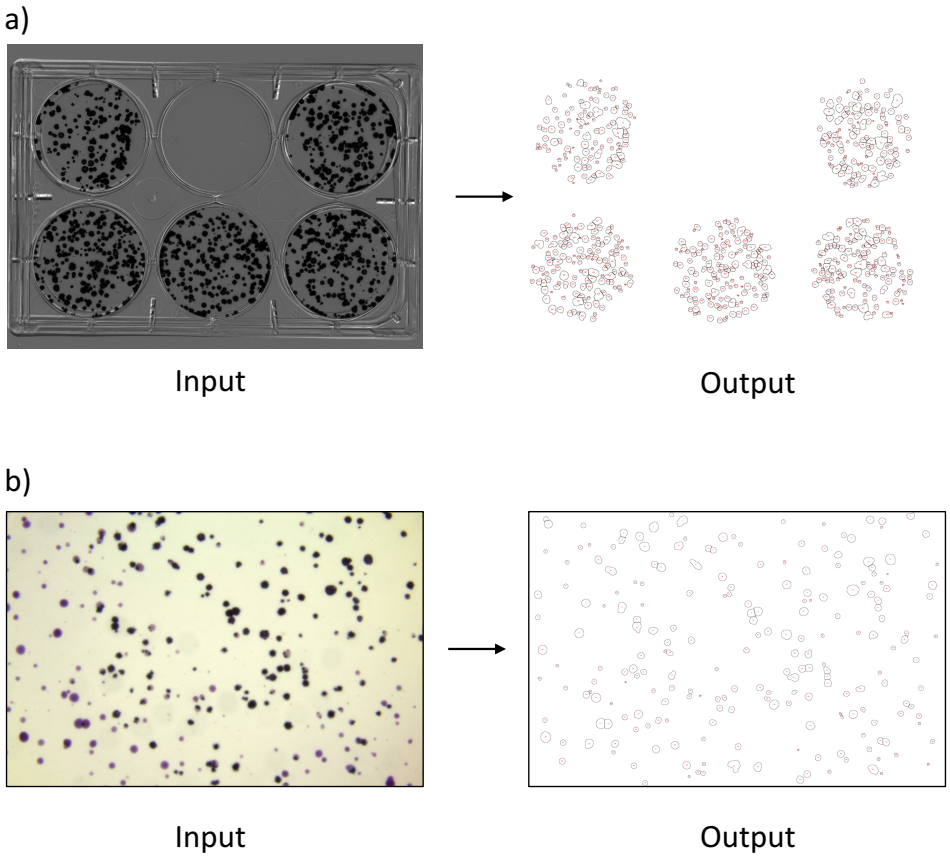

Figure 2.2 ***Colony quantification process with Image J.***
Process showing image capture of cell colonies in crystal violet assay and use of Image J software to detect and quantify colonies against a baseline threshold. B) Process showing representative image of single soft agar well with colonies stained with crystal violet and quantified using image J software.

2.10 Immunocytochemistry

This technique developed over 80 years ago by Coons *et al*[147] has been an important component in visually validating the effect of CRISPR KO and the activation of MiniTurbo system *in vitro.* Cover slips were sterilised in 70% ethanol and placed in wells of 6 well plate to completely dry. Once dry, cells being investigated were counted and seeded at the appropriate density for the treatment. Cells were carefully washed with PBS (room temperature) twice and fixed with 4% formaldehyde-phosphate buffered saline (FA-PBS) for 10 minutes.

Then cells were washed 3 times, and the cell membrane was permeabilised with 0.2% Triton-PBS for 5 minutes. Following permeabilization, cells were washed again 3 times and then blocked with filtered 3% BSA-PBST solution for 30 mins. Next, a master mix of primary antibodies to be tested was prepared in 3% BSA-PBST according to the recommended antibody dilution shown in **Table 2.1**, and carefully pipetted (60 μl) onto parafilm with the coverslip placed cell side down to incubate for 1.5 hours. Following incubation, cover slips were washed 3 times with PBST and in a similar manner secondary antibodies (including DAPI) were applied according to recommended dilutions for 40 minutes. Coverslips were washed 3 times again with PBST and prepared for mounting onto microscope slides. The cover slips were dipped in MilliQ™ water and carefully dried and placed onto microscope slides containing a drop of Mowiol® mounting solution to fix the cover slip to the slide. The microscope slides were subject to Leica fluorescent microscope at the following exposure times: DAPI-280.9ms, gfp-2.764s, dsRED-1.528s, cy5-3.573s. Images were processed using Leica X software and Image J.

2.11 Nuclear fractionation (nuclear enrichment)

It is well understood that β-catenin interacts with protein complexes in the nucleus to exert various downstream signaling observed in cancer. The purpose of employing this technique was to enrich the nuclear protein pool in the WT and β-catenin KO U2OS cell samples prior to subjecting it to mass spectrometry to magnify the nuclear proteins and increase signal to noise ratio by discarding the cytoplasmic and membrane proteins. This protocol was adapted from Blobbel and Potter[148]. Firstly, cells were trypsinised and resuspended in media. Then cell suspension was centrifuged at 4°C at 300 x *g* for 4 minutes. Following the centrifugation, the media was taken off with an aspirator needle and turned upside down, properly dried with tissue. Next, by mechanical agitation the pellet was disrupted and washed with ice cold PBS and subjected to centrifugation at 300 x *g* for 4 minutes. The PBS was removed, and the pellet was disrupted again and 1ml of ice-cold hypotonic buffer (20 mM Tris-HCl (pH 7.4), 10 mM KCl, 2 mM $MgCl_2$, 1 mM EGTA, 0.5 mM DTT, 0.5 mM PMSF) was added drop by drop to the pellet by vortexing the tube and homogenised by pipetting to avoid effervescence.

After 5 minutes of incubation, the homogenised pellet was put through a 22.2-gauge needle 10 times to disrupt and break open the cell membrane.

The disrupted cell lysate was then very carefully pipetted drop by drop against the wall of the tube containing 0.32 mM sucrose (cushion) to form a top layer in the tube and centrifuged at 700 x *g* for 5 minutes. Following this, the top 1ml was carefully removed which was comprised of the membrane and cytosol fraction. Any remaining membrane fraction around the edge of the tube was aspirated first followed by rest of buffer till only nuclear pellet remained. The nuclear pellet was washed twice with fractionation wash buffer (PBS, 0.1% SDS) and centrifuged at 700 x *g* for 5 minutes for the first wash and for 3 minutes at 500 x *g* for the second wash. The supernatant was removed, and the nuclear fraction pellet was snap frozen.

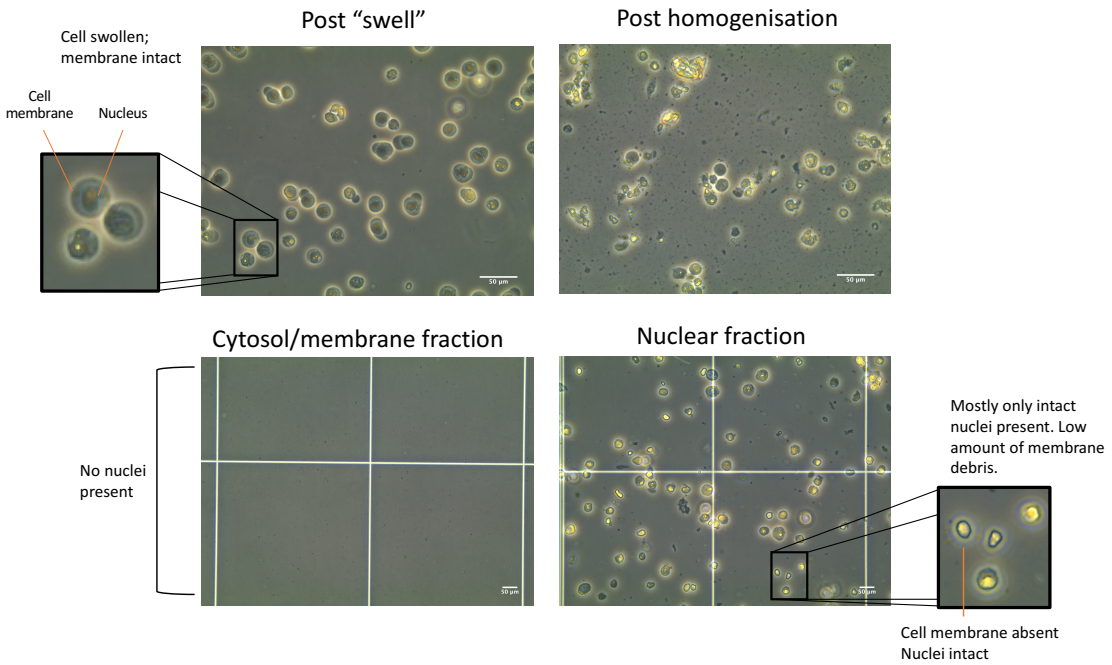

Figure 2.3 Stages of Cell Fractionation process.
Microscope images showing different stages of cell fractionation. "Swell" phase is after hypotonic buffer has been added. The post-homogenisation was carried out with a 22.2-gauge needle. The image of the cytosol/membrane fraction was taken post centrifugation of the homogenised lysate and separation of the nuclear pellet. Scale bar=50 μm. n=3.

2.12 General molecular cloning for generation of MiniTurbo expressing stable cell line

2.12.1 Primer Design

Table 2.6 Primer sequences and characteristics used for MiniTurbo Cloning

Primer	Sequence	Direction	Length	GC %	Tm (°C)
Forward_CTNNB1_slice_ Miniturbo	CGATGTTCCAGATTACG CCGAATTCATGGCTACT CAAGCTGATTTGATGG	Forward	50-mer	46	70
For_Primer_1_CTNNB1	AACTTGCCACACGTGCA ATC	Forward	20-mer	50	59
For_Primer_2_CTNNB1	GCAGAGTGCTGAAGGT GCTA	Forward	20-mer	55	58
For_Primer_3_CTNNB1	TGGACTACCAGTTGTGG TTAAG	Forward	22-mer	45	56
For_Primer_4_CTNNB1	TGAGGACAAGCCACAA GATTAC	Forward	22-mer	45	57
Reverse_CTNNB1_slice_ Miniturbo	GCAGCGGGATGCTAGC CGCGGCCGCCAGGTCA GTATCAAACCAGGCCAG C	Reverse	50-mer	64	80
For_LNCX_Primer	AGCTCGTTTAGTGAACC GTCAGATC	Forward	25-mer	46	60

2.12.2 Polymerase Chain Reaction (PCR)

Forward and reverse MiniTurbo primers were designed with Integrated DNA Technologies (**Table 2.6**). Reconstituted in nuclease free water. To conduct the PCR, we used the qPCRBIO Kit (PCRBIOSYSTEMS, Cat no. PB20.15-01) including PCRBIO HiFi polymerase (PCRBIOSYSTEMS, Cat no. PB10.41-02) in the constituents listed in **Table 2.7** below. Magnesium was added as a cofactor to enhance the enzymatic activity of DNA polymerase[140].

Table 2.7 PCR conditions with qPCRBIO kit

Reagent	50µl reaction	Final Concentration
5x PCRBIO Reaction buffer	10µl	1x
Forward primer (100µM)	0.2µl	400nM
Reverse Primer (100µM)	0.2µl	400nM
Template DNA (1:100)	1	N/A
PCRBIO HiFi Polymerase (2µg/µl)	0.5µl	N/A
PCR grade dH_20	38.6ul	N/A

The PCR conditions were as follows:

1. Denaturation at 92-95°C
2. Anneal at 55-60°C (57°C melting temperature)
3. Extend at 72°C

2.12.3 Agarose gel electrophoresis and DNA purification

For verification of correct DNA sizes and pure band DNA extraction of CTNNB1 DNA we conducted gel electrophoresis[149]. Given the approximate 2700kB size of CTNNB1 gene, 0.8% agarose gel was made in TAE buffer. Cybersafe blue dye was used instead of gel red for the samples to decrease probability of introducing nicks into the DNA. The gel was run for 1 hour at 50V till 75-80% was run through the gel to try to achieve good band separation and resolution for gel purification. Once the gel had run it was carefully removed from the tank and transferred to an open UV box on a glass plate. Using a sterile razor blade the desired CTNNB1 DNA band (**Figure 4.3**a) was cut out trying to minimize any excess gel being extracted and placed into a 15 ml falcon tube and weighed. Then 3x volume of Guanidine thiocyanate was added and incubated at 37°C for 5-10 minutes till gel dissolved. Then 1x volume of isopropanol was added to help binding. Solution was then mixed and pipetted to column under vacuum. The column was washed twice with PCR buffer and spun down to remove excess ethanol from buffer. The flow-through was placed into new columns and eluted with 50µl elution buffer. See **Figure 4.3**a for DNA bands from gel electrophoresis.

2.12.4 Restriction enzyme digest and Ligation

Xho1 restriction enzyme was used to cut the vector backbone to allow SLiCE cloning to be performed. The Seamless Ligation Cloning Extract (SLiCE) cloning method[150] was utilised to construct recombinant DNA. The components included the PCR template DNA (100 ng, 1:1 insert to vector, vector plasmid (100 ng, 1 µl SLiCE buffer and 1 µl SLiCE extract, to a total of 10 µl reaction mixture. The mix was incubated at 37°C for 15 minutes-1 hour. See **Figure 4.2**.

2.12.5 Bacterial transformation and DNA plasmid extraction

Following successful ligation, competent Stable 3 cells were transformed[151] with the recombinant DNA in the following conditions: 15 minutes on ice, 1 minute at 42°C, followed by 2 minutes on ice. LB broth was then added to transformed bacteria and kept in shaking incubator at 37°C for 30 minutes. Agar plates that were supplemented with ampicillin (100 µg/ml) and control agar plates were streaked with the transformed bacteria and incubated overnight at 37°C. Single colonies were then picked and transferred to 10ml of LB broth supplemented with selection antibiotic (ampicillin-100 µg/ml) for overnight growth.

In order to extract the DNA plasmid from bacterial cells, a miniprep was performed using the QIAprep Spin Miniprep kit (QIAGEN, Cat no.27104) following the manufacturer's instructions. The DNA plasmid concentration and purity was measured on a spectrophotometer using the NanoDropTM 2000 software (ThermoFisher, Cat no. ND-2000) for Nucleic acids.

2.13 Implementation of Mini Turbo affinity purification-mass spectrometry

In this section, the experimental procedure of coupling Streptavidin pulldown with Mass spectrometry is described. **Figure 2.4** below schematically illustrates the pipeline from cell culture to proteomic analysis.

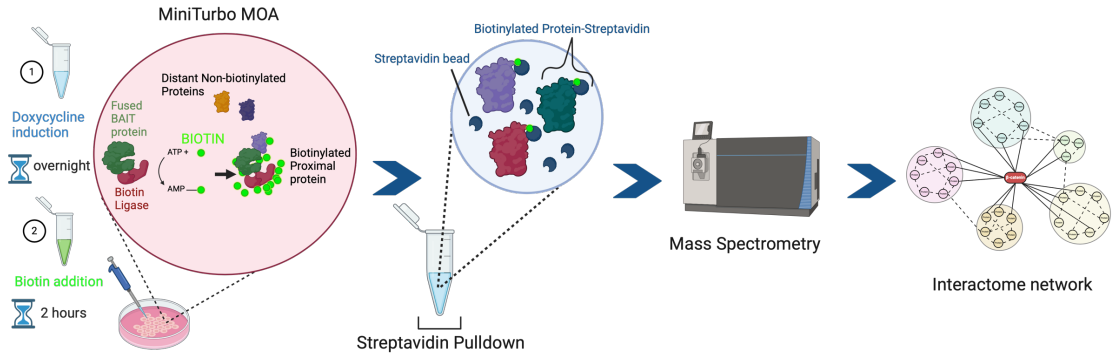

Figure 2.4 Schematic of MiniTurbo AP-MS pipeline
The experimental pipeline from MiniTurbo ID cell Biotinylation to generation of interactome network by subjecting streptavidin pulldown to mass spectrometry. Created using Biorender.com.

2.13.1 Cell culture preparation for AP-MS

For a representative MiniTurbo AP-MS experiment[152] both the U2OS MiniTurbo Empty vector (control) and U2OS MiniTurbo CTNNB1 (test) cells were cultured, treated, and processed under the same conditions with 3 biological replicates.

Day 0: 2.5×10^6 cells were plated in 10cm dishes and left overnight.
Day 1: Cells were treated with 0.5µg/ml doxycycline overnight.
Day 2: Biotinylation was induced by adding exogenous biotin at a final concentration of 50µM for 2 hours.

After 2 hours, cells were washed twice with 1ml ice cold PBS and then placed on ice. Each 10 cm dish of cells (each repeat) were lysed with 1ml RIPA buffer (20 mM NaH_2PO_4, 0.15 M NaCl, 1% deoxycholate, 1% NP-40, 0.1% SDS, 2mM EDTA, pH 7.5) containing Protease and Phosphatase inhibitors and left on ice for 10 minutes. After 10 minutes, the cells were scraped using a cell scraper and collect lysate into 1.5ml Eppendorf and water sonicated for 3 minutes (5 seconds on, 5 seconds off setting). The water needed to be ice cold before starting and re calibrated after each run. Following sonication, the lysates were centrifuged at 4°C at 12000rpm for 5 minutes and the supernatant was removed to a new Eppendorf ready for affinity purification.

2.13.2 Affinity purification of Biotinylation proteins coupled to mass spectrometry

One of the major advantages of this technique[152] as mentioned in the introduction is the high affinity with which streptavidin binds Biotin (K_d=10^{-14-15} M).[153] This extremely high affinity enables stringent washes to be carried out to remove impurities and artefacts following cell lysis which is not possible with standard co-immunoprecipitation methods as the proteins bound to the antibody may fall off. Furthermore, as biotinylation takes place while cells are viable and intact it may represent a more accurate picture of the cell environment compared to standard CO-IP procedure where only post cell-lysis the lysates are subjected to conjugated antibody for protein binding. The procedure carried out to achieve affinity purification is described below.
To increase the purity of the cell lysates prior to subjecting it to streptavidin beads, the samples were desalted. This process removed low molecular weight impurities, such as salts and other contaminants using the G25 sephadex column for chromatography and eluted in 0.5ml fractions. Following Bradford protein assay verification, the two protein containing fractions from each sample were collected and pooled.

The streptavidin agarose beads (ThermoFisher, Cat no. 20353) were formulated in a 50% slurry. So, for 25ul packed beads, 50ul must be aspirated. This was measured out as a batch to incorporate enough for all samples (6=350µl slurry). The beads were washed with RIPA buffer and centrifuged (2000 *x g*, 30 seconds), removing the supernatant leaving about 50µl on top of the beads and then re-centrifuged, removing the last dregs with a Hamilton syringe. The beads are then resuspended in RIPA buffer sufficient to add 100ul into each sample tube. Once the streptavidin beads were added to the desalted samples the tubes were rotated for 1.5 hours at 4°C. Following this, the samples underwent a series of wash steps by centrifugation (10000rpm, 30 seconds)

1. 0.8ml RIPA was added and centrifuged (5600 *x g*, 30 seconds) and then most of the buffer was removed. This was repeated with 2x 1ml RIPA washes.
2. 2 x washes with 1ml of RIPA: 8M urea (3 parts RIPA: 1-part 8M urea, 0.2% SDS, 0.2% Tx100, 20mM Tris pH 7.6)
3. 2x wash with RIPA.
4. 2x wash with 100µl 10mM Tris pH 7.4 (not mixed).

During the last wash, the supernatant was collected to check on SDS PAGE. After the last centrifugation, the last dregs were removed with a Hamilton syringe. The sample pellets were then freeze dried and given for on-bead trypsin digestion subjected to mass spectrometry for proteomic analysis (Proteomics-Prof Skipp lab, University of Southampton). Streptavidin antibody reveals the biotinylation status. A reduction of biotinylated proteins can be observed after desalting.

2.14 Generation of knockout cell lines using CRISPR/Cas9 gene editing

2.14.1 Guide RNA selection for CTNNB1

CRISPR/Cas9 works by cutting the DNA in a specific location guided by the single guide RNA (sgRNA)[154]. For the generation of the CRISPR plasmid, exon 3 of CTNNB1 was utilised to generate the sgRNA as this exon was present in all the splice variants. **Figure 2.5**a below shows the sequence map highlighting the 3 targets for sgRNA selected. These were intentionally spaced out to increase the knockout efficiency by avoiding overlaps and were near the start of the sequence to increase the probability of a frameshift, inducing a knockout with CRISPR-Cas9. The guide sequence is directly upstream of an NGG PAM sequence which is recognised by the spCas9 that was utilised, highlighted in red in **Figure 2.5**. The specific forward and reverse sequences of the DNA template are shown in **Figure 2.5**b. Important to note, the forward guide sequences had CACC added to the 5' end and the reverse guide had AAAC added at the 5' end. This was to ensure compatibility with the BSMB1 digested pLenti_CRISPR_V1 plasmids. Furthermore, to allow compatibility with the U6 promoter any forward sequences that didn't start with a G (see sgRNA2 and sgRNA3) had an additional G added after the CACC and this was mirrored with an additional C on the reverse strand for the purpose of annealing. This work was carried out in collaboration with Professor Nullin Divecha (University of Southampton), Amy Lewington (University of Southampton), and Chloe King (University of Southampton).

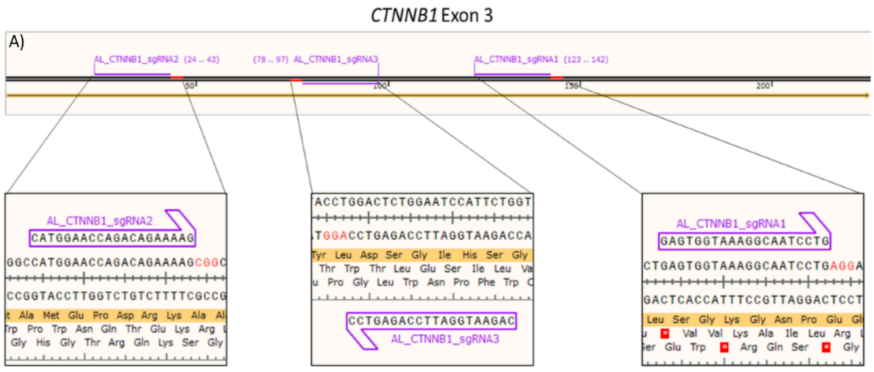

B)

sgRNA	Forward Sequence	Reverse Sequence
AL_CTNNB1_sgRNA1	CACCGAGTGGTAAAGGCAATCCTG	AAACCAGGATTGCCTTTACCACTC
AL_CTNNB1_sgRNA2	CACCGCATGGAACCAGACAGAAAAG	AAACCTTTTCTGTCTGGTTCCATGC
AL_CTNNB1_sgRNA3	CACCGCAGAATGGATTCCAGAGTCC	AAACGGACTCTGGAATCCATTCTGC

Figure 2.5 An overview of the sgRNA designs.

A) The 20 base pair guides designed to target exon 3. NGG PAM sequence highlighted in red. B) For each guide, a forward and reverse oligonucleotide was ordered with the corresponding forward and reverse sequences are shown, adapted for compatibility with the BSMB1 cut plasmid and U6 promoter.

2.14.2 Lentiviral transfection and transduction

Lentiviruses[155] are often used instead of other retroviral transduction as they can infect and introduce their DNA into the genome of non-replicating cells whereas other methods require the cells to be going through the cell cycle[156].

Firstly, $1x10^6$ HEK293FT cells were plated in each well of a 6 well plate in DMEM media (10% FBS and 1% Pen/Strep) and incubated for 2 hours at 37°C/5% CO_2. These were highly transfectable cells that grew well and enabled the virus packaging at high titre. Lentiviral transfection of HEK293T cells was carried out by combining 1.14μg of plasmid, 0.57μg of gag pol and 0.28μg of the VSVG plasmid in a ratio of 4:2:1 respectively with 100μl of serum free DMEM (no antibiotics). This mix was left to incubate at room temperature for 10 minutes and then 6μl of PEI transfection reagent was added followed by a further 20 minutes incubation. After this period, 100μl of this solution was added drop wise to the cells in each well and then left to incubate overnight at 37°C/5% CO_2. The next day the serum free media was replaced with 2ml of DMEM (10% FBS, 1% Pen/Strep) per well. Once the virus was packaged using the host cell machinery, it is exocytosed into the media. Virus containing media was collected and stored after 24/48/72 hours post-transfection. Prior to transduction this media was filtered through a 0.45μm filter.

For transduction, host U2OS cells were plated at $2.5\text{-}3x10^5$ seeding density in a 6-well plate with DMEM media (10% FBS and 1% Pen/Strep). The solution for transduction was prepared with 0.5ml of filtered virus, diluted to 2ml with DMEM (10% FBS, 1% Pen/Strep) with 20μl of polybrene (1:100 dilution). The media was replaced with 2ml of virus containing media to each well except the negative control well which was only given serum supplemented DMEM media. The cells were incubated overnight at 37 °C/5% CO_2. The next day the viral media was replaced with DMEM (10% FBS and 1% Pen/Strep). The cells were left to recover for one more day before replacing with media containing the selection antibiotic puromycin (2 μg/ml). The cells were incubated and grown and the cells in the control well died in the presence of the antibiotic, which was a good measure of transduction efficiency as the surviving cells in the other wells were puromycin selected transduced cells containing the CRISPR KO construct in the genome. The cell lysates were then collected and validated for a KO by western blot and immunocytochemistry.

2.15 Proteomic sample preparation

2.15.1 Cell culture preparation

Cells were cultured as mentioned in 2.2 but at a larger density to achieve a cell density of $1x10^7$ cells per biological repeat. During harvest, cells were washed in PBS, scraped, and pelleted ready for Trypsin treatment.

2.15.2 Proteomic sample preparation-off the bead digestion

This proteomic sample preparation and execution was carried out in collaboration with Dr Andy Shapanis (University of Southampton) and Dr Luis Coy (University of Southampton) in Professor Paul Skipp's lab. The samples were resuspended in 100µl of 0.25% RapiGest™ in 50mM ammonium bicarbonate. The samples were then subjected to centrifugation for 10 minutes at 1000RPM at 70°C. Next, 5mM DTT was added, and samples were incubated at 57°C for 30 minutes at 1000RPM. After that, 15mM Iodoacetamide was added, and the samples were left to incubate at room temperature in dark environment for 30 minutes. Next, 2µg of Trypsin was added to digest the peptides, and the samples were incubated overnight at 37°C. The next day, samples were spun at full speed for 20 minutes and the supernatant was collected. The samples were then acidified with 0.05% trifluoroacetic acid and incubated for 30 minutes at 37°C. Following this, samples were centrifuged at full speed for 20 minutes again with the supernatant being retained. Next, 100µl Buffer A was added, and a C18 column peptide purification clean-up was conducted. This step using reverse phased columns was conducted to remove salts and buffers from the peptides for cleaner signal to noise ratio. Samples were then resuspended in 20µl Buffer A and from that 18µl was injected into the mass spectrometer on a 4-hour gradient.

2.16 Statistical analysis

Statistical analysis to determine significance where applicable was carried out using the appropriate test (t-test, ANOVA) in the GraphPad Prism 10.1 software with significance represented by $P<0.05$. For proteomic analyses, PEAKS software was utilised for peptide identification. Two methods were used to assess significance for MiniTurbo proximity-biotinylation AP-MS. One was based on stringent exclusion, where the protein was selected if it was present in 2 out of 3 repeats and not present in any of the control samples. The second method involved using the Significance Analysis of INTeractome (SAINT) algorithm developed by Choi *et al*[157] to model spectral count distributions for true and false interactions aiding to calculate the Saint Probability (SP) through application of Bayes rule. The input utilises the protein-spectrum match(PSM) scoring function assigning a numerical value to a peptide spectrum pair.[158] To visualise the protein networks, primarily STRING[159] database was used alongside the network imbedded in the SAINT analysis on the Contaminant Repository for Affinity Purification-mass spectrometry (CRAPome) website.[160]

Chapter 3 CRISPR-Cas9-mediated CTNNB1 knockout and proteomic profiling

3.1 Introduction

The emergence of CRISPR-Cas9 gene-editing technology has revolutionized the study of cell and molecular biology, providing an unparalleled tool for targeted genetic modification. This ancient bacterial defense mechanism, repurposed for precise gene editing, has opened entirely new fields of inquiry while simultaneously expanding existing ones. With its ability to induce highly specific gene knockouts (KO) or knock-ins, CRISPR has quickly become an indispensable tool for researchers. As described in the methodology, guide RNA (gRNA) directs the Cas9 endonuclease to cut a few nucleotides upstream of the protospacer adjacent motif (PAM) sequence, which serves as a recognition signal for Cas9 to locate the correct DNA site[161]. The introduction of a double-strand break (DSB) in the DNA triggers the cell's error-prone repair machinery, leading to non-homologous end joining (NHEJ). This process often results in insertions or deletions (indels) that cause frameshift mutations, rendering the resulting protein truncated and non-functional. This disruption of gene function enables researchers to study the effects of gene loss in a controlled system.

The use of lentiviral vectors for plasmid delivery offers a permanent solution for gene knockout by integrating the CRISPR/Cas9 sequence into the host genome. This method ensures long-term gene editing and is particularly useful in generating stable knockout models. The technology has accelerated the progress of gene therapy while remaining an invaluable tool for scientists aiming to understand basic biological processes by depleting a specific protein in in vitro or in vivo systems.

β-Catenin, encoded by the CTNNB1 gene, has been extensively studied due to its dual function as a structural component of cell junctions and a key transcriptional co-activator in Wnt signaling. Its primary role in cell proliferation and differentiation makes it a critical player in cancer progression. U2OS cells, a Wnt-dependent osteosarcoma cell line, represent an ideal model for studying the influence of β-catenin in cancer biology. Previous studies have examined β-catenin expression patterns in 78 malignant bone tumor patients and 75 benign bone tumor patients, revealing elevated β-catenin mRNA and protein levels that correlate positively with tumor malignancy [26]. These findings highlight the oncogenic potential of β-catenin in bone tumors and provide a rationale for further research into its functional networks.

In our study, we employed CRISPR-Cas9 technology to knock out CTNNB1 in U2OS cells to identify the proteomic changes that emerge in the absence of β-catenin. This exploratory approach aims to map the downstream proteomic patterns and pathways affected by β-catenin loss. Given that siRNA-mediated CTNNB1 knockdown in colon cancer cells (SW480) has been shown to affect proliferation, apoptosis, and invasion [(147)], we hypothesize that similar alterations will be observed in U2OS cells.

The study conducted by Ewing *et al*. [(148)] exemplifies the value of a multi-omic approach in understanding β-catenin's role. By integrating transcriptomic and proteomic data, they were able to uncover novel β-catenin protein-protein interactions and functional networks, which provided valuable insights into how β-catenin mutations influence cellular behavior. Inspired by this work, our goal is to extend the understanding of β-catenin's impact by focusing on its proteomic signature in U2OS cells. By analyzing the changes in the proteome following CTNNB1 knockout, we aim to identify potential β-catenin-dependent protein interactions and novel downstream targets that could shed light on the molecular mechanisms underlying its role in cancer progression. This investigation into the absence of β-catenin represents a first step in establishing a broader proteomic framework that can be expanded with multi-omic approaches in future studies. Such integration will allow us to better understand the context-specific effects of β-catenin loss, providing deeper insights into its role across various cancer subtypes and microenvironments.

3.2 Results

3.2.1 Phenotype of CTNNB1 KO cells

The U2OS CTNNB1 knockout cells were tested against wildtype U2OS cells by Western blot and validated a CTNNB1 KO (**Figure 3.1**). Three repeat constructs are shown here. The area highlighted in red shows the difference between the U2OS WT control and the KO positive samples. In addition, immunofluorescence was carried out on the control and CTNNB1 KO samples.

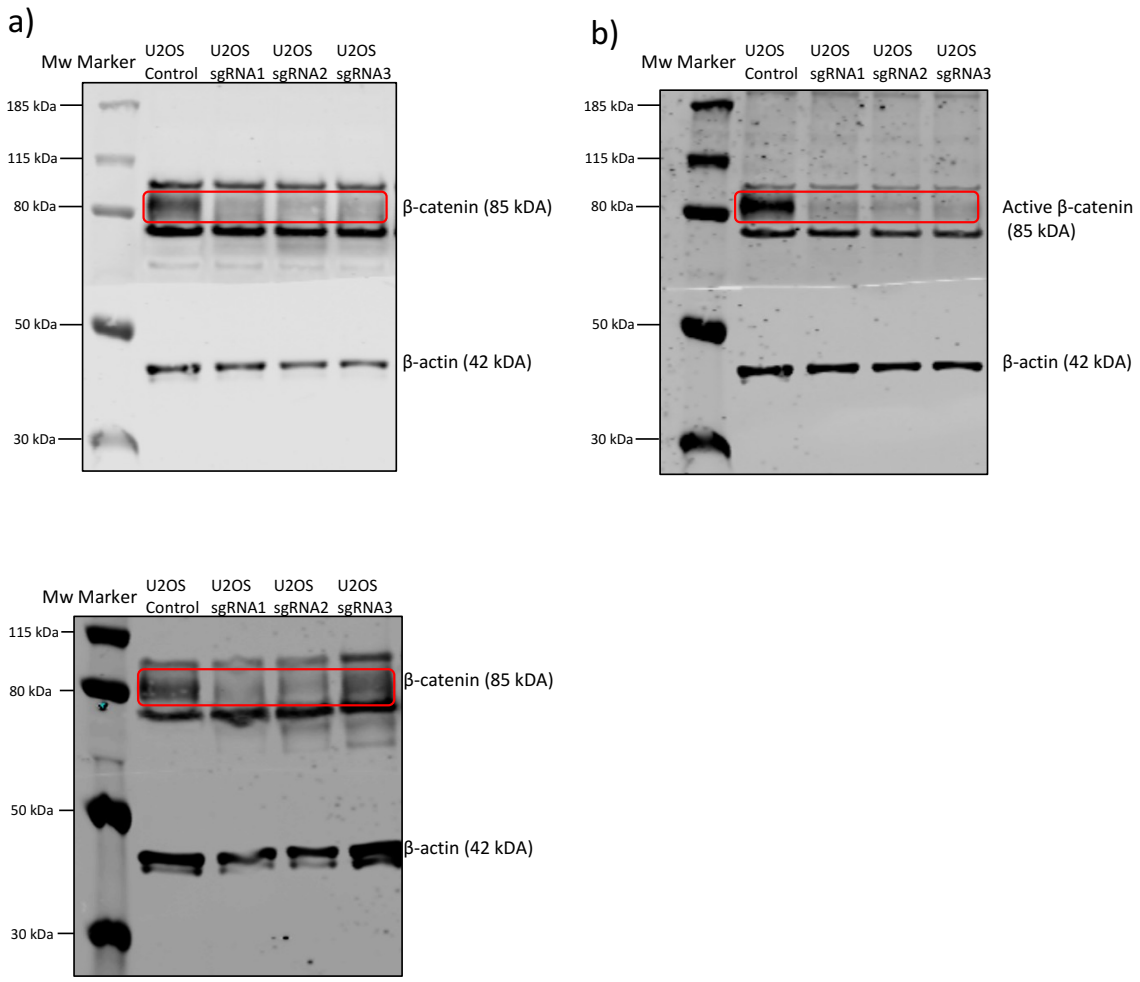

Figure 3.1 ***Western blot images of U2OS CRISPR CTNNB1 KO validation.***

a) Application of whole β-catenin antibody for all 3 guides and control vector. Two repeats shown here. b) Application of unphosphorylated (active) β-catenin antibody as a second source of validation. There are two non-specific bands above and below that are seen with the central β-catenin band, this is present and noted on the manufacturer's website β-actin used as loading control. n=1.

As seen in **Figure 3.2** below, the U2OS wildtype cells fluoresced brightly as expected when subject to.β-catenin antibody, especially distinct on the cell membrane lining as expected given one of its function at the cell-cell junction. Secondly, the presence of nuclear β-catenin was also observed using the active β-catenin (unphosphorylated) antibody consistent with its role as a transcriptional co-activator. Conversely, in the CTNNB1 KO cells the β-catenin signal was significantly reduced at both the membrane and in the nucleus. This increased our confidence alongside the western blots that the CRISPR/Cas9 induced KO of CTNNB1 was successful and can be utilised for further characterisation and proteomic investigation.

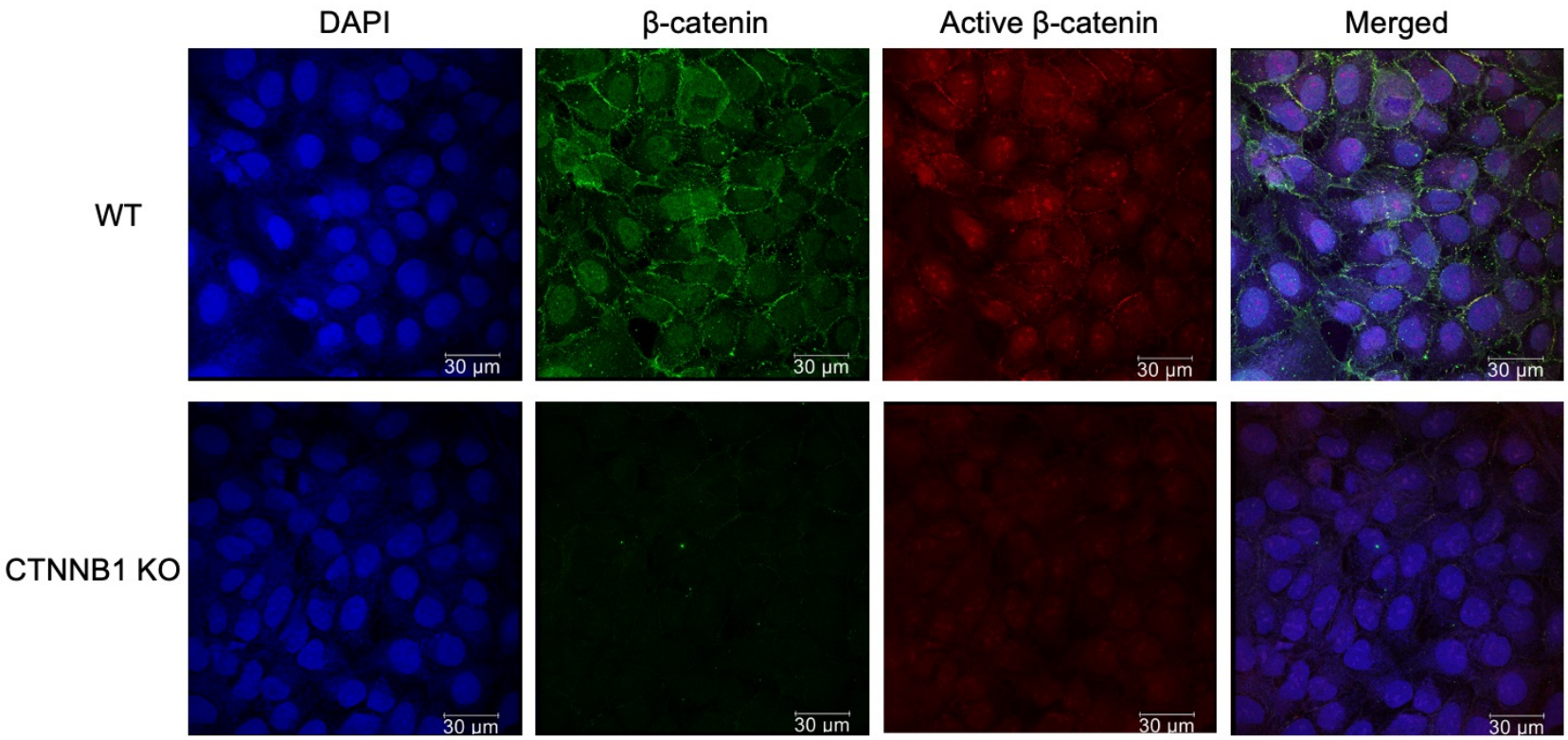

Figure 3.2 Immunofluorescence of U2OS WT and CTNNB1 CRISPR KO cells.

Immunofluorescence images highlighting the difference between WT and CTNNB1 KO cells. DAPI used to observe cell nuclei. β-catenin antibody (Alexa fluor 488) showing general levels at the cell-cell junctions and cytoplasm. Active (unphosphorylated) β-catenin (Alexa fluor 594) highlights nuclear β-catenin activity. Scale bar =30µm. n=1

We cultured CTNNB1 KO cells in the presence of 2μgμl puromycin to help maintain a selective KO sensitive population since these cells were not picked from single cell populations meaning they are a heterogenous population. With respect to rate of cell growth compared to wildtype cells we didn't observe any significant differences.

To ascertain the ability of U2OS CTNNB1 deficient cells to migrate and assess cell-cell interactions we carried out a wound healing (scratch) assay. The procedure was carried out as explained in methods section 2.8. The results show that at 24 hours the wound width in the U2OS WT cells had migrated and reduced the gap by 66% compared to only 39% by CTNNB1 KO cells. By 48 hours the wound in the WT cells had fully healed whereas CTNNB1 KO U2OS cells took more than 24 hours longer to migrate and close the wound as shown in figure 3.4. The paired T-test informs the values to be statistically significant (P=0.01 24hr, P=0.008 48hr) consistent with reported data from Cheon *et al*[162] and *et al*[163] suggesting the importance of β-catenin levels in driving cell migration and invasion. In an *in vitro* cancer context, the assay also provides some insight into metastases as the slower migration rate of CTNNB1 KO U2OS cells indicates that β-catenin plays an important role in cell migration and the cell's ability to metastasize. Additionally, tumourigenic growth was compared between WT and CTNNB1 KO cells in soft agar. After 10 days of culture the colonies were counted, and in our hands, we didn't observe any statistically significant differences between the WT and CTNNB1 KO cells as shown in **Figure 3.3**. The colony counts were indistinguishable with averages of 120 to 160.

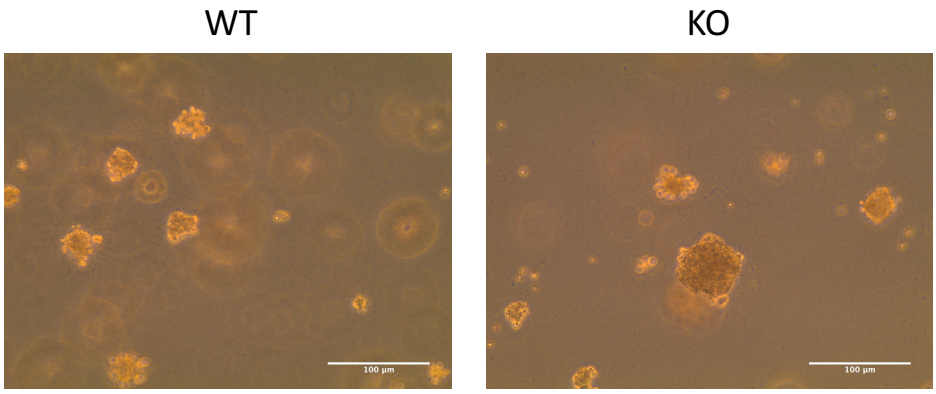

Figure 3.3 Representative image of U2OS cell colony formation in soft agar.
CTNNB1 wildtype and knockout variants after 10 days of colony growth. Visible colonies were counted in quadrants of the well. Of 12 well plate. Light microscope used with 100x magnification. Scale bar 100μm. n=3

This observation was unexpected and might be cancer cell line specific because Salomon *et al*[164] demonstrated when adrenocortical cancer cells had β-catenin expression silenced it caused growth inhibition and when transplanted in mice, it suppressed tumour growth. They also reported a reversal of epithelial-to-mesenchymal transition with an increase in apoptotic cells. Similarly, in a study for breast cancer, reduced tumour growth and an increase in apoptotic cells were observed in β-catenin deficient cells[165]. A caveat in our investigations is the lack of data on apoptosis in this knockout cell line. This needs to be addressed in future studies by administering the caspase detection assay.

Buechel and colleagues[165] address an important point on the difficulty of establishing a completely β-catenin deficient cell line certain cell lines due to the resulting mass cell apoptosis, lending to the insight that the presence of β-catenin is indispensable for the survival of the cells. It's possible here, that in the U2OS cell line, there are low levels of β-catenin still driving cell proliferation and colony growth and hence not decreasing colony growth. It may also be the case that U2OS cell line is not entirely dependent on β-catenin unlike the mammary tumour cell line. An experiment that would have provided further clarity as to the effect on canonical Wnt transcriptional output would have been to transfect the cell line with TOPflash promoter reporter constructs along with Wnt3a stimulation.

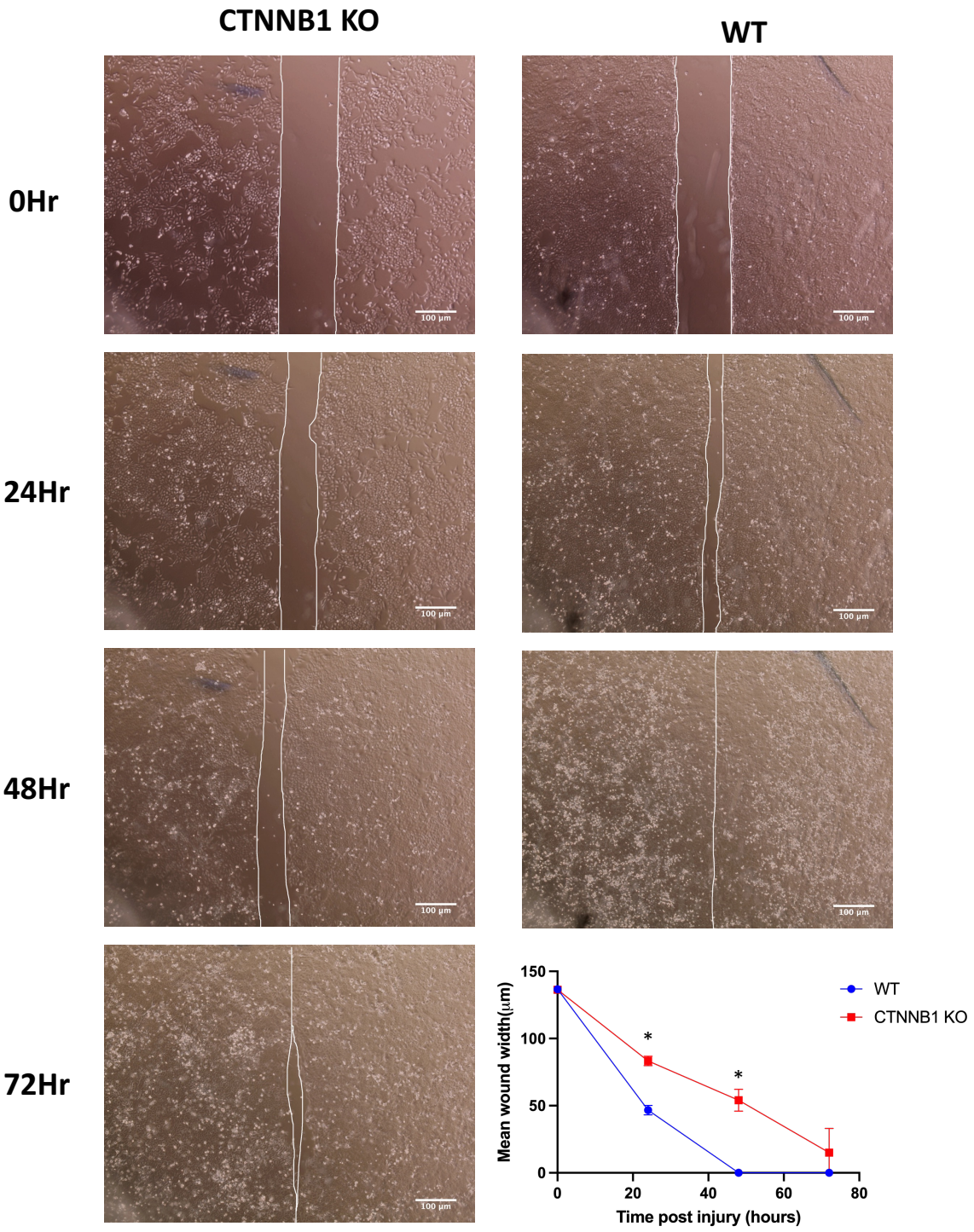

Figure 3.4 Wound healing assay on WT and CTNNB1 KO U2OS cells.
*Wound made and monitored over 72-hour period. Image taken using light microscope at 10x magnification. Wound closure measured using Image J and analysed using 1-way ANOVA in GraphPad software. Scale bar=100µm. *, P<0.05. n=3*

3.2.2 Functional enrichment analyses of the impact of CTNNB1 deficiency in U2OS cells

Our first aim was to improve our understanding of protein and pathway regulation when β-catenin levels are perturbed. In this instance as we validated the knockdown of β-catenin, we cultured the WT and CTNNB1 KO cells and attempted to enrich the nuclei to study the nuclear proteome with more emphasis. The procedure wasn't the cleanest, according to COMPARTMENT analysis that was carried out with the proteomic data it identified 18% of proteins that localised to the nucleus alone and 45% of proteins that localised to the nucleus and cytoplasm and 35% that localised to the cytoplasm (**Table 3.1**). Therefore, it is important to bear in mind we may be observing a weak nuclear enriched proteome profile. For future consideration, a western blot using specific cytoplasmic and nuclear markers would be more accurate in determining the nuclear enrichment of the sample. Following nuclear enrichment, the cells were pelleted and prepared for mass spectrometry analysis as described in the methods section. PEAKS software was used to analyse the mass spectrometry data.

Table 3.1 Results from COMPARTMENT analysis.
Assessing nuclei enrichment efficacy for U2OS cells for Mass Spectrometry analysis. "n" denotes number of proteins alongside the respective percentage out of total proteins.

Localisation	n	%
Cytoplasm	1295	35.92
Cytoplasm/Nucleus	1633	45.30
Nucleus	677	18.78
NA	375	NA

Firstly, principal component analysis was performed to identify the directions (principal components) that capture the most variation in the data and project it onto the principal components. Here the data illustrates that for PC1 accounts for 43.2% of the explained variance and PC2 accounts for 19.6% of the explained variance. This gives a total variance of 63.1% providing moderate confidence for the variance observed under these two conditions. In addition, the biological repeats between the two conditions are distinct and do not overlap as shown by blue (U2OS WT-Control) and orange (U2OS CTNNB1 KO-Treated) ellipses on the graph respectively in **Figure 3.5**a.

The proteomic analysis, **Figure 3.5**b illustrates the volcano plot highlighting in red and green the significantly elevated and reduced level of proteins in U2OS CTNNB1 KO dataset compared to control U2OS WT dataset respectively. The complete list of significant proteins is shown in **Supplementary Table 1.** It documents log fold and p-value of proteins (gene names displayed) that have been up- and down-regulated. **Figure 3.5**c provides a heatmap illustrating the proteomic landscape of differentially expressed proteins between the WT and CTNNB2 KO dataset.

Following LC-MS/MS proteomics with CTNNB1 WT and KD, **Figure 3.5**b highlights the top 10 most significant proteins that have been upregulated and down regulated. Interestingly, as β-catenin plays a structural role in cells, when it is down regulated the cells are responding by upregulating proteins for cell adhesion such as integrin alpha -2 (ITGA2) and junctional cadherin. In addition to this, there is an increase in proteins involved with mitochondrial function and maintenance. For example, L-cysteine transaminase which plays a key role in electron transport chain in mitochondria as well as Selenoprotein H which promotes mitochondrial biogenesis and function. Conversely, the proteins that are down regulated are involved in nuclear migration, cell component organisation, cell division and proliferation. Among the down regulated proteins are also prominent components of the Wnt and MTOR signalling pathway including GSK3B, CK1, TGFB1/2, RPTOR. the knockdown of β-catenin has seen a decrease in oncogenic proteins such as Tensin1 and APOBEC3B which is overexpressed in a wide range of cancers resulting in formation of unexpected clusters of mutations.

Furthermore, the Kyoto Encyclopedia of Genes and Genomes (KEGG) enrichment analysis in **Figure 3.5**d shows between 1.5-2-fold positive enrichments for proteins associated with “mitophagy”, “lysosome” and “splicesome” biological pathways. Conversely, highlighted in green bars are the almost 2-fold downregulation of the following biological processes with respect to the differentially expressed proteins: “Gastric cancer”, “Thyroid hormone signaling pathway” and “Hepatocellular carcinoma”. The references to these two cancer pathways being down-regulated corroborates what has been studied before about the prominent role of β-catenin in driving these cancers.

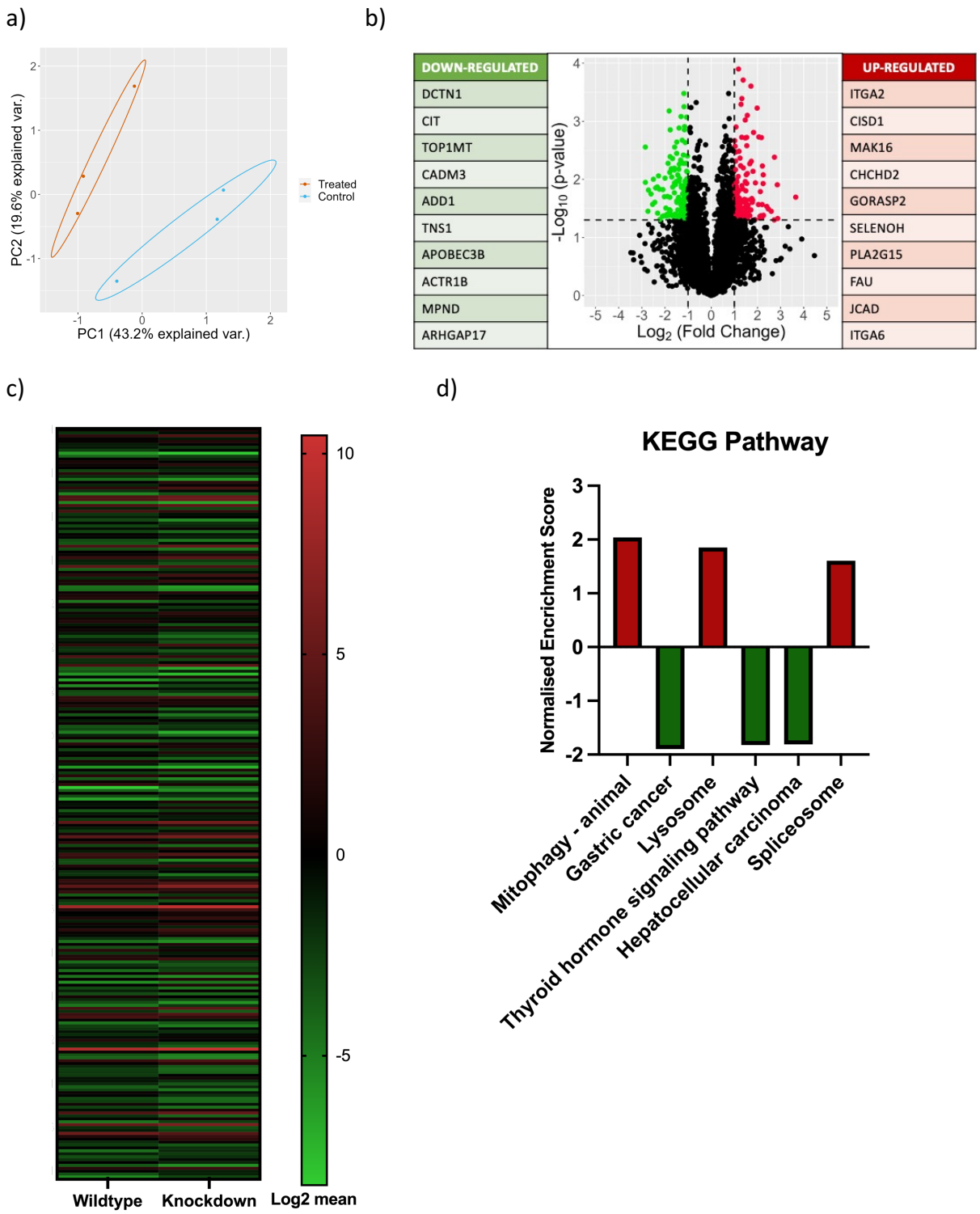

Figure 3.5 Proteomic analysis of CTNNB1 KO in U2OS cells.

a) PCA plot illustrating the variance for the U2OS WT and U2OS CTNNB1 KO datasets. b) Volcano plot highlighting up and down regulated proteins with gene symbols of 10 highest significant hits with respect to p-value (P<0.05). c) Heatmap showing the log2 mean values of significantly differentially expressed genes between Wildtype and knockdown of CTNNB1. d) Graph showing normalised enrichment score from KEGG analysis showing up or down regulated proteins in a pathway.

3.3 Discussion

This chapter focusses on the CRISPR/Cas9 driven manipulation of β-catenin levels In U2OS cells. We successfully managed to implement a KO of CTNNB1 in U2OS cells as a heterogenous pool controlled by puromycin resistance. One of the main findings and point of discussion is the method behind obtaining the CRISPR/Cas9 KO. Traditionally, when knocking out a gene in this manner, single cell clones are selected and cultured to obtain a homogeneous pool of cells. However, we proceeded with a heterogenous model, where KO cell selection was based on the puromycin antibiotic resistance. The advantage of this method is it does not force a cell population to grow that may not be what is natural for that cell and reduces the workload for selecting and growing colonies and the time involved in screening the colonies for successful KO. This allows for cell homeostasis by withdrawing compulsory competition and a sudden change in intracellular characteristics.

In contrast, there are also some limitations associated with this method which need to be considered. Firstly, as it is not a single cell clonal population of cells, there is a low percentage of cells that replicate that do not carry the CTNNB1 KO gene and this may dampen down the effect of the knockout. Secondly, an observation that with time, the KO property of the cell diminishes, with the gene expression being restored to WT levels. This results in shorter experimental window to investigate the effect due to the transient nature of the knockout, which is not a hinderance with single cell populations. In the future, the results obtained from single cell colonies and antibiotic resistance selection should be compared and scrutinized to enable further informed decisions as to which method captures a more accurate and representative picture of knockout conditions in the cell proteome.

Proteomic research conducted on the WT and CTNNB1 KO U2OS samples yielded interesting results. A deeper look into the proteins **Figure 3.5**b reveals the effects of knocking out Beta-catenin. Downregulation of these genes may lead to a combination of impaired cell division, reduced adhesion, mitochondrial dysfunction, and altered cytoskeletal organization, affecting U2OS cell viability and metastatic potential. Proteins such as Dynactin Subunit 1 (DCTN1) play a critical role in intracellular transport and mitotic spindle organisation[(166)]. The potential effect of this is reduced cell division, impaired intracellular transport, and decreased cancer cell viability. Another protein that was downregulated here was Mitochondrial Topoisomerase I (TOP1MT), which helps maintain mitochondrial DNA integrity. Its downregulation in the absence of Beta-catenin can lead to increased mitochondrial dysfunction, impaired energy metabolism, and enhanced sensitivity to apoptosis[(167)].

Closely tied with Mitochondrial Fission 1 protein (FIS1) and Ribosome-Releasing Factor 2 (GFM2) it maintains mitochondrial function and energy homeostasis. Recent research highlights that Wnt/β-catenin signaling supports mitochondrial biogenesis and metabolic reprogramming in cancer cells[168]. Importantly, disruption of mitochondrial genes reveals the crucial role of Wnt signaling in maintaining cancer cell metabolism in cancer cells[169]. Take home message could be that targeting metabolic vulnerabilities in Wnt-active tumours could become a promising strategy.

Chapter 4 Mapping the B-catenin interactome via proximity dependent biotinylation

4.1 Introduction

4.1.1 Current knowledge on previous attempts to characterize the β-catenin interactome.

As the previous section highlighted the multiple binding sites present on β-catenin it is no surprise that the β-catenin interactome has been the subject of considerable research due to β-catenin's dual role in cell-cell adhesion (at adherens junctions) and as a key transcriptional co-activator in Wnt signaling. Early studies focused on its structural role in epithelial integrity, while more recent work has explored its nuclear functions, identifying protein-protein interactions (PPIs) that regulate transcription and oncogenic signaling pathways. Below is an overview of previous efforts:

Initial attempts to characterize the β-catenin interactome were largely focused on co-immunoprecipitation (Co-IP)[170] experiments and mass spectrometry(MS)[171]. These studies identified core components of the β-catenin signaling machinery such as TCF/LEF transcription factors[23]) as primary β-catenin-binding partners for gene transcription regulation as mentioned above and E-cadherin and α-catenin[92], which anchor β-catenin at adherens junctions, were some of the earliest characterized interactors, emphasizing its structural role.

The use of high-resolution MS gave a more robust view of the β-catenin interactome. Several large-scale proteomics studies aimed at identifying β-catenin-associated complexes revealed new binding partners in both the cytoplasmic and nuclear compartments. Affinity purification-mass spectrometry (AP-MS) became a cornerstone method for interactome studies, identifying hundreds of potential interactors. Ewing *et al*[172] conducted large scale immunoprecipitation of flag-tagged versions of 338 bait proteins which when subjected to Liquid Chromatography-Electrospray ionization Mass Spectrometry (LC-ESI-MS/MS) yielded 24,540 potential protein interactions and within that discovered a subset of novel β-catenin PPIs involved in transcriptional regulation and Wnt target gene activation. Functional interactors, including chromatin remodelers, transcriptional regulators (e.g., CBP/p300, BCL9, Pygo)[58], and components of nuclear transport machinery, were also discovered with this approach.

Recent advances in proximity-dependent biotinylation (BioID[173, 174], APEX[175], and MiniTurbo[153]) have allowed for more sensitive detection of dynamic interactors in living cells. These techniques help capture transient interactions that are often missed in traditional pulldown assays.

4.1.2 Introduction to MiniTurbo and other Proximity labelling methods

Identifying protein-protein interactions is crucial to our understanding of cell biology and signaling and as discussed in the introduction it is key for finding new therapeutic targets. Recently, affinity purification methods have improved to be more advantageous than traditional methods for determining PPI methods such as co-immunoprecipitation[176] . Immunoprecipitation is effective for proteins that are of higher abundance but can fail to detect lower abundance or transient proteins due to the stringent washing procedures during purification.[177] An advantage of affinity purification such as Biotin Ligase methods is the high binding affinity of Streptavidin to Biotin ((K_d=10^{-14-15} M).[153] allowing for more stringent washes. Furthermore, immunoprecipitation is carried out after cell lysis with the conjugated antibody beads, due to the in vitro scaffold there is a risk of artefacts and debris and it may not accurately reflect the interaction environment taking place physiologically.[177]

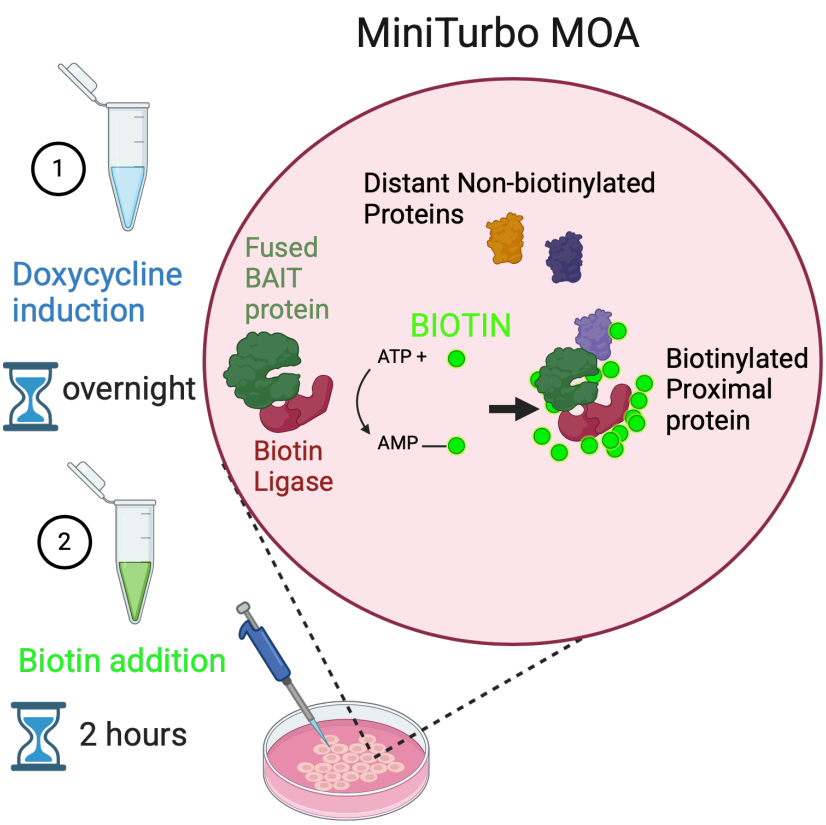

Figure 4.1 Cartoon diagram of MiniTurbo mechanism of action.
When cells are induced by doxycycline overnight, the MiniTurbo Biotin Ligase fused to BAIT protein is expressed. Upon addition of exogenous Biotin for an average of 2 hours, it enables the biotin ligase to activate the Biotin within its vicinity using ATP to Biotin-AMP which is able to bind to Lysine residues on proteins that are in close proximity to the BAIT protein (~10nm radius). Effectively tagging the proximal proteins not the distal proteins. Schematic created using Biorender.com.

MiniTurbo (**Figure 4.1**) represents an optimized variant of TurboID, engineered to achieve faster biotinylation kinetics with significantly reduced labeling time (~10 minutes compared to TurboID's ~30 minutes). This accelerated reaction reduces the likelihood of off-target biotinylation while retaining high sensitivity and specificity in proximity labeling studies. MiniTurbo offers superior temporal control and low cytotoxicity[178], making it particularly well-suited for live-cell proximity labeling in diverse subcellular environments, including the nucleus, cytoplasm, and organelles. When coupled with affinity purification and mass spectrometry (AP-MS), MiniTurbo allows for the precise identification of protein-protein interactions (PPIs) and dynamic interactors that may otherwise be challenging to capture with traditional biochemical approaches. Its broad applicability and rapid reaction kinetics make it a powerful tool for interactome mapping and cellular signaling studies.

Biotin Ligase Mini Turbo technology is based on an engineered mutant of Biotin Ligase[153] with a 13 amino acid deletion, when activated in the presence of doxycycline it induces the expression of the enzyme-coupled to a protein of interest, and when biotin is added the ligase converts it into the active form in the presence of ATP (**Error! Reference source not found.**) and has a proximity distance of ~10 nm and hence can be ideal as a measure of investigating dynamic and transient PPI. **Table 4.1** below expands on and compares the different proximity labelling methods.

Table 4.1. Detailed comparison of proximity labelling methods.
Information adapted from Samavarchi et al[178]

Feature	TurboID / MiniTurbo	BioID	APEX (Ascorbate Peroxidase)	HRP (Horseradish Peroxidase)
Enzyme Type	Biotin ligase (MiniTurbo: enhanced kinetics)	Biotin ligase	Peroxidase	Peroxidase
Reaction Mechanism	Catalyzes biotinylation of lysine residues within a 10 nm radius	Catalyzes biotinylation of lysine residues within a ~10 nm radius	Catalyzes oxidation of biotin-phenol in the presence of H_2O_2	Catalyzes oxidation of DAB or biotin-tyramide in the presence of H_2O_2
Biotinylation Speed	TurboID: Fast (seconds to minutes); MiniTurbo: Very fast (~10 min)	Slow (18–24 hrs)	Moderate (minutes)	Slow (minutes to hours)
Proximity Labeling Resolution	High (~10 nm)	High (~10 nm)	Moderate (~10–20 nm)	Low (>20 nm, diffuse labeling)
Requirement for External Cofactors	Requires ATP	Requires ATP	Requires H_2O_2	Requires H_2O_2
Cellular Compartmentalization	Effective in cytoplasm, nucleus, and organelles	Effective in cytoplasm, nucleus, and organelles	Effective in cytoplasm and mitochondria	Primarily used for membrane-bound and extracellular proteins
Live-Cell Labeling	Yes (non-toxic, minimal cytotoxicity)	Yes (low cytotoxicity but slower)	Limited (H_2O_2 can be toxic at high concentrations)	No (used in fixed cells)
Temporal Control	High (short-lived and rapid labeling)	Low (slow labeling time)	Moderate	Low
Labeling Specificity	High (TurboID: excellent; MiniTurbo: reduced off-target biotinylation)	Moderate (higher background noise compared to TurboID)	Moderate	Moderate to Low
Compatibility with Mass Spectrometry	High	High	High	Moderate to Low
Ease of Use	Easy (genetic fusion and short reaction time)	Moderate (requires long labeling time)	Moderate (requires careful control of H_2O_2 exposure)	Complex (requires optimized reaction conditions)
Molecular Weight	~28 kDa	~35 kDa	~27 kDa	~44 kDa
Key Advantage	Rapid biotinylation; excellent temporal control (MiniTurbo: fastest kinetics)	Proven track record for proximity labeling studies	High spatial resolution for subcellular compartments	Strong signal amplification for imaging
Key Disadvantage	TurboID: Over-biotinylation risk if uncontrolled; MiniTurbo: potential abundant protein labeling	Long reaction time (~18–24 hrs)	H_2O_2-induced toxicity in live cells	Limited to fixed cells; potential for non-specific labeling

4.2 Results

4.2.1 The design and implementation of CTNNB1-MiniTurbo vector

The backbone vector for MiniTurbo originally derived from Alice Ting's[153] lab was modified incorporating the following components. Firstly, the MiniTurbo element itself, 778 base pairs that translates to a 28kDa bioengineered *E.coli* Biotin ligase with an N-terminus truncation mutation enhancing the catalytic efficiency of the enzyme[153]. There are two selection markers present, it contains β-lactamase which confer resistance to ampicillin which is important when selecting bacterial colonies that have successfully been transformed following cloning.

Secondly, the vector codes for puromycin *N*-acetyltransferase which confers resistance to puromycin which is critical for selecting host cells that have been successfully transfected. In addition, there is a transactivator, (Tet-on system, rtTA advanced) which binds to the Tet responsive element and activates transcription in conjunction with tet operators and 3rd generation Tet-responsive (TRE3G) promoter only in the presence of tetracycline or doxycycline. This is advantageous at it means we can control the induction and activation of the MiniTurbo system. Furthermore, there is a human influenza haemagglutinin (HA) epitope tag that serves as a critical feature to help verify the expression of the MiniTurbo upon activation in host cells via Western Blotting or Immunofluorescence. **Figure 4.2** illustrates the empty vector construct and the CTNNB1 inserted version. The diagram also includes the forward and reverse primer positions for the insertion of CTNNB1 into the backbone vector highlighted in purple. **Figure 4.3**a shows a gel electrophoresis image of the PCR amplified product of *CTNNB1* plasmid along with the MiniTurbo vector backbone.

SLiCE cloning was carried out as described in Chapter 2.12.4 and following that we performed two methods of verification. Firstly, we conducted an enzyme digestion using *EcoR1* and *Mlu1* as it has restriction sites in the middle and edges of CTNNB1 and MiniTurbo (**Figure 4.3**b) and selected two independent plasmids that showed successful digestion (**Figure 4.3**c) for sequence verification. We designed 4 forward primers and included the LNCX primer mentioned earlier (**Table 2.6**) to cover the entire region from the HA tag to the MiniTurbo section to send for sequencing with Eurofins. This step was crucial to verify the molecular cloning was performed successfully with full alignment and no major errors. The results of the verification were positive as both selected plasmid constructs showed almost identical alignment with very minor mismatches or gap/insertions, and this has been shown in **Figure 4.4** below in red and blue arrows.

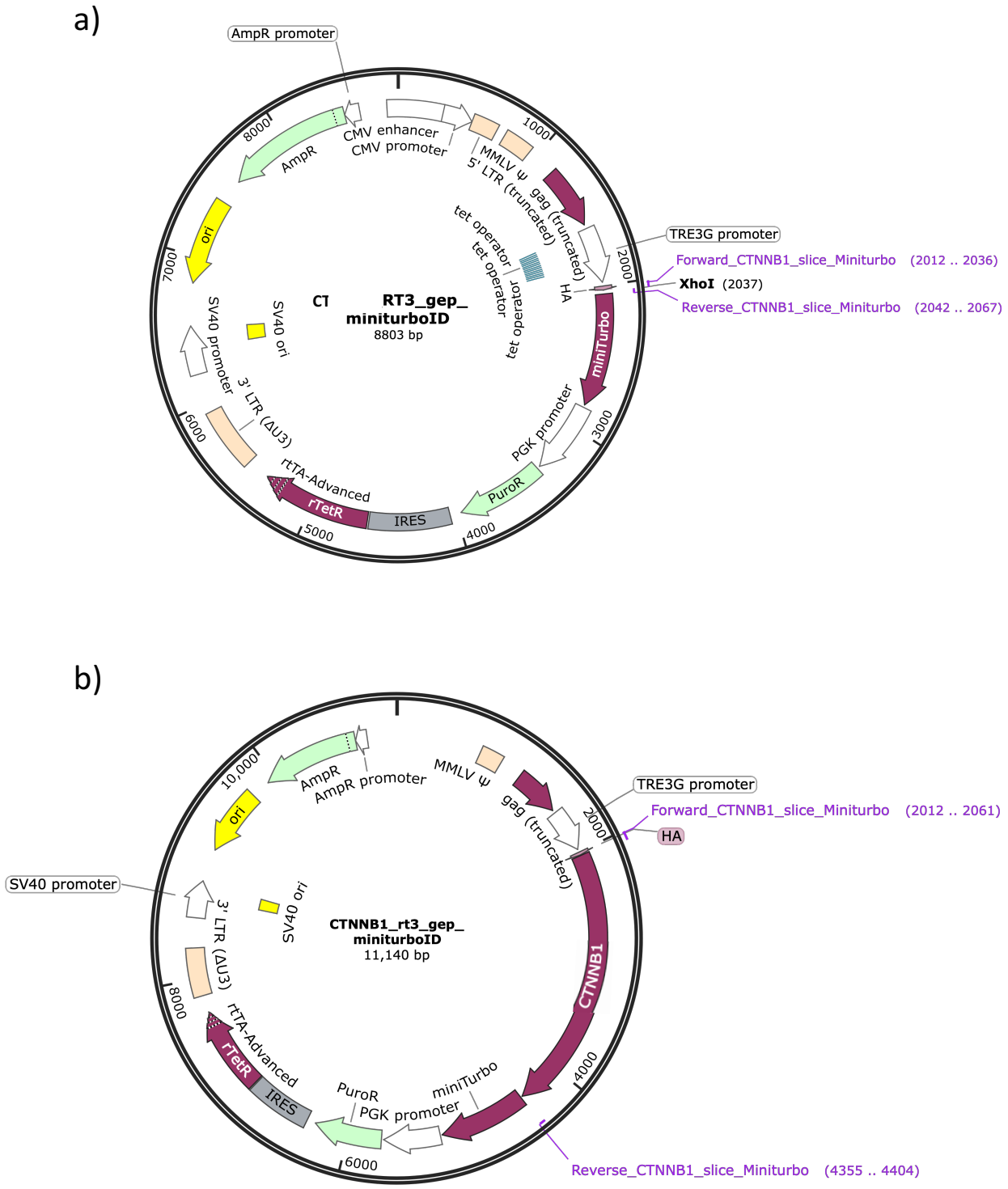

Figure 4.2 ***Plasmid maps of pre- and -post SLiCE cloning.***
a) Plasmid map of Mini Turbo empty vector construct b) Plasmid map of MiniTurbo vector showing insertion of CTNNB1 gene. Locations of forward and reverse MiniTurbo primer shown in purple. Xho1 restriction enzyme used to cut vector for SLiCE cloning.

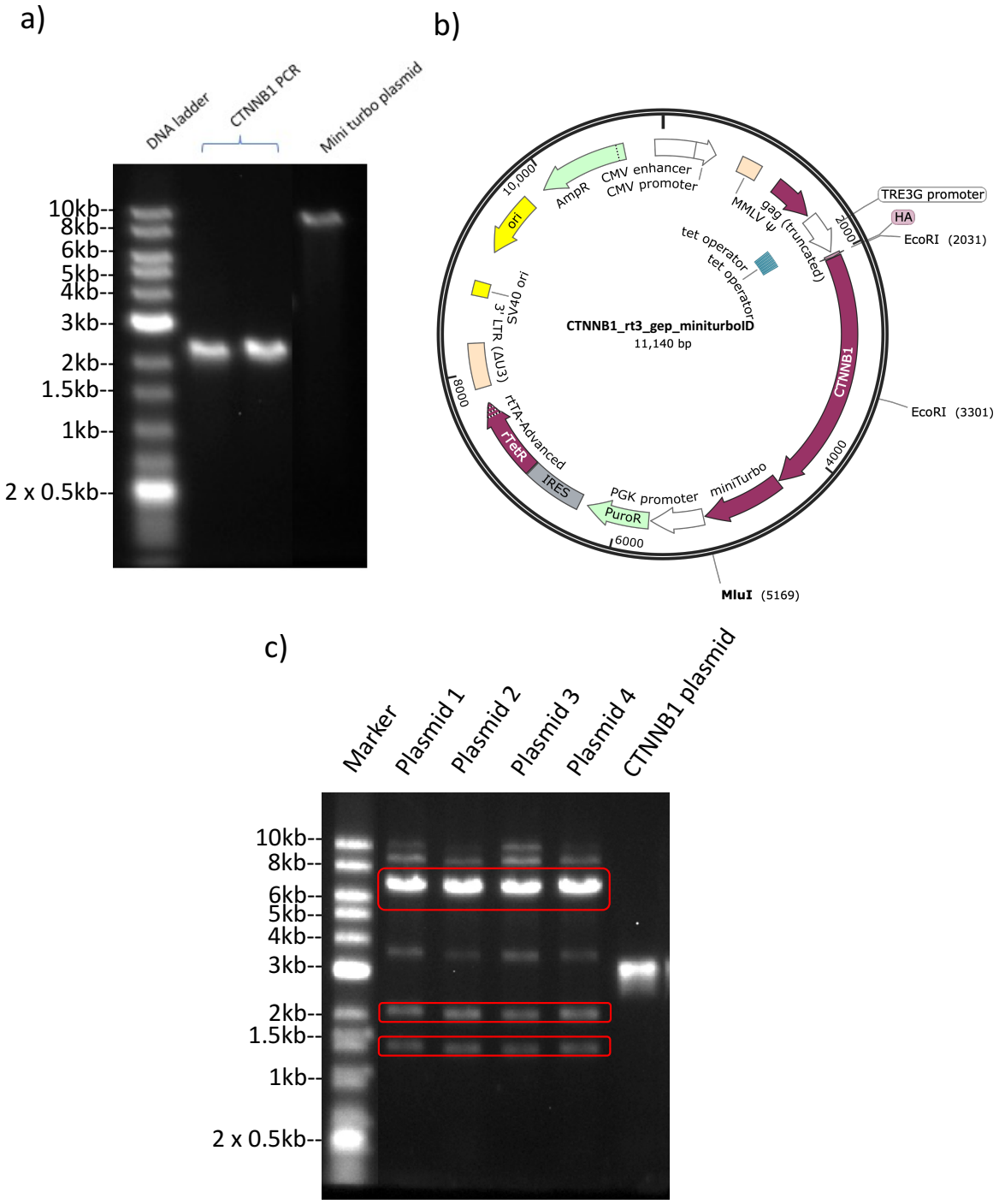

Figure 4.3 Cloning verification by restriction enzyme digest.
a) Gel electrophoresis image of PCR amplified CTNNB1 plasmid (2343bp) and MiniTurbo plasmid (8803bp) b) Plasmid map of CTNNB1-MiniTurbo following cloning highlighting the restriction enzymes EcoR1 and Mlu1 used for digestion. The image position of the 'Mini Turbo Plasmid' lane has been rearranged and spliced together for better clarity when comparing to 'CTNNB1 PCR' lanes. c) Image of gel electrophoresis showing independent purified plasmids that have undergone enzyme digestion. Expected bands are circled in red: 8002bp = Mlu1(5160)-EcoR1(2031), 1868bp = EcoR1(3301)-Mlu1(5169), 1270bp = EcoR1(2031)-EcoR1(3301). Marker lane and CTNNB1 plasmid spliced into image for clarity and reference.

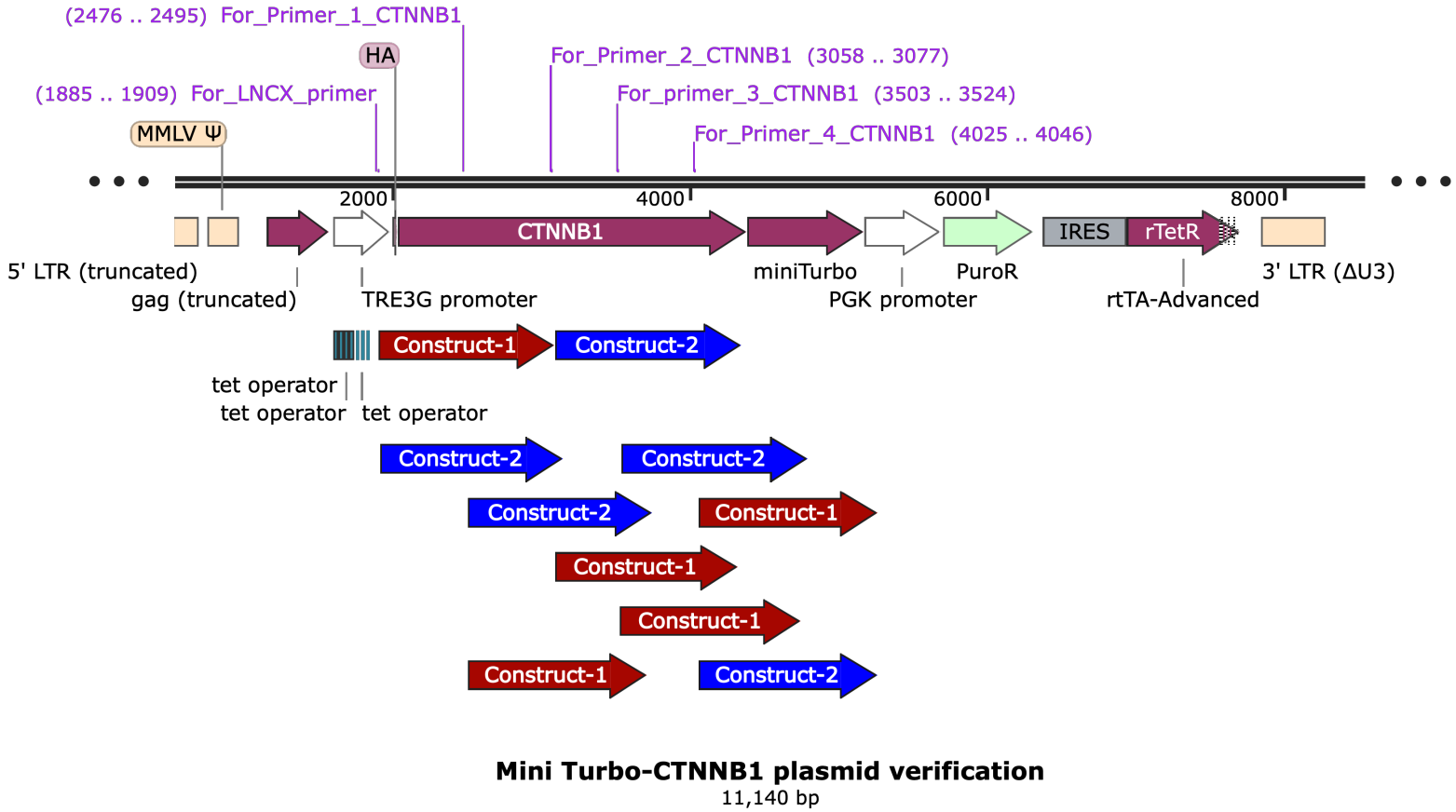

Figure 4.4 ***Plasmid map showing successful sequence alignment in two independent constructs***
Constructs shown in red and blue. Forward primers shown in purple text covered the length of the open reading frame to encompass the full MiniTurbo-CTNNB1 construct. Including HA tag at 5' end of CTNNB1 right past the MiniTurbo Biotin ligase gene. The primers were designed to purposely enable overlap between them to improve chances of 100% coverage. n=2

4.2.2 Verification of MiniTurbo construct in U2OS cells

Retroviral transfection and transduction of MiniTurbo plasmid was carried out as described in Chapter 2.14.2 with the main difference being the viral production was done in Plat-E cells to help further improve the transfection efficiency. Once the U2OS cells were transduced and one day after the virus was taken off, we added 2μg/ml puromycin to begin positively selecting for cells that had taken up the MiniTurbo plasmid. **Figure 4.5**a shows the images of the U2OS cells that are surviving in the presence of puromycin and thus MiniTurbo positive cells (left image) and the control WT U2OS cells without the MiniTurbo construct on the right where all the cells have succumbed to the puromycin cytotoxicity without the puromycin resistance gene. We then sought to obtain in vitro verification using western blotting and Immunofluorescence. Due to the HA tag in the MiniTurbo plasmid vector and streptavidin strongly binding to biotin, it offers an ideal method to verify using the antibody counterpart. As mentioned earlier, this system can be activated with doxycycline which drives the transcription and translation of the β-catenin-MiniTurbo construct (111kDa) and MiniTurbo alone (29kDa).

Figure 4.5b shows the western blot of U2OS CTNNB1-MiniTurbo (MT) and U2OS MiniTurbo empty vector (EV) cell lysates under different doxycycline (0.5μg/ml) and biotin (50μM) conditions showing important elements of MiniTurbo verification. Firstly, when neither Doxycycline or Biotin are applied there is no expression of the HA tag in the MT and EV lane showing that Doxycycline is required for MiniTurbo activation. Similarly, when only biotin is applied without doxycycline there is no HA(MiniTurbo) expression. In contrast, when the MT and EV cells are induced with doxycycline without biotin, we see MiniTurbo activation in the EV and MT lanes. The EV lane clearly shows the HA tag on its own with a band at 29kDa while the MT shows a band at approximately 111kDa which is the Mini Turbo-HA tag co-expressed with β-catenin and no band at 29kDa. The β-catenin (85kDa) band can be seen for reference. Unexpectedly, even though biotin wasn't exogenously applied a streak was observed in the MT lane when probed with streptavidin antibody. Research groups have shown no labelling unless biotin is applied so this result in our hands was surprising. Finally, on the right-hand side of the blot they are all MT lysates that had both doxycycline and biotin treatment and the β-catenin + Ha Tag band at 111kDa was observed in all the MT lanes with no band seen at 29kDa.

In addition to the western blot, immunofluorescence verification of the MiniTurbo-CTNNB1 system was carried out. We induced the cells with doxycycline and treated with Biotin for 4 hours. Using the protocol outlined in chapter 2.10 we captured images of U2OS MT cells (**Figure 4.5**c) showing clear differential staining with some cells clearly expressing MiniTurbo with high levels of Biotin labelling and also showing cells which haven't been transduced or with very low levels of activation and have no HA and streptavidin staining.

Alongside this, we conducted a time course with Biotin application ranging from 10 minutes to 4 hours (**Figure 4.5**b) as one of the advantages of this optimized system is the reduced Biotin exposure time needed for protein labelling. This data shows biotin labelling was observed from 10 minutes with the level of biotin labelling being positively correlated with exposure time. We unfortunately didn't obtain consistent actin bands for the time course segment which does weaken the interpretation and thus needs to be obtained in future work. However, we carried out the biotin time course for immunofluorescence validation under the same time frames and conditions shown in **Figure 4.5**d which strengthens the data and demonstrates successful implementation of the CTNNB1-Miniturbo system in U2OS cells. This gave us confidence to proceed to carry out affinity purification and subsequent coupling to mass spectrometry.

a)

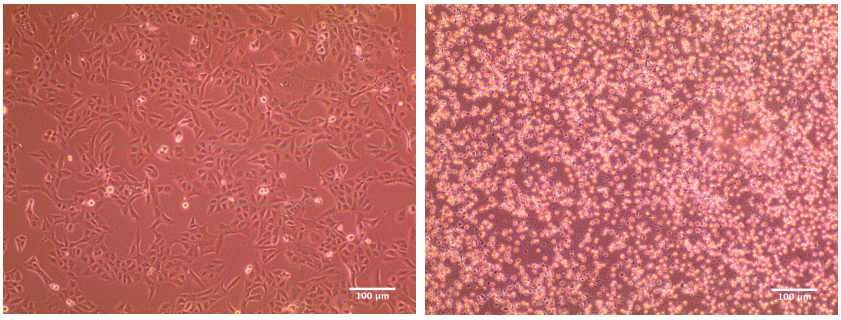

b)

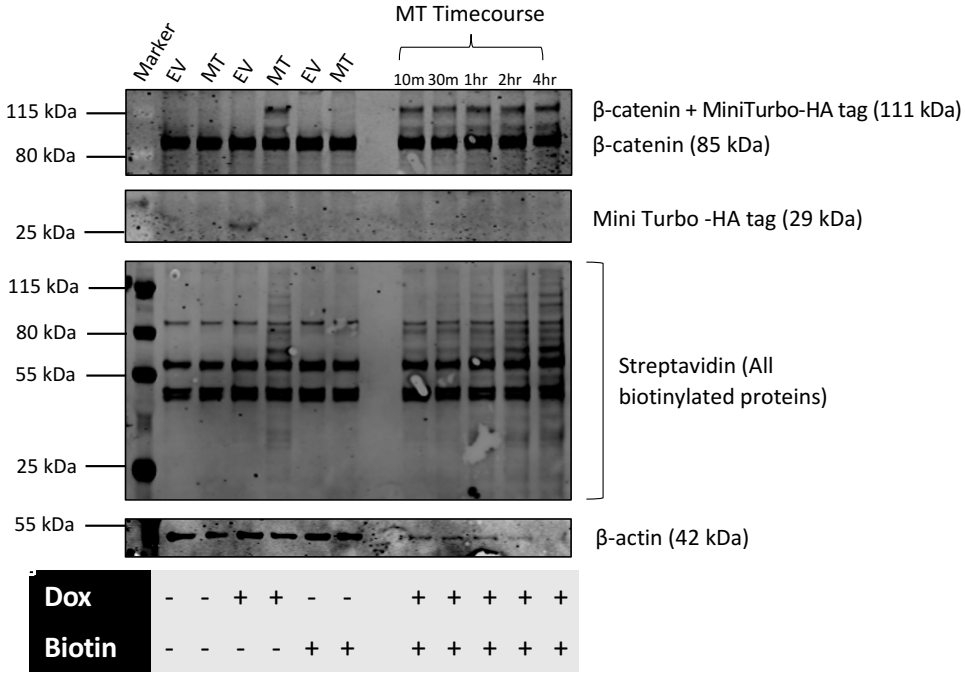

Figure 4.5 Verification of MiniTurbo system in U2OS cells.
U2OS CTNNB1 MiniTurbo transduced cells (left) and U2OS WT cells (right) following application of 2µg/ml puromycin as a selection marker. White rounded cells indicate dead cells. Scale bar = 100µm. n=1. b) Western blot detecting β-catenin and MiniTurbo construct via the HA tag or Biotinylation (streptavidin antibody) in either Empty Vector (EV) or β-catenin-MiniTurbo (MT) U2OS cell lines. Both in the presence/absence of Doxycycline (Dox 0.5µg/ml) and Biotin (50µM). Right hand side of the blot depicts time course with Biotin. n=1. c) Immunofluorescence images showing DAPI, HA(CY5) and Streptavidin (DSRED) staining in MiniTurbo-β-catenin (MT) and Empty Vector (EV) U2OS cells. Cells induced under different conditions with or without Doxycycline(D) and Biotin(B). Scale bar=100µm. d) Immunofluorescence images of β-catenin-MiniTurbo (MT) U2OS cells in a timecourse with Biotin(50µM) exposure (10 minutes-4 hours). Scale bar=100µm. n=1.

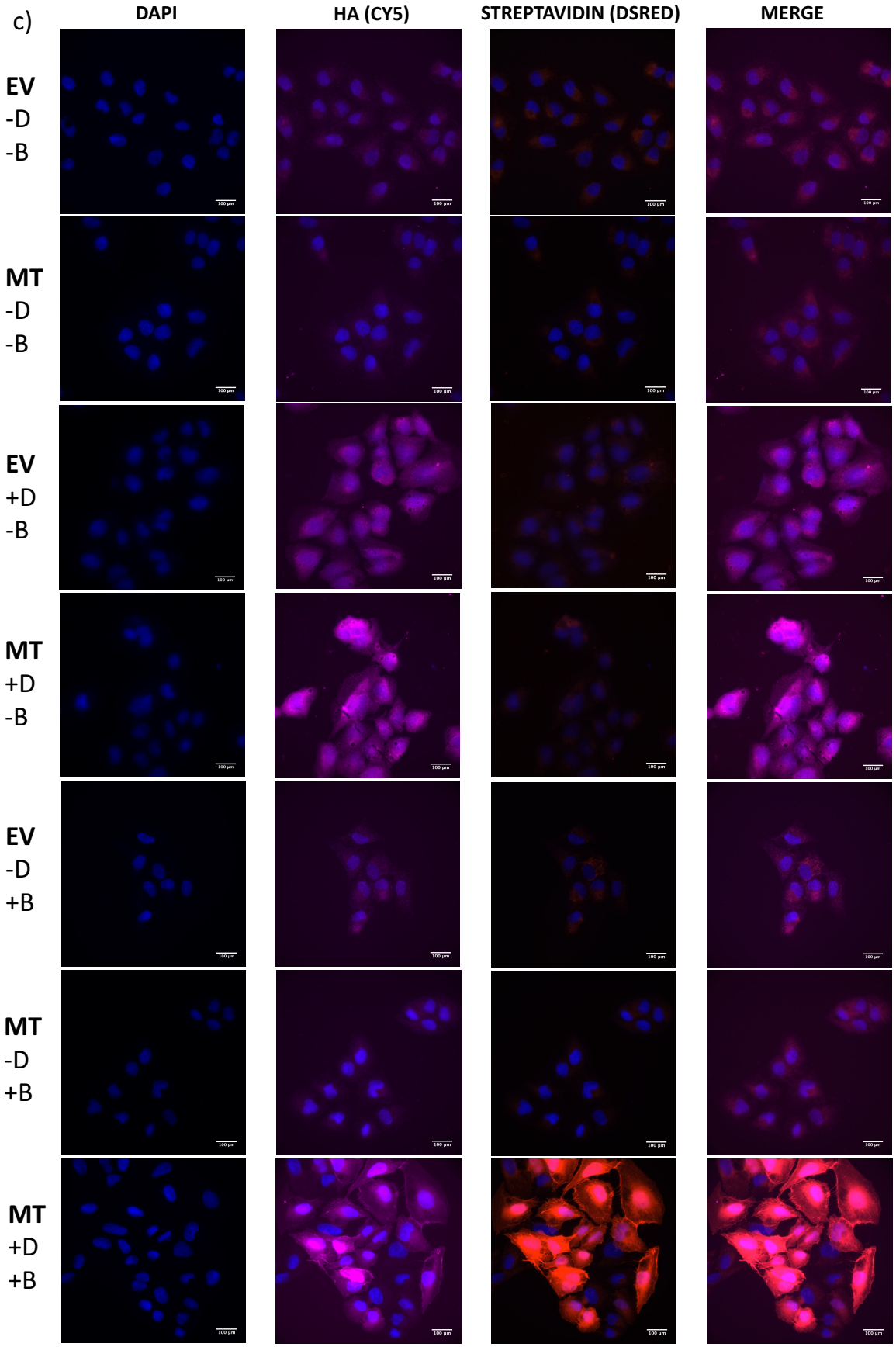
c)
DAPI
HA (CY5)
STREPTAVIDIN (DSRED)
MERGE
EV
-D
-B
MT
-D
-B
EV
+D
-B
MT
+D
-B
EV
-D
+B
MT
-D
+B
MT
+D
+B

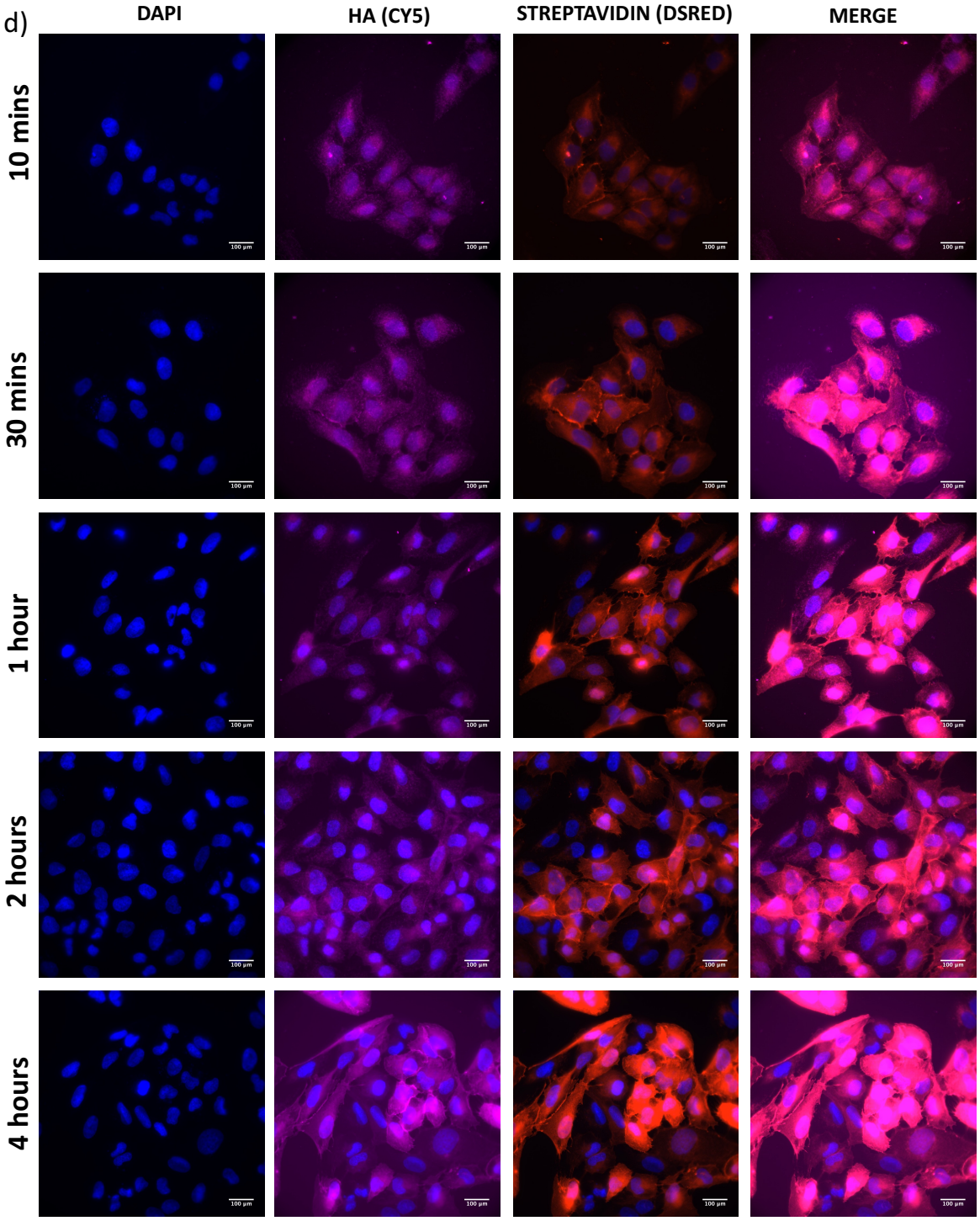
d)
DAPI
HA (CY5)
STREPTAVIDIN (DSRED)
MERGE
10 mins
30 mins
1 hour
2 hours
4 hours

4.2.3 Proteomic functional enrichment analysis confirms β-catenin associated terms

When investigating protein-protein interactions of a protein of interest by AP-MS, identifying known and verified interactions is a crucial indicator of the technique's success. The MiniTurbo biotinylation method yielded a very positive result with many known β-catenin interactors identified as being within very close proximity. Analysis of the functional enrichment of these proteins obtained using the SAINT analysis software set at high SAINT probability score of >0.95 is highlighted here.

Firstly, via gene ontology (GO) biological process analysis yielded high scores for "maintenance of apical and basal polarity" ($-Log_{10}$ P value =5.4), "adherens junction organisation" ($-Log_{10}$ P value =4.47), "canonical Wnt signaling pathway" ($-Log_{10}$ P value =3.63) and "beta-catenin-TCF complex assembly" (($-Log_{10}$ P value =2.58) among other enriched values linked to β-catenin activity (**Figure 4.6**a). In addition, pathways analysis yielded many significant connotations including "deactivation of beta-catenin transactivating complex" ($-Log_{10}$ P value =4.65), "Signaling by Wnt in cancer" ($-Log_{10}$ P value = 2.43) and "Beta-catenin phosphorylation cascade" ($-Log_{10}$ P value =2.37) and "Degradation of beta-catenin by the destruction complex" ($-Log_{10}$ P value =1.57)
. (see **Figure 4.6**b)

Furthermore, the GO molecular function analysis strongly illustrated that the MiniTurbo system worked as "beta-catenin binding" and "armadillo repeat domain binding" are significant terms picked up with $-Log_{10}$ P value of 8.05 and 2.32 respectively. Other significant β-catenin associated terms are also included in **Figure 4.6**c. The final GO analysis involving cellular component further corroborated the success of this technique with significant terms associated with "cell-cell junction" ($-Log_{10}$ P value = 8.34) and "catenin-complex" ($-Log_{10}$ P value = 6.23) being flagged with the labelled proteins(see **Figure 4.6**d). Each of these functional enrichment analyses strengthens the interpretation of the data, clearly showing that the proteins that have been biotinylated by β-catenin are direct binding partners and are associated with its functions at the cell membrane and within cell signaling and the Wnt signaling pathway.

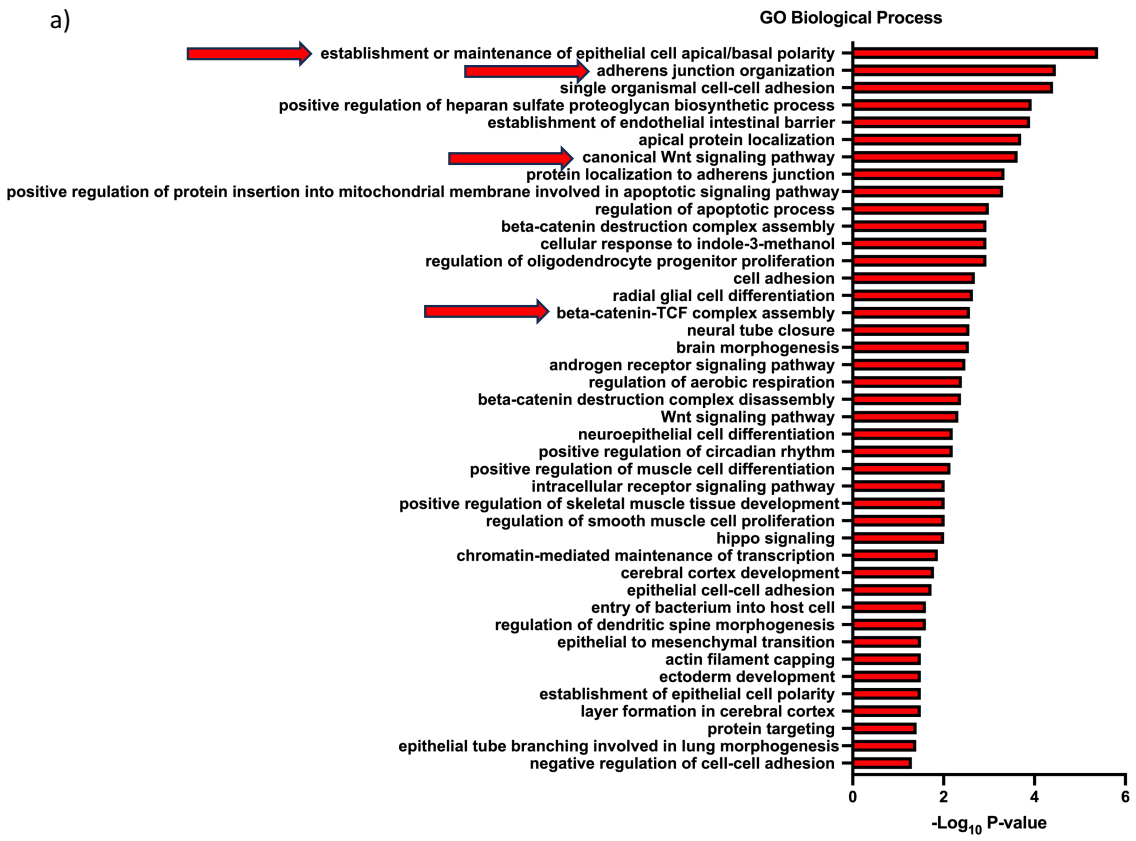
a)
GO Biological Process
establishment or maintenance of epithelial cell apical/basal polarity
adherens junction organization
single organismal cell-cell adhesion
positive regulation of heparan sulfate proteoglycan biosynthetic process
establishment of endothelial intestinal barrier
apical protein localization
canonical Wnt signaling pathway
protein localization to adherens junction
positive regulation of protein insertion into mitochondrial membrane involved in apoptotic signaling pathway
regulation of apoptotic process
beta-catenin destruction complex assembly
cellular response to indole-3-methanol
regulation of oligodendrocyte progenitor proliferation
cell adhesion
radial glial cell differentiation
beta-catenin-TCF complex assembly
neural tube closure
brain morphogenesis
androgen receptor signaling pathway
regulation of aerobic respiration
beta-catenin destruction complex disassembly
Wnt signaling pathway
neuroepithelial cell differentiation
positive regulation of circadian rhythm
positive regulation of muscle cell differentiation
intracellular receptor signaling pathway
positive regulation of skeletal muscle tissue development
regulation of smooth muscle cell proliferation
hippo signaling
chromatin-mediated maintenance of transcription
cerebral cortex development
epithelial cell-cell adhesion
entry of bacterium into host cell
regulation of dendritic spine morphogenesis
epithelial to mesenchymal transition
actin filament capping
ectoderm development
establishment of epithelial cell polarity
layer formation in cerebral cortex
protein targeting
epithelial tube branching involved in lung morphogenesis
negative regulation of cell-cell adhesion
0
2
4
6
-Log10 P-value

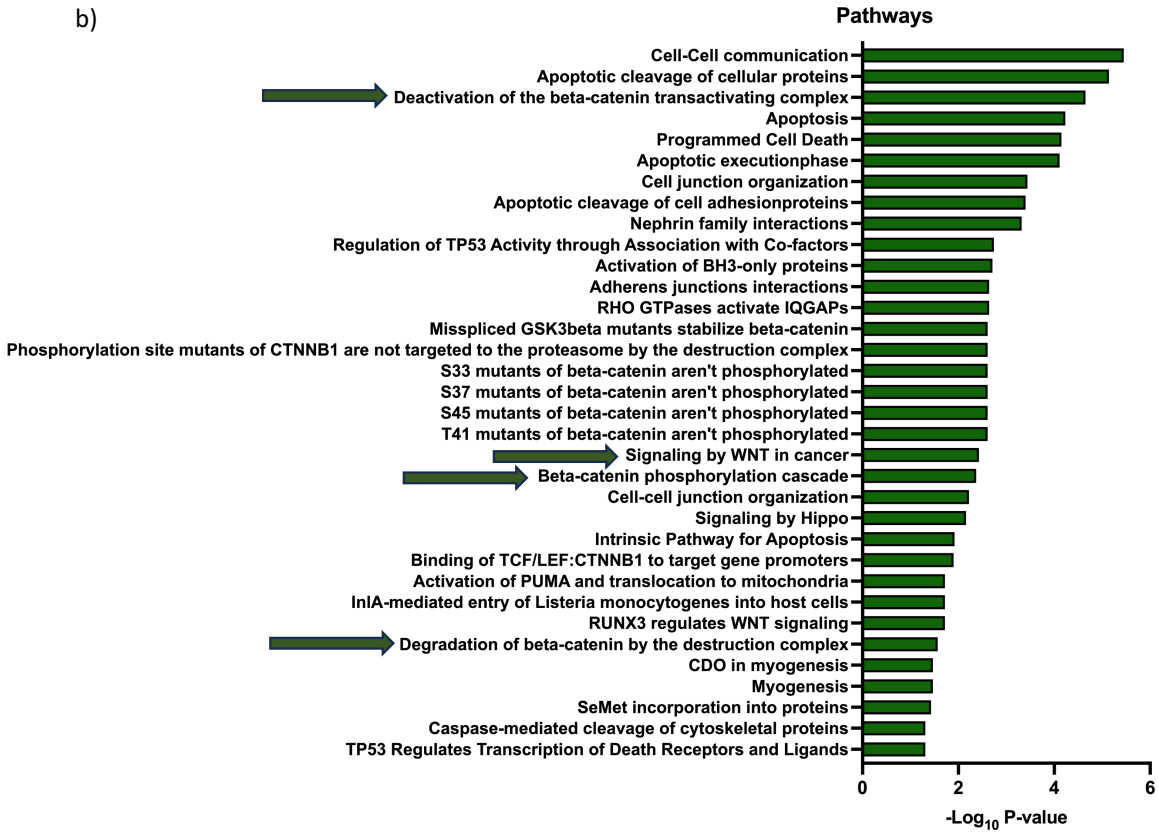
b)
Pathways
Cell-Cell communication
Apoptotic cleavage of cellular proteins
Deactivation of the beta-catenin transactivating complex
Apoptosis
Programmed Cell Death
Apoptotic executionphase
Cell junction organization
Apoptotic cleavage of cell adhesionproteins
Nephrin family interactions
Regulation of TP53 Activity through Association with Co-factors
Activation of BH3-only proteins
Adherens junctions interactions
RHO GTPases activate IQGAPs
Misspliced GSK3beta mutants stabilize beta-catenin
Phosphorylation site mutants of CTNNB1 are not targeted to the proteasome by the destruction complex
S33 mutants of beta-catenin aren't phosphorylated
S37 mutants of beta-catenin aren't phosphorylated
S45 mutants of beta-catenin aren't phosphorylated
T41 mutants of beta-catenin aren't phosphorylated
Signaling by WNT in cancer
Beta-catenin phosphorylation cascade
Cell-cell junction organization
Signaling by Hippo
Intrinsic Pathway for Apoptosis
Binding of TCF/LEF:CTNNB1 to target gene promoters
Activation of PUMA and translocation to mitochondria
InlA-mediated entry of Listeria monocytogenes into host cells
RUNX3 regulates WNT signaling
Degradation of beta-catenin by the destruction complex
CDO in myogenesis
Myogenesis
SeMet incorporation into proteins
Caspase-mediated cleavage of cytoskeletal proteins
TP53 Regulates Transcription of Death Receptors and Ligands
0
2
4
6
-Log10 P-value

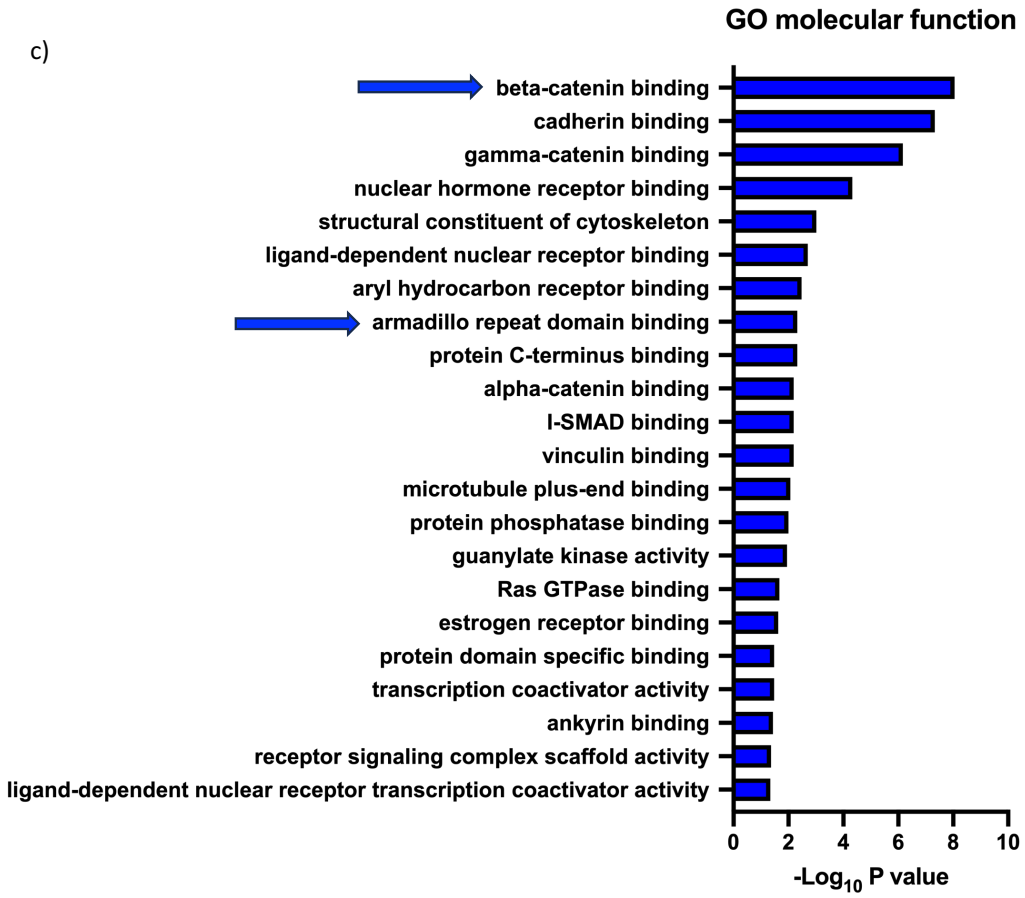

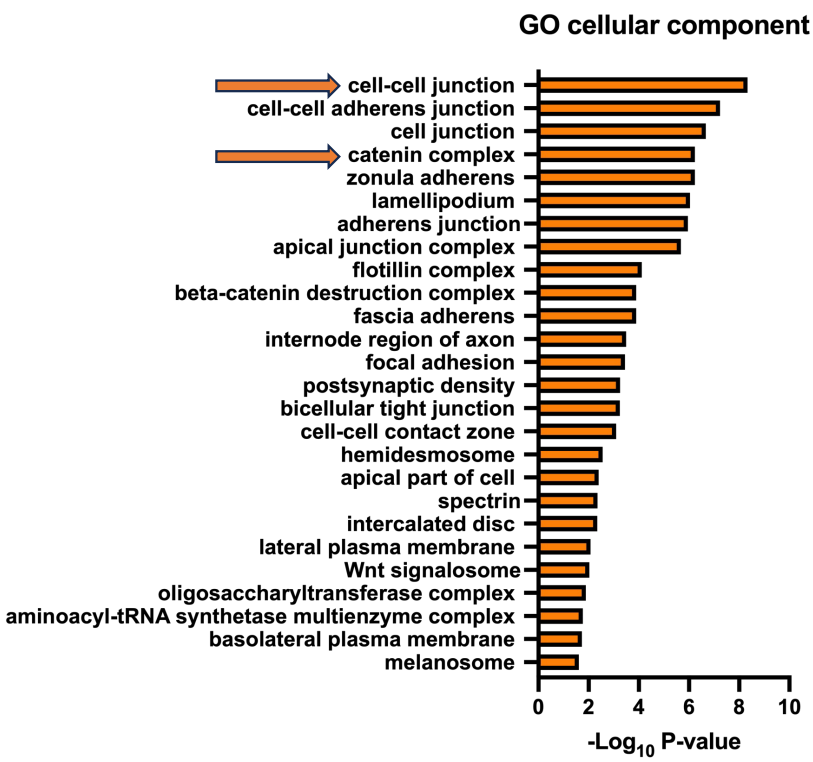

Figure 4.6 Functional enrichment analysis shows significant β-catenin associations.
Proteins identified through proximity labelled affinity purification-mass spectrometry subjected to SAINT analysis with functional enrichment. A) GO Biological Process b) pathways c) GO Molecular Function d) GO Cellular component. All displaying the -Log of P value, where P<0.05 is significant. n=1.

4.2.4 Interactome analysis and database comparisons reveals network of novel candidates for β-catenin direct binding

Affinity purification methods as described earlier have "BAIT" and "PREY/HITS" connotations given when referring to analysis. The bait here is CTNNB1 fused with the BirA* enzyme biotin ligase biotinylating the proximal proteins that are the prey. The previous section detailed our experimental design involving 3 biological repeats from both the MiniTurbo β-catenin positive U2OS cells and the empty vector control cells. Both qualitative and quantitative approaches were used to allocate significance to biotinylated proteins that could be novel candidates as β-catenin interactors. The qualitative approach involved stringent exclusion where for the β-catenin MiniTurbo samples each protein had to be present in at least 2 out of 3 repeats while simultaneously not be present in any of the empty vector control repeats. The quantitative method used SAINT analysis software using the Bayesian method to predict true interactions.

Figure 4.7a shows the qualitative analysis outcome with database comparisons by a Venn diagram. This comparative analysis produced 112 verified interactors that are present in either or both the BIOGrid and INTact databases. **Figure 4.7**b illustrates the string network of known β-catenin interactions with highlighted edges of prominent Wnt signaling proteins. In addition to this result, 315 unique potential interactors were identified (see **Figure 4.7**c). This figure points out 3 GO annotations. 153 proteins were annotated to be present in/associated with the 'nucleus' (FDR; P=0.002). 72 proteins were involved with 'RNA binding' to some degree (FDR; $P=2.3x10^{-11}$) and 69 with 'nucleotide binding' ($P=6.5x10^{-6}$). These GO terms were highlighted due to the high proportion of proteins that were associated with those terms. With the role that β-catenin plays as a transcriptional co-activator, to have this many proteins have 'nuclear' associations could potentially indicate the number of proteins that β-catenin are in close proximity with or if not binding that has not been documented yet. This full list of the qualitatively selected proteins is **Supplementary Table 2.**

Quantitative analysis showed 39 unique proteins not found in the BIOGRID and INTACT databases (see **Figure 4.8**a) that need further in vitro validation to be verified as direct interactors. 31 of these proteins have been annotated as "phosphoproteins" by UniProt with an FDR of P=0.00083 which is significant when considering the role phosphorylation plays in the regulation of the Wnt signaling pathway. In addition, 18 of these proteins have been annotated to be involved with "acetylation" (FDR; P=0.03). The full list of analysed proteins is in **Supplementary Table 3.** Furthermore, GO analysis of these 39 proteins revealed that 16 are implicated at the cell junction (FDR; P=0.002), 14 with extracellular exosome (FDR; P=0.02, 9 at anchoring junction (FDR; P=0.02) and 6 at focal adhesions (FDR; P=0.03).

MINITURBO: STRINGENT QUALITATIVE CUT OFF
→PREY PRESENT IN 2/3 REPEATS
& NOT PRESENT IN ANY CONTROLS

a)

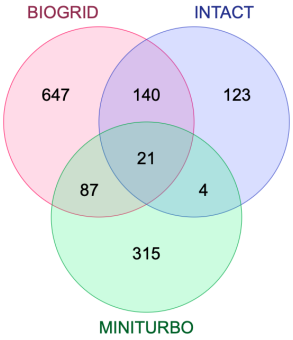

b)

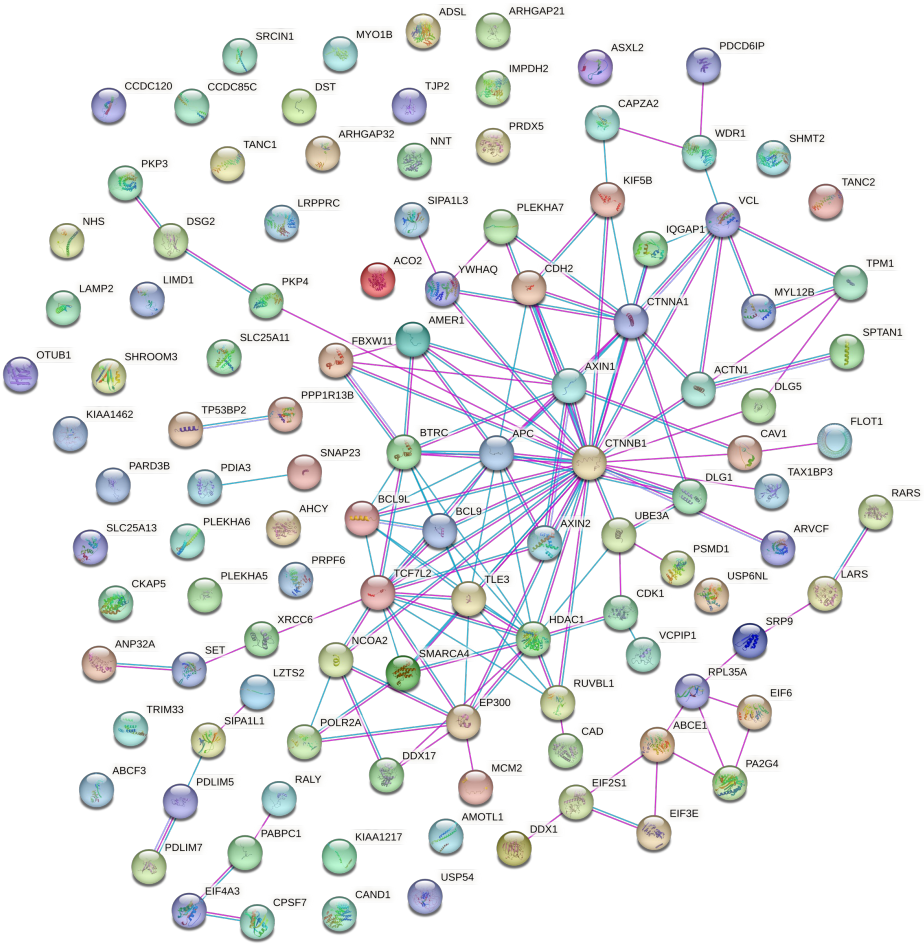

87 + 21 + 4 = 112 database verified interactors

.

c) Key: GO Cellular component=Nucleus GO Molecular Function=Nucleotide binding GO Molecular Function=RNA binding

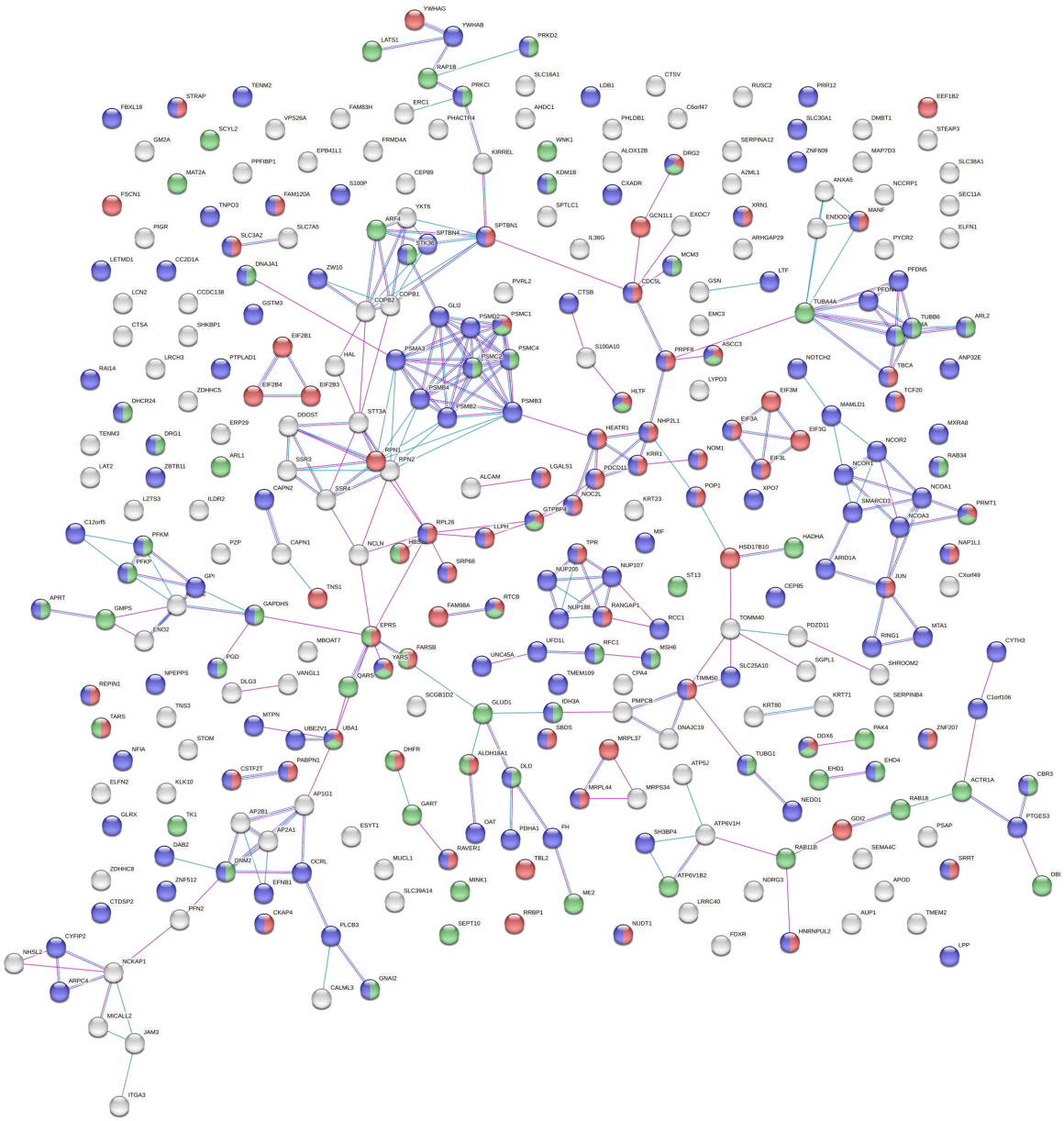

315 unique Biotinylated proteins → potential novel direct interactors

Figure 4.7 Qualitative interactome analysis of B-catenin by proximity dependent biotinylation. *a) Venn diagram showing database comparisons of known and unique interactors. b) STRING network of verified interactions with databases. Verified in this context means, the proteins that MiniTurbo has identified matches with the proteins in the database for having physical associations with β-catenin c) STRING network showing total amount of unique proteins identified through the stringent method, with the following GO terms highlighted: GO cellular component=nucleus, GO molecular function=nucleotide binding and RNA binding. Purpose of displaying. This network is intended for visual purposes only the large proportion of nuclear involved proteins highlighted. n=3*

Figure 4.8b shows comparisons within the database that have the same "BAIT" protein, β-catenin and have employed the proximity labelling. The difference here is the model cell line used, which is HEK293 compared to our U2OS cell model. Out of the total number of proteins from our dataset (SP>0.95), 34 were common with the HEK293T dataset. The HEK293T cohort had 41 unique hits and our U2OS set had 53 unique hits. When all types of physical interactions were set as the selection criteria, 48 proteins were found to be correlating with hits found in either or both BIOGriD and INTact databases which strengthens the argument that proximity labelling is identifying correct known targets. In addition to this, 39 proteins were not characterized in either of the databases a being interactor, which reveals that these 39 candidates need further investigation to ascertain if they are possibly direct interactors of β-catenin by co-immunoprecipitation.

MINITURBO: STRINGENT QUANTITATIVE CUT OFF- SP ≥ 0.95

a) Databases: Proximity Label-MS only- BAIT and HITS

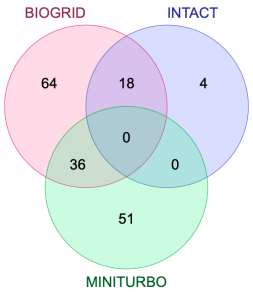

b) Databases: Proximity Label-MS only- BAIT BCAT only

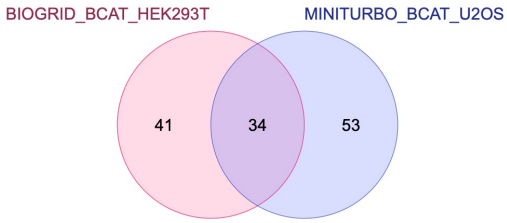

c) Databases: All physical interactions

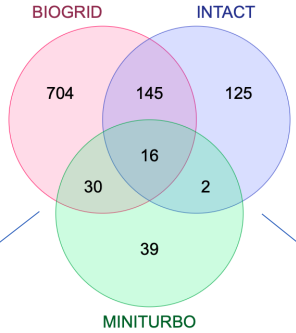

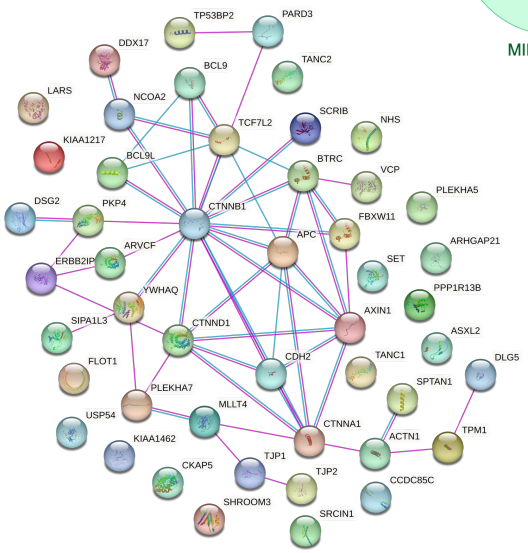

30 + 16 + 2 = 48 database verified interactors

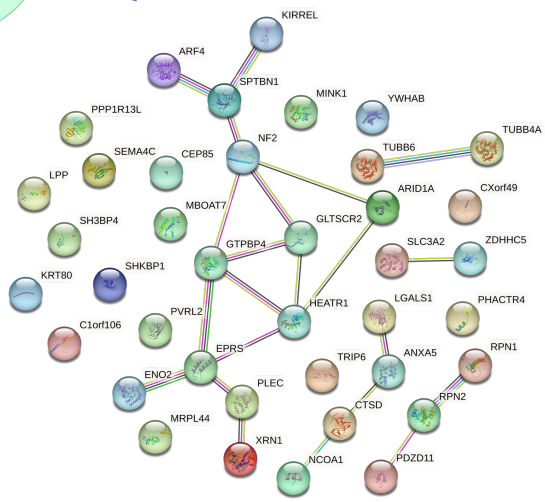

39 unique Biotinylated proteins → potential novel direct interactors

Figure 4.8 Quantitative analysis of β-catenin using SAINT.
a-b) Database comparisons of verified and unique interactors with proximity labelling only. c) Database comparison including all physical associations. Left, verified interactors. Right, unique interactors. 'Verified' in this context means the proteins that MiniTurbo has identified matches with the proteins in the database for having physical associations with β-catenin. 'Direct' in this context is implying direct protein-protein interaction given the close proximity of the PREY to the BAIT protein of about 10nm. n=1

4.3 Discussion

Proximity-based affinity capture is proving to be a trustworthy tool for investigating protein-protein interactions, especially when coupled with proteomics. There aren't many written works using the MiniTurbo proximity label system as it is still relatively new technology compared to the pre-existing proximity labelling systems. However, the work by Alice Ting's group[153] has clearly shown how the modified Biotin ligase is advantageous when considering other methods that require longer labelling time or need the cells/living organism to be dead for labelling. In addition, as described above, the high affinity of streptavidin and biotin helps to overcome limitations of stringent washing seen with immunoprecipitation along with artefacts. The enzyme-catalysed proximity labelling described here reflects a more accurate picture of the interactome landscape in an *in vitro* cellular environment due to the Tet on Biotin activation in the Mini Turbo system enabling PPI study in living cells.

Many papers have been published with reference to protein-protein interaction methods, including the well-established process of immunoprecipitation. In contrast, there are relatively few on MiniTurbo. One of the wider applications of this method was put in the spotlight in 2021 when Go *et al*[179] published a massive project on mapping the human cell using the proximity dependent biotinylation. This beautiful work provided accurate insight into the protein compartmentalisation and interactions within the cell, fuelling future investigations for novel protein interactions.

The primary aim of this study was to implement this MiniTurbo system genetically fused to β-catenin in a cancer cell line (U2OS) which was achieved as demonstrated by **Figure 4.4** and **Figure 4.5**. Thanks to the widely available Addgene repository, this plasmid construct was accessible at low cost and the robust lentiviral vector transduction system, the process was not overly arduous. Due to the tet-repressor component, the advantage of selectively activating this enzyme activity was immediately realised. It would enable timed and context specific analysis of the interactome rather than having a constitutively active system enabling the study of the influence of drugs on the cell interactome. In our hands, however, we did observe the system to be a bit 'leaky' as **Figure 4.5** showed that just inducing the cells with doxycycline in the absence of biotin addition led to the biotinylation of proteins as seen by the streptavidin antibody.

In addition, the experiment design missed a key control arm which should have been tested during the validation steps. There are no western blots or immunofluorescence images of the control empty vector after induction with doxycycline and addition of Biotin. This should have been included as a direct comparison to the β-catenin MiniTurbo vector. Therefore, this should be included in future experiment and analysis.

A second arm of this research was to carry out affinity purification with the MiniTurbo biotinylation capture coupled to mass spectrometry. Perhaps the most compelling result was the observance of expected proteins being captured by this method. The verification of over 100 proteins by two independent databases (BIOGrid and INTact) increased confidence that novel proteins being observed warrant further investigation for being direct interactors of β-catenin. There needs to be caution when interpreting the analysis from the interactome. We can infer from this data the proximity labelling is correctly identifying known interactors, but this method does not verify for certain they are direct interactors just that they in very close proximity. Therefore, one of the future experiments that need to be carried out is co-immunoprecipitation of the unique interactors that were identified in the interactome to verify by western blot whether it is a direct interaction. As this proximity labelling is done when cells are viable, there is a potential risk, if the fusion of Biotin-ligase to the N-terminus of β-catenin may be potentially hindering important PPI as it is the ARM region of the protein. A counter argument to that notion would be that among the proteins that were pulled down by streptavidin, E-Cadherin, TCF-7 and Axin, BCL-9 were present. These proteins bind in the groove near the N-terminus and are not being hindered from coming into close proximity. However, perhaps TOPflash assay would shed more light as to the effect on Wnt transcriptional activation comparing WT and Biotin-ligase fused β-catenin.

A point of discussion is which method of selection is more accurate, the qualitative or the quantitative method. The reasoning behind the qualitative method uses the inclusion-exclusion principle as part of the sieve method, where the proteins selected had to be present in at least 2 out of the 3 repeats and not be present in any of the control repeats. The reason for opting for this method over proteins being present in all 3 repeats is because of the unequal protein count between each repeat and to expand selection for identifying potentially lower abundance proteins that might be true interactors but aren't picked up in all 3 repeats.

In contrast, the quantitative method uses an algorithm to calculate the probability it is a direct interaction by assessing the occurrence and frequency of peptide spectra providing a probability score between 0 and 1. There is a compromise here as only proteins with an SP score of 0.95 or higher have been selected with a risk that genuine interactors but less abundant may be missed due to a lower SP score.

There is a level of subjectivity being administered when the threshold cut off is decided which is important to note when drawing conclusions about the number of unique hits. A further limitation with the data analysis is the lack of more control datasets to increase confidence and further refine the unique hits. The plan involved utilising CRAPome[160] to add further proximity label control datasets to filter out false positive unique hits.

With this in mind, the gene ontology results of the unique hits from both the qualitative and quantitative analysis highlight the dual function of β-catenin as a structural protein and a transcriptional co-activator. It is well documented that β-catenin interacts with multiple proteins, but it was still fascinating to find the such a high number of biotinylated proteins that were nanometers from β-catenin that are potential direct interactors ranging from cell junction to the nucleolus, demonstrating the widespread reach of β-catenin. Over 50% of the unique proteins qualitatively identified were associated with 'RNA binding'. RNA binding proteins (RBPs) play a crucial part in regulating post-transcriptional gene expression, with dysregulated RBPs leading to the development and progression of cancer[180].

Mutations or deletions in RBPs may promote cancer cell proliferation and dysregulated maintenance of RBPs leads to higher expression in tumour cells resulting in poor prognosis. One of the other key annotations was "acetylation". This is suggestive of involvement with gene regulation as one of the primary purposes of acetylation in signaling is to control gene transcription, Narita *et al*[181] reported that over 100 non-histone proteins implicated in regulating transcription are in turn regulated by acetylation. These include transcription factors, transcriptional co-activators, and nuclear receptors. β-catenin, as a transcriptional co-activator is acetylated by CBP at position K49[182]. A site that is frequently found to be mutated in cancer resulting in aberrant activation of the c-myc oncogene. It could be cautiously speculated from this result that the proteins identified here to be associated with acetylation, being in close proximity and potential interactors of β-catenin may be playing a part in regulating Wnt target gene transcription alongside β-catenin.

In summary, the aim of this chapter is met with the successful employment of the MiniTurbo proximity labelling system enabling the capture of dynamic interactions within the B-catenin interactome. This will serve as a foundation to access further bait proteins in Wnt, Hippo and Notch signaling pathways to build a comprehensive map of the interlinked interactomes.

Chapter 5 Investigating the impact of small molecule modulators on the β-catenin interactome

5.1 Introduction

This final results chapter builds on the β-catenin/Wnt signaling narrative by investigating how small-molecule modulators affect β-catenin-dependent signaling and protein interactions in living cells. As outlined in the Introduction chapter, significant research has been directed toward targeting the Wnt signaling pathway as a potential therapeutic strategy for various diseases, especially cancer. Despite promising preclinical data, no Wnt-targeted therapies have reached clinical approval. Several small molecules have entered Phase I and II clinical trials (**Table 1.3**), but many were paused or discontinued due to lack of efficacy or off-target effects, underscoring the need for more targeted and mechanistic approaches to disrupt this critical signaling pathway. The primary aim of this study is to profile both known small-molecule modulators of Wnt signaling and novel derivatives of carnosic acid (CA) to assess their impact on β-catenin interactions. CA, a naturally occurring small molecule, has previously been shown to induce β-catenin degradation, as reported by Marc de la Roche *et al*[120]. To extend these findings, we explored a couple of CA derivatives for their potential to selectively modulate β-catenin activity and signaling. By performing cell-based assays, including cell viability and colony formation assays, we assessed the phenotypic impact of these compounds on both cancerous and non-cancerous cell models, focusing on their cytotoxicity and selectivity.

A key component of this investigation involved using the MiniTurbo system, a proximity-dependent biotinylation tool fused to β-catenin[153], to determine how small-molecule treatments alter the β-catenin interactome in living cells. This system enabled us to capture dynamic changes in β-catenin's interaction network following treatment with MAM4-141, a promising carnosic acid derivative. By coupling MiniTurbo-based biotinylation with advanced proteomic platforms, including LC-MS/MS (Liquid Chromatography-Tandem Mass Spectrometry) and AP-MS (Affinity Purification-Mass Spectrometry), we mapped the β-catenin interactome and identified changes in functional networks in response to these compounds. The integration of high-resolution proteomics and cell-based assays provided a comprehensive overview of how small-molecule modulators affect β-catenin-dependent signaling and protein interactions. The findings from this chapter contribute to a deeper understanding of β-catenin modulation in cancer and highlight the potential for MAM4-141 and related derivatives to be developed as therapeutic agents targeting the Wnt pathway. Ultimately, this work lays the foundation for identifying novel β-catenin interactors and functional networks that may serve as therapeutic targets in Wnt-driven cancers.

5.2 Results

5.2.1 Influence of CA on β-catenin levels in HCT116 and SW480 cell lines

Based on the work of Marc de la Roche and colleagues[120], CA was shown to induce a decrease in active β-catenin levels in SW480 cells after 8 hours at 25μM, illustrated by Western blotting. This work was sought to be replicated in both HCT-116 and SW480 human colorectal cell lines, under the same experimental conditions. In a first series of experiments, treatment of HCT-116 cells with 2.5μM CA (**Figure 5.1a**) concentration over a time-course ranging from 0-4 hours did not produce an appreciable decrease in active β-catenin (**Figure 5.1b**). This was verified with 3 biological repeats giving rise to the same results.

To extend the range of concentrations and to investigate whether an effect could be observed at higher doses of CA, time-course assays with 12.5μM, 25μM, 50μM and 100μM were also performed using the same methodology as described above. Once again, upon western blot analysis, no significant decrease was observed in the level of active β-catenin (**Figure 5.1c**) in HCT-116 cells. This experiment is lacking a DMSO vehicle control to mirror the 100μM CA concentration. Therefore, these results must be interpreted cautiously.

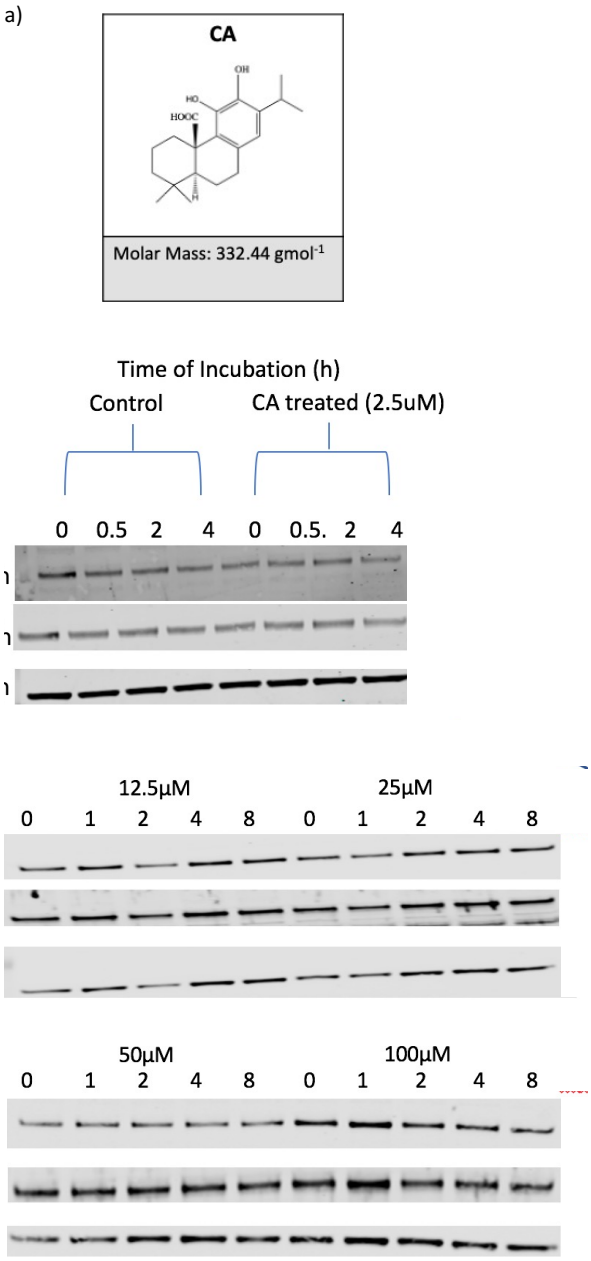

Figure 5.1 ***CA treatment on HCT116 cells.***
a) Structure of CA b-c) Western blot analysis of active β-catenin levels in HCT-116 cells following CA treatment for the indicated hours (0-8) and concentrations (2.5 µM-100 µM) specified respectively. DMSO used as vehicle control for b), but no vehicle control used for c). n=3

Strictly speaking, the effect by Roche *et al* was reported in SW480 cells and not HCT-116 cells, possibly suggesting a cell specific effect. Thus, after obtaining the SW480 cells (**Figure 5.2**a), CA was applied at 25μM in the same conditions. The western blot results were negative once again with virtually no decrease in the unphosphorylated "active" β-catenin pool after 8 hours (**Figure 5.2**b), contrasting with reports by De la Roche[119].

A couple of troubleshooting options were addressed to investigate whether the observed result was due to technical issues. Firstly, we employed 1H NMR to assess the quality of the commercial sample of CA employed and ensure no degradation occurred over time. CA is a chemical quencher for reactive oxygen species being an active antioxidant.[132] Within a cellular environment, it is still unclear the amount of time CA stays active. Pleasingly, NMR analysis confirmed the high purity of the sample, and did not identify any noticeable impurity and/or degradation product.

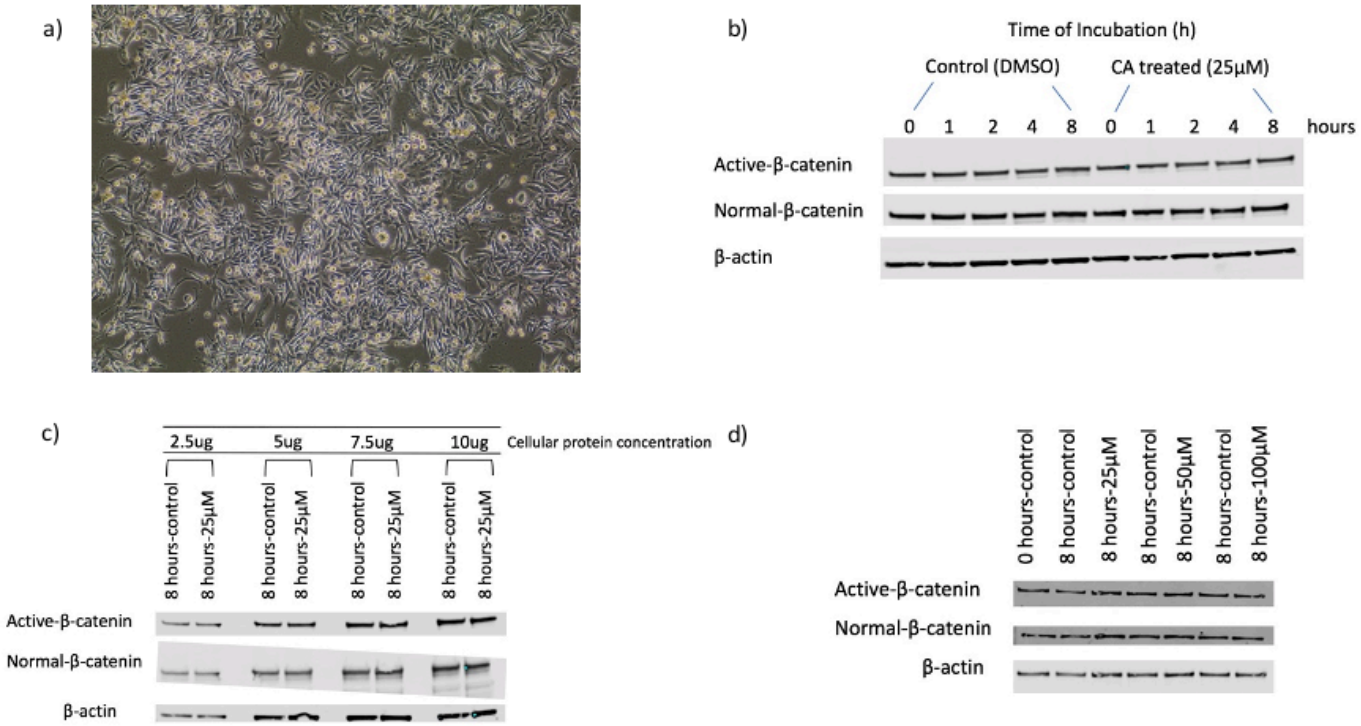

Figure 5.2. CA treatment on SW480 cells.
Image of SW480 cells. (b) Western blot analysis of active β-catenin levels of SW480 cell lysates following 8-hour time-course treated with 25μM CA.(c) Western blot analysis of active β-catenin levels of SW480 cell lysates applied at various cellular protein concentrations treated with 25μM CA at the 8-hour timepoint. d) Western blot analysis of active β-catenin levels of independent SW480 cell lysates to the ones used in a) treated with 25μM, 50μM and 100μM CA at the 8-hour timepoint. DMSO used as control. n=3

Secondly, we questioned whether the high steady state level of β-catenin present within SW480 cells due to APC gene mutation could mask the effect of CA compared to Wnt- independent cell lines. In this context, Wnt-independent cell lines are not as actively reliant on Wnt signaling for viability or Wnt signaling is not constitutively active in those cell lines.

Therefore, in an attempt to address this, we varied the concentration of cellular protein being loaded for Western blot analysis ranging from as low as 2.5μg to 10μg for the 8-hour time-point (**Figure 5.2**c). However, this still failed to demonstrate any decrease in the CA treated cells compared to control.

Thirdly, we repeated these experiments using a distinct set of SW480 cells from Professor Graham Packham at the Southampton General Hospital, independent to the ones we cultured and treated with 25μM, 50μM and 100μM of CA for 8 hours (**Figure 5.2**d), which yielded an indiscriminating result, as levels of active β-catenin were not significantly different between the control and treated samples. This was a frustrating result, as we wanted CA to act as a reference or positive model when testing the derivatives. However, there are variables that hinder the reproducibility of results between research groups.

5.2.2 HEK293T as a model cell line for induced Wnt activity for compounds CA and MSAB

Following up on the above results and observations, we decided to further investigate the cellular activity of CA and MSAB in cell lines displaying lower steady state β-catenin levels. We hypothesised that reduced baseline levels of β-catenin may allow a more accurate quantification and validation of CA inhibitory activity. HEK293T represents a particularly suitable model cell line and is a routinely used cell line to study the activation of Wnt signalling following extracellular stimulation/induction. This is more challenging in cell lines that are more Wnt dependent (heavy reliance on Wnt signaling for viability) and display constitutively high levels of β-catenin, like HCT116 and SW480. Here we purposed to study the inhibitory effect of CA in HEK293T with the goal that it may shed more light on its effect on β-catenin and Wnt target genes. **Figure 5.3** displays the experimental data on HEK293T when treated with increasing concentrations of CA at a transcriptional and protein level following initial Wnt induction with the 40kDa Wnt3a ligand for 24 hours at a concentration of 50 ng/ml. Wnt3a binds to the Frizzled-LRP5/6 co-receptors and subsequently activates the pathway.

Firstly, to observe Wnt transcriptional activity the TOPFlash dual luciferase assay was employed. **Figure 5.3**a displays the trend between the DMSO control and the 25uM CA treated where the relative fold change in firefly over renilla luciferase was lower in the treated compared to the control, however it was not statistically significant ($P>0.05$). CA has been reported to reduce Wnt transcriptional activity and although the TOPFlash assay gives a general picture of transcriptional activity, one of the drawbacks is the sensitivity of the instruments that measure luciferase activity; therefore, optimisation is still required.

In addition, it needs to be acknowledged that from the results (**Figure 5.3**a, b) that no Wnt induction was observed from Wnt3A exposure. Critically, **Figure 5.3**b shows cellular β-catenin levels following treatment of HEK293T with 25μM, 50μM, and 100μM CA for 24 hours, and shows potent β-catenin depletion at all 3 concentrations. Total B-catenin was not tested here and that is a limitation as it would have provided insight as to whether the decrease in B-catenin levels being observed is specific to Wnt signaling or not.

After observing this clear change in unphosphorylated β-catenin levels, lower concentrations of CA were applied as shown in **Figure 5.3**c for 12 hours. The results were inconclusive showing no real change in active β-catenin levels compared to control over the 5-25μM concentration range. When the same doses were administered for 24 hours (**Figure 5.3**d), a dose dependent decrease of β-catenin could be observed. The mechanism behind β-catenin being targeted for degradation is unclear although it has been proposed to be through inducing β-catenin to aggregate upon CA binding[120].

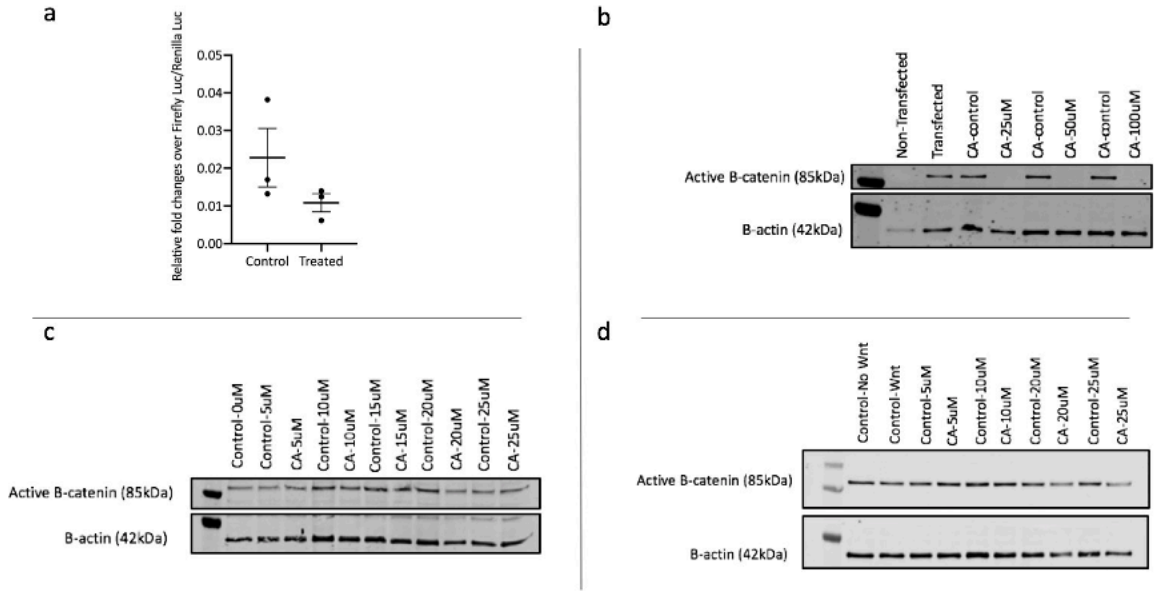

Figure 5.3 HEK293T cells respond to CA treatment.

a) TOPflash assay with 20μM CA treatment for 24 hours, t-test performed, not statistically significant. b) Western blot of HEK293T cells with CA treatment of 25μM, 50μM, and 100μM respectively for a period of 24 hours. C) Western blot of HEK293T cells with CA treatment of 5-25μM for a period of 12 hours. d) Western blot of HEK293T cells with CA treatment of 5-25μM for a period of 24 hours. The HEK293T cells were induced with 50ng/ml Wnt-3a for 24 hours prior to CA application. DMSO was used as a negative control. n=1

Following a similar stepwise approach, MSAB (**Figure 5.4**a) was applied to HEK293T cells to assess its effect on Wnt-driven transcriptional activity and active β-catenin protein levels. The result from the dual luciferase assay in **Figure 5.4**b illustrates a significant decrease in the level of luciferase signal for the HEK293T cells treated with 20μM MSAB compared to control (p =0.028) thus demonstrating a decrease in TCF/LEF triggered transcriptional activation.

This was then investigated in a 24-hour time course with 10-20μM MSAB treatment in cells which were then lysed for western blot analysis. **Figure 5.4**c shows a concentration dependent decrease in the level of active β-catenin, in line with the data in Wnt dependent cell line SW480 reported by Huang *et al*[129]. Following this result, we altered the parameters to a 12-hour time course to observe whether a decrease of active β-catenin levels could be observed on a shorter time scale in the same concentration range. We also added a concentration of 5μM as we observed a decrease at 10μM compound concentration after 24h. The result as shown in **Figure 5.4**d confirms that after 12 hours, MSAB treatment leads to depletion of β-catenin in a concentration dependent manner compared to control.

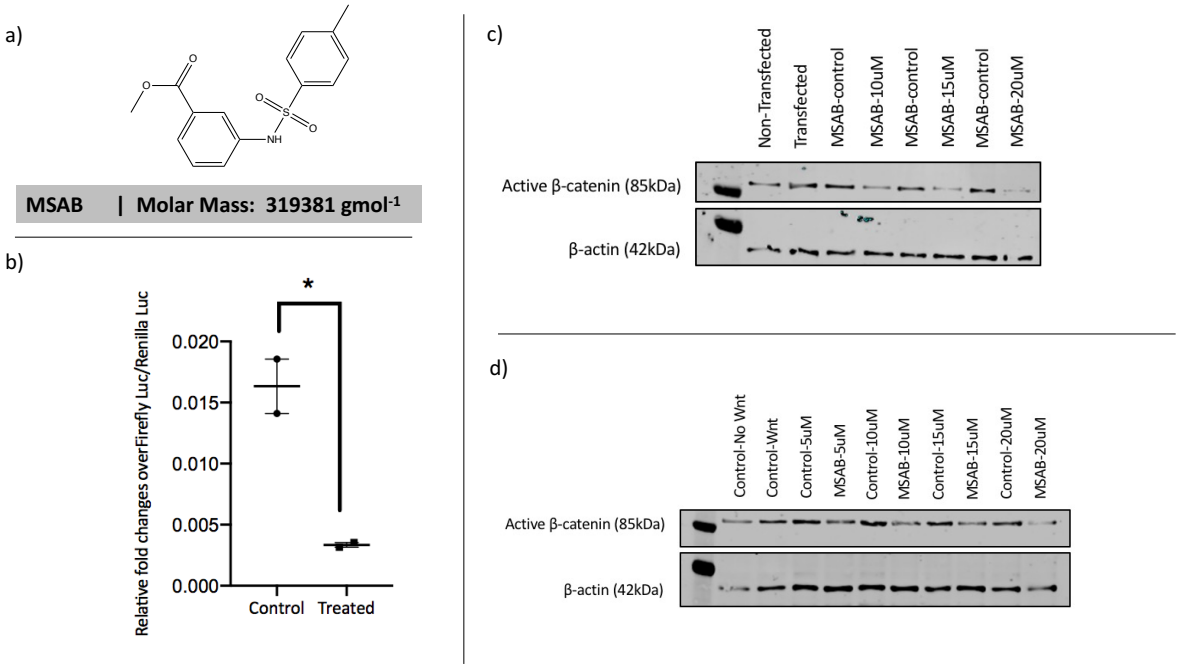

Figure 5.4 HEK293T cells respond to MSAB treatment.
*a) Chemical structure and Molar Mass of MSAB b) TOPflash assay with 20μM MSAB treatment for 24 hours. Statistical t-test performed. *, p<0.05 c) Western blot of HEK293T cells with MSAB treatment of 10μM, 15μM and 20μM respectively for a period of 24 hours. d) Western blot of HEK293T cells with MSAB treatment of 5-20μM for a period of 12 hours. The HEK293T cells were induced with 50ng/ml Wnt3a for 24 hours prior to MSAB application. DMSO was used as a negative control. n=1.*

Furthermore, to investigate the expression levels of some Wnt target genes when the cells are treated with CA, qPCR was conducted. The HEK293T cells were induced with Wnt-3a and treated with 25μM CA for 24 hours. The cells were then harvested, and the RNA was extracted. Then following reverse transcription, it was subjected to qPCR for analysis.

The results shown in **Error! Reference source not found.** demonstrate that the expression of BMP4 (p=0.017), CCND1 (p=0.023), and AXIN2 (p=0.036) has decreased significantly compared to untreated cells. This result supports the hypothesis that CA binding to β-catenin and inhibiting the BCL9 interaction subsequently hinders its efficiency in promoting transcription.

They also hypothesise degradation of B-catenin by means of CA binding and causing protein aggregation, marking it for lysosomal degradation. There is a lack of experimental evidence to explain this. In contrast, c-myc expression did not decrease and perhaps an explanation could be due to its crosstalk and involvement across signalling pathways. For example, c-myc is also known to be regulated by other nuclear effectors such as brd4, a member of the Bromo- and Extra-Terminal (BET) domain family involved in epigenetic regulation of gene expression.

Inhibition of brd4 by prototypical small molecule Brd4 inhibitors such as iBET and JQ1 is an established strategy for downregulation of oncogenic myc. Of note, there was no significant difference in the expression levels of β-catenin in the western blot between the HEK293T cells that were exposed to WNT3A and cells that weren't exposed. A possible explanation may be that the expression levels are naturally high and therefore mask the effect of induction and therefore higher doses of wnt3a is required. This is not conclusive, however a system wide investigation into the dynamics of Wnt signalling in HEK293 cells carried out by Gujral and Macbeath[133] carried out a qPCR screen of Wnt ligands that the HEK293 cells express Wnt 3, Wnt5a at high levels, along with the range of Fzd receptors, suggesting an already intact Wnt pathway. In the future, an alternative to Wnt3A is molecule CHIR99021, a GSK3β inhibitor and used in research to stimulate Wnt signaling. Furthermore, it is important to note that the decrease in β-catenin protein levels and Wnt target levels in qPCR were normalized against viability with the house keeping protein β-actin and gene 36B4 respectively. This increases confidence that the decrease observed is attributed to inhibition as opposed to cell toxicity.

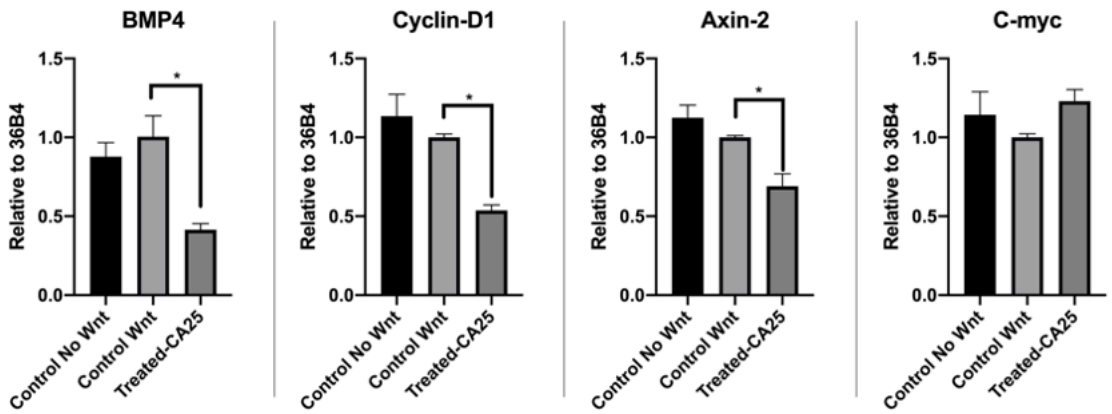

Figure 5.5. CA induces changes in the expression of Wnt target genes.

HEK293T cells were induced with 50ng/ml Wnt3a for 24 hours and subsequently treated with 25μM CA for 24 hours. The expression levels were normalized to house-keeping gene 36B4. Data analysed using ANOVA statistics. n=1

5.2.3 Working with CA derivatives in cell lines and proteomics

Thus far, in our hands CA activity in cell lines has yielded mixed results. De la Roche and colleagues[120] proposed that CA is binding directly to the N-terminal region of the ARD domain of β-catenin in vitro evidenced with NMR spectra. However, recent work by McCoy *et al*[131] surveyed a range of small molecules found in literature including CA, conducted gold standard biophysical experiments to determine the binding profile of CA with respect to β-catenin. The differential scanning fluorimetry (DSF) yielded a small 2.7°C perturbation thermal stabilisation of β-catenin in the presence of CA. When subjected to isothermal calorimetry no binding was detected. Therefore, the definitive binding site of CA remains elusive. There is evidence that CA is prone to oxidisation in mild aerobic conditions[183] and in cellular conditions it is not clear whether it is CA or one of its oxidised metabolites responsible for the biological activity.

In an attempt to understand further, we collaborated with Dr Michael McCoy (University of Southampton) to synthesise CA derivatives and cellular investigations were conducted on two of these: MAM7-139 and MAM4-141. These were chosen as there was sufficient purified material to work with and portrayed interesting R groups that may shed light on SAR properties of this catechol molecule. Figure 5.6 illustrates the structural differences between CA and these analogues. The MAM4-141 molecule has a stabilised oxidised ring structure while MAM7-139 also has the oxidised ring but in addition has a benzyl group substituted for the hydroxyl group.

CA	MAM4-141	MAM7-139
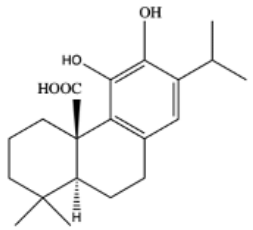	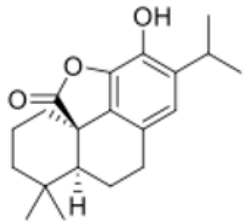	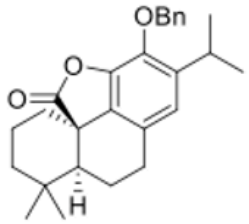
Molar Mass: 332.44 $gmol^{-1}$	Molar Mass: 314.19 $gmol^{-1}$	Molar Mass: 404.24 $gmol^{-1}$

Figure 5.6 ***CA and derivative structures with molar mass***

We investigated the phenotypic effect of MAM4-141 and MAM7-139 in cancer cell lines to ascertain if there was any noticeable cytotoxicity. We investigated cytotoxicity at a range of concentrations from 0-40μM in Wnt dependent cancer cell lines (SW480, HCT116, U2OS, MDAMB231) and non-cancer cell lines (MCF10A and ARPE-19). Cells were treated for 24 hours with either MAM4-141 or MAM7-139. Figures 5.7 to 5.11 depict cell images taken with the light microscope at 40x magnification following drug treatment.

Interestingly, in contrast to CA over the same timecourse, both derivatives show cell toxicity across the cell lines. MAM4-141 is more potent than MAM7-139 and broader spectrum compared to MAM7-139. The efficacy of these derivatives needs further optimisation as both compounds displayed toxicity in non-cancer cells as shown in **Figure 5.12** In normal breast cell line, MCF10A, MAM7-139 had an IC_{50} of 16μM while MAM4-141 produced an IC_{50} of 11μM. Similarly in retinal epithelial cell line, ARPE-19, both compounds had an IC_{50} below 10μM. Though we must acknowledge these compounds are not ready to be in the therapeutic arena and need further investigation to be more selective we might be able to start understanding some characteristics and mechanism of action that contribute to the cell toxicity compared to CA.

Furthermore, 2D crystal violet (figure 5.13, figure 5.14) and 3D soft agar (figure 5.15) cellular assays with MAM4-141 and MAM7-139 in HCT116 and SW480 cells respectively show MAM4-141 to be more potent than MAM7-139 with significant cell death occurring at 20μM with MAM4-141 compared to 40μM with MAM7-139. Therefore, due to time I prioritised MAM4-141 for the proteomic analysis.

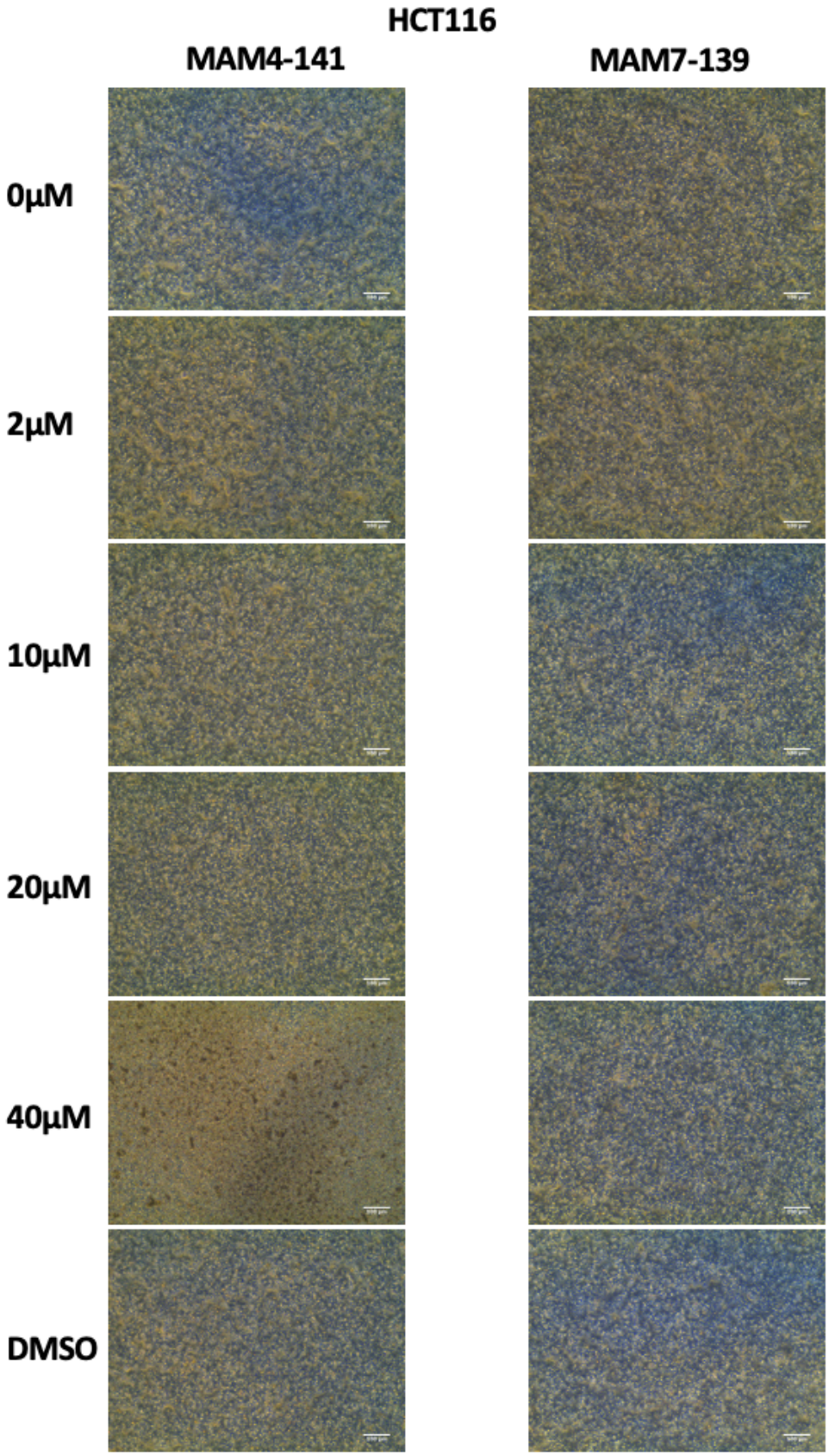

Figure 5.7 HCT116 cells with 24-hour MAM4-141 and MAM7-139 treatment.
In these images, the bright yellow colouration indicates cell death. At 40µM MAM4-141 high volume of cell death is observed. n=3

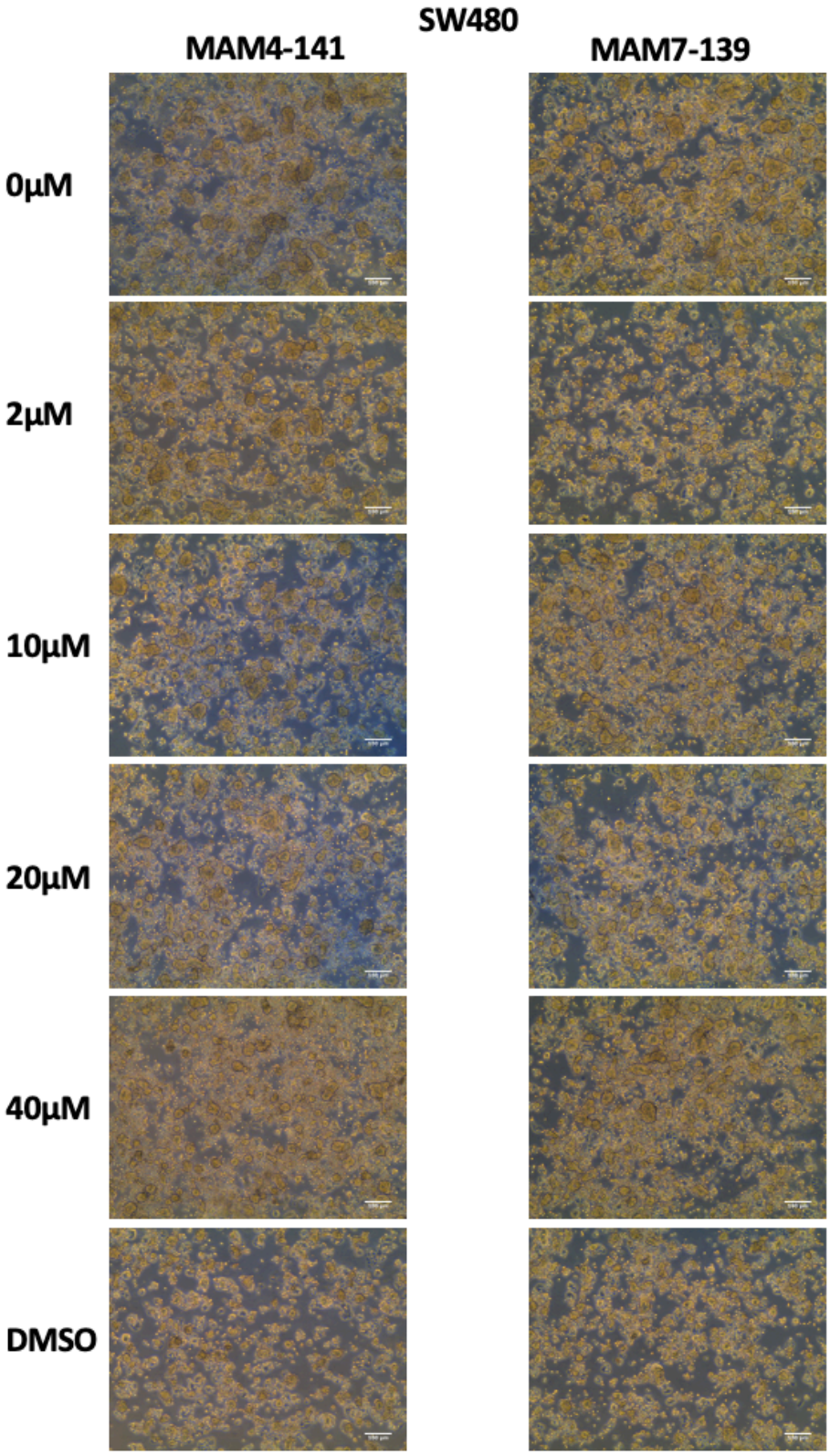

Figure 5.8 SW480 cells with 24-hour MAM4-141 and MAM7-139 treatment.
Cell death is not easily observed here due to the clustered growth style of SW80 cells. Cell death is hidden within the cluster of cells. n=3

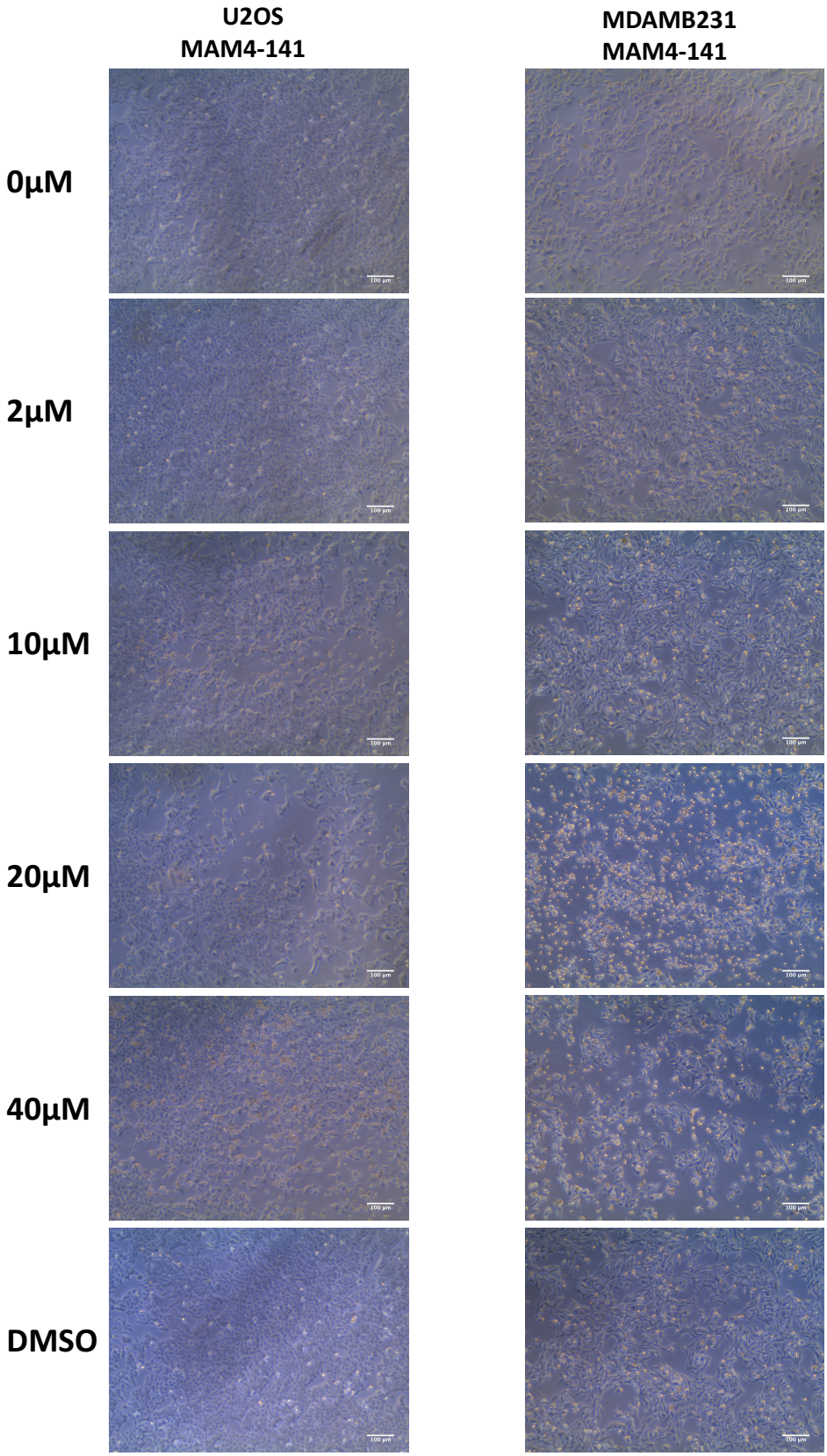

Figure 5.9 U2OS and MDAMB231 cells treated with MAM4-141 for 24 hours.
Cell death can be observed here by the yellow/brown speckles and the disruption in the ubiquitous monolayer contrasted with the control DMSO image. n=3

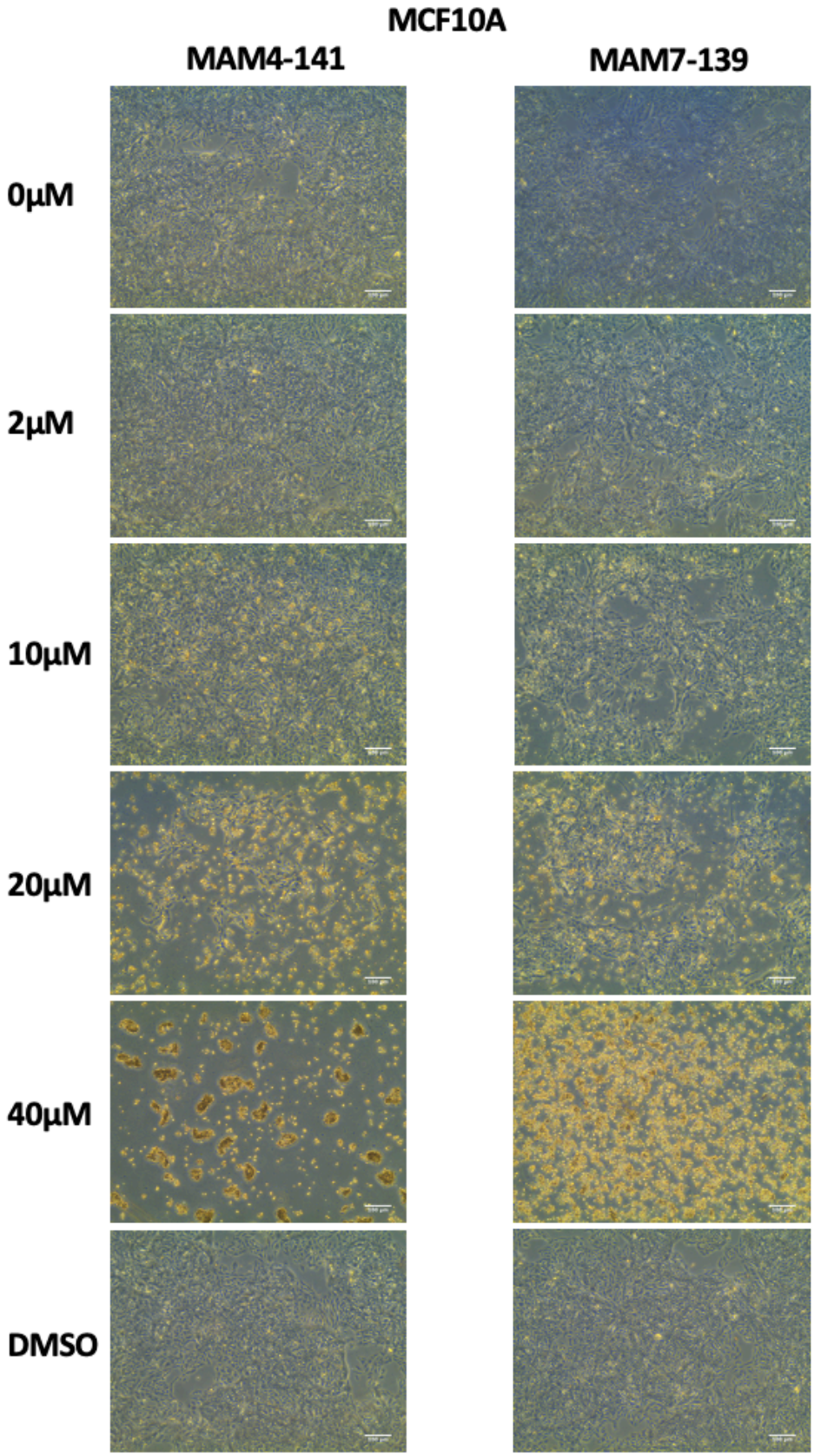

Figure 5.10 MCF10A cells treated with MAM4-141 and MAM7-139 for 24 hours.
Cell death is denoted here by the yellow spots and clumps the cells form. n=3.

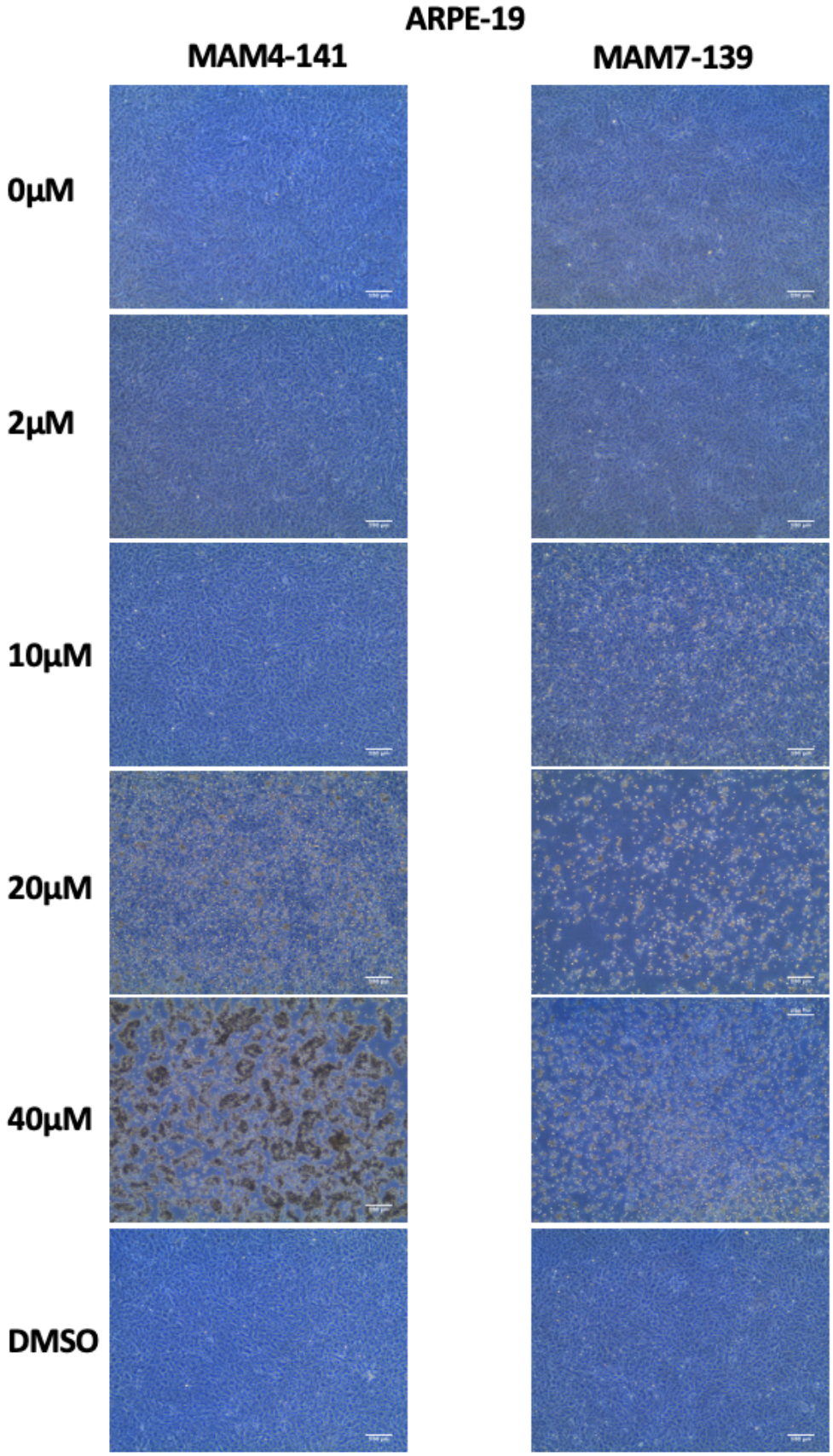

Figure 5.11 ARPE-19 cells treated with MAM4-141 and MAM7-139 for 24 hours.
Cell death is observed by the yellow to dark-coloured spots and clumps formed as cells lose their adherence and detach. n=3

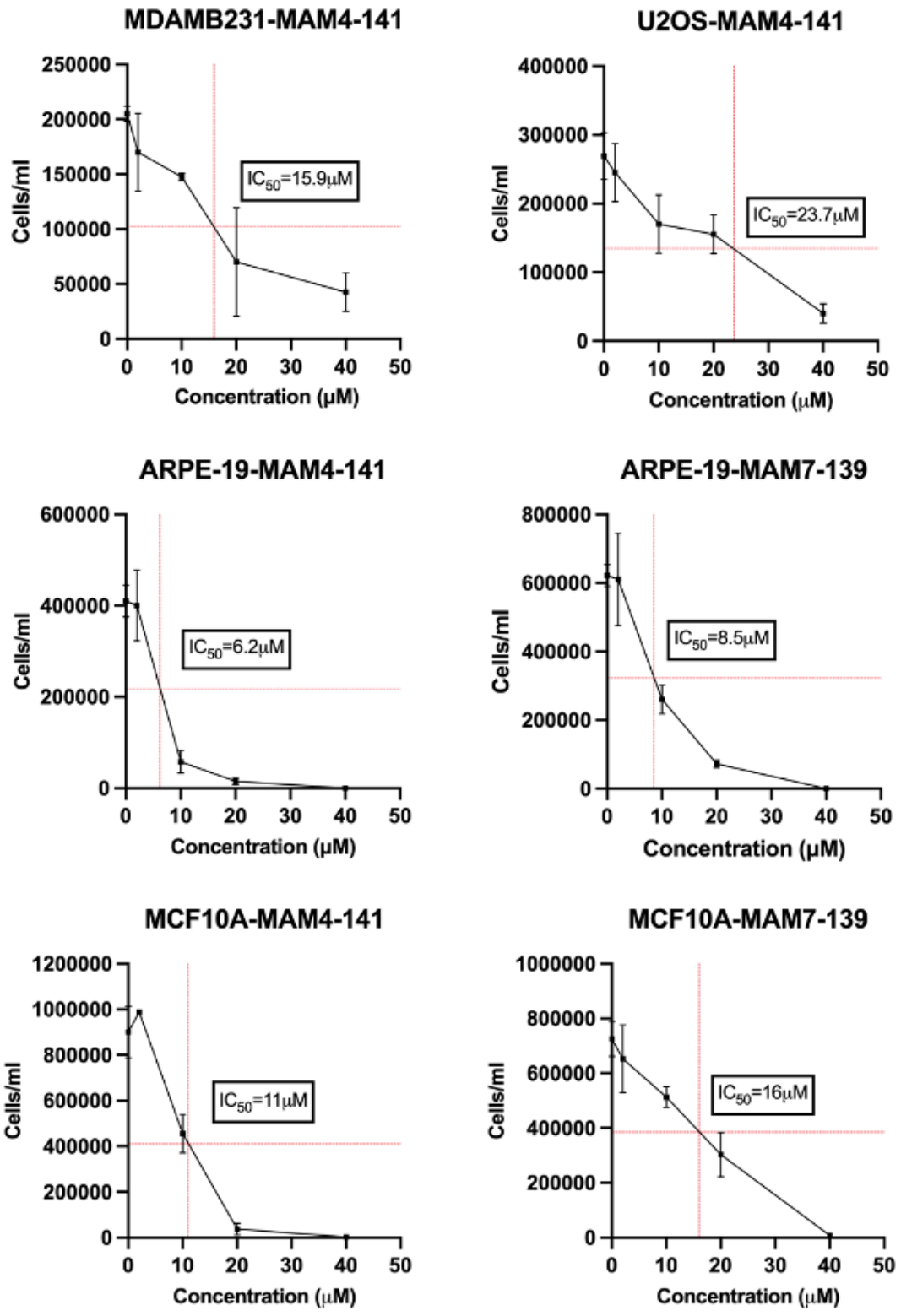

Figure 5.12 ***IC_{50} calculations of MAM4-141 and MAM7-139.***
Tested *in both cancer (MDAMB231, U2OS) and non-cancer cell lines (MCF10A, ARPE-19). IC_{50} was estimated at 50% of cell concentration. Cells were treated with compounds for24 hours and then manually counted for viability using a haemocytometer. n=3.*

Furthermore, 2D crystal violet assays (**Error! Reference source not found.**, **Figure 5.14**) were performed with a dose range between 0-40 μM of MAM4-141 and MAM7-139 compounds on HCT-116 and SW480 cells respectively over a 7 day period. The colonies were fixed dyed with crystal violet and counted using ImageJ software as described in section 2.9.1 The result is very clear showing that in HCT116 and SW480 cells, there is no observable change in number of colonies up to 10 μM of MAM4-141 treatment with 212 colonies in HCT116 and 993 colonies present in SW480 plates respectively. However, at 20 μM there is a significant drop in number of colonies with just 6 colonies in HCT116 and 126 colonies in SW480 plates respectively. At 40 μM just 2 colonies are present in HCT116 and 26 colonies in SW480 plates respectively. This indicates that MAM4-141 compound toxicity begins to occur within the range of 10-20 μM.

With respect to MAM7-139 treatment on HCT116 and SW480 cells, no significant difference in number of colonies was observed between treated and DMSO control at 20 μM. There were 121 colonies in HCT-116 and 769 colonies in SW480 plates respectively. At 40 μM there is a significant decrease where there no colonies present in HCT116 and 26 colonies in SW480 plates respectively, indicating the cell toxicity dose is between 20 and 40 μM. A limitation in this result is not having an IC_{50} value for either compound in the HCT116 and SW480 cell line. Although cell images were taken with dose treatment (**Figure 5.7** and **Figure 5.8**) cell viability calculations were not performed. An additional caveat that needs to be acknowledged is the lack of sufficient technical and biological repeats which hinders any statistical significance to be calculated. The reason was lack of laboratory time, but these experiments need to be repeated to hold accurate experimental interpretation.

To assess the three-dimensional colony tumourigenic growth, soft agar (**Figure 5.15**) cellular assays with MAM4-141 and MAM7-139 in HCT116 and SW480 cells were performed. Again, due to time a single dose of 20 μM was administered and after 14 days of cell culture, the plate was imaged with a stereo microscope and the colonies were counted using ImageJ software as described in chapter 2.9.2. The result shows that at 20 μM no significant difference was observed in number of colonies present between MAM7-139 treated and DMSO control, with an average of 184 and 195 colonies respectively in HCT116 with 560 and 733 colonies respectively in SW480 plates. in complete contrast, there were no colonies present in either the HCT116 or SW480 wells that were treated with MAM4-141 with a statistically significant difference of $p<0.0001$. Due to this clear difference in potency within these CRC cell lines MAM4-141 was prioritized for proteomic investigations.

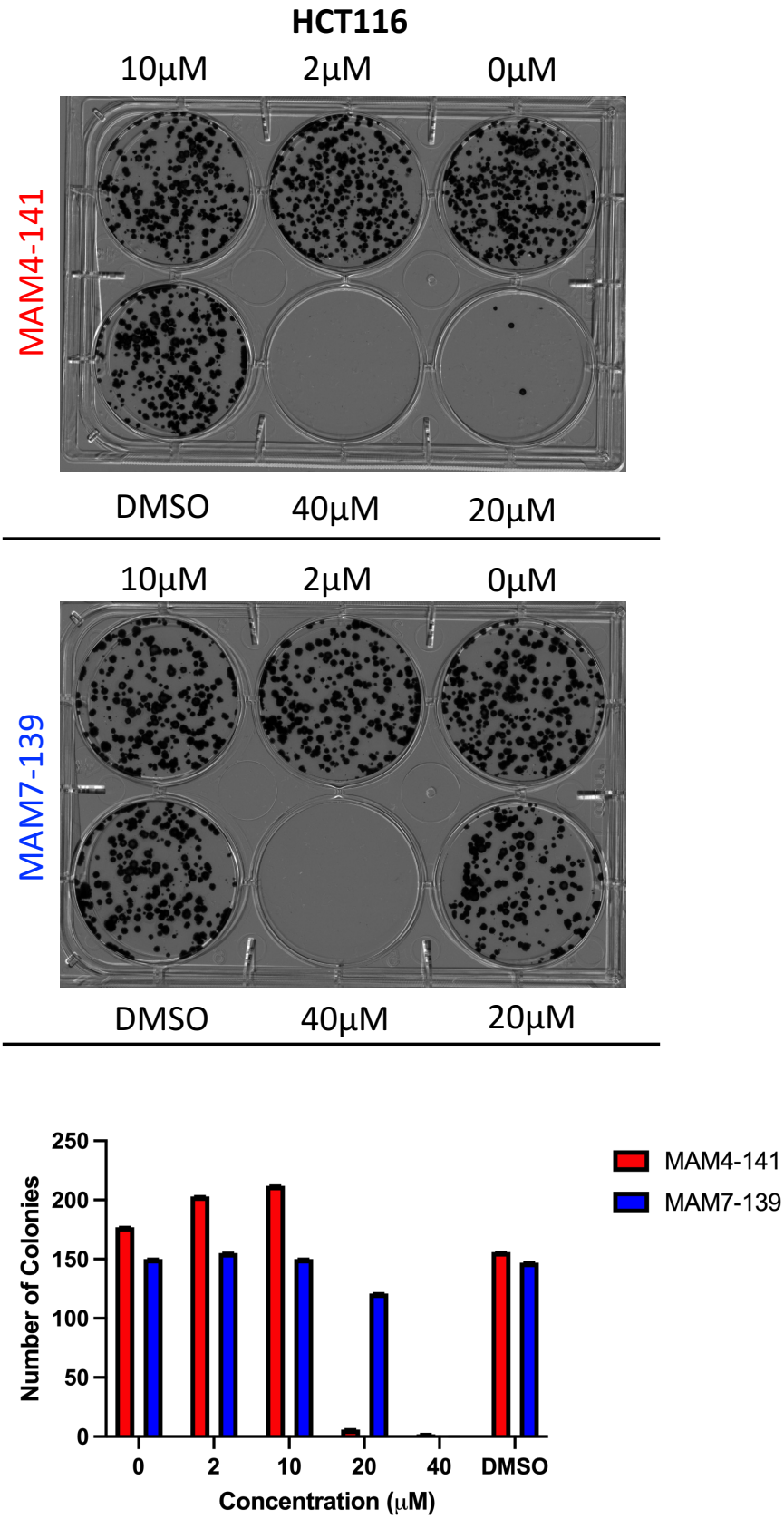

Figure 5.13. Crystal violet assay of HCT116 cells with treatment of MAM7-139 and MAM4-141. *Plate fixed after 7 days of cell culture with compound treatment. Number of colonies were counted using semi-automated procedure outlined in section 2.9.1. Statistical analysis not performed due to insufficient technical and biological repeat. n=1*

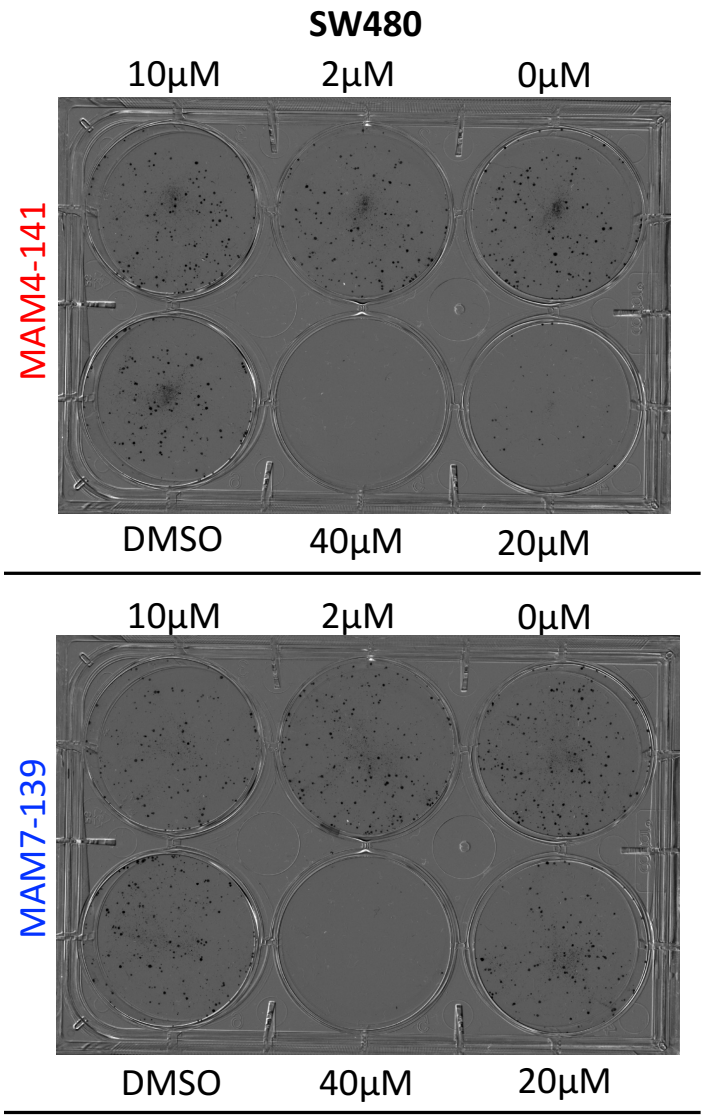

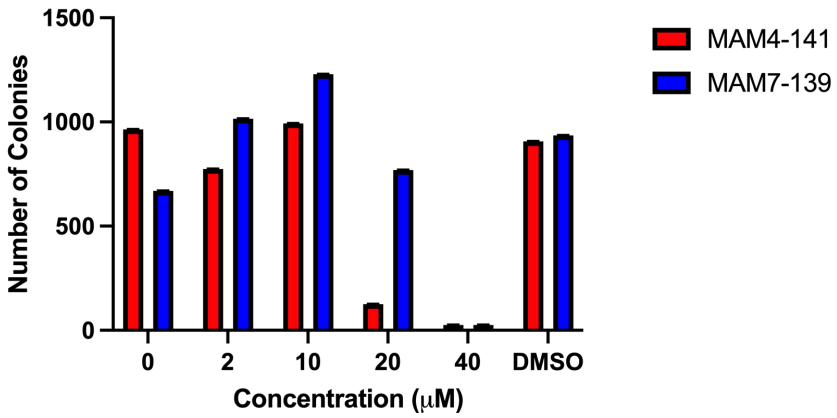

Figure 5.14 Crystal violet assay of SW480 cells treated with MAM7-139 and MAM4-141.
Plate fixed after 7 days of cell culture with compound treatment. Number of colonies were counted using semi-automated procedure outlined in section 2.9.1. Statistical analysis not performed due to insufficient technical and biological repeat. n=1

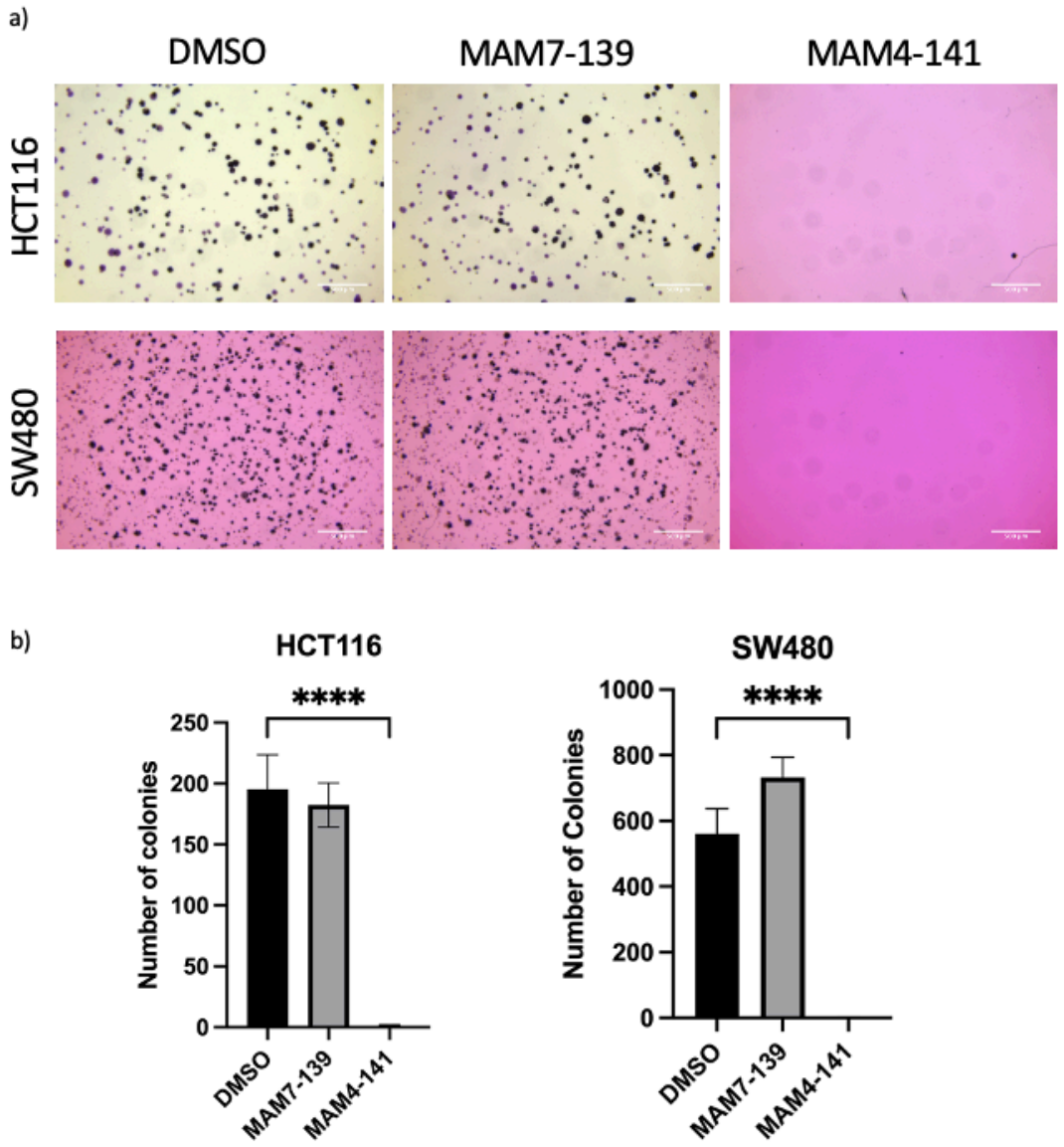

Figure 5.15 Soft agar analysis of MAM7-139 and MAM4-141.
*a) Soft agar assay images of HCT116 and SW480 cells treated with 20μM of MAM7-139 and MAM4-141 for 14 days. Images were taken with Leica Stereomicroscope. Scale bar =100 μm. b) Graph showing quantitative analysis of number of colonies Statistical T-test performed. P<0.001;****. n=3*

5.2.3.1 Proteomic analysis reveals down regulation of key carcinogenic signaling proteins with MAM4-141 treatment in SW480 cells

The SW480 cells were treated with 10μM MAM4-141 alongside DMSO control for 24 hours and subjected to Proteomic analysis (0). The rationale was based on cell viability images of SW480 cells (**Figure 5.8**), complete cell death in Clonogenic assays at 20μM and IC_{50} of 23.7μM for MAM4-141 in U2OS cells (**Figure 5.12**) to try and capture optimal conditions for effect of MAM4-141 on proteins prior to inducing cell death. The PCA plot suggests that there is sufficient data variance between control and MAM4-141 treated data (**Figure 5.16a**). The volcano plot (**Figure 5.16b**) depicting the significantly differentially expressed proteins revealed the most down-regulated protein in the MAM4-141 treated group is RIN1 (Ras and Rab interactor 1), ($p=2.85x10^{-4}$). RIN1 is present in most cancers[184] and has been reported as a key intracellular signaling protein in driving carcinogenesis in CRC[185]. Similarly, HOOK3 (Hook microtubule tethering protein 3), an adaptor protein for intracellular vesicle and protein trafficking often observed to be mutated in CRC[186] is significantly down regulated in the MAM4-141 treated sample (p=0.0097). Another down-regulated protein FASTKD5(Fast Kinase Domains 5) with p=0.014 is also frequently mutated in solid cancers.[187] The full list of differentially expressed proteins is in **Supplementary Table 4.**

Conversely, in the treated dataset DCTN5(Dynactin subunit 5) was the most significantly upregulated protein ($p=8.67x10^{-7}$). This protein is a subunit of dynactin which plays a role in microtubule dependent organelle transport and high levels are correlated with poor prognosis in various cancers.[188] Hypothetically, this could be an argument for its upregulation when treated with MAM4-141, increased expression would lead to increased transport of mRNA crucial to maintain proliferation and slow down apoptosis.

The heatmap (**Figure 5.16c**) illustrates the differences in expression through log_2 mean values between the control and treated samples. The KEGG normalised enrichment analysis for biological processes that are significantly affected are highlighted in **Figure 5.16**d. Positively enriched pathways upon treatment with MAM4-141 with 1.5-2 fold enrichment include “oxidative phosphorylation”, “chemical carcinogenesis-Reactive oxygen species”, “Thermogenesis” and “diabetic cardiomyopathy”. In contrast, the following processes were almost 2-fold negatively enriched when treated with MAM4-141, “Alcoholic liver disease” and “IL-17 signaling pathway”.

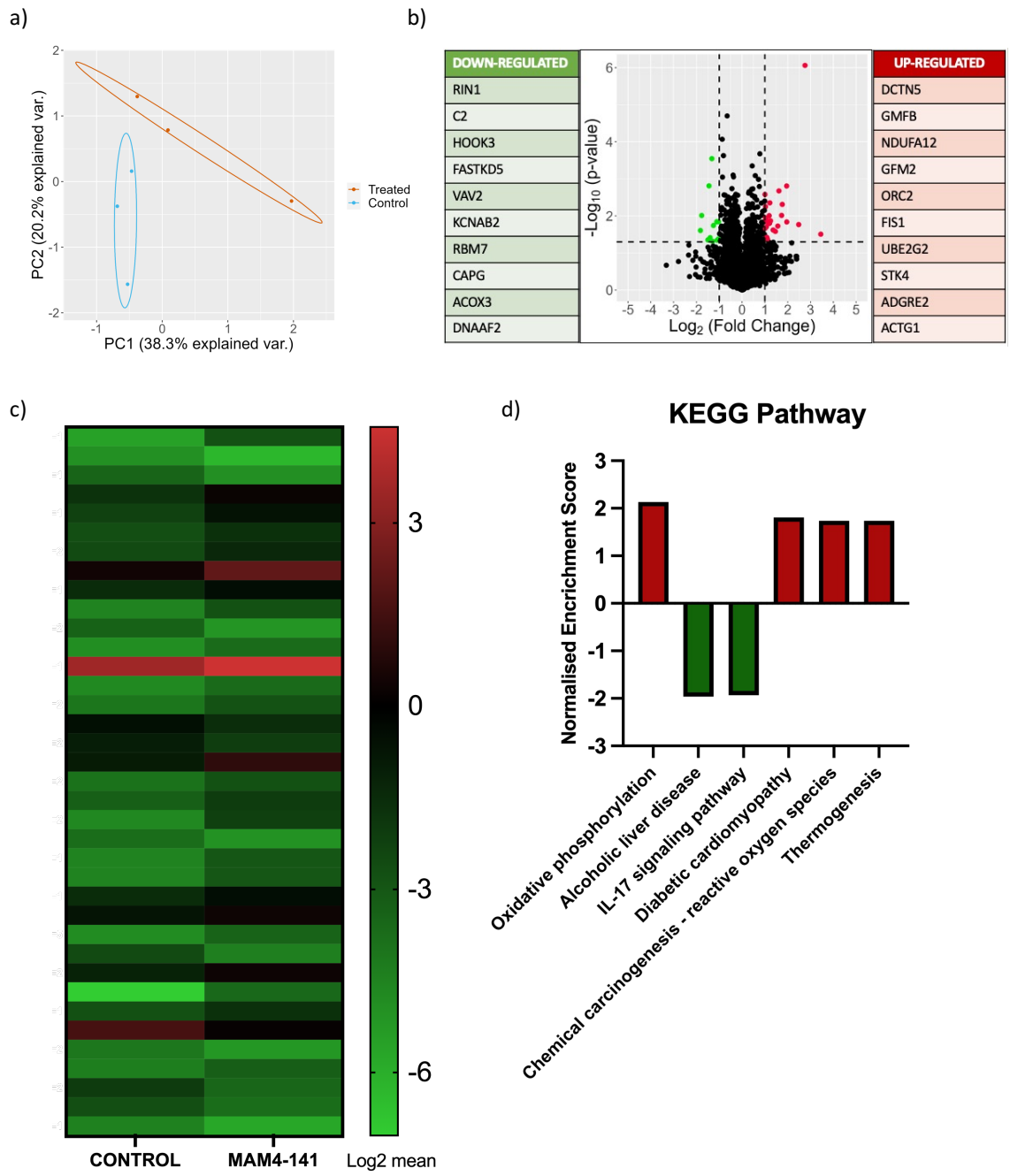

Figure 5.16 Proteomic analysis of MAM4-141 treatment in SW480 cells.
a) PCA plot illustrating the variance for the SW480 control and MAM4-141 treated datasets. b) Volcano plot highlighting up and down regulated proteins with gene symbols of 10 most significant hits with respect to p-value (P<0.05). c) Heatmap showing the log2 mean values of significantly differentially expressed genes between control and MAM4-141 treated samples. d) Graph showing normalised enrichment score from KEGG analysis showing differentially enriched pathways.

5.2.3.2 Interactome analysis reveals β-catenin selective proximity with junctional proteins when treated with MAM4-141 in U2OS cells

In the previous chapter, we demonstrated the successful implementation of the MiniTurbo system fused to β-catenin in U2OS cell model system. Employing this technique for AP-MS successfully biotinylated several known β-catenin interactors and identified potential novel interactors. Here, we thought to use this proven method to get an idea of the β-catenin interactome specifically when treated with MAM4-141 and subsequently add another dimension to the proteomic analysis of the effect of MAM4-141.

The experimental design involved treating both U2OS β-catenin MiniTurbo positive cells (MT) and the U2OS empty vector control cells (EV) with 10μM MAM4-141(T) and the equivalent volume of DMSO(C) as vehicle control having 3 biological replicates for each. This layout enabled us to achieve representative data as we had two-layer controls. Both qualitative and quantitative analysis was conducted. For qualitative stringent selection, the list of biotinylated proteins from all the biological repeats (R1 OR R2 OR R3) of the EV(T) were removed if present in the MT(T) set. The MT set consisted of proteins present in at least 2 out of 3 biological repeats (R1&R2 OR R1&R3 OR R2&R3). This was repeated for the MT(C) and EV(C) sets respectively. The second step was to now subtract the proteins from updated MT(C) that are present in the updated MT(T). The resulting group of biotinylated proteins are shown in **Figure 5.17a**. However, a limitation with the study is that β-catenin levels in U2OS cells were not assessed by western blot prior to interactome analysis to ensure the levels of B-catenin were not adversely affected so that levels of interactions were not skewed.

For the quantitative SAINT[1(157)] analysis, PSM values for each biological repeat CONTROL input was selected in the following manner [MT(C)-R minus EV (C)-R1 OR R2 OR R3] and the same format for each treated (BAIT) biological repeat input: [MT(T)-R minus EV (T)-R1 OR R2 OR R3]. This was submitted in a tabular format into the SAINT software. The software using Bayesian formula predicted the SAINT probability score for true interactions. The resulting BAIT-PREY network and corresponding figures are shown below in **Figure 5.17**b**.** The full list of proteins from SAINT analysis can be found in **Supplementary Table 5.** The network generated from the qualitative analysis has more hits than the quantitative method due to the applied threshold, but there are strong overlaps. Of note, **Figure 5.17**a highlights a string of biotinylated proteins that have physical associations and the GO cell component has flagged up these proteins as being associated with cell-cell junction and junction complex and highlighting that β-catenin is in close proximity and possibly directly binding.

The role of β-catenin at the cell junction is well established and perhaps an extrapolated argument that would need further investigation could be that MAM4-141 is indirectly affecting the cell polarity and anchoring the cells decreasing migration and EMT.

a)

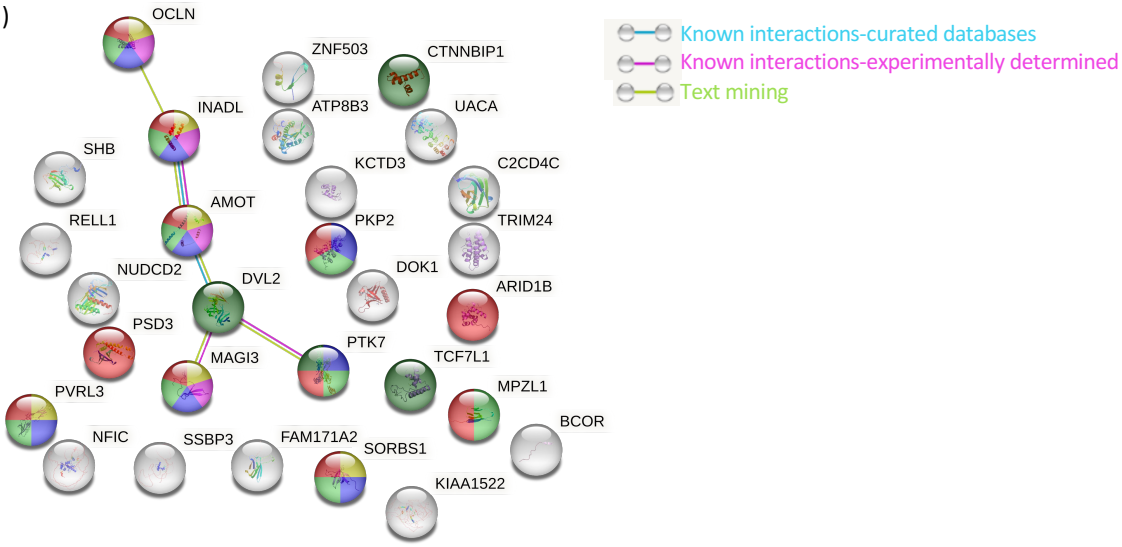

Cellular Component (Gene Ontology)				
GO-term	*description*	*count in network*	*strength*	*false discovery rate*
GO:0043296	Apical junction complex	6 of 143	1.45	0.00012
GO:0005923	Bicellular tight junction	4 of 122	1.34	0.0145
GO:0005911	Cell-cell junction	8 of 490	1.04	0.00037
GO:0070161	Anchoring junction	9 of 820	0.87	0.0011
GO:0030054	Cell junction	11 of 2075	0.55	0.0307

b)

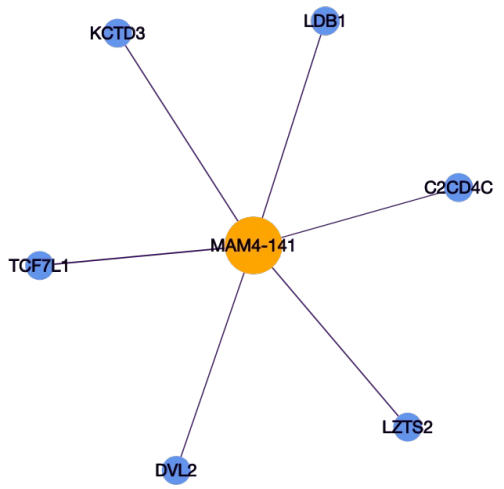

Gene name	MaxFCA	SAINT Probability
KCTD3	9.12	0.96
TCF7L1	7.46	0.88
LZTS2	5.52	0.64
DVL2	6.09	0.62
LDB1	4.97	0.58
C2CD42	3.95	0.52
NFIC	3.83	0.47
CTNNBIP1	7.36	0.46
AMOTL1	3.64	0.42
RELL1	3.09	0.41

Figure 5.17 β-catenin interactome analysis with MAM4-141 treatment by proximity-dependent biotinylation.
a)Protein network produced from qualitative analysis using STRING[(159)] software, nodes coloured according to table showing terms for GO Cellular component. Edges illustrate physical associations between proteins colour coded by key. The nodes highlighted with darker green shade. b) Protein network of BAIT and PREY derived from SAINT analysis with a threshold (above red line) set at SAINT Probability score >0.5 AND Max Fold Change (FCA) >3. Figures shown in table on Right Hand Side. MAM4-141 shown in centre in yellow for illustrative purpose only, authentic BAIT is CTNNB1. n=3.

5.3 Discussion

As mentioned in the literature review, there have been extensive efforts from various research groups to target Wnt signaling components and bring a Wnt signaling inhibitor to the clinic for the treatment of various diseases, especially cancer. This has proven to be extremely challenging given the complexities involved with the Wnt signaling being involved in regulatory processes such as stem cell homeostasis and tissue regeneration. β-catenin, has been central to these efforts.

One of the aims of this study was to investigate the effect of novel small molecules on cells on *in vitro* systems and this highlighted the difficulty that comes with reproducing previously published results because in our hands regardless of whether HCT116 or SW480 cells were used, we didn't observe any significant degradation when treated with Carnosic acid. However, the stabilised derivatives of CA (MAM7-139 and MAM4-141) certainly displayed cytotoxic properties when applied at higher concentrations (10-40 μM) across a range of cancer cell lines. However, further work is required on altering structure activity relationship to achieve selective toxicity because our results show that both derivatives displayed toxicity in healthy cells (ARPE-19, MCF10A). Therefore, we must proceed cautiously when interpreting results.

The combination of treating cells with MAM4-141 and subjecting it to whole proteomic and targeted affinity purification offers insights for discussion. The analysis of these genes highlights a complex and multi-dimensional relationship between Wnt/β-catenin signaling and essential cellular processes, including cell adhesion, cytoskeletal dynamics, intracellular trafficking, transcriptional regulation, and angiogenesis. The findings emphasize how Wnt signaling acts as a central hub connecting diverse molecular pathways to drive cancer progression and how dysregulation of these genes influences the tumour microenvironment, immune response, and therapeutic resistance.

The down regulation of proteins like Ras and Rab interactor 1 (RIN1) reduces Ras signaling activity, which may cause decreased β-catenin nuclear localization due to the loss of Ras/ERK cross-regulation with Wnt[189]. This can impair tumour growth and invasion and it may protect uncontrolled growth. Similarly, Vav Guanine Nucleotide Exchange Factor 2 (VAV2)[190] and Capping Actin Protein Gelsolin-Like (CAPG) proteins both regulate actin cytoskeleton dynamics. Their down-regulation in the MAM4-141 treated SW480 sample set, disrupts actin remodelling, impairing epithelial-mesenchymal transition and thus reducing cell migration and metastatic potential. From this analysis, further investigation is warranted for understanding the mechanism of action of MAM4-141 if it may be playing a role in reducing tumour characteristics.

Interestingly, among the significant proteins that were selected by stringent analysis in **Figure 5.17**a are β-catenin interacting protein 1 (CTNNBIP1) and Membrane associated guanylate kinase (MAGI3). Both these proteins function as negative regulators of β-catenin-dependent transcription by promoting its degradation or preventing its interaction with TCF/LEF transcription factors. A hypothesis to test is perhaps what role and mechanism is MAM4-141 playing to help promote β-catenin degradation.

From the cell viability and colony formation results, we have observed that MAM4-141 when administered across both cancer and healthy cell lines, results in cell death. It is highly probable that it is driving apoptosis. It is worth investigating and confirming by Western blot if levels of B-catenin are decreased in the presence of MAM4-141 treatment. In a wider context, uncovering the mechanism of action of MAM4-141 could help to refine its structure activity relationship to achieve selectivity in potently targeting cancer cells and not healthy cells. In summary, combining research tools like small molecules with targeted mass spectrometry, allows a greater a breadth of analysis to uncover the effect of compounds on cell proteomes and interactomes.

Chapter 6 Overall Discussion

The overarching aim of this research project was to explore β-catenin signaling and its protein-protein interactions (PPIs) using modern proteomic tools, particularly through the application of CRISPR-induced β-catenin knockout (KO) in the U2OS osteosarcoma cell model system. The successful implementation and verification of β-catenin KO not only corroborated previously published work but also provided reproducible insights into β-catenin's role in cancer biology. The significant downregulation of cancer-associated proteins in the CTNNB1-depleted dataset underlines β-catenin's influence in cancer propagation and pathology.

6.1 Insights and Reproducibility

The data generated in this study highlighted the power of CRISPR-based β-catenin KO to elucidate the roles of β-catenin in signaling and cancer biology. Several pathways identified in this study align with previously published research, reaffirming the robustness and reproducibility of the findings. This congruence with the literature enhances the confidence in the β-catenin interactome and the biological significance of the identified protein candidates.
However, while the data offer valuable insights into β-catenin's regulatory network, its interpretation is limited by the absence of multi-cell-line validation and complementary approaches such as siRNA-induced knockdown. The lack of cumulative proteomic data across multiple cell models restricts the broader applicability of these findings. Expanding the study to include additional cancer cell lines and different genetic backgrounds would provide a more comprehensive picture of β-catenin's context-dependent roles.

6.2 Multi-Omic Integration and Functional Analysis

To further enhance the understanding of β-catenin's role in cancer, multi-omic studies integrating transcriptomic and proteomic data should be conducted. As demonstrated by Ewing *et al*[191], the integration of multiple omic layers can reveal distinct molecular signatures and provide deeper insights into the cancer-specific niches and tumour microenvironment. Transcriptomic data would help to elucidate mRNA-level changes that correlate with proteomic observations, offering a more holistic view of β-catenin-driven oncogenic pathways.
Additionally, the functional enrichment analysis of key signaling pathways affected by MAM4-141, including the observed downregulation of cancer driver proteins and the upregulation of reactive oxygen species (ROS)-related proteins, highlights the potential mechanistic role of β-catenin in controlling cellular redox balance and oncogenic signaling. This warrants further investigation to explore how junctional proteins and oxidative stress pathways intersect with β-catenin's oncogenic function.

6.3 MiniTurbo and Proximity Biotinylation for β-Catenin Interactome Mapping

The optimized MiniTurbo biotin ligase system has proven to be a highly sensitive approach for studying β-catenin protein-protein interactions (PPIs), revealing over 30 high-confidence interactors (SP > 0.95) and identifying 315 unique prey candidates. These candidates represent a valuable starting point for understanding β-catenin's interactome in living cells.
While this qualitative approach has generated a rich dataset, it is crucial for future work to include CRAPome (Contaminant Repository for Affinity Purification) analysis once it is functioning. This would allow for rigorous cross-referencing against large datasets of known contaminants and negative background controls, significantly reducing the false discovery rate and increasing the confidence in the identified interactors. Such analysis would ensure that the high-confidence hits are truly β-catenin-specific interactors rather than general background proteins.

An exciting future direction would be to adapt MiniTurbo to be a platform for compound treatment experiments as tested here with the effects of MAM4-141 on β-catenin's interactome. Although this approach does not directly reveal the compound's target protein or binding site, it offers valuable insights into how the β-catenin interactome shifts in response to treatment. Coupling this with functional analysis would help elucidate the mechanism of action and uncover potential therapeutic targets.

6.4 Expanding Beyond a Single Bait Protein

A key limitation of the current study is that it utilized only one bait protein (β-catenin), providing a single perspective on the interactome. While the cross-validation of hits across multiple baits enhances confidence in interactors, the lack of additional baits restricts the broader applicability of the findings. In contrast, the Human Cell Map® developed by Go *et al*[179] successfully implemented proximity-biotinylation for 192 bait proteins in HEK293 cells, identifying over 4,000 unique proteins and mapping their subcellular localization.
Adapting this approach to incorporate multiple bait proteins that are key cancer biomarkers—especially in different cancer cell lines—would help create a comprehensive map of the cancer interactome. This would not only shed light on cellular context-specific networks but also facilitate compound screening for drugs like MAM4-141, helping to optimize efficacy and target selectivity. Another limitation that has been observed is the absence of complementary knockdown approaches. While CRISPR KO is powerful, integrating siRNA-induced knockdown would provide additional validation and offer insights into transient versus permanent loss of β-catenin.

Furthermore, the lack of transcriptomic data means the study does not capture the gene expression changes associated with β-catenin loss, which could reveal regulatory networks missed at the protein level. Finally, throughout out the chapters, assertions and suggestions have been made with respect to functional analysis of the proteomic data. However, functional validation of several identified interactors is still lacking. Confirming their roles in cell proliferation, migration or apoptosis for example would increase the biological relevance of the findings.

6.5 Future work and research directions

As mentioned above, conducting multi-omic and cross-validation studies by integrating transcriptomic and proteomic datasets would provide a more comprehensive understanding of β-catenin's influence on cancer signaling. This should be coupled with validating key findings across multiple cancer cell lines to ensure broad applicability. The data would be enhanced if it were to be expanded to multi-bait systems. Future work should include additional bait proteins in the Wnt signaling pathway in different cellular contexts to create a more comprehensive cancer interactome map. Focus should begin on proteins involved in oncogenic signaling, cell adhesion and DNA repair linked to poor disease prognosis for deeper insights. There is potential to expand this system for other applications too. In 2024, Hanswillemenke and colleagues[(192)] developed "Drug-ID", a novel methodology applying proximity biotinylation to identify protein-drug interactions in living cells potentially identifying excellent molecules for hard to treat diseases.

One of the limitations involved having an incomplete functional analysis for the unique identified interactors. So next steps should focus on conducting functional enrichment analysis to validate the role of key interactors in processes like cell migration and proliferation that drive tumour growth. It would also be beneficial to investigate the mechanism of action of MAM4-141 using targeted proteomics and biochemical assays to identify its precise targets. Co-immunoprecipitation could be carried out to validate the potential interactor candidates of interest. Finally, in a similar vein, to identify further targets within β-catenin's interactome, MiniTurbo could be adapted for high-throughput screening. This could lead to new therapeutic strategies for targeting β-catenin-driven cancers.

In conclusion, although Wnt signaling and β-catenin biology have been studied for over 40 years, there remain many unanswered questions regarding its basic biology and therapeutic targeting. Modern tools like CRISPR, MiniTurbo, and multi-omic integration are bringing us closer to addressing these gaps. This study provides a foundation for future work aimed at understanding β-catenin's interactome and optimizing targeted therapies for β-catenin-driven cancers.

Appendix

Supplementary Table 1. Full list of gene names of respective proteins that are differentially expressed with CRISPR KO of CTNNB1 in U2OS cells. '-' connotation indicates downregulation of that protein. p<0.05, n=3

Gene name	Treated log2 mean	Control log2 mean	log2fold	P value
ITGA2	1.624713	0.441950	1.182763	0.000126
CISD1	-0.482188	-1.867282	1.385094	0.000195
MAK16	3.900769	2.179619	1.721150	0.000248
DCTN1	-0.936264	0.241937	-1.178201	0.000331
CHCHD2	1.730549	0.403622	1.326927	0.000406
GORASP2	0.229205	-1.062424	1.291629	0.000510
CIT	-2.117188	-0.943917	-1.173270	0.000560
SELENOH	-0.537543	-2.524337	1.986794	0.000592
TOP1MT	-8.090358	-6.272724	-1.817634	0.000662
PLA2G15	-2.532810	-4.094980	1.562170	0.000789
CADM3	-1.484783	-0.181796	-1.302986	0.000827
ADD1	0.146253	1.207674	-1.061420	0.000850
FAU	2.115854	0.643102	1.472751	0.000950
TNS1	-1.023309	0.127046	-1.150355	0.001232
JCAD	-1.630593	-2.704365	1.073773	0.001250
APOBEC3B	0.522419	1.910379	-1.387960	0.001304
ACTR1B	-2.818932	-1.663343	-1.155589	0.001399
MPND	-6.079451	-4.309297	-1.770154	0.001403
ITGA6	1.955872	0.121607	1.834265	0.001555
SQSTM1	0.576938	-1.484592	2.061530	0.001857
GRPEL1	3.517052	2.196710	1.320342	0.001881
SRSF8	-0.366515	-1.903467	1.536952	0.001890
DDAH1	-3.193787	-5.365683	2.171896	0.001904
HSPA1A	5.378252	3.899081	1.479171	0.001934
HSPA1B	5.378252	3.899081	1.479171	0.001934
ARHGAP17	-6.668353	-5.414071	-1.254282	0.002115
AATF	4.774604	3.756618	1.017986	0.002155
SIPA1	-2.742590	-1.255442	-1.487148	0.002274
PLOD1	2.447262	3.566878	-1.119616	0.002317
FLYWCH1	-0.623848	-2.165028	1.541180	0.002633
NEXN	-0.221600	-1.256947	1.035347	0.002691
KRT17	-5.683965	-2.839636	-2.844329	0.002776
MOV10	-2.067499	-0.487127	-1.580373	0.002780
NGRN	-1.535007	-2.739531	1.204524	0.003289
RSRC1	0.409550	-0.657139	1.066689	0.003379
TLK1	-4.193548	-2.702170	-1.491378	0.003564
FN1	-0.913689	0.286960	-1.200649	0.003809

Gene name	Treated log2 mean	Control log2 mean	log2fold	P value
PHLDB1	-1.225844	-0.201099	-1.024745	0.003958
PARP14	-4.783157	-3.007186	-1.775971	0.004063
CAVIN2	-0.656497	-3.393332	2.736834	0.004147
RNPS1	5.064211	3.817652	1.246559	0.004300
SPCS1	-4.801782	-3.129302	-1.672480	0.004382
TGFB2	-1.442448	-0.121325	-1.321123	0.004655
NDUFAF2	1.648891	0.596446	1.052444	0.004849
THRAP3	4.388456	2.651873	1.736583	0.004888
DCTN4	-2.389761	-1.188002	-1.201758	0.005292
CSPG4	-3.343390	-1.478291	-1.865098	0.005292
RPS16	3.625091	4.706273	-1.081183	0.005293
CLEC11A	-2.161559	-3.829442	1.667884	0.005390
DNM1	-0.833916	0.544285	-1.378201	0.005484
M6PR	3.218066	1.944360	1.273706	0.005811
CALCOCO2	0.519346	-1.695404	2.214749	0.005877
AKAP8L	2.651749	1.259066	1.392684	0.006348
COL6A1	-0.420776	1.170580	-1.591356	0.006411
ADGRG1	-6.266258	-4.542829	-1.723429	0.006563
GSK3B	-5.665011	-4.267080	-1.397930	0.006699
RACGAP1	1.627277	0.574006	1.053271	0.006809
SMARCA1	-0.221001	1.374304	-1.595305	0.006899
TLN1	0.629645	1.688757	-1.059112	0.007249
RBMS2	-3.029257	-4.838308	1.809051	0.007271
DNM2	-0.097458	0.933765	-1.031222	0.007493
VCL	-2.167175	-0.373940	-1.793235	0.007569
MRPL34	-0.760222	-2.321836	1.561614	0.007934
HTATSF1	2.224658	0.705961	1.518698	0.008322
LLPH	1.323711	-0.929018	2.252730	0.008355
ACTR1A	-0.447254	1.001212	-1.448466	0.008386
EIF3L	0.260172	1.702958	-1.442786	0.008464
SLC5A3	-3.255593	-0.979203	-2.276389	0.008707
MMTAG2	1.493821	0.321582	1.172239	0.008919
FASN	-0.957908	0.746813	-1.704721	0.009131
CERS6	-2.952081	-0.954682	-1.997399	0.009514
STAT1	-4.380219	-3.012617	-1.367603	0.009579
TOR1A	-2.211035	-1.163934	-1.047101	0.009703
COPG2	-3.132832	-0.635012	-2.497819	0.009960
LMAN1	3.377850	2.285314	1.092536	0.010338
TIMM22	-0.800947	-1.895506	1.094559	0.010500
RPS27	-3.478820	-2.093691	-1.385129	0.010743
EXOC2	-1.733130	-0.597371	-1.135759	0.010766

Gene name	Treated log2 mean	Control log2 mean	log2fold	P value
PALLD	2.321581	3.824074	-1.502493	0.010802
PBK	-2.942588	-1.876128	-1.066460	0.010822
PHC2	-0.286438	-1.760295	1.473857	0.010921
SART1	4.677387	3.569722	1.107665	0.011117
ZCCHC3	-6.714477	-3.871907	-2.842570	0.011262
RMND1	-1.449098	-3.362447	1.913349	0.011478
LMF2	-7.439577	-5.851149	-1.588428	0.011536
GPATCH4	1.205791	-0.333474	1.539265	0.011734
RNF114	-4.282261	-6.528940	2.246679	0.011794
NCAPG	-0.881058	0.665963	-1.547021	0.012335
ZZZ3	-2.688199	-5.548405	2.860206	0.012408
LSS	-0.727791	0.417691	-1.145481	0.012658
SNRNP48	-1.935380	-2.941297	1.005916	0.012737
PDK1	-4.458852	-3.167376	-1.291476	0.012802
AKAP2	3.678024	2.350339	1.327685	0.012822
POR	1.242649	2.343150	-1.100501	0.013085
CLASRP	1.655879	0.565352	1.090528	0.013219
DRG1	0.457382	1.628017	-1.170635	0.013310
GEMIN4	-4.084327	-1.753412	-2.330915	0.013515
CYFIP1	-1.256802	0.408117	-1.664919	0.013559
ARL 3.00	-4.721929	-3.435810	-1.286119	0.013707
FOSB	-2.426592	-0.026216	-2.400376	0.014044
SURF6	0.260380	-1.103771	1.364151	0.014628
DHCR7	-1.645791	0.592946	-2.238737	0.014784
TMEM147	-2.185488	-3.296083	1.110595	0.014813
PPTC7	-1.701774	-2.855160	1.153386	0.014978
PPP6C	-7.055112	-4.969467	-2.085645	0.015007
COL1A1	-4.166115	-1.452013	-2.714103	0.015298
ANAPC7	-0.543107	0.629035	-1.172142	0.015527
ACAD8	-2.679269	-4.180530	1.501262	0.015733
ACLY	0.909830	2.075893	-1.166064	0.015823
MCAM	1.333138	0.142914	1.190224	0.015913
LUZP1	-1.559642	-2.595327	1.035685	0.016209
BAG3	1.730026	-0.394435	2.124461	0.016228
MICALL2	-1.382879	0.206790	-1.589669	0.017036
DHX57	-3.942327	-2.850057	-1.092270	0.017720
SEPTIN10	-0.034499	1.202935	-1.237435	0.017746
VPS16	-3.612029	-1.009915	-2.602114	0.017834
LNPK	-7.216877	-6.025271	-1.191605	0.017949
ARG2	1.338386	0.212052	1.126335	0.017980
MEAK7	-3.399344	-2.393046	-1.006298	0.018230

Gene name	Treated log2 mean	Control log2 mean	log2fold	P value
LRWD1	0.977567	1.991094	-1.013527	0.018510
SHKBP1	-5.552560	-3.663538	-1.889022	0.019631
NCAPD3	-1.544424	0.478944	-2.023368	0.019905
SAP18	1.223209	2.325008	-1.101799	0.020244
DCXR	-4.571532	-8.227355	3.655823	0.020252
UBP1	-5.587941	-3.801577	-1.786365	0.020350
FDFT1	-1.219241	0.192212	-1.411453	0.020483
BANP	-2.107631	-3.157854	1.050223	0.020818
TFDP2	-5.309425	-6.523963	1.214537	0.020977
RBMXL1	1.393585	-0.365921	1.759506	0.021368
CAMK2D	-1.928049	-0.741028	-1.187021	0.021401
ATF7IP	1.153375	0.116907	1.036468	0.021441
EMB	-2.359303	-3.492854	1.133551	0.021529
ZNF185	0.669896	-1.091097	1.760993	0.021607
SQLE	-0.998021	0.160186	-1.158207	0.021956
CCDC102A	-0.867298	-2.310460	1.443161	0.022007
HSD17B10	5.877132	4.767878	1.109254	0.022188
REXO4	2.052684	0.353438	1.699246	0.022285
PLCB3	-2.459513	-1.120319	-1.339194	0.022407
ALDH5A1	-0.808609	-2.333741	1.525132	0.022785
RPL35	2.940202	1.149088	1.791114	0.022853
SRSF9	5.975669	4.633351	1.342318	0.023007
ATP6AP2	-1.226184	0.260456	-1.486640	0.023454
ACSL3	1.116323	2.270939	-1.154615	0.023743
CDK6	-4.247148	-2.849068	-1.398080	0.023994
LUC7L2	1.876490	0.498167	1.378323	0.024106
RSL24D1	0.143478	-1.077495	1.220973	0.024219
EWSR1	4.301168	2.952676	1.348492	0.024721
CTNNA1	1.144817	2.438342	-1.293525	0.024744
FAM210B	-5.476470	-3.038400	-2.438070	0.024825
TFPT	-1.209751	-2.988923	1.779172	0.024865
JUN	2.839493	1.774565	1.064927	0.024886
NCAPD2	-1.080038	0.404901	-1.484939	0.024964
PCM1	-0.215805	-1.731605	1.515800	0.025907
TGFB1	-4.682332	-2.149801	-2.532531	0.026921
SGF29	-1.573551	-0.365386	-1.208165	0.026940
GTF2I	1.419712	2.562307	-1.142595	0.026970
RRP15	3.985719	1.941998	2.043722	0.027066
SRSF7	6.928316	4.723196	2.205120	0.027078
RANBP1	2.549241	1.391442	1.157800	0.027440
ADNP	1.281762	2.581039	-1.299277	0.027602

Gene name	Treated log2 mean	Control log2 mean	log2fold	P value
GOLM1	-2.039770	-3.601356	1.561586	0.027710
HTRA2	1.766326	0.170428	1.595899	0.027790
RAB3GAP2	-3.278925	-2.018758	-1.260167	0.029212
LMBRD1	-0.435840	-2.840628	2.404788	0.029256
HSPE1	9.802071	8.304032	1.498040	0.029483
PLIN3	3.601412	2.064117	1.537294	0.029513
GNS	1.175339	0.073809	1.101530	0.029551
C2	1.040024	-0.213343	1.253367	0.029664
ITGA3	2.594300	1.523110	1.071189	0.029852
EZH2	0.017425	-1.210295	1.227720	0.029978
ITGB5	1.945535	0.727003	1.218532	0.030024
GPI	-1.320498	-0.264325	-1.056173	0.030602
RCN3	3.254219	2.099680	1.154539	0.030826
CAAP1	2.014625	0.426302	1.588322	0.030902
CHMP4B	0.641435	-0.390788	1.032223	0.031112
NHSL2	-3.962262	-2.003361	-1.958902	0.031177
PUM2	-5.682278	-4.573868	-1.108410	0.031214
RPL32	1.628048	0.280852	1.347196	0.031423
PFN2	-0.715792	-3.188035	2.472243	0.032310
BAIAP2	0.965323	2.091499	-1.126176	0.032471
NUDC	-1.060233	-2.123338	1.063105	0.032540
SUN2	-0.212913	1.593916	-1.806829	0.033251
TERF2IP	3.258421	1.868626	1.389795	0.033259
SLX4	-2.605045	-4.324446	1.719401	0.033589
PFKP	-3.345655	-1.899406	-1.446250	0.033652
SCFD2	-2.388198	-1.033593	-1.354605	0.033980
GON4L	-2.663594	-4.347528	1.683933	0.033999
MRPS12	1.485424	0.006439	1.478985	0.034106
RPTOR	-5.701334	-4.588577	-1.112757	0.034237
SYPL1	1.496839	0.268895	1.227944	0.034251
TOPORS	-4.702183	-5.765611	1.063427	0.034480
CNPY3	1.412710	-0.082616	1.495326	0.034494
ZNF462	-4.653786	-2.885898	-1.767888	0.034532
GPATCH8	0.336741	-1.298259	1.635000	0.034621
UBE2N	-4.104733	-3.031797	-1.072937	0.034911
TMEM256	-0.093437	1.034044	-1.127481	0.035345
CSNK1A1	-2.668639	-1.606955	-1.061684	0.035399
ZNF608	-5.873491	-3.139074	-2.734417	0.035399
RRAS2	-2.124790	-4.723013	2.598223	0.035482
NUP43	4.609978	3.456010	1.153968	0.035494
USP48	-3.632772	-1.840405	-1.792366	0.035828

Gene name	Treated log2 mean	Control log2 mean	log2fold	P value
TCOF1	4.041209	2.949990	1.091219	0.036099
TMEM43	2.498014	3.685409	-1.187395	0.036657
ARID2	-0.799477	0.407298	-1.206775	0.037278
SUGT1	-3.493639	-4.691515	1.197876	0.038054
OSBPL10	-4.914064	-2.597556	-2.316509	0.038178
PHF23	-0.496162	-2.048042	1.551879	0.038781
UBXN4	-1.922729	-0.856000	-1.066729	0.039131
LSM 7.00	-0.363787	-1.729939	1.366152	0.039244
EFEMP1	0.439384	-0.590624	1.030007	0.039295
THBS1	0.136342	1.691232	-1.554890	0.039617
NBAS	-2.633704	-1.412843	-1.220862	0.039823
COL6A2	-3.656522	-1.748544	-1.907978	0.039858
HSPD1	10.453768	9.177010	1.276758	0.039869
ZMYM3	-0.491291	0.641088	-1.132379	0.040045
MAP2K1	-5.094384	-3.331904	-1.762480	0.040381
VPS41	-5.302116	-3.953558	-1.348558	0.040506
ZCCHC8	3.801522	2.639265	1.162256	0.040754
SCP2	1.862069	0.298206	1.563863	0.040862
POLRMT	-3.516720	-1.595902	-1.920818	0.041069
HUWE1	-4.067793	-2.433227	-1.634566	0.041249
PALM3	-3.790483	-2.209240	-1.581243	0.041497
GXYLT1	-0.082775	-2.345874	2.263099	0.041663
SP1	0.910795	-0.759422	1.670217	0.042160
CLASP1	-1.871827	-0.850930	-1.020897	0.042229
ZDHHC4	-3.474134	-1.626494	-1.847641	0.042241
CLIP1	-1.593660	-3.758898	2.165238	0.042269
HOOK3	-4.683965	-2.636181	-2.047784	0.042557
ADD3	-0.839985	0.531080	-1.371065	0.042557
DPY19L1	-1.852809	-0.237474	-1.615335	0.042744
PAIP1	-4.175655	-2.783413	-1.392242	0.042786
CNOT10	-4.120089	-2.457513	-1.662576	0.042797
NCKAP1	-0.685091	0.738904	-1.423995	0.042890
COPS2	-4.520768	-2.588347	-1.932421	0.043114
PFDN2	1.440995	-0.667862	2.108857	0.043173
PRKCSH	5.076024	3.978260	1.097763	0.043180
SLC4A7	-3.991827	-1.889841	-2.101986	0.043244
ACBD3	1.082005	-0.368808	1.450813	0.043584
MITF	-2.535761	-4.717655	2.181894	0.043993
RBBP4	6.417368	5.124605	1.292763	0.044276
PGD	-3.161576	-1.760382	-1.401194	0.044279
TTYH3	-2.580110	-0.950606	-1.629504	0.044316

Gene name	Treated log2 mean	Control log2 mean	log2fold	P value
DHRS2	4.279451	5.603299	-1.323849	0.044515
BIRC5	2.811707	1.593827	1.217880	0.045268
GPX1	2.252566	0.064245	2.188321	0.046038
NPTN	0.362406	-1.756919	2.119325	0.046494
TNFRSF12A	-3.485642	-2.422286	-1.063356	0.046625
CHTF18	-1.881718	-0.333084	-1.548634	0.046955
EEA1	-1.573107	-4.450312	2.877205	0.047245
GCFC2	-2.396134	-1.248112	-1.148021	0.047301
CMPK1	-1.912602	-3.142145	1.229543	0.047377
ZNF106	-0.481092	-2.039343	1.558251	0.047396
TRRAP	-1.541684	-0.133901	-1.407783	0.047893
TXLNG	-5.764638	-3.547273	-2.217366	0.048970
IWS1	2.918619	1.897191	1.021428	0.049126
SEPTIN5	-1.144770	-0.094532	-1.050239	0.049151
CCDC9B	-1.386121	-3.284019	1.897898	0.049303
BAG4	-2.859636	-5.586957	2.727321	0.049797

Supplementary Table 2. Full list of proteins following stringent exclusion analysis with two out of three BCAT(MT) repeats included while excluding all control (EV) samples included. n=3

Protein ID	Protein Name
A8K2U0	Alpha-2-macroglobulin-like protein 1 OS=Homo sapiens OX=9606 GN=A2ML1 PE=1 SV=3
A8MYA2	Uncharacterized protein CXorf49 OS=Homo sapiens OX=9606 GN=CXorf49 PE=2 SV=3
O14497	AT-rich interactive domain-containing protein 1A OS=Homo sapiens OX=9606 GN=ARID1A PE=1 SV=3
O14556	Glyceraldehyde-3-phosphate dehydrogenase, testis-specific OS=Homo sapiens OX=9606 GN=GAPDHS PE=1 SV=2
O14595	Carboxy-terminal domain RNA polymerase II polypeptide A small phosphatase 2 OS=Homo sapiens OX=9606 GN=CTDSP2 PE=1 SV=2
O15014	Zinc finger protein 609 OS=Homo sapiens OX=9606 GN=ZNF609 PE=1 SV=2
O15269	Serine palmitoyltransferase 1 OS=Homo sapiens OX=9606 GN=SPTLC1 PE=1 SV=1
O15498	Synaptobrevin homolog YKT6 OS=Homo sapiens OX=9606 GN=YKT6 PE=1 SV=1
O43240	Kallikrein-10 OS=Homo sapiens OX=9606 GN=KLK10 PE=1 SV=3
O43264	Centromere/kinetochore protein zw10 homolog OS=Homo sapiens OX=9606 GN=ZW10 PE=1 SV=3
O43670	BUB3-interacting and GLEBS motif-containing protein ZNF207 OS=Homo sapiens OX=9606 GN=ZNF207 PE=1 SV=1
O43739	Cytohesin-3 OS=Homo sapiens OX=9606 GN=CYTH3 PE=1 SV=2
O43747	AP-1 complex subunit gamma-1 OS=Homo sapiens OX=9606 GN=AP1G1 PE=1 SV=5
O60299	Leucine zipper putative tumor suppressor 3 OS=Homo sapiens OX=9606 GN=LZTS3 PE=2 SV=1
O60911	Cathepsin L2 OS=Homo sapiens OX=9606 GN=CTSV PE=1 SV=2
O75342	Arachidonate 12-lipoxygenase, 12R-type OS=Homo sapiens OX=9606 GN=ALOX12B PE=1 SV=1
O75347	Tubulin-specific chaperone A OS=Homo sapiens OX=9606 GN=TBCA PE=1 SV=3

Protein ID	Protein Name
O75376	Nuclear receptor corepressor 1 OS=Homo sapiens OX=9606 GN=NCOR1 PE=1 SV=2
O75436	Vacuolar protein sorting-associated protein 26A OS=Homo sapiens OX=9606 GN=VPS26A PE=1 SV=2
O75439	Mitochondrial-processing peptidase subunit beta OS=Homo sapiens OX=9606 GN=PMPCB PE=1 SV=2
O75821	Eukaryotic translation initiation factor 3 subunit G OS=Homo sapiens OX=9606 GN=EIF3G PE=1 SV=2
O75828	Carbonyl reductase [NADPH] 3 OS=Homo sapiens OX=9606 GN=CBR3 PE=1 SV=3
O94919	Endonuclease domain-containing 1 protein OS=Homo sapiens OX=9606 GN=ENDOD1 PE=1 SV=2
O95274	Ly6/PLAUR domain-containing protein 3 OS=Homo sapiens OX=9606 GN=LYPD3 PE=1 SV=2
O95470	Sphingosine-1-phosphate lyase 1 OS=Homo sapiens OX=9606 GN=SGPL1 PE=1 SV=3
O95625	Zinc finger and BTB domain-containing protein 11 OS=Homo sapiens OX=9606 GN=ZBTB11 PE=1 SV=2
O95782	AP-2 complex subunit alpha-1 OS=Homo sapiens OX=9606 GN=AP2A1 PE=1 SV=3
O95835	Serine/threonine-protein kinase LATS1 OS=Homo sapiens OX=9606 GN=LATS1 PE=1 SV=1
O95873	Uncharacterized protein C6orf47 OS=Homo sapiens OX=9606 GN=C6orf47 PE=1 SV=2
O95969	Secretoglobin family 1D member 2 OS=Homo sapiens OX=9606 GN=SCGB1D2 PE=2 SV=1
O96008	Mitochondrial import receptor subunit TOM40 homolog OS=Homo sapiens OX=9606 GN=TOMM40 PE=1 SV=1
O96013	Serine/threonine-protein kinase PAK 4 OS=Homo sapiens OX=9606 GN=PAK4 PE=1 SV=1
P0C7U0	Protein ELFN1 OS=Homo sapiens OX=9606 GN=ELFN1 PE=1 SV=2
P0DOX2	Immunoglobulin alpha-2 heavy chain OS=Homo sapiens OX=9606 PE=1 SV=2

Protein ID	Protein Name
P00367	Glutamate dehydrogenase 1, mitochondrial OS=Homo sapiens OX=9606 GN=GLUD1 PE=1 SV=2
P00374	Dihydrofolate reductase OS=Homo sapiens OX=9606 GN=DHFR PE=1 SV=2
P01833	Polymeric immunoglobulin receptor OS=Homo sapiens OX=9606 GN=PIGR PE=1 SV=4
P01861	Immunoglobulin heavy constant gamma 4 OS=Homo sapiens OX=9606 GN=IGHG4 PE=1 SV=1
P02788	Lactotransferrin OS=Homo sapiens OX=9606 GN=LTF PE=1 SV=6
P04181	Ornithine aminotransferase, mitochondrial OS=Homo sapiens OX=9606 GN=OAT PE=1 SV=1
P04183	Thymidine kinase, cytosolic OS=Homo sapiens OX=9606 GN=TK1 PE=1 SV=2
P04350	Tubulin beta-4A chain OS=Homo sapiens OX=9606 GN=TUBB4A PE=1 SV=2
P04843	Dolichyl-diphosphooligosaccharide--protein glycosyltransferase subunit 1 OS=Homo sapiens OX=9606 GN=RPN1 PE=1 SV=1
P04844	Dolichyl-diphosphooligosaccharide--protein glycosyltransferase subunit 2 OS=Homo sapiens OX=9606 GN=RPN2 PE=1 SV=3
P04899	Guanine nucleotide-binding protein G(i) subunit alpha-2 OS=Homo sapiens OX=9606 GN=GNAI2 PE=1 SV=3
P05090	Apolipoprotein D OS=Homo sapiens OX=9606 GN=APOD PE=1 SV=1
P05412	Transcription factor AP-1 OS=Homo sapiens OX=9606 GN=JUN PE=1 SV=2
P06396	Gelsolin OS=Homo sapiens OX=9606 GN=GSN PE=1 SV=1
P06744	Glucose-6-phosphate isomerase OS=Homo sapiens OX=9606 GN=GPI PE=1 SV=4
P07108	Acyl-CoA-binding protein OS=Homo sapiens OX=9606 GN=DBI PE=1 SV=2
P07384	Calpain-1 catalytic subunit OS=Homo sapiens OX=9606 GN=CAPN1 PE=1 SV=1
P07602	Prosaposin OS=Homo sapiens OX=9606 GN=PSAP PE=1 SV=2
P07741	Adenine phosphoribosyltransferase OS=Homo sapiens OX=9606 GN=APRT PE=1 SV=2

Protein ID	Protein Name
P07814	Bifunctional glutamate/proline--tRNA ligase OS=Homo sapiens OX=9606 GN=EPRS1 PE=1 SV=5
P07858	Cathepsin B OS=Homo sapiens OX=9606 GN=CTSB PE=1 SV=3
P07954	Fumarate hydratase, mitochondrial OS=Homo sapiens OX=9606 GN=FH PE=1 SV=3
P08195	4F2 cell-surface antigen heavy chain OS=Homo sapiens OX=9606 GN=SLC3A2 PE=1 SV=3
P08237	ATP-dependent 6-phosphofructokinase, muscle type OS=Homo sapiens OX=9606 GN=PFKM PE=1 SV=2
P08559	Pyruvate dehydrogenase E1 component subunit alpha, somatic form, mitochondrial OS=Homo sapiens OX=9606 GN=PDHA1 PE=1 SV=3
P08758	Annexin A5 OS=Homo sapiens OX=9606 GN=ANXA5 PE=1 SV=2
P09104	Gamma-enolase OS=Homo sapiens OX=9606 GN=ENO2 PE=1 SV=3
P09382	Galectin-1 OS=Homo sapiens OX=9606 GN=LGALS1 PE=1 SV=2
P09622	Dihydrolipoyl dehydrogenase, mitochondrial OS=Homo sapiens OX=9606 GN=DLD PE=1 SV=2
P09972	Fructose-bisphosphate aldolase C OS=Homo sapiens OX=9606 GN=ALDOC PE=1 SV=2
P10070	Zinc finger protein GLI2 OS=Homo sapiens OX=9606 GN=GLI2 PE=1 SV=4
P10619	Lysosomal protective protein OS=Homo sapiens OX=9606 GN=CTSA PE=1 SV=2
P12270	Nucleoprotein TPR OS=Homo sapiens OX=9606 GN=TPR PE=1 SV=3
P14174	Macrophage migration inhibitory factor OS=Homo sapiens OX=9606 GN=MIF PE=1 SV=4
P17655	Calpain-2 catalytic subunit OS=Homo sapiens OX=9606 GN=CAPN2 PE=1 SV=6
P17900	Ganglioside GM2 activator OS=Homo sapiens OX=9606 GN=GM2A PE=1 SV=4
P18085	ADP-ribosylation factor 4 OS=Homo sapiens OX=9606 GN=ARF4 PE=1 SV=3
P18754	Regulator of chromosome condensation OS=Homo sapiens OX=9606 GN=RCC1 PE=1 SV=1

Protein ID	Protein Name
P18859	ATP synthase-coupling factor 6, mitochondrial OS=Homo sapiens OX=9606 GN=ATP5PF PE=1 SV=1
P20742	Pregnancy zone protein OS=Homo sapiens OX=9606 GN=PZP PE=1 SV=4
P21266	Glutathione S-transferase Mu 3 OS=Homo sapiens OX=9606 GN=GSTM3 PE=1 SV=3
P21281	V-type proton ATPase subunit B, brain isoform OS=Homo sapiens OX=9606 GN=ATP6V1B2 PE=1 SV=3
P22102	Trifunctional purine biosynthetic protein adenosine-3 OS=Homo sapiens OX=9606 GN=GART PE=1 SV=1
P22314	Ubiquitin-like modifier-activating enzyme 1 OS=Homo sapiens OX=9606 GN=UBA1 PE=1 SV=3
P22570	NADPH:adrenodoxin oxidoreductase, mitochondrial OS=Homo sapiens OX=9606 GN=FDXR PE=1 SV=3
P23258	Tubulin gamma-1 chain OS=Homo sapiens OX=9606 GN=TUBG1 PE=1 SV=2
P23368	NAD-dependent malic enzyme, mitochondrial OS=Homo sapiens OX=9606 GN=ME2 PE=1 SV=1
P24534	Elongation factor 1-beta OS=Homo sapiens OX=9606 GN=EEF1B2 PE=1 SV=3
P25205	DNA replication licensing factor MCM3 OS=Homo sapiens OX=9606 GN=MCM3 PE=1 SV=3
P25788	Proteasome subunit alpha type-3 OS=Homo sapiens OX=9606 GN=PSMA3 PE=1 SV=2
P25815	Protein S100-P OS=Homo sapiens OX=9606 GN=S100P PE=1 SV=2
P26006	Integrin alpha-3 OS=Homo sapiens OX=9606 GN=ITGA3 PE=1 SV=5
P26196	Probable ATP-dependent RNA helicase DDX6 OS=Homo sapiens OX=9606 GN=DDX6 PE=1 SV=2
P26639	Threonine--tRNA ligase 1, cytoplasmic OS=Homo sapiens OX=9606 GN=TARS1 PE=1 SV=3
P27105	Stomatin OS=Homo sapiens OX=9606 GN=STOM PE=1 SV=3
P27482	Calmodulin-like protein 3 OS=Homo sapiens OX=9606 GN=CALML3 PE=1 SV=2

Protein ID	Protein Name
P28070	Proteasome subunit beta type-4 OS=Homo sapiens OX=9606 GN=PSMB4 PE=1 SV=4
P30040	Endoplasmic reticulum resident protein 29 OS=Homo sapiens OX=9606 GN=ERP29 PE=1 SV=4
P31153	S-adenosylmethionine synthase isoform type-2 OS=Homo sapiens OX=9606 GN=MAT2A PE=1 SV=1
P31689	DnaJ homolog subfamily A member 1 OS=Homo sapiens OX=9606 GN=DNAJA1 PE=1 SV=2
P31946	14-3-3 protein beta/alpha OS=Homo sapiens OX=9606 GN=YWHAB PE=1 SV=3
P35080	Profilin-2 OS=Homo sapiens OX=9606 GN=PFN2 PE=1 SV=3
P35251	Replication factor C subunit 1 OS=Homo sapiens OX=9606 GN=RFC1 PE=1 SV=4
P35606	Coatomer subunit beta' OS=Homo sapiens OX=9606 GN=COPB2 PE=1 SV=2
P35754	Glutaredoxin-1 OS=Homo sapiens OX=9606 GN=GLRX PE=1 SV=2
P35998	26S proteasome regulatory subunit 7 OS=Homo sapiens OX=9606 GN=PSMC2 PE=1 SV=3
P36404	ADP-ribosylation factor-like protein 2 OS=Homo sapiens OX=9606 GN=ARL2 PE=1 SV=4
P36639	7,8-dihydro-8-oxoguanine triphosphatase OS=Homo sapiens OX=9606 GN=NUDT1 PE=1 SV=3
P39656	Dolichyl-diphosphooligosaccharide--protein glycosyltransferase 48 kDa subunit OS=Homo sapiens OX=9606 GN=DDOST PE=1 SV=4
P40616	ADP-ribosylation factor-like protein 1 OS=Homo sapiens OX=9606 GN=ARL1 PE=1 SV=1
P40939	Trifunctional enzyme subunit alpha, mitochondrial OS=Homo sapiens OX=9606 GN=HADHA PE=1 SV=2
P41743	Protein kinase C iota type OS=Homo sapiens OX=9606 GN=PRKCI PE=1 SV=2
P42357	Histidine ammonia-lyase OS=Homo sapiens OX=9606 GN=HAL PE=1 SV=1
P43686	26S proteasome regulatory subunit 6B OS=Homo sapiens OX=9606 GN=PSMC4 PE=1 SV=2

Protein ID	Protein Name
P46060	Ran GTPase-activating protein 1 OS=Homo sapiens OX=9606 GN=RANGAP1 PE=1 SV=1
P46977	Dolichyl-diphosphooligosaccharide--protein glycosyltransferase subunit STT3A OS=Homo sapiens OX=9606 GN=STT3A PE=1 SV=2
P47897	Glutamine--tRNA ligase OS=Homo sapiens OX=9606 GN=QARS1 PE=1 SV=1
P48594	Serpin B4 OS=Homo sapiens OX=9606 GN=SERPINB4 PE=1 SV=2
P49720	Proteasome subunit beta type-3 OS=Homo sapiens OX=9606 GN=PSMB3 PE=1 SV=2
P49721	Proteasome subunit beta type-2 OS=Homo sapiens OX=9606 GN=PSMB2 PE=1 SV=1
P49915	GMP synthase [glutamine-hydrolyzing] OS=Homo sapiens OX=9606 GN=GMPS PE=1 SV=1
P50213	Isocitrate dehydrogenase [NAD] subunit alpha, mitochondrial OS=Homo sapiens OX=9606 GN=IDH3A PE=1 SV=1
P50395	Rab GDP dissociation inhibitor beta OS=Homo sapiens OX=9606 GN=GDI2 PE=1 SV=2
P50502	Hsc70-interacting protein OS=Homo sapiens OX=9606 GN=ST13 PE=1 SV=2
P50570	Dynamin-2 OS=Homo sapiens OX=9606 GN=DNM2 PE=1 SV=2
P51571	Translocon-associated protein subunit delta OS=Homo sapiens OX=9606 GN=SSR4 PE=1 SV=1
P52209	6-phosphogluconate dehydrogenase, decarboxylating OS=Homo sapiens OX=9606 GN=PGD PE=1 SV=3
P52701	DNA mismatch repair protein Msh6 OS=Homo sapiens OX=9606 GN=MSH6 PE=1 SV=2
P53618	Coatomer subunit beta OS=Homo sapiens OX=9606 GN=COPB1 PE=1 SV=3
P53985	Monocarboxylate transporter 1 OS=Homo sapiens OX=9606 GN=SLC16A1 PE=1 SV=3
P54577	Tyrosine--tRNA ligase, cytoplasmic OS=Homo sapiens OX=9606 GN=YARS1 PE=1 SV=4
P54886	Delta-1-pyrroline-5-carboxylate synthase OS=Homo sapiens OX=9606 GN=ALDH18A1 PE=1 SV=2

Protein ID	Protein Name
P55039	Developmentally-regulated GTP-binding protein 2 OS=Homo sapiens OX=9606 GN=DRG2 PE=1 SV=1
P55145	Mesencephalic astrocyte-derived neurotrophic factor OS=Homo sapiens OX=9606 GN=MANF PE=1 SV=3
P55209	Nucleosome assembly protein 1-like 1 OS=Homo sapiens OX=9606 GN=NAP1L1 PE=1 SV=1
P55769	NHP2-like protein 1 OS=Homo sapiens OX=9606 GN=SNU13 PE=1 SV=3
P55786	Puromycin-sensitive aminopeptidase OS=Homo sapiens OX=9606 GN=NPEPPS PE=1 SV=2
P57740	Nuclear pore complex protein Nup107 OS=Homo sapiens OX=9606 GN=NUP107 PE=1 SV=1
P58546	Myotrophin OS=Homo sapiens OX=9606 GN=MTPN PE=1 SV=2
P59998	Actin-related protein 2/3 complex subunit 4 OS=Homo sapiens OX=9606 GN=ARPC4 PE=1 SV=3
P60903	Protein S100-A10 OS=Homo sapiens OX=9606 GN=S100A10 PE=1 SV=2
P61163	Alpha-centractin OS=Homo sapiens OX=9606 GN=ACTR1A PE=1 SV=1
P61224	Ras-related protein Rap-1b OS=Homo sapiens OX=9606 GN=RAP1B PE=1 SV=1
P61254	60S ribosomal protein L26 OS=Homo sapiens OX=9606 GN=RPL26 PE=1 SV=1
P61981	14-3-3 protein gamma OS=Homo sapiens OX=9606 GN=YWHAG PE=1 SV=2
P62191	26S proteasome regulatory subunit 4 OS=Homo sapiens OX=9606 GN=PSMC1 PE=1 SV=1
P63010	AP-2 complex subunit beta OS=Homo sapiens OX=9606 GN=AP2B1 PE=1 SV=1
P67812	Signal peptidase complex catalytic subunit SEC11A OS=Homo sapiens OX=9606 GN=SEC11A PE=1 SV=1
P68366	Tubulin alpha-4A chain OS=Homo sapiens OX=9606 GN=TUBA4A PE=1 SV=1
P78310	Coxsackievirus and adenovirus receptor OS=Homo sapiens OX=9606 GN=CXADR PE=1 SV=1

Protein ID	Protein Name
P80188	Neutrophil gelatinase-associated lipocalin OS=Homo sapiens OX=9606 GN=LCN2 PE=1 SV=2
P82930	28S ribosomal protein S34, mitochondrial OS=Homo sapiens OX=9606 GN=MRPS34 PE=1 SV=2
P98082	Disabled homolog 2 OS=Homo sapiens OX=9606 GN=DAB2 PE=1 SV=3
P98172	Ephrin-B1 OS=Homo sapiens OX=9606 GN=EFNB1 PE=1 SV=1
Q01082	Spectrin beta chain, non-erythrocytic 1 OS=Homo sapiens OX=9606 GN=SPTBN1 PE=1 SV=2
Q01650	Large neutral amino acids transporter small subunit 1 OS=Homo sapiens OX=9606 GN=SLC7A5 PE=1 SV=2
Q01813	ATP-dependent 6-phosphofructokinase, platelet type OS=Homo sapiens OX=9606 GN=PFKP PE=1 SV=2
Q01968	Inositol polyphosphate 5-phosphatase OCRL OS=Homo sapiens OX=9606 GN=OCRL PE=1 SV=3
Q01970	1-phosphatidylinositol 4,5-bisphosphate phosphodiesterase beta-3 OS=Homo sapiens OX=9606 GN=PLCB3 PE=1 SV=2
Q04721	Neurogenic locus notch homolog protein 2 OS=Homo sapiens OX=9606 GN=NOTCH2 PE=1 SV=3
Q06587	E3 ubiquitin-protein ligase RING1 OS=Homo sapiens OX=9606 GN=RING1 PE=1 SV=2
Q07065	Cytoskeleton-associated protein 4 OS=Homo sapiens OX=9606 GN=CKAP4 PE=1 SV=2
Q1KMD3	Heterogeneous nuclear ribonucleoprotein U-like protein 2 OS=Homo sapiens OX=9606 GN=HNRNPUL2 PE=1 SV=1
Q3KP66	Innate immunity activator protein OS=Homo sapiens OX=9606 GN=INAVA PE=1 SV=2
Q3SY84	Keratin, type II cytoskeletal 71 OS=Homo sapiens OX=9606 GN=KRT71 PE=1 SV=3
Q3ZCQ8	Mitochondrial import inner membrane translocase subunit TIM50 OS=Homo sapiens OX=9606 GN=TIMM50 PE=1 SV=2
Q5C9Z4	Nucleolar MIF4G domain-containing protein 1 OS=Homo sapiens OX=9606 GN=NOM1 PE=1 SV=1
Q5EBL8	PDZ domain-containing protein 11 OS=Homo sapiens OX=9606 GN=PDZD11 PE=1 SV=2

Protein ID	Protein Name
Q5HYW2	NHS-like protein 2 OS=Homo sapiens OX=9606 GN=NHSL2 PE=1 SV=2
Q5R3F8	Protein phosphatase 1 regulatory subunit 29 OS=Homo sapiens OX=9606 GN=ELFN2 PE=1 SV=1
Q5SRE5	Nucleoporin NUP188 OS=Homo sapiens OX=9606 GN=NUP188 PE=1 SV=1
Q5TGY3	AT-hook DNA-binding motif-containing protein 1 OS=Homo sapiens OX=9606 GN=AHDC1 PE=1 SV=1
Q6KB66	Keratin, type II cytoskeletal 80 OS=Homo sapiens OX=9606 GN=KRT80 PE=1 SV=2
Q6P1N0	Coiled-coil and C2 domain-containing protein 1A OS=Homo sapiens OX=9606 GN=CC2D1A PE=1 SV=1
Q6P1Q0	LETM1 domain-containing protein 1 OS=Homo sapiens OX=9606 GN=LETMD1 PE=1 SV=1
Q6P2H3	Centrosomal protein of 85 kDa OS=Homo sapiens OX=9606 GN=CEP85 PE=1 SV=1
Q6P2Q9	Pre-mRNA-processing-splicing factor 8 OS=Homo sapiens OX=9606 GN=PRPF8 PE=1 SV=2
Q6P3W7	SCY1-like protein 2 OS=Homo sapiens OX=9606 GN=SCYL2 PE=1 SV=1
Q6STE5	SWI/SNF-related matrix-associated actin-dependent regulator of chromatin subfamily D member 3 OS=Homo sapiens OX=9606 GN=SMARCD3 PE=1 SV=1
Q6ZRV2	Protein FAM83H OS=Homo sapiens OX=9606 GN=FAM83H PE=1 SV=3
Q6ZVX7	F-box only protein 50 OS=Homo sapiens OX=9606 GN=NCCRP1 PE=1 SV=1
Q7L2H7	Eukaryotic translation initiation factor 3 subunit M OS=Homo sapiens OX=9606 GN=EIF3M PE=1 SV=1
Q8IUD2	ELKS/Rab6-interacting/CAST family member 1 OS=Homo sapiens OX=9606 GN=ERC1 PE=1 SV=1
Q8IW75	Serpin A12 OS=Homo sapiens OX=9606 GN=SERPINA12 PE=1 SV=1
Q8IWC1	MAP7 domain-containing protein 3 OS=Homo sapiens OX=9606 GN=MAP7D3 PE=1 SV=2

Protein ID	Protein Name
Q8IY33	MICAL-like protein 2 OS=Homo sapiens OX=9606 GN=MICALL2 PE=1 SV=1
Q8IY67	Ribonucleoprotein PTB-binding 1 OS=Homo sapiens OX=9606 GN=RAVER1 PE=1 SV=1
Q8IZ21	Phosphatase and actin regulator 4 OS=Homo sapiens OX=9606 GN=PHACTR4 PE=1 SV=1
Q8IZH2	5'-3' exoribonuclease 1 OS=Homo sapiens OX=9606 GN=XRN1 PE=1 SV=1
Q8N2Y8	Iporin OS=Homo sapiens OX=9606 GN=RUSC2 PE=1 SV=3
Q8N3C0	Activating signal cointegrator 1 complex subunit 3 OS=Homo sapiens OX=9606 GN=ASCC3 PE=1 SV=3
Q8N4C8	Misshapen-like kinase 1 OS=Homo sapiens OX=9606 GN=MINK1 PE=1 SV=2
Q8NB78	Lysine-specific histone demethylase 1B OS=Homo sapiens OX=9606 GN=KDM1B PE=1 SV=3
Q8NCA5	Protein FAM98A OS=Homo sapiens OX=9606 GN=FAM98A PE=1 SV=2
Q8NHV4	Protein NEDD1 OS=Homo sapiens OX=9606 GN=NEDD1 PE=1 SV=1
Q8TAA9	Vang-like protein 1 OS=Homo sapiens OX=9606 GN=VANGL1 PE=1 SV=1
Q8TBC3	SH3KBP1-binding protein 1 OS=Homo sapiens OX=9606 GN=SHKBP1 PE=1 SV=2
Q9BRK3	Matrix remodeling-associated protein 8 OS=Homo sapiens OX=9606 GN=MXRA8 PE=1 SV=1
Q9BRT6	Protein LLP homolog OS=Homo sapiens OX=9606 GN=LLPH PE=1 SV=1
Q9BSJ8	Extended synaptotagmin-1 OS=Homo sapiens OX=9606 GN=ESYT1 PE=1 SV=1
Q9BTT0	Acidic leucine-rich nuclear phosphoprotein 32 family member E OS=Homo sapiens OX=9606 GN=ANP32E PE=1 SV=1
Q9BUF5	Tubulin beta-6 chain OS=Homo sapiens OX=9606 GN=TUBB6 PE=1 SV=1
Q9BVC6	Transmembrane protein 109 OS=Homo sapiens OX=9606 GN=TMEM109 PE=1 SV=1

Protein ID	Protein Name
Q9BWE0	Replication initiator 1 OS=Homo sapiens OX=9606 GN=REPIN1 PE=1 SV=1
Q9BX67	Junctional adhesion molecule C OS=Homo sapiens OX=9606 GN=JAM3 PE=1 SV=1
Q9BXP5	Serrate RNA effector molecule homolog OS=Homo sapiens OX=9606 GN=SRRT PE=1 SV=1
Q9BZE1	39S ribosomal protein L37, mitochondrial OS=Homo sapiens OX=9606 GN=MRPL37 PE=1 SV=2
Q9BZE4	GTP-binding protein 4 OS=Homo sapiens OX=9606 GN=GTPBP4 PE=1 SV=3
Q9BZG1	Ras-related protein Rab-34 OS=Homo sapiens OX=9606 GN=RAB34 PE=1 SV=1
Q9BZL6	Serine/threonine-protein kinase D2 OS=Homo sapiens OX=9606 GN=PRKD2 PE=1 SV=3
Q9C0B5	Palmitoyltransferase ZDHHC5 OS=Homo sapiens OX=9606 GN=ZDHHC5 PE=1 SV=2
Q9C0C4	Semaphorin-4C OS=Homo sapiens OX=9606 GN=SEMA4C PE=1 SV=2
Q9C075	Keratin, type I cytoskeletal 23 OS=Homo sapiens OX=9606 GN=KRT23 PE=1 SV=2
Q9GZY6	Linker for activation of T-cells family member 2 OS=Homo sapiens OX=9606 GN=LAT2 PE=1 SV=1
Q9H0L4	Cleavage stimulation factor subunit 2 tau variant OS=Homo sapiens OX=9606 GN=CSTF2T PE=1 SV=1
Q9H2H9	Sodium-coupled neutral amino acid transporter 1 OS=Homo sapiens OX=9606 GN=SLC38A1 PE=1 SV=1
Q9H3U1	Protein unc-45 homolog A OS=Homo sapiens OX=9606 GN=UNC45A PE=1 SV=1
Q9H4A3	Serine/threonine-protein kinase WNK1 OS=Homo sapiens OX=9606 GN=WNK1 PE=1 SV=2
Q9H4G0	Band 4.1-like protein 1 OS=Homo sapiens OX=9606 GN=EPB41L1 PE=1 SV=2
Q9H4M9	EH domain-containing protein 1 OS=Homo sapiens OX=9606 GN=EHD1 PE=1 SV=2

Protein ID	Protein Name
Q9H9A6	Leucine-rich repeat-containing protein 40 OS=Homo sapiens OX=9606 GN=LRRC40 PE=1 SV=1
Q9H9J2	39S ribosomal protein L44, mitochondrial OS=Homo sapiens OX=9606 GN=MRPL44 PE=1 SV=1
Q9H223	EH domain-containing protein 4 OS=Homo sapiens OX=9606 GN=EHD4 PE=1 SV=1
Q9H254	Spectrin beta chain, non-erythrocytic 4 OS=Homo sapiens OX=9606 GN=SPTBN4 PE=1 SV=2
Q9H583	HEAT repeat-containing protein 1 OS=Homo sapiens OX=9606 GN=HEATR1 PE=1 SV=3
Q9HBL0	Tensin-1 OS=Homo sapiens OX=9606 GN=TNS1 PE=1 SV=2
Q9NP72	Ras-related protein Rab-18 OS=Homo sapiens OX=9606 GN=RAB18 PE=1 SV=1
Q9NQ39	Putative 40S ribosomal protein S10-like OS=Homo sapiens OX=9606 GN=RPS10P5 PE=5 SV=1
Q9NQ88	Fructose-2,6-bisphosphatase TIGAR OS=Homo sapiens OX=9606 GN=TIGAR PE=1 SV=1
Q9NQP4	Prefoldin subunit 4 OS=Homo sapiens OX=9606 GN=PFDN4 PE=1 SV=1
Q9NR50	Translation initiation factor eIF-2B subunit gamma OS=Homo sapiens OX=9606 GN=EIF2B3 PE=1 SV=1
Q9NRP7	Serine/threonine-protein kinase 36 OS=Homo sapiens OX=9606 GN=STK36 PE=1 SV=2
Q9NSD9	Phenylalanine--tRNA ligase beta subunit OS=Homo sapiens OX=9606 GN=FARSB PE=1 SV=3
Q9NT68	Teneurin-2 OS=Homo sapiens OX=9606 GN=TENM2 PE=1 SV=3
Q9NZB2	Constitutive coactivator of PPAR-gamma-like protein 1 OS=Homo sapiens OX=9606 GN=FAM120A PE=1 SV=2
Q9NZH8	Interleukin-36 gamma OS=Homo sapiens OX=9606 GN=IL36G PE=1 SV=1
Q9P0I2	ER membrane protein complex subunit 3 OS=Homo sapiens OX=9606 GN=EMC3 PE=1 SV=3
Q9P0K7	Ankycorbin OS=Homo sapiens OX=9606 GN=RAI14 PE=1 SV=2
Q9P0V3	SH3 domain-binding protein 4 OS=Homo sapiens OX=9606 GN=SH3BP4 PE=1 SV=1

Protein ID	Protein Name
Q9P0V9	Septin-10 OS=Homo sapiens OX=9606 GN=SEPTIN10 PE=1 SV=2
Q9P035	Very-long-chain (3R)-3-hydroxyacyl-CoA dehydratase 3 OS=Homo sapiens OX=9606 GN=HACD3 PE=1 SV=2
Q9P2E9	Ribosome-binding protein 1 OS=Homo sapiens OX=9606 GN=RRBP1 PE=1 SV=5
Q9P2Q2	FERM domain-containing protein 4A OS=Homo sapiens OX=9606 GN=FRMD4A PE=1 SV=3
Q9P273	Teneurin-3 OS=Homo sapiens OX=9606 GN=TENM3 PE=2 SV=3
Q9UBX3	Mitochondrial dicarboxylate carrier OS=Homo sapiens OX=9606 GN=SLC25A10 PE=1 SV=2
Q9UGM3	Deleted in malignant brain tumors 1 protein OS=Homo sapiens OX=9606 GN=DMBT1 PE=1 SV=2
Q9UGU0	Transcription factor 20 OS=Homo sapiens OX=9606 GN=TCF20 PE=1 SV=3
Q9UGV2	Protein NDRG3 OS=Homo sapiens OX=9606 GN=NDRG3 PE=1 SV=2
Q9UHB9	Signal recognition particle subunit SRP68 OS=Homo sapiens OX=9606 GN=SRP68 PE=1 SV=2
Q9UHN6	Cell surface hyaluronidase OS=Homo sapiens OX=9606 GN=CEMIP2 PE=1 SV=1
Q9UI10	Translation initiation factor eIF-2B subunit delta OS=Homo sapiens OX=9606 GN=EIF2B4 PE=1 SV=2
Q9UI12	V-type proton ATPase subunit H OS=Homo sapiens OX=9606 GN=ATP6V1H PE=1 SV=1
Q9UI42	Carboxypeptidase A4 OS=Homo sapiens OX=9606 GN=CPA4 PE=1 SV=2
Q9UIA9	Exportin-7 OS=Homo sapiens OX=9606 GN=XPO7 PE=1 SV=3
Q9ULC8	Palmitoyltransferase ZDHHC8 OS=Homo sapiens OX=9606 GN=ZDHHC8 PE=1 SV=3
Q9ULL5	Proline-rich protein 12 OS=Homo sapiens OX=9606 GN=PRR12 PE=1 SV=3
Q9UNL2	Translocon-associated protein subunit gamma OS=Homo sapiens OX=9606 GN=SSR3 PE=1 SV=1
Q9UPT5	Exocyst complex component 7 OS=Homo sapiens OX=9606 GN=EXOC7 PE=1 SV=3

Protein ID	Protein Name
Q9Y2A7	Nck-associated protein 1 OS=Homo sapiens OX=9606 GN=NCKAP1 PE=1 SV=1
Q9Y3A5	Ribosome maturation protein SBDS OS=Homo sapiens OX=9606 GN=SBDS PE=1 SV=4
Q9Y3F4	Serine-threonine kinase receptor-associated protein OS=Homo sapiens OX=9606 GN=STRAP PE=1 SV=1
Q9Y3I0	RNA-splicing ligase RtcB homolog OS=Homo sapiens OX=9606 GN=RTCB PE=1 SV=1
Q9Y3T9	Nucleolar complex protein 2 homolog OS=Homo sapiens OX=9606 GN=NOC2L PE=1 SV=4
Q9Y4P3	Transducin beta-like protein 2 OS=Homo sapiens OX=9606 GN=TBL2 PE=1 SV=1
Q9Y5L0	Transportin-3 OS=Homo sapiens OX=9606 GN=TNPO3 PE=1 SV=3
Q9Y6M5	Zinc transporter 1 OS=Homo sapiens OX=9606 GN=SLC30A1 PE=1 SV=3
Q9Y6Q9	Nuclear receptor coactivator 3 OS=Homo sapiens OX=9606 GN=NCOA3 PE=1 SV=1
Q9Y262	Eukaryotic translation initiation factor 3 subunit L OS=Homo sapiens OX=9606 GN=EIF3L PE=1 SV=1
Q9Y295	Developmentally-regulated GTP-binding protein 1 OS=Homo sapiens OX=9606 GN=DRG1 PE=1 SV=1
Q9Y450	HBS1-like protein OS=Homo sapiens OX=9606 GN=HBS1L PE=1 SV=1
Q9Y618	Nuclear receptor corepressor 2 OS=Homo sapiens OX=9606 GN=NCOR2 PE=1 SV=3
Q9Y679	Lipid droplet-regulating VLDL assembly factor AUP1 OS=Homo sapiens OX=9606 GN=AUP1 PE=1 SV=2
Q52LW3	Rho GTPase-activating protein 29 OS=Homo sapiens OX=9606 GN=ARHGAP29 PE=1 SV=2
Q68CZ2	Tensin-3 OS=Homo sapiens OX=9606 GN=TNS3 PE=1 SV=2
Q71H61	Immunoglobulin-like domain-containing receptor 2 OS=Homo sapiens OX=9606 GN=ILDR2 PE=2 SV=1
Q86U42	Polyadenylate-binding protein 2 OS=Homo sapiens OX=9606 GN=PABPN1 PE=1 SV=3

Protein ID	Protein Name
Q86U70	LIM domain-binding protein 1 OS=Homo sapiens OX=9606 GN=LDB1 PE=1 SV=2
Q86UU1	Pleckstrin homology-like domain family B member 1 OS=Homo sapiens OX=9606 GN=PHLDB1 PE=1 SV=1
Q86W92	Liprin-beta-1 OS=Homo sapiens OX=9606 GN=PPFIBP1 PE=1 SV=2
Q96C36	Pyrroline-5-carboxylate reductase 2 OS=Homo sapiens OX=9606 GN=PYCR2 PE=1 SV=1
Q96DA6	Mitochondrial import inner membrane translocase subunit TIM14 OS=Homo sapiens OX=9606 GN=DNAJC19 PE=1 SV=3
Q96DR8	Mucin-like protein 1 OS=Homo sapiens OX=9606 GN=MUCL1 PE=1 SV=1
Q96F07	Cytoplasmic FMR1-interacting protein 2 OS=Homo sapiens OX=9606 GN=CYFIP2 PE=1 SV=2
Q96II8	DISP complex protein LRCH3 OS=Homo sapiens OX=9606 GN=LRCH3 PE=1 SV=2
Q96J84	Kin of IRRE-like protein 1 OS=Homo sapiens OX=9606 GN=KIRREL1 PE=1 SV=2
Q96M89	Coiled-coil domain-containing protein 138 OS=Homo sapiens OX=9606 GN=CCDC138 PE=1 SV=1
Q96ME1	F-box/LRR-repeat protein 18 OS=Homo sapiens OX=9606 GN=FBXL18 PE=1 SV=2
Q96ME7	Zinc finger protein 512 OS=Homo sapiens OX=9606 GN=ZNF512 PE=1 SV=2
Q96N66	Lysophospholipid acyltransferase 7 OS=Homo sapiens OX=9606 GN=MBOAT7 PE=1 SV=2
Q96ST8	Centrosomal protein of 89 kDa OS=Homo sapiens OX=9606 GN=CEP89 PE=1 SV=3
Q658P3	Metalloreductase STEAP3 OS=Homo sapiens OX=9606 GN=STEAP3 PE=1 SV=2
Q969V3	Nicalin OS=Homo sapiens OX=9606 GN=NCLN PE=1 SV=2
Q12857	Nuclear factor 1 A-type OS=Homo sapiens OX=9606 GN=NFIA PE=1 SV=2
Q13200	26S proteasome non-ATPase regulatory subunit 2 OS=Homo sapiens OX=9606 GN=PSMD2 PE=1 SV=3

Protein ID	Protein Name
Q13330	Metastasis-associated protein MTA1 OS=Homo sapiens OX=9606 GN=MTA1 PE=1 SV=2
Q13404	Ubiquitin-conjugating enzyme E2 variant 1 OS=Homo sapiens OX=9606 GN=UBE2V1 PE=1 SV=2
Q13495	Mastermind-like domain-containing protein 1 OS=Homo sapiens OX=9606 GN=MAMLD1 PE=1 SV=2
Q13601	KRR1 small subunit processome component homolog OS=Homo sapiens OX=9606 GN=KRR1 PE=1 SV=4
Q13740	CD166 antigen OS=Homo sapiens OX=9606 GN=ALCAM PE=1 SV=2
Q13796	Protein Shroom2 OS=Homo sapiens OX=9606 GN=SHROOM2 PE=1 SV=1
Q14152	Eukaryotic translation initiation factor 3 subunit A OS=Homo sapiens OX=9606 GN=EIF3A PE=1 SV=1
Q14232	Translation initiation factor eIF-2B subunit alpha OS=Homo sapiens OX=9606 GN=EIF2B1 PE=1 SV=1
Q14527	Helicase-like transcription factor OS=Homo sapiens OX=9606 GN=HLTF PE=1 SV=2
Q14690	Protein RRP5 homolog OS=Homo sapiens OX=9606 GN=PDCD11 PE=1 SV=3
Q15043	Metal cation symporter ZIP14 OS=Homo sapiens OX=9606 GN=SLC39A14 PE=1 SV=3
Q15185	Prostaglandin E synthase 3 OS=Homo sapiens OX=9606 GN=PTGES3 PE=1 SV=1
Q15392	Delta(24)-sterol reductase OS=Homo sapiens OX=9606 GN=DHCR24 PE=1 SV=2
Q15788	Nuclear receptor coactivator 1 OS=Homo sapiens OX=9606 GN=NCOA1 PE=1 SV=3
Q15907	Ras-related protein Rab-11B OS=Homo sapiens OX=9606 GN=RAB11B PE=1 SV=4
Q16658	Fascin OS=Homo sapiens OX=9606 GN=FSCN1 PE=1 SV=3
Q92616	eIF-2-alpha kinase activator GCN1 OS=Homo sapiens OX=9606 GN=GCN1 PE=1 SV=6
Q92621	Nuclear pore complex protein Nup205 OS=Homo sapiens OX=9606 GN=NUP205 PE=1 SV=3

Protein ID	Protein Name
Q92692	Nectin-2 OS=Homo sapiens OX=9606 GN=NECTIN2 PE=1 SV=1
Q92796	Disks large homolog 3 OS=Homo sapiens OX=9606 GN=DLG3 PE=1 SV=2
Q92890	Ubiquitin recognition factor in ER-associated degradation protein 1 OS=Homo sapiens OX=9606 GN=UFD1 PE=1 SV=3
Q93052	Lipoma-preferred partner OS=Homo sapiens OX=9606 GN=LPP PE=1 SV=1
Q99459	Cell division cycle 5-like protein OS=Homo sapiens OX=9606 GN=CDC5L PE=1 SV=2
Q99471	Prefoldin subunit 5 OS=Homo sapiens OX=9606 GN=PFDN5 PE=1 SV=2
Q99575	Ribonucleases P/MRP protein subunit POP1 OS=Homo sapiens OX=9606 GN=POP1 PE=1 SV=2
Q99714	3-hydroxyacyl-CoA dehydrogenase type-2 OS=Homo sapiens OX=9606 GN=HSD17B10 PE=1 SV=3
Q99873	Protein arginine N-methyltransferase 1 OS=Homo sapiens OX=9606 GN=PRMT1 PE=1 SV=3

Supplementary Table 3. Full list of proteins following SAINT analysis.
"Quant" and "User Control" column depict number of peptide spectra for each across all 3 repeats. "SP" Saint probability score confers confidence in how probable the interaction is significant. For analysis SP>0.95 was used. n=3

prey Gene	Quant (SPC or Intensities)	User Controls (SPC or Intensities)	SP	Description of protein
ACTN1	13|5|4	0|0|0	1	Alpha-actinin-1 OS=Homo sapiens OX=9606 GN=ACTN1 PE=1 SV=2
AFDN	45|35|33	0|4|0	1	Afadin OS=Homo sapiens OX=9606 GN=AFDN PE=1 SV=3
APC	54|38|53	0|0|0	1	Adenomatous polyposis coli protein OS=Homo sapiens OX=9606 GN=APC PE=1 SV=2
ARF4	6|6|5	0|0|0	1	ADP-ribosylation factor 4 OS=Homo sapiens OX=9606 GN=ARF4 PE=1 SV=3
ARHGAP21	30|30|24	0|0|0	1	Rho GTPase-activating protein 21 OS=Homo sapiens OX=9606 GN=ARHGAP21 PE=1 SV=2
ARVCF	9|7|6	0|0|0	1	Armadillo repeat protein deleted in velo-cardio-facial syndrome OS=Homo sapiens OX=9606 GN=ARVCF PE=1 SV=1
AXIN1	7|4|4	0|0|0	1	Axin-1 OS=Homo sapiens OX=9606 GN=AXIN1 PE=1 SV=2
BTRC	6|7|7	0|0|0	1	F-box/WD repeat-containing protein 1A OS=Homo sapiens OX=9606 GN=BTRC PE=1 SV=1
CDH2	28|19|18	0|0|0	1	Cadherin-2 OS=Homo sapiens OX=9606 GN=CDH2 PE=1 SV=4
CKAP5	12|7|12	0|0|0	1	Cytoskeleton-associated protein 5 OS=Homo sapiens OX=9606 GN=CKAP5 PE=1 SV=3
CTNNA1	67|46|45	0|0|0	1	Catenin alpha-1 OS=Homo sapiens OX=9606 GN=CTNNA1 PE=1 SV=1

prey Gene	Quant (SPC or Intensities)	User Controls (SPC or Intensities)	SP	Description of protein
CTNNB1	41|29|26	0|0|0	1	Catenin beta-1 OS=Homo sapiens OX=9606 GN=CTNNB1 PE=1 SV=1
CTNND1	92|73|89	1|0|0	1	Catenin delta-1 OS=Homo sapiens OX=9606 GN=CTNND1 PE=1 SV=1
DLG5	15|12|13	0|0|0	1	Disks large homolog 5 OS=Homo sapiens OX=9606 GN=DLG5 PE=1 SV=4
DSG2	7|7|7	0|0|0	1	Desmoglein-2 OS=Homo sapiens OX=9606 GN=DSG2 PE=1 SV=2
ENO2	20|11|9	0|0|0	1	Gamma-enolase OS=Homo sapiens OX=9606 GN=ENO2 PE=1 SV=3
ERBIN	113|80|73	1|2|0	1	Erbin OS=Homo sapiens OX=9606 GN=ERBIN PE=1 SV=2
FBXW11	6|8|7	0|0|0	1	F-box/WD repeat-containing protein 11 OS=Homo sapiens OX=9606 GN=FBXW11 PE=1 SV=1
KIAA1217	28|25|30	0|0|0	1	Sickle tail protein homolog OS=Homo sapiens OX=9606 GN=KIAA1217 PE=1 SV=2
KIAA1462	7|4|6	0|0|0	1	Junctional protein associated with coronary artery disease OS=Homo sapiens OX=9606 GN=JCAD PE=1 SV=3
KIRREL	11|9|9	0|0|0	1	Kin of IRRE-like protein 1 OS=Homo sapiens OX=9606 GN=KIRREL1 PE=1 SV=2
KRT80	16|17|12	0|0|0	1	Keratin, type II cytoskeletal 80 OS=Homo sapiens OX=9606 GN=KRT80 PE=1 SV=2
PARD3	16|14|17	0|1|0	1	Partitioning defective 3 homolog OS=Homo sapiens OX=9606 GN=PARD3 PE=1 SV=2
PDZD11	9|6|9	0|0|0	1	PDZ domain-containing protein 11 OS=Homo sapiens OX=9606 GN=PDZD11 PE=1 SV=2

prey Gene	Quant (SPC or Intensities)	User Controls (SPC or Intensities)	SP	Description of protein
PKP4	14|12|9	0|0|0	1	Plakophilin-4 OS=Homo sapiens OX=9606 GN=PKP4 PE=1 SV=2
PLEKHA5	87|78|72	0|0|0	1	Pleckstrin homology domain-containing family A member 5 OS=Homo sapiens OX=9606 GN=PLEKHA5 PE=1 SV=1
PLEKHA7	14|13|15	0|0|0	1	Pleckstrin homology domain-containing family A member 7 OS=Homo sapiens OX=9606 GN=PLEKHA7 PE=1 SV=2
PPP1R13B	11|7|5	0|0|0	1	Apoptosis-stimulating of p53 protein 1 OS=Homo sapiens OX=9606 GN=PPP1R13B PE=1 SV=3
PPP1R13L	26|25|20	4|2|0	1	RelA-associated inhibitor OS=Homo sapiens OX=9606 GN=PPP1R13L PE=1 SV=4
SCRIB	35|33|34	1|2|0	1	Protein scribble homolog OS=Homo sapiens OX=9606 GN=SCRIB PE=1 SV=4
SH3BP4	12|13|16	0|0|0	1	SH3 domain-binding protein 4 OS=Homo sapiens OX=9606 GN=SH3BP4 PE=1 SV=1
SHKBP1	7|4|4	0|0|0	1	SH3KBP1-binding protein 1 OS=Homo sapiens OX=9606 GN=SHKBP1 PE=1 SV=2
SHROOM3	24|18|19	0|0|0	1	Protein Shroom3 OS=Homo sapiens OX=9606 GN=SHROOM3 PE=1 SV=2
SIPA1L3	15|6|10	0|0|0	1	Signal-induced proliferation-associated 1-like protein 3 OS=Homo sapiens OX=9606 GN=SIPA1L3 PE=1 SV=3
SLC3A2	12|7|6	0|0|0	1	4F2 cell-surface antigen heavy chain OS=Homo sapiens OX=9606 GN=SLC3A2 PE=1 SV=3

prey Gene	Quant (SPC or Intensities)	User Controls (SPC or Intensities)	SP	Description of protein
SPTAN1	10|5|6	0|0|0	1	Spectrin alpha chain, non-erythrocytic 1 OS=Homo sapiens OX=9606 GN=SPTAN1 PE=1 SV=3
SPTBN1	11|4|8	0|0|0	1	Spectrin beta chain, non-erythrocytic 1 OS=Homo sapiens OX=9606 GN=SPTBN1 PE=1 SV=2
SRCIN1	16|16|11	0|0|0	1	SRC kinase signaling inhibitor 1 OS=Homo sapiens OX=9606 GN=SRCIN1 PE=1 SV=4
TANC1	10|6|11	0|0|0	1	Protein TANC1 OS=Homo sapiens OX=9606 GN=TANC1 PE=1 SV=3
TJP1	43|36|33	2|0|0	1	Tight junction protein ZO-1 OS=Homo sapiens OX=9606 GN=TJP1 PE=1 SV=3
TP53BP2	17|13|12	0|0|0	1	Apoptosis-stimulating of p53 protein 2 OS=Homo sapiens OX=9606 GN=TP53BP2 PE=1 SV=2
TRIP6	9|8|9	0|1|0	1	Thyroid receptor-interacting protein 6 OS=Homo sapiens OX=9606 GN=TRIP6 PE=1 SV=3
TUBB4A	47|37|36	0|0|0	1	Tubulin beta-4A chain OS=Homo sapiens OX=9606 GN=TUBB4A PE=1 SV=2
TUBB6	16|17|16	0|0|0	1	Tubulin beta-6 chain OS=Homo sapiens OX=9606 GN=TUBB6 PE=1 SV=1
USP54	14|12|9	0|0|0	1	Inactive ubiquitin carboxyl-terminal hydrolase 54 OS=Homo sapiens OX=9606 GN=USP54 PE=1 SV=4
YWHAB	7|4|5	0|0|0	1	14-3-3 protein beta/alpha OS=Homo sapiens OX=9606 GN=YWHAB PE=1 SV=3
YWHAQ	7|6|5	0|0|0	1	14-3-3 protein theta OS=Homo sapiens OX=9606 GN=YWHAQ PE=1 SV=1

prey Gene	Quant (SPC or Intensities)	User Controls (SPC or Intensities)	SP	Description of protein
BCL9	12|3|5	0|0|0	0.99	B-cell CLL/lymphoma 9 protein OS=Homo sapiens OX=9606 GN=BCL9 PE=1 SV=4
BCL9L	6|3|4	0|0|0	0.99	B-cell CLL/lymphoma 9-like protein OS=Homo sapiens OX=9606 GN=BCL9L PE=1 SV=1
C1ORF106	6|3|3	0|0|0	0.99	Innate immunity activator protein OS=Homo sapiens OX=9606 GN=INAVA PE=1 SV=2
CTSD	8|7|13	1|1|0	0.99	Cathepsin D OS=Homo sapiens OX=9606 GN=CTSD PE=1 SV=1
CXORF49B; CXORF49	4|4|5	0|0|0	0.99	Uncharacterized protein CXorf49 OS=Homo sapiens OX=9606 GN=CXorf49 PE=2 SV=3
EPRS	6|3|3	0|0|0	0.99	Bifunctional glutamate/proline--tRNA ligase OS=Homo sapiens OX=9606 GN=EPRS1 PE=1 SV=5
LARS	5|4|4	0|0|0	0.99	Leucine--tRNA ligase, cytoplasmic OS=Homo sapiens OX=9606 GN=LARS1 PE=1 SV=2
MINK1	5|4|4	0|0|0	0.99	Misshapen-like kinase 1 OS=Homo sapiens OX=9606 GN=MINK1 PE=1 SV=2
NCOA2	5|3|3	0|0|0	0.99	Nuclear receptor coactivator 2 OS=Homo sapiens OX=9606 GN=NCOA2 PE=1 SV=2
NHS	7|3|7	0|0|0	0.99	Nance-Horan syndrome protein OS=Homo sapiens OX=9606 GN=NHS PE=1 SV=2
SEMA4C	6|5|4	0|0|0	0.99	Semaphorin-4C OS=Homo sapiens OX=9606 GN=SEMA4C PE=1 SV=2
TANC2	8|4|4	0|0|0	0.99	Protein TANC2 OS=Homo sapiens OX=9606 GN=TANC2 PE=1 SV=3

prey Gene	Quant (SPC or Intensities)	User Controls (SPC or Intensities)	SP	Description of protein
TPM1	6|3|3	0|0|0	0.99	Tropomyosin alpha-1 chain OS=Homo sapiens OX=9606 GN=TPM1 PE=1 SV=2
ASXL2	6|2|5	0|0|0	0.98	Putative Polycomb group protein ASXL2 OS=Homo sapiens OX=9606 GN=ASXL2 PE=1 SV=1
CCDC85C	4|3|4	0|0|0	0.98	Coiled-coil domain-containing protein 85C OS=Homo sapiens OX=9606 GN=CCDC85C PE=1 SV=1
HEATR1	4|3|4	0|0|0	0.98	HEAT repeat-containing protein 1 OS=Homo sapiens OX=9606 GN=HEATR1 PE=1 SV=3
LPP	7|3|4	0|0|0	0.98	Lipoma-preferred partner OS=Homo sapiens OX=9606 GN=LPP PE=1 SV=1
MRPL44	4|2|4	0|0|0	0.98	39S ribosomal protein L44, mitochondrial OS=Homo sapiens OX=9606 GN=MRPL44 PE=1 SV=1
SET	3|3|4	0|0|0	0.98	Protein SET OS=Homo sapiens OX=9606 GN=SET PE=1 SV=3
ZDHHC5	4|4|3	0|0|0	0.98	Palmitoyltransferase ZDHHC5 OS=Homo sapiens OX=9606 GN=ZDHHC5 PE=1 SV=2
CEP85	7|2|3	0|0|0	0.97	Centrosomal protein of 85 kDa OS=Homo sapiens OX=9606 GN=CEP85 PE=1 SV=1
DDX17	3|2|3	0|0|0	0.97	Probable ATP-dependent RNA helicase DDX17 OS=Homo sapiens OX=9606 GN=DDX17 PE=1 SV=2
FLOT1	6|2|5	0|0|0	0.97	Flotillin-1 OS=Homo sapiens OX=9606 GN=FLOT1 PE=1 SV=3
NCOA1	3|3|3	0|0|0	0.97	Nuclear receptor coactivator 1 OS=Homo sapiens OX=9606 GN=NCOA1 PE=1 SV=3

prey Gene	Quant (SPC or Intensities)	User Controls (SPC or Intensities)	SP	Description of protein
NECTIN2	8|2|6	0|0|0	0.97	Nectin-2 OS=Homo sapiens OX=9606 GN=NECTIN2 PE=1 SV=1
NF2	7|11|10	0|2|1	0.97	Merlin OS=Homo sapiens OX=9606 GN=NF2 PE=1 SV=1
NOP53	7|5|6	1|1|0	0.97	Ribosome biogenesis protein NOP53 OS=Homo sapiens OX=9606 GN=NOP53 PE=1 SV=2
ANXA5	4|3|2	0|0|0	0.96	Annexin A5 OS=Homo sapiens OX=9606 GN=ANXA5 PE=1 SV=2
ARID1A	3|2|6	0|0|0	0.96	AT-rich interactive domain-containing protein 1A OS=Homo sapiens OX=9606 GN=ARID1A PE=1 SV=3
LGALS1	4|3|2	0|0|0	0.96	Galectin-1 OS=Homo sapiens OX=9606 GN=LGALS1 PE=1 SV=2
PHACTR4	4|2|3	0|0|0	0.96	Phosphatase and actin regulator 4 OS=Homo sapiens OX=9606 GN=PHACTR4 PE=1 SV=1
PLEC	31|18|27	7|1|4	0.96	Plectin OS=Homo sapiens OX=9606 GN=PLEC PE=1 SV=3
RPN1	3|2|4	0|0|0	0.96	Dolichyl-diphosphooligosaccharide--protein glycosyltransferase subunit 1 OS=Homo sapiens OX=9606 GN=RPN1 PE=1 SV=1
RPN2	4|5|2	0|0|0	0.96	Dolichyl-diphosphooligosaccharide--protein glycosyltransferase subunit 2 OS=Homo sapiens OX=9606 GN=RPN2 PE=1 SV=3
TCF7L2	4|3|2	0|0|0	0.96	Transcription factor 7-like 2 OS=Homo sapiens OX=9606 GN=TCF7L2 PE=1 SV=2

prey Gene	Quant (SPC or Intensities)	User Controls (SPC or Intensities)	SP	Description of protein
VCP	12|4|7	0|1|1	0.96	Transitional endoplasmic reticulum ATPase OS=Homo sapiens OX=9606 GN=VCP PE=1 SV=4
XRN1	6|2|3	0|0|0	0.96	5'-3' exoribonuclease 1 OS=Homo sapiens OX=9606 GN=XRN1 PE=1 SV=1
GTPBP4	2|3|4	0|0|0	0.95	GTP-binding protein 4 OS=Homo sapiens OX=9606 GN=GTPBP4 PE=1 SV=3
MBOAT7	3|2|3	0|0|0	0.95	Lysophospholipid acyltransferase 7 OS=Homo sapiens OX=9606 GN=MBOAT7 PE=1 SV=2
TJP2	8|4|2	0|0|0	0.95	Tight junction protein ZO-2 OS=Homo sapiens OX=9606 GN=TJP2 PE=1 SV=2
ACTN4	13|7|6	0|2|1	0.94	Alpha-actinin-4 OS=Homo sapiens OX=9606 GN=ACTN4 PE=1 SV=2
ALDH18A1	4|2|2	0|0|0	0.94	Delta-1-pyrroline-5-carboxylate synthase OS=Homo sapiens OX=9606 GN=ALDH18A1 PE=1 SV=2
DARS	5|4|6	1|1|0	0.94	Aspartate--tRNA ligase, cytoplasmic OS=Homo sapiens OX=9606 GN=DARS1 PE=1 SV=2
ELFN1	4|2|2	0|0|0	0.94	Protein ELFN1 OS=Homo sapiens OX=9606 GN=ELFN1 PE=1 SV=2
HACD3	3|2|2	0|0|0	0.94	Very-long-chain (3R)-3-hydroxyacyl-CoA dehydratase 3 OS=Homo sapiens OX=9606 GN=HACD3 PE=1 SV=2
PFKM	2|2|3	0|0|0	0.94	ATP-dependent 6-phosphofructokinase, muscle type OS=Homo sapiens OX=9606 GN=PFKM PE=1 SV=2

prey Gene	Quant (SPC or Intensities)	User Controls (SPC or Intensities)	SP	Description of protein
PFN1	9|3|3	1|0|0	0.94	Profilin-1 OS=Homo sapiens OX=9606 GN=PFN1 PE=1 SV=2
PKP3	3|2|2	0|0|0	0.94	Plakophilin-3 OS=Homo sapiens OX=9606 GN=PKP3 PE=1 SV=1
RPS14	8|5|5	1|1|0	0.94	40S ribosomal protein S14 OS=Homo sapiens OX=9606 GN=RPS14 PE=1 SV=3
TLE3	6|4|2	0|0|0	0.94	Transducin-like enhancer protein 3 OS=Homo sapiens OX=9606 GN=TLE3 PE=1 SV=2
VDAC3	7|4|4	1|1|0	0.94	Voltage-dependent anion-selective channel protein 3 OS=Homo sapiens OX=9606 GN=VDAC3 PE=1 SV=1
XRCC6	5|2|2	0|0|0	0.94	X-ray repair cross-complementing protein 6 OS=Homo sapiens OX=9606 GN=XRCC6 PE=1 SV=2
CLTC	4|4|6	0|0|1	0.93	Clathrin heavy chain 1 OS=Homo sapiens OX=9606 GN=CLTC PE=1 SV=5
GNAI2	2|2|3	0|0|0	0.93	Guanine nucleotide-binding protein G(i) subunit alpha-2 OS=Homo sapiens OX=9606 GN=GNAI2 PE=1 SV=3
NCOA3	6|2|2	0|0|0	0.93	Nuclear receptor coactivator 3 OS=Homo sapiens OX=9606 GN=NCOA3 PE=1 SV=1
PIGR	3|2|2	0|0|0	0.93	Polymeric immunoglobulin receptor OS=Homo sapiens OX=9606 GN=PIGR PE=1 SV=4
ALDOA	6|2|5	0|0|1	0.92	Fructose-bisphosphate aldolase A OS=Homo sapiens OX=9606 GN=ALDOA PE=1 SV=2
ASCC3	3|2|2	0|0|0	0.91	Activating signal cointegrator 1 complex subunit 3 OS=Homo sapiens

prey Gene	Quant (SPC or Intensities)	User Controls (SPC or Intensities)	SP	Description of protein
				OX=9606 GN=ASCC3 PE=1 SV=3
CXADR	2|2|2	0|0|0	0.91	Coxsackievirus and adenovirus receptor OS=Homo sapiens OX=9606 GN=CXADR PE=1 SV=1
MIF	2|2|2	0|0|0	0.91	Macrophage migration inhibitory factor OS=Homo sapiens OX=9606 GN=MIF PE=1 SV=4
IGKC	3|3|2	1|0|0	0.9	Immunoglobulin kappa constant OS=Homo sapiens OX=9606 GN=IGKC PE=1 SV=2
KRT23	3|1|3	0|0|0	0.9	Keratin, type I cytoskeletal 23 OS=Homo sapiens OX=9606 GN=KRT23 PE=1 SV=2
MAGI1	11|5|9	3|1|0	0.9	Membrane-associated guanylate kinase, WW and PDZ domain-containing protein 1 OS=Homo sapiens OX=9606 GN=MAGI1 PE=1 SV=3
RAI14	2|2|2	0|0|0	0.9	Ankycorbin OS=Homo sapiens OX=9606 GN=RAI14 PE=1 SV=2
RPS25	4|5|4	2|0|0	0.9	40S ribosomal protein S25 OS=Homo sapiens OX=9606 GN=RPS25 PE=1 SV=1
RAB2A	3|2|4	0|1|0	0.89	Ras-related protein Rab-2A OS=Homo sapiens OX=9606 GN=RAB2A PE=1 SV=1
STRAP	3|1|4	0|0|0	0.89	Serine-threonine kinase receptor-associated protein OS=Homo sapiens OX=9606 GN=STRAP PE=1 SV=1
CCT7	4|4|3	0|0|1	0.88	T-complex protein 1 subunit eta OS=Homo sapiens OX=9606 GN=CCT7 PE=1 SV=2
EFNB1	2|1|2	0|0|0	0.88	Ephrin-B1 OS=Homo sapiens OX=9606 GN=EFNB1 PE=1 SV=1

prey Gene	Quant (SPC or Intensities)	User Controls (SPC or Intensities)	SP	Description of protein
CCT5	5|4|4	1|1|0	0.87	T-complex protein 1 subunit epsilon OS=Homo sapiens OX=9606 GN=CCT5 PE=1 SV=1
DLG1	3|1|5	0|0|0	0.87	Disks large homolog 1 OS=Homo sapiens OX=9606 GN=DLG1 PE=1 SV=2
EIF3L	2|1|2	0|0|0	0.87	Eukaryotic translation initiation factor 3 subunit L OS=Homo sapiens OX=9606 GN=EIF3L PE=1 SV=1
FLNB	9|7|8	0|0|5	0.87	Filamin-B OS=Homo sapiens OX=9606 GN=FLNB PE=1 SV=2
MCM2	3|1|2	0|0|0	0.87	DNA replication licensing factor MCM2 OS=Homo sapiens OX=9606 GN=MCM2 PE=1 SV=4
PGK1	8|6|6	2|1|1	0.87	Phosphoglycerate kinase 1 OS=Homo sapiens OX=9606 GN=PGK1 PE=1 SV=3
PHB	6|4|6	2|1|0	0.87	Prohibitin OS=Homo sapiens OX=9606 GN=PHB PE=1 SV=1
PHGDH	7|3|4	2|0|0	0.87	D-3-phosphoglycerate dehydrogenase OS=Homo sapiens OX=9606 GN=PHGDH PE=1 SV=4
RPL35A	3|1|2	0|0|0	0.87	60S ribosomal protein L35a OS=Homo sapiens OX=9606 GN=RPL35A PE=1 SV=2
TGM3	6|4|9	1|2|0	0.87	Protein-glutamine gamma-glutamyltransferase E OS=Homo sapiens OX=9606 GN=TGM3 PE=1 SV=4
CALML3	1|2|3	0|0|0	0.86	Calmodulin-like protein 3 OS=Homo sapiens OX=9606 GN=CALML3 PE=1 SV=2
COPB2	2|1|2	0|0|0	0.86	Coatomer subunit beta' OS=Homo sapiens OX=9606 GN=COPB2 PE=1 SV=2

prey Gene	Quant (SPC or Intensities)	User Controls (SPC or Intensities)	SP	Description of protein
FAM83H	3|1|3	0|0|0	0.86	Protein FAM83H OS=Homo sapiens OX=9606 GN=FAM83H PE=1 SV=3
OAT	2|1|2	0|0|0	0.86	Ornithine aminotransferase, mitochondrial OS=Homo sapiens OX=9606 GN=OAT PE=1 SV=1
PDCD6IP	2|1|3	0|0|0	0.86	Programmed cell death 6-interacting protein OS=Homo sapiens OX=9606 GN=PDCD6IP PE=1 SV=1
RALY	3|3|1	0|0|0	0.86	RNA-binding protein Raly OS=Homo sapiens OX=9606 GN=RALY PE=1 SV=1
CASP14	9|7|11	1|3|1	0.85	Caspase-14 OS=Homo sapiens OX=9606 GN=CASP14 PE=1 SV=2
CCDC120	4|1|2	0|0|0	0.85	Coiled-coil domain-containing protein 120 OS=Homo sapiens OX=9606 GN=CCDC120 PE=1 SV=1
DDX6	3|1|2	0|0|0	0.85	Probable ATP-dependent RNA helicase DDX6 OS=Homo sapiens OX=9606 GN=DDX6 PE=1 SV=2
DYNC1H1	11|5|12	2|2|0	0.85	Cytoplasmic dynein 1 heavy chain 1 OS=Homo sapiens OX=9606 GN=DYNC1H1 PE=1 SV=5
JUP	16|26|39	0|12|2	0.85	Junction plakoglobin OS=Homo sapiens OX=9606 GN=JUP PE=1 SV=3
LZTS3	3|2|1	0|0|0	0.85	Leucine zipper putative tumor suppressor 3 OS=Homo sapiens OX=9606 GN=LZTS3 PE=2 SV=1
PSAP	2|1|2	0|0|0	0.85	Prosaposin OS=Homo sapiens OX=9606 GN=PSAP PE=1 SV=2

prey Gene	Quant (SPC or Intensities)	User Controls (SPC or Intensities)	SP	Description of protein
PSMD2	3|2|1	0|0|0	0.85	26S proteasome non-ATPase regulatory subunit 2 OS=Homo sapiens OX=9606 GN=PSMD2 PE=1 SV=3
VDAC1	4|3|3	0|0|2	0.85	Voltage-dependent anion-selective channel protein 1 OS=Homo sapiens OX=9606 GN=VDAC1 PE=1 SV=2
CSE1L	4|2|3	0|1|0	0.84	Exportin-2 OS=Homo sapiens OX=9606 GN=CSE1L PE=1 SV=3
EIF3A	5|1|4	0|0|0	0.84	Eukaryotic translation initiation factor 3 subunit A OS=Homo sapiens OX=9606 GN=EIF3A PE=1 SV=1
GART	5|1|2	0|0|0	0.84	Trifunctional purine biosynthetic protein adenosine-3 OS=Homo sapiens OX=9606 GN=GART PE=1 SV=1
GDI2	2|2|1	0|0|0	0.84	Rab GDP dissociation inhibitor beta OS=Homo sapiens OX=9606 GN=GDI2 PE=1 SV=2
LZTS2	3|2|1	0|0|0	0.84	Leucine zipper putative tumor suppressor 2 OS=Homo sapiens OX=9606 GN=LZTS2 PE=1 SV=2
PA2G4	2|2|1	0|0|0	0.84	Proliferation-associated protein 2G4 OS=Homo sapiens OX=9606 GN=PA2G4 PE=1 SV=3
PARK7	2|2|4	1|0|0	0.84	Parkinson disease protein 7 OS=Homo sapiens OX=9606 GN=PARK7 PE=1 SV=2
PDIA3	3|2|1	0|0|0	0.84	Protein disulfide-isomerase A3 OS=Homo sapiens OX=9606 GN=PDIA3 PE=1 SV=4

prey Gene	Quant (SPC or Intensities)	User Controls (SPC or Intensities)	SP	Description of protein
POP1	2|1|3	0|0|0	0.84	Ribonucleases P/MRP protein subunit POP1 OS=Homo sapiens OX=9606 GN=POP1 PE=1 SV=2
QARS	2|1|2	0|0|0	0.84	Glutamine--tRNA ligase OS=Homo sapiens OX=9606 GN=QARS1 PE=1 SV=1
SLC25A10	2|2|1	0|0|0	0.84	Mitochondrial dicarboxylate carrier OS=Homo sapiens OX=9606 GN=SLC25A10 PE=1 SV=2
VCL	5|1|6	0|0|0	0.84	Vinculin OS=Homo sapiens OX=9606 GN=VCL PE=1 SV=4
YWHAE	9|6|6	5|0|0	0.84	14-3-3 protein epsilon OS=Homo sapiens OX=9606 GN=YWHAE PE=1 SV=1
CDK1	5|1|1	0|0|0	0.83	Cyclin-dependent kinase 1 OS=Homo sapiens OX=9606 GN=CDK1 PE=1 SV=3
EEF1G	6|2|5	2|0|0	0.83	Elongation factor 1-gamma OS=Homo sapiens OX=9606 GN=EEF1G PE=1 SV=3
ELFN2	2|1|2	0|0|0	0.83	Protein phosphatase 1 regulatory subunit 29 OS=Homo sapiens OX=9606 GN=ELFN2 PE=1 SV=1
FH	1|2|2	0|0|0	0.83	Fumarate hydratase, mitochondrial OS=Homo sapiens OX=9606 GN=FH PE=1 SV=3
MRPS34	3|1|1	0|0|0	0.83	28S ribosomal protein S34, mitochondrial OS=Homo sapiens OX=9606 GN=MRPS34 PE=1 SV=2
NCOR1	2|2|2	0|0|0	0.83	Nuclear receptor corepressor 1 OS=Homo sapiens OX=9606 GN=NCOR1 PE=1 SV=2
PRR12	3|2|1	0|0|0	0.83	Proline-rich protein 12 OS=Homo sapiens

prey Gene	Quant (SPC or Intensities)	User Controls (SPC or Intensities)	SP	Description of protein
				OX=9606 GN=PRR12 PE=1 SV=3
SNAP23	2|2|1	0|0|0	0.83	Synaptosomal-associated protein 23 OS=Homo sapiens OX=9606 GN=SNAP23 PE=1 SV=1
VPS26A	2|2|1	0|0|0	0.83	Vacuolar protein sorting-associated protein 26A OS=Homo sapiens OX=9606 GN=VPS26A PE=1 SV=2
XRCC5	6|3|4	1|1|0	0.83	X-ray repair cross-complementing protein 5 OS=Homo sapiens OX=9606 GN=XRCC5 PE=1 SV=3
10-Sep	1|2|3	0|0|0	0.82	Septin-10 OS=Homo sapiens OX=9606 GN=SEPTIN10 PE=1 SV=2
ATP1A1	6|3|2	1|0|0	0.82	Sodium/potassium-transporting ATPase subunit alpha-1 OS=Homo sapiens OX=9606 GN=ATP1A1 PE=1 SV=1
ATP2A2	3|2|3	1|0|0	0.82	Sarcoplasmic/endoplasmic reticulum calcium ATPase 2 OS=Homo sapiens OX=9606 GN=ATP2A2 PE=1 SV=1
LTF	3|1|10	0|0|0	0.82	Lactotransferrin OS=Homo sapiens OX=9606 GN=LTF PE=1 SV=6
PRDX5	2|1|1	0|0|0	0.82	Peroxiredoxin-5, mitochondrial OS=Homo sapiens OX=9606 GN=PRDX5 PE=1 SV=4
SMARCD3	1|2|2	0|0|0	0.82	SWI/SNF-related matrix-associated actin-dependent regulator of chromatin subfamily D member 3 OS=Homo sapiens OX=9606 GN=SMARCD3 PE=1 SV=1
XPO1	4|4|3	1|1|0	0.82	Exportin-1 OS=Homo sapiens OX=9606 GN=XPO1 PE=1 SV=1

prey Gene	Quant (SPC or Intensities)	User Controls (SPC or Intensities)	SP	Description of protein
CCT2	6|2|2	0|1|0	0.81	T-complex protein 1 subunit beta OS=Homo sapiens OX=9606 GN=CCT2 PE=1 SV=4
JAM3	2|1|1	0|0|0	0.81	Junctional adhesion molecule C OS=Homo sapiens OX=9606 GN=JAM3 PE=1 SV=1
MSH6	3|1|2	0|0|0	0.81	DNA mismatch repair protein Msh6 OS=Homo sapiens OX=9606 GN=MSH6 PE=1 SV=2
PLIN2	2|3|2	1|0|0	0.81	Perilipin-2 OS=Homo sapiens OX=9606 GN=PLIN2 PE=1 SV=2
SBDS	2|1|1	0|0|0	0.81	Ribosome maturation protein SBDS OS=Homo sapiens OX=9606 GN=SBDS PE=1 SV=4
TPI1	7|4|6	3|1|0	0.81	Triosephosphate isomerase OS=Homo sapiens OX=9606 GN=TPI1 PE=1 SV=4
CKAP4	5|1|1	0|0|0	0.8	Cytoskeleton-associated protein 4 OS=Homo sapiens OX=9606 GN=CKAP4 PE=1 SV=2
COPG1	5|2|2	0|1|0	0.8	Coatomer subunit gamma-1 OS=Homo sapiens OX=9606 GN=COPG1 PE=1 SV=1
CPA4	1|1|2	0|0|0	0.8	Carboxypeptidase A4 OS=Homo sapiens OX=9606 GN=CPA4 PE=1 SV=2
EIF4A3	4|1|1	0|0|0	0.8	Eukaryotic initiation factor 4A-III OS=Homo sapiens OX=9606 GN=EIF4A3 PE=1 SV=4
FDXR	2|1|1	0|0|0	0.8	NADPH: adrenodoxin oxidoreductase, mitochondrial OS=Homo sapiens OX=9606 GN=FDXR PE=1 SV=3
NHSL2	1|2|2	0|0|0	0.8	NHS-like protein 2 OS=Homo sapiens OX=9606 GN=NHSL2 PE=1 SV=2

prey Gene	Quant (SPC or Intensities)	User Controls (SPC or Intensities)	SP	Description of protein
PHB2	5|1|3	0|0|1	0.8	Prohibitin-2 OS=Homo sapiens OX=9606 GN=PHB2 PE=1 SV=2
RPS27	2|2|2	0|1|0	0.8	40S ribosomal protein S27 OS=Homo sapiens OX=9606 GN=RPS27 PE=1 SV=3
UBE2V1	2|1|1	0|0|0	0.8	Ubiquitin-conjugating enzyme E2 variant 1 OS=Homo sapiens OX=9606 GN=UBE2V1 PE=1 SV=2
ALDOC	1|1|2	0|0|0	0.79	Fructose-bisphosphate aldolase C OS=Homo sapiens OX=9606 GN=ALDOC PE=1 SV=2
CISD2	2|1|4	0|0|1	0.79	CDGSH iron-sulfur domain-containing protein 2 OS=Homo sapiens OX=9606 GN=CISD2 PE=1 SV=1
DDOST	3|1|1	0|0|0	0.79	Dolichyl-diphosphooligosaccharide--protein glycosyltransferase 48 kDa subunit OS=Homo sapiens OX=9606 GN=DDOST PE=1 SV=4
FUBP1	3|2|2	1|0|0	0.79	Far upstream element-binding protein 1 OS=Homo sapiens OX=9606 GN=FUBP1 PE=1 SV=3
GSDMA	2|3|3	0|1|0	0.79	Gasdermin-A OS=Homo sapiens OX=9606 GN=GSDMA PE=1 SV=4
IQGAP1	7|1|4	0|0|0	0.79	Ras GTPase-activating-like protein IQGAP1 OS=Homo sapiens OX=9606 GN=IQGAP1 PE=1 SV=1
MAPRE1	2|2|2	0|1|0	0.79	Microtubule-associated protein RP/EB family member 1 OS=Homo sapiens OX=9606 GN=MAPRE1 PE=1 SV=3
MCAM	8|8|5	2|1|1	0.79	Cell surface glycoprotein MUC18 OS=Homo sapiens OX=9606 GN=MCAM PE=1 SV=2

prey Gene	Quant (SPC or Intensities)	User Controls (SPC or Intensities)	SP	Description of protein
MXRA8	2|1|1	0|0|0	0.79	Matrix remodeling-associated protein 8 OS=Homo sapiens OX=9606 GN=MXRA8 PE=1 SV=1
PSMA6	3|2|2	0|0|1	0.79	Proteasome subunit alpha type-6 OS=Homo sapiens OX=9606 GN=PSMA6 PE=1 SV=1
RCC1	2|1|1	0|0|0	0.79	Regulator of chromosome condensation OS=Homo sapiens OX=9606 GN=RCC1 PE=1 SV=1
RPL23	15|6|7	6|1|0	0.79	60S ribosomal protein L23 OS=Homo sapiens OX=9606 GN=RPL23 PE=1 SV=1
S100A10	3|1|1	0|0|0	0.79	Protein S100-A10 OS=Homo sapiens OX=9606 GN=S100A10 PE=1 SV=2
AUP1	1|1|2	0|0|0	0.78	Lipid droplet-regulating VLDL assembly factor AUP1 OS=Homo sapiens OX=9606 GN=AUP1 PE=1 SV=2
DHRS2	2|2|2	0|0|1	0.78	Dehydrogenase/reductase SDR family member 2, mitochondrial OS=Homo sapiens OX=9606 GN=DHRS2 PE=1 SV=4
DSC1	4|6|11	0|4|0	0.78	Desmocollin-1 OS=Homo sapiens OX=9606 GN=DSC1 PE=1 SV=2
PDHA1	2|1|1	0|0|0	0.78	Pyruvate dehydrogenase E1 component subunit alpha, somatic form, mitochondrial OS=Homo sapiens OX=9606 GN=PDHA1 PE=1 SV=3
PEBP1	2|2|2	1|0|0	0.78	Phosphatidylethanolamine-binding protein 1 OS=Homo sapiens OX=9606 GN=PEBP1 PE=1 SV=3
PES1	4|1|5	0|1|0	0.78	Pescadillo homolog OS=Homo sapiens OX=9606 GN=PES1 PE=1 SV=1

prey Gene	Quant (SPC or Intensities)	User Controls (SPC or Intensities)	SP	Description of protein
PHLDB1	3|2|1	0|0|0	0.78	Pleckstrin homology-like domain family B member 1 OS=Homo sapiens OX=9606 GN=PHLDB1 PE=1 SV=1
RPL26	1|2|1	0|0|0	0.78	60S ribosomal protein L26 OS=Homo sapiens OX=9606 GN=RPL26 PE=1 SV=1
RPS18	3|1|2	1|0|0	0.78	40S ribosomal protein S18 OS=Homo sapiens OX=9606 GN=RPS18 PE=1 SV=3
RUVBL1	2|1|1	0|0|0	0.78	RuvB-like 1 OS=Homo sapiens OX=9606 GN=RUVBL1 PE=1 SV=1
TNRC6B	10|3|5	1|2|0	0.78	Trinucleotide repeat-containing gene 6B protein OS=Homo sapiens OX=9606 GN=TNRC6B PE=1 SV=4
EPB41L5	5|2|2	0|1|0	0.77	Band 4.1-like protein 5 OS=Homo sapiens OX=9606 GN=EPB41L5 PE=1 SV=3
MRPL43	3|1|2	1|0|0	0.77	39S ribosomal protein L43, mitochondrial OS=Homo sapiens OX=9606 GN=MRPL43 PE=1 SV=1
MTA1	3|1|1	0|0|0	0.77	Metastasis-associated protein MTA1 OS=Homo sapiens OX=9606 GN=MTA1 PE=1 SV=2
PSMC1	2|1|1	0|0|0	0.77	26S proteasome regulatory subunit 4 OS=Homo sapiens OX=9606 GN=PSMC1 PE=1 SV=1
RARS	3|1|1	0|0|0	0.77	Arginine--tRNA ligase, cytoplasmic OS=Homo sapiens OX=9606 GN=RARS1 PE=1 SV=2
SPRR1B	1|2|3	0|1|0	0.77	Cornifin-B OS=Homo sapiens OX=9606 GN=SPRR1B PE=1 SV=2
STEAP3	1|1|2	0|0|0	0.77	Metalloreductase STEAP3 OS=Homo sapiens OX=9606 GN=STEAP3 PE=1 SV=2

prey Gene	Quant (SPC or Intensities)	User Controls (SPC or Intensities)	SP	Description of protein
FABP5	4|7|6	0|2|2	0.76	Fatty acid-binding protein 5 OS=Homo sapiens OX=9606 GN=FABP5 PE=1 SV=3
FSCN1	2|1|1	0|0|0	0.76	Fascin OS=Homo sapiens OX=9606 GN=FSCN1 PE=1 SV=3
HBS1L	2|1|1	0|0|0	0.76	HBS1-like protein OS=Homo sapiens OX=9606 GN=HBS1L PE=1 SV=1
ILF3	5|2|4	1|1|0	0.76	Interleukin enhancer-binding factor 3 OS=Homo sapiens OX=9606 GN=ILF3 PE=1 SV=3
MTHFD1	12|8|6	2|4|0	0.76	C-1-tetrahydrofolate synthase, cytoplasmic OS=Homo sapiens OX=9606 GN=MTHFD1 PE=1 SV=4
NEDD1	2|1|1	0|0|0	0.76	Protein NEDD1 OS=Homo sapiens OX=9606 GN=NEDD1 PE=1 SV=1
NUP205	3|1|2	0|0|0	0.76	Nuclear pore complex protein Nup205 OS=Homo sapiens OX=9606 GN=NUP205 PE=1 SV=3
P0DOX2	1|3|1	0|0|0	0.76	Immunoglobulin alpha-2 heavy chain OS=Homo sapiens OX=9606 PE=1 SV=2
SSR4	1|1|2	0|0|0	0.76	Translocon-associated protein subunit delta OS=Homo sapiens OX=9606 GN=SSR4 PE=1 SV=1
USP6NL	1|1|2	0|0|0	0.76	USP6 N-terminal-like protein OS=Homo sapiens OX=9606 GN=USP6NL PE=1 SV=3
ARHGAP32	4|1|2	0|0|0	0.75	Rho GTPase-activating protein 32 OS=Homo sapiens OX=9606 GN=ARHGAP32 PE=1 SV=1
CALM3	2|1|3	0|1|0	0.75	Calmodulin-3 OS=Homo sapiens OX=9606 GN=CALM3 PE=1 SV=1

prey Gene	Quant (SPC or Intensities)	User Controls (SPC or Intensities)	SP	Description of protein
CCDC102A	7|4|3	3|0|0	0.75	Coiled-coil domain-containing protein 102A OS=Homo sapiens OX=9606 GN=CCDC102A PE=1 SV=2
PLEKHA6	3|1|1	0|0|0	0.75	Pleckstrin homology domain-containing family A member 6 OS=Homo sapiens OX=9606 GN=PLEKHA6 PE=1 SV=4
ZDHHC8	2|1|1	0|0|0	0.75	Palmitoyltransferase ZDHHC8 OS=Homo sapiens OX=9606 GN=ZDHHC8 PE=1 SV=3
ZG16B	2|3|1	0|0|1	0.75	Zymogen granule protein 16 homolog B OS=Homo sapiens OX=9606 GN=ZG16B PE=1 SV=3
CAT	2|5|8	1|1|0	0.74	Catalase OS=Homo sapiens OX=9606 GN=CAT PE=1 SV=3
COPA	2|5|4	2|0|0	0.74	Coatomer subunit alpha OS=Homo sapiens OX=9606 GN=COPA PE=1 SV=2
EP300	5|1|2	0|0|0	0.74	Histone acetyltransferase p300 OS=Homo sapiens OX=9606 GN=EP300 PE=1 SV=2
SCYL2	2|1|1	0|0|0	0.74	SCY1-like protein 2 OS=Homo sapiens OX=9606 GN=SCYL2 PE=1 SV=1
SERPINH1	8|4|8	3|2|0	0.74	Serpin H1 OS=Homo sapiens OX=9606 GN=SERPINH1 PE=1 SV=2
DLG3	2|1|1	0|0|0	0.73	Disks large homolog 3 OS=Homo sapiens OX=9606 GN=DLG3 PE=1 SV=2
P0DOX5	1|3|4	1|0|0	0.73	Immunoglobulin gamma-1 heavy chain OS=Homo sapiens OX=9606 PE=1 SV=2
TGM1	2|3|4	0|2|0	0.73	Protein-glutamine gamma-glutamyltransferase K OS=Homo sapiens

prey Gene	Quant (SPC or Intensities)	User Controls (SPC or Intensities)	SP	Description of protein
				OX=9606 GN=TGM1 PE=1 SV=4
2-Sep	7|4|4	3|1|0	0.71	Septin-2 OS=Homo sapiens OX=9606 GN=SEPTIN2 PE=1 SV=1
BAIAP2	3|2|1	0|1|0	0.71	Brain-specific angiogenesis inhibitor 1-associated protein 2 OS=Homo sapiens OX=9606 GN=BAIAP2 PE=1 SV=1
CAND1	4|1|1	0|0|0	0.71	Cullin-associated NEDD8-dissociated protein 1 OS=Homo sapiens OX=9606 GN=CAND1 PE=1 SV=2
KPNA2	4|3|2	2|0|0	0.71	Importin subunit alpha-1 OS=Homo sapiens OX=9606 GN=KPNA2 PE=1 SV=1
NSFL1C	4|2|2	0|2|0	0.71	NSFL1 cofactor p47 OS=Homo sapiens OX=9606 GN=NSFL1C PE=1 SV=2
RPS16	7|3|7	0|3|1	0.71	40S ribosomal protein S16 OS=Homo sapiens OX=9606 GN=RPS16 PE=1 SV=2
ATAD2	2|2|3	1|0|0	0.7	ATPase family AAA domain-containing protein 2 OS=Homo sapiens OX=9606 GN=ATAD2 PE=1 SV=1
KIF5B	3|1|1	0|0|0	0.7	Kinesin-1 heavy chain OS=Homo sapiens OX=9606 GN=KIF5B PE=1 SV=1
RPS19	3|1|1	1|0|0	0.7	40S ribosomal protein S19 OS=Homo sapiens OX=9606 GN=RPS19 PE=1 SV=2
GOT2	3|2|3	2|0|0	0.69	Aspartate aminotransferase, mitochondrial OS=Homo sapiens OX=9606 GN=GOT2 PE=1 SV=3

prey Gene	Quant (SPC or Intensities)	User Controls (SPC or Intensities)	SP	Description of protein
MED15	7|4|6	2|2|0	0.69	Mediator of RNA polymerase II transcription subunit 15 OS=Homo sapiens OX=9606 GN=MED15 PE=1 SV=2
MYO6	7|3|8	2|2|0	0.69	Unconventional myosin-VI OS=Homo sapiens OX=9606 GN=MYO6 PE=1 SV=4
PARVA	2|1|2	1|0|0	0.69	Alpha-parvin OS=Homo sapiens OX=9606 GN=PARVA PE=1 SV=1
PDIA6	2|3|3	0|0|2	0.69	Protein disulfide-isomerase A6 OS=Homo sapiens OX=9606 GN=PDIA6 PE=1 SV=1
ZC3HAV1	10|7|8	2|3|2	0.69	Zinc finger CCCH-type antiviral protein 1 OS=Homo sapiens OX=9606 GN=ZC3HAV1 PE=1 SV=3
CAD	2|2|1	0|0|0	0.68	CAD protein OS=Homo sapiens OX=9606 GN=CAD PE=1 SV=3
CAP1	2|3|1	0|1|0	0.68	Adenylyl cyclase-associated protein 1 OS=Homo sapiens OX=9606 GN=CAP1 PE=1 SV=5
CC2D1A	1|1|2	0|0|0	0.68	Coiled-coil and C2 domain-containing protein 1A OS=Homo sapiens OX=9606 GN=CC2D1A PE=1 SV=1
CS	3|1|2	1|0|0	0.68	Citrate synthase, mitochondrial OS=Homo sapiens OX=9606 GN=CS PE=1 SV=2
EIF4A1	9|7|8	0|7|0	0.68	Eukaryotic initiation factor 4A-I OS=Homo sapiens OX=9606 GN=EIF4A1 PE=1 SV=1
ESYT1	2|1|1	0|0|0	0.68	Extended synaptotagmin-1 OS=Homo sapiens OX=9606 GN=ESYT1 PE=1 SV=1
FRMD4A	2|1|1	0|0|0	0.68	FERM domain-containing protein 4A OS=Homo

prey Gene	Quant (SPC or Intensities)	User Controls (SPC or Intensities)	SP	Description of protein
				sapiens OX=9606 GN=FRMD4A PE=1 SV=3
GLS	3|2|1	0|1|0	0.68	Glutaminase kidney isoform, mitochondrial OS=Homo sapiens OX=9606 GN=GLS PE=1 SV=1
RPLP1	1|1|2	0|0|1	0.68	60S acidic ribosomal protein P1 OS=Homo sapiens OX=9606 GN=RPLP1 PE=1 SV=1
RPS20	3|4|4	2|1|0	0.68	40S ribosomal protein S20 OS=Homo sapiens OX=9606 GN=RPS20 PE=1 SV=1
EPS15L1	5|4|3	2|1|0	0.67	Epidermal growth factor receptor substrate 15-like 1 OS=Homo sapiens OX=9606 GN=EPS15L1 PE=1 SV=1
LATS1	2|1|1	0|0|0	0.67	Serine/threonine-protein kinase LATS1 OS=Homo sapiens OX=9606 GN=LATS1 PE=1 SV=1
PAGE2B	5|3|3	0|0|3	0.67	Putative G antigen family E member 3 OS=Homo sapiens OX=9606 GN=PAGE2B PE=3 SV=1
SERPINB12	2|5|5	0|2|1	0.67	Serpin B12 OS=Homo sapiens OX=9606 GN=SERPINB12 PE=1 SV=1
SERPINB3	3|4|9	0|4|0	0.67	Serpin B3 OS=Homo sapiens OX=9606 GN=SERPINB3 PE=1 SV=2
YBX1	7|2|3	2|1|0	0.67	Y-box-binding protein 1 OS=Homo sapiens OX=9606 GN=YBX1 PE=1 SV=3
KRT71	0|8|9	0|0|0	0.65	Keratin, type II cytoskeletal 71 OS=Homo sapiens OX=9606 GN=KRT71 PE=1 SV=3
NOP58	5|3|3	2|1|0	0.65	Nucleolar protein 58 OS=Homo sapiens OX=9606 GN=NOP58 PE=1 SV=1

prey Gene	Quant (SPC or Intensities)	User Controls (SPC or Intensities)	SP	Description of protein
SERPINB4	0|4|8	0|0|0	0.65	Serpin B4 OS=Homo sapiens OX=9606 GN=SERPINB4 PE=1 SV=2
TUBA4A	38|30|0	0|0|0	0.65	Tubulin alpha-4A chain OS=Homo sapiens OX=9606 GN=TUBA4A PE=1 SV=1
TUBB2A	44|0|41	0|25|0	0.65	Tubulin beta-2A chain OS=Homo sapiens OX=9606 GN=TUBB2A PE=1 SV=1
ADD3	1|2|3	1|0|0	0.64	Gamma-adducin OS=Homo sapiens OX=9606 GN=ADD3 PE=1 SV=1
ELAVL1	3|1|1	0|0|1	0.64	ELAV-like protein 1 OS=Homo sapiens OX=9606 GN=ELAVL1 PE=1 SV=2
HDLBP	3|1|2	1|0|0	0.64	Vigilin OS=Homo sapiens OX=9606 GN=HDLBP PE=1 SV=2
YWHAG	6|0|5	0|0|0	0.64	14-3-3 protein gamma OS=Homo sapiens OX=9606 GN=YWHAG PE=1 SV=2
EIF3B	4|0|5	1|0|0	0.63	Eukaryotic translation initiation factor 3 subunit B OS=Homo sapiens OX=9606 GN=EIF3B PE=1 SV=3
NOTCH2	2|1|2	0|0|0	0.63	Neurogenic locus notch homolog protein 2 OS=Homo sapiens OX=9606 GN=NOTCH2 PE=1 SV=3
STOML2	3|1|1	1|0|0	0.63	Stomatin-like protein 2, mitochondrial OS=Homo sapiens OX=9606 GN=STOML2 PE=1 SV=1
ACOT7	3|1|1	1|0|0	0.62	Cytosolic acyl coenzyme A thioester hydrolase OS=Homo sapiens OX=9606 GN=ACOT7 PE=1 SV=3

prey Gene	Quant (SPC or Intensities)	User Controls (SPC or Intensities)	SP	Description of protein
PSMD3	5|4|4	1|3|0	0.62	26S proteasome non-ATPase regulatory subunit 3 OS=Homo sapiens OX=9606 GN=PSMD3 PE=1 SV=2
TNKS1BP1	10|5|9	4|2|0	0.62	182 kDa tankyrase-1-binding protein OS=Homo sapiens OX=9606 GN=TNKS1BP1 PE=1 SV=4
TPM3	6|0|3	1|0|0	0.62	Tropomyosin alpha-3 chain OS=Homo sapiens OX=9606 GN=TPM3 PE=1 SV=2
ZNF609	2|1|1	0|0|0	0.62	Zinc finger protein 609 OS=Homo sapiens OX=9606 GN=ZNF609 PE=1 SV=2
AHCY	3|2|0	0|0|0	0.61	Adenosylhomocysteinase OS=Homo sapiens OX=9606 GN=AHCY PE=1 SV=4
MCM7	6|2|1	2|0|0	0.61	DNA replication licensing factor MCM7 OS=Homo sapiens OX=9606 GN=MCM7 PE=1 SV=4
PABPC4	4|4|0	0|1|0	0.61	Polyadenylate-binding protein 4 OS=Homo sapiens OX=9606 GN=PABPC4 PE=1 SV=1
PRDX6	4|4|4	3|1|0	0.61	Peroxiredoxin-6 OS=Homo sapiens OX=9606 GN=PRDX6 PE=1 SV=3
SUCLG1	1|1|2	1|0|0	0.61	Succinate--CoA ligase [ADP/GDP-forming] subunit alpha, mitochondrial OS=Homo sapiens OX=9606 GN=SUCLG1 PE=1 SV=4
TUBGCP3	4|2|2	1|1|0	0.61	Gamma-tubulin complex component 3 OS=Homo sapiens OX=9606 GN=TUBGCP3 PE=1 SV=2
CANX	1|1|2	0|0|1	0.6	Calnexin OS=Homo sapiens OX=9606 GN=CANX PE=1 SV=2
EIF3CL	3|1|3	1|1|0	0.6	Eukaryotic translation initiation factor 3 subunit C-

prey Gene	Quant (SPC or Intensities)	User Controls (SPC or Intensities)	SP	Description of protein
				like protein OS=Homo sapiens OX=9606 GN=EIF3CL PE=1 SV=1
HDAC1	4|0|2	0|0|0	0.6	Histone deacetylase 1 OS=Homo sapiens OX=9606 GN=HDAC1 PE=1 SV=1
HSPA4	7|2|3	0|3|0	0.6	Heat shock 70 kDa protein 4 OS=Homo sapiens OX=9606 GN=HSPA4 PE=1 SV=4
MYO1C	10|7|11	4|4|0	0.6	Unconventional myosin-Ic OS=Homo sapiens OX=9606 GN=MYO1C PE=1 SV=4
PSMC2	4|0|2	0|0|0	0.6	26S proteasome regulatory subunit 7 OS=Homo sapiens OX=9606 GN=PSMC2 PE=1 SV=3
PSMC5	3|2|2	1|1|0	0.6	26S proteasome regulatory subunit 8 OS=Homo sapiens OX=9606 GN=PSMC5 PE=1 SV=1
RANBP1	2|1|3	1|1|0	0.6	Ran-specific GTPase-activating protein OS=Homo sapiens OX=9606 GN=RANBP1 PE=1 SV=1
RPS4X	5|3|6	2|1|1	0.6	40S ribosomal protein S4, X isoform OS=Homo sapiens OX=9606 GN=RPS4X PE=1 SV=2
TMEM33	2|2|2	1|1|0	0.6	Transmembrane protein 33 OS=Homo sapiens OX=9606 GN=TMEM33 PE=1 SV=2
IMPDH2	3|0|2	0|0|0	0.59	Inosine-5'-monophosphate dehydrogenase 2 OS=Homo sapiens OX=9606 GN=IMPDH2 PE=1 SV=2
MYO1B	4|0|3	0|0|0	0.59	Unconventional myosin-Ib OS=Homo sapiens OX=9606 GN=MYO1B PE=1 SV=3
PABPC1	8|0|2	0|0|0	0.59	Polyadenylate-binding protein 1 OS=Homo sapiens OX=9606 GN=PABPC1 PE=1 SV=2

prey Gene	Quant (SPC or Intensities)	User Controls (SPC or Intensities)	SP	Description of protein
11-Sep	7|3|3	1|3|0	0.58	Septin-11 OS=Homo sapiens OX=9606 GN=SEPTIN11 PE=1 SV=3
AIMP2	1|2|1	0|0|1	0.58	Aminoacyl tRNA synthase complex-interacting multifunctional protein 2 OS=Homo sapiens OX=9606 GN=AIMP2 PE=1 SV=2
APOD	0|3|2	0|0|0	0.58	Apolipoprotein D OS=Homo sapiens OX=9606 GN=APOD PE=1 SV=1
AZGP1	5|6|10	2|3|1	0.58	Zinc-alpha-2-glycoprotein OS=Homo sapiens OX=9606 GN=AZGP1 PE=1 SV=2
EIF6	2|0|2	0|0|0	0.58	Eukaryotic translation initiation factor 6 OS=Homo sapiens OX=9606 GN=EIF6 PE=1 SV=1
MRPL20	3|3|3	1|2|0	0.58	39S ribosomal protein L20, mitochondrial OS=Homo sapiens OX=9606 GN=MRPL20 PE=1 SV=1
NME1	4|5|4	2|2|0	0.58	Nucleoside diphosphate kinase A OS=Homo sapiens OX=9606 GN=NME1 PE=1 SV=1
PSMA1	2|1|1	0|1|0	0.58	Proteasome subunit alpha type-1 OS=Homo sapiens OX=9606 GN=PSMA1 PE=1 SV=1
RAB6A	2|3|3	0|3|0	0.58	Ras-related protein Rab-6A OS=Homo sapiens OX=9606 GN=RAB6A PE=1 SV=3
STK36	0|3|4	0|0|0	0.58	Serine/threonine-protein kinase 36 OS=Homo sapiens OX=9606 GN=STK36 PE=1 SV=2
UBA1	5|2|0	0|0|0	0.58	Ubiquitin-like modifier-activating enzyme 1 OS=Homo sapiens OX=9606 GN=UBA1 PE=1 SV=3

prey Gene	Quant (SPC or Intensities)	User Controls (SPC or Intensities)	SP	Description of protein
ARPC4	2|2|0	0|0|0	0.57	Actin-related protein 2/3 complex subunit 4 OS=Homo sapiens OX=9606 GN=ARPC4 PE=1 SV=3
DDX21	10|6|8	6|2|0	0.57	Nucleolar RNA helicase 2 OS=Homo sapiens OX=9606 GN=DDX21 PE=1 SV=5
KIF2C	2|1|1	1|0|0	0.57	Kinesin-like protein KIF2C OS=Homo sapiens OX=9606 GN=KIF2C PE=1 SV=2
KRT19	0|14|22	0|0|16	0.57	Keratin, type I cytoskeletal 19 OS=Homo sapiens OX=9606 GN=KRT19 PE=1 SV=4
KRT81	1|1|2	1|0|0	0.57	Keratin, type II cuticular Hb1 OS=Homo sapiens OX=9606 GN=KRT81 PE=1 SV=3
PSMA7	2|3|3	2|1|0	0.57	Proteasome subunit alpha type-7 OS=Homo sapiens OX=9606 GN=PSMA7 PE=1 SV=1
RNH1	2|1|1	1|0|0	0.57	Ribonuclease inhibitor OS=Homo sapiens OX=9606 GN=RNH1 PE=1 SV=2
EHD1	2|0|2	0|0|0	0.56	EH domain-containing protein 1 OS=Homo sapiens OX=9606 GN=EHD1 PE=1 SV=2
LMNA	9|6|9	3|3|2	0.56	Prelamin-A/C OS=Homo sapiens OX=9606 GN=LMNA PE=1 SV=1
SIPA1L1	3|1|1	0|0|0	0.56	Signal-induced proliferation-associated 1-like protein 1 OS=Homo sapiens OX=9606 GN=SIPA1L1 PE=1 SV=4
TENM2	8|0|3	0|0|0	0.56	Teneurin-2 OS=Homo sapiens OX=9606 GN=TENM2 PE=1 SV=3
YBX3	0|2|3	0|0|1	0.56	Y-box-binding protein 3 OS=Homo sapiens OX=9606 GN=YBX3 PE=1 SV=4

prey Gene	Quant (SPC or Intensities)	User Controls (SPC or Intensities)	SP	Description of protein
ANP32A	2|0|2	0|0|0	0.55	Acidic leucine-rich nuclear phosphoprotein 32 family member A OS=Homo sapiens OX=9606 GN=ANP32A PE=1 SV=1
CTPS1	6|2|3	1|2|0	0.55	CTP synthase 1 OS=Homo sapiens OX=9606 GN=CTPS1 PE=1 SV=2
DRG1	2|0|2	0|0|0	0.55	Developmentally-regulated GTP-binding protein 1 OS=Homo sapiens OX=9606 GN=DRG1 PE=1 SV=1
EIF2B4	2|0|2	0|0|0	0.55	Translation initiation factor eIF-2B subunit delta OS=Homo sapiens OX=9606 GN=EIF2B4 PE=1 SV=2
EPB41L2	8|5|7	3|3|0	0.55	Band 4.1-like protein 2 OS=Homo sapiens OX=9606 GN=EPB41L2 PE=1 SV=1
ERP29	3|1|0	0|0|0	0.55	Endoplasmic reticulum resident protein 29 OS=Homo sapiens OX=9606 GN=ERP29 PE=1 SV=4
HSD17B10	4|0|1	0|0|0	0.55	3-hydroxyacyl-CoA dehydrogenase type-2 OS=Homo sapiens OX=9606 GN=HSD17B10 PE=1 SV=3
LMNB1	4|2|1	1|0|1	0.55	Lamin-B1 OS=Homo sapiens OX=9606 GN=LMNB1 PE=1 SV=2
PKP1	0|2|8	0|1|0	0.55	Plakophilin-1 OS=Homo sapiens OX=9606 GN=PKP1 PE=1 SV=2
SLC25A13	2|2|0	0|0|0	0.55	Calcium-binding mitochondrial carrier protein Aralar2 OS=Homo sapiens OX=9606 GN=SLC25A13 PE=1 SV=2
7-Sep	9|4|3	2|3|0	0.54	Septin-7 OS=Homo sapiens OX=9606 GN=SEPTIN7 PE=1 SV=2
DDX27	2|2|2	2|0|0	0.54	Probable ATP-dependent RNA helicase DDX27

prey Gene	Quant (SPC or Intensities)	User Controls (SPC or Intensities)	SP	Description of protein
				OS=Homo sapiens OX=9606 GN=DDX27 PE=1 SV=2
DSP	19|29|49	3|17|9	0.54	Desmoplakin OS=Homo sapiens OX=9606 GN=DSP PE=1 SV=3
ITIH2	2|1|1	1|0|0	0.54	Inter-alpha-trypsin inhibitor heavy chain H2 OS=Homo sapiens OX=9606 GN=ITIH2 PE=1 SV=2
LAMP2	0|1|2	0|0|0	0.54	Lysosome-associated membrane glycoprotein 2 OS=Homo sapiens OX=9606 GN=LAMP2 PE=1 SV=2
LDHA	9|8|9	1|4|3	0.54	L-lactate dehydrogenase A chain OS=Homo sapiens OX=9606 GN=LDHA PE=1 SV=2
MCM6	3|2|0	1|0|0	0.54	DNA replication licensing factor MCM6 OS=Homo sapiens OX=9606 GN=MCM6 PE=1 SV=1
PRMT1	3|1|0	0|0|0	0.54	Protein arginine N-methyltransferase 1 OS=Homo sapiens OX=9606 GN=PRMT1 PE=1 SV=3
RPS15A	6|6|4	2|2|1	0.54	40S ribosomal protein S15a OS=Homo sapiens OX=9606 GN=RPS15A PE=1 SV=2
SRPRA	2|1|1	1|0|0	0.54	Signal recognition particle receptor subunit alpha OS=Homo sapiens OX=9606 GN=SRPRA PE=1 SV=2
YKT6	2|1|0	0|0|0	0.54	Synaptobrevin homolog YKT6 OS=Homo sapiens OX=9606 GN=YKT6 PE=1 SV=1
CAPZA2	2|1|0	0|0|0	0.53	F-actin-capping protein subunit alpha-2 OS=Homo sapiens OX=9606 GN=CAPZA2 PE=1 SV=3

prey Gene	Quant (SPC or Intensities)	User Controls (SPC or Intensities)	SP	Description of protein
DEPDC7	7|3|5	1|4|0	0.53	DEP domain-containing protein 7 OS=Homo sapiens OX=9606 GN=DEPDC7 PE=2 SV=1
GGCT	2|5|6	2|2|0	0.53	Gamma-glutamylcyclotransferase OS=Homo sapiens OX=9606 GN=GGCT PE=1 SV=1
GM2A	0|1|2	0|0|0	0.53	Ganglioside GM2 activator OS=Homo sapiens OX=9606 GN=GM2A PE=1 SV=4
RPS2	10|8|6	4|2|1	0.53	40S ribosomal protein S2 OS=Homo sapiens OX=9606 GN=RPS2 PE=1 SV=2
A2ML1	0|2|3	0|0|0	0.52	Alpha-2-macroglobulin-like protein 1 OS=Homo sapiens OX=9606 GN=A2ML1 PE=1 SV=3
ARF3	8|5|6	3|2|1	0.52	ADP-ribosylation factor 3 OS=Homo sapiens OX=9606 GN=ARF3 PE=1 SV=2
EIF3E	3|0|1	0|0|0	0.52	Eukaryotic translation initiation factor 3 subunit E OS=Homo sapiens OX=9606 GN=EIF3E PE=1 SV=1
PARP1	3|1|2	0|2|0	0.52	Poly [ADP-ribose] polymerase 1 OS=Homo sapiens OX=9606 GN=PARP1 PE=1 SV=4
PLEKHO2	3|2|1	2|0|0	0.52	Pleckstrin homology domain-containing family O member 2 OS=Homo sapiens OX=9606 GN=PLEKHO2 PE=1 SV=1
PSMA5	2|0|2	1|0|0	0.52	Proteasome subunit alpha type-5 OS=Homo sapiens OX=9606 GN=PSMA5 PE=1 SV=3
RAB18	2|0|1	0|0|0	0.52	Ras-related protein Rab-18 OS=Homo sapiens OX=9606 GN=RAB18 PE=1 SV=1

prey Gene	Quant (SPC or Intensities)	User Controls (SPC or Intensities)	SP	Description of protein
SPATA2	14|7|8	6|1|2	0.52	Spermatogenesis-associated protein 2 OS=Homo sapiens OX=9606 GN=SPATA2 PE=1 SV=2
STAT1	3|0|2	0|1|0	0.52	Signal transducer and activator of transcription 1-alpha/beta OS=Homo sapiens OX=9606 GN=STAT1 PE=1 SV=2
TUBG1	0|2|1	0|0|0	0.52	Tubulin gamma-1 chain OS=Homo sapiens OX=9606 GN=TUBG1 PE=1 SV=2
ALOX12B	0|1|5	0|0|0	0.51	Arachidonate 12-lipoxygenase, 12R-type OS=Homo sapiens OX=9606 GN=ALOX12B PE=1 SV=1
CALML5	4|6|5	2|1|2	0.51	Calmodulin-like protein 5 OS=Homo sapiens OX=9606 GN=CALML5 PE=1 SV=2
CFL1	7|5|3	0|5|0	0.51	Cofilin-1 OS=Homo sapiens OX=9606 GN=CFL1 PE=1 SV=3
CTSB	1|0|2	0|0|0	0.51	Cathepsin B OS=Homo sapiens OX=9606 GN=CTSB PE=1 SV=3
EEF1B2	2|0|1	0|0|0	0.51	Elongation factor 1-beta OS=Homo sapiens OX=9606 GN=EEF1B2 PE=1 SV=3
ENDOD1	0|1|2	0|0|0	0.51	Endonuclease domain-containing 1 protein OS=Homo sapiens OX=9606 GN=ENDOD1 PE=1 SV=2
FARSB	4|0|1	0|0|0	0.51	Phenylalanine--tRNA ligase beta subunit OS=Homo sapiens OX=9606 GN=FARSB PE=1 SV=3
FHL2	1|2|2	1|1|0	0.51	Four and a half LIM domains protein 2 OS=Homo sapiens OX=9606 GN=FHL2 PE=1 SV=3

prey Gene	Quant (SPC or Intensities)	User Controls (SPC or Intensities)	SP	Description of protein
LYZ	1|1|3	0|2|0	0.51	Lysozyme C OS=Homo sapiens OX=9606 GN=LYZ PE=1 SV=1
PIK3C2A	2|1|2	1|0|0	0.51	Phosphatidylinositol 4-phosphate 3-kinase C2 domain-containing subunit alpha OS=Homo sapiens OX=9606 GN=PIK3C2A PE=1 SV=2
PSMB3	2|0|1	0|0|0	0.51	Proteasome subunit beta type-3 OS=Homo sapiens OX=9606 GN=PSMB3 PE=1 SV=2
PSMC4	2|0|1	0|0|0	0.51	26S proteasome regulatory subunit 6B OS=Homo sapiens OX=9606 GN=PSMC4 PE=1 SV=2
SLC16A1	3|0|1	0|0|0	0.51	Monocarboxylate transporter 1 OS=Homo sapiens OX=9606 GN=SLC16A1 PE=1 SV=3
TK1	2|0|1	0|0|0	0.51	Thymidine kinase, cytosolic OS=Homo sapiens OX=9606 GN=TK1 PE=1 SV=2
CMSS1	3|1|0	1|0|0	0.5	Protein CMSS1 OS=Homo sapiens OX=9606 GN=CMSS1 PE=1 SV=2
DHCR24	2|0|1	0|0|0	0.5	Delta(24)-sterol reductase OS=Homo sapiens OX=9606 GN=DHCR24 PE=1 SV=2
LAT2	2|0|1	0|0|0	0.5	Linker for activation of T-cells family member 2 OS=Homo sapiens OX=9606 GN=LAT2 PE=1 SV=1
PPFIBP1	2|0|2	0|0|0	0.5	Liprin-beta-1 OS=Homo sapiens OX=9606 GN=PPFIBP1 PE=1 SV=2
SLC30A1	2|0|1	0|0|0	0.5	Zinc transporter 1 OS=Homo sapiens OX=9606 GN=SLC30A1 PE=1 SV=3
SRP68	2|1|0	0|0|0	0.5	Signal recognition particle subunit SRP68 OS=Homo sapiens OX=9606 GN=SRP68 PE=1 SV=2

prey Gene	Quant (SPC or Intensities)	User Controls (SPC or Intensities)	SP	Description of protein
VCPIP1	2|0|2	0|0|0	0.5	Deubiquitinating protein VCPIP1 OS=Homo sapiens OX=9606 GN=VCPIP1 PE=1 SV=2
AMOTL1	4|1|0	0|0|0	0.49	Angiomotin-like protein 1 OS=Homo sapiens OX=9606 GN=AMOTL1 PE=1 SV=1
DLD	1|0|2	0|0|0	0.49	Dihydrolipoyl dehydrogenase, mitochondrial OS=Homo sapiens OX=9606 GN=DLD PE=1 SV=2
NCCRP1	0|1|2	0|0|0	0.49	F-box only protein 50 OS=Homo sapiens OX=9606 GN=NCCRP1 PE=1 SV=1
SLC39A14	1|0|2	0|0|0	0.49	Metal cation symporter ZIP14 OS=Homo sapiens OX=9606 GN=SLC39A14 PE=1 SV=3
TGM2	3|1|2	1|1|0	0.49	Protein-glutamine gamma-glutamyltransferase 2 OS=Homo sapiens OX=9606 GN=TGM2 PE=1 SV=2
TIMM50	1|0|2	0|0|0	0.49	Mitochondrial import inner membrane translocase subunit TIM50 OS=Homo sapiens OX=9606 GN=TIMM50 PE=1 SV=2
VPS13C	7|3|9	3|3|0	0.49	Vacuolar protein sorting-associated protein 13C OS=Homo sapiens OX=9606 GN=VPS13C PE=1 SV=1
ABCE1	2|0|1	0|0|0	0.48	ATP-binding cassette sub-family E member 1 OS=Homo sapiens OX=9606 GN=ABCE1 PE=1 SV=1
ACTR1A	2|0|1	0|0|0	0.48	Alpha-centractin OS=Homo sapiens OX=9606 GN=ACTR1A PE=1 SV=1

prey Gene	Quant (SPC or Intensities)	User Controls (SPC or Intensities)	SP	Description of protein
FBL	3|2|0	0|2|0	0.48	rRNA 2'-O-methyltransferase fibrillarin OS=Homo sapiens OX=9606 GN=FBL PE=1 SV=2
HAL	1|0|4	0|0|0	0.48	Histidine ammonia-lyase OS=Homo sapiens OX=9606 GN=HAL PE=1 SV=1
IGHG4	1|0|2	0|0|0	0.48	Immunoglobulin heavy constant gamma 4 OS=Homo sapiens OX=9606 GN=IGHG4 PE=1 SV=1
JMJD1C	3|1|2	1|0|0	0.48	Probable JmjC domain-containing histone demethylation protein 2C OS=Homo sapiens OX=9606 GN=JMJD1C PE=1 SV=2
PGD	1|2|0	0|0|0	0.48	6-phosphogluconate dehydrogenase, decarboxylating OS=Homo sapiens OX=9606 GN=PGD PE=1 SV=3
STT3A	1|0|3	0|0|0	0.48	Dolichyl-diphosphooligosaccharide--protein glycosyltransferase subunit STT3A OS=Homo sapiens OX=9606 GN=STT3A PE=1 SV=2
TALDO1	2|2|1	1|1|0	0.48	Transaldolase OS=Homo sapiens OX=9606 GN=TALDO1 PE=1 SV=2
9-Sep	7|6|3	2|4|0	0.47	Septin-9 OS=Homo sapiens OX=9606 GN=SEPTIN9 PE=1 SV=2
AXIN2	2|1|0	0|0|0	0.47	Axin-2 OS=Homo sapiens OX=9606 GN=AXIN2 PE=1 SV=1
GPI	1|2|0	0|0|0	0.47	Glucose-6-phosphate isomerase OS=Homo sapiens OX=9606 GN=GPI PE=1 SV=4

prey Gene	Quant (SPC or Intensities)	User Controls (SPC or Intensities)	SP	Description of protein
HNRNPDL	4|1|1	1|1|0	0.47	Heterogeneous nuclear ribonucleoprotein D-like OS=Homo sapiens OX=9606 GN=HNRNPDL PE=1 SV=3
KDM1B	4|0|1	0|0|0	0.47	Lysine-specific histone demethylase 1B OS=Homo sapiens OX=9606 GN=KDM1B PE=1 SV=3
LIMD1	2|0|1	0|0|0	0.47	LIM domain-containing protein 1 OS=Homo sapiens OX=9606 GN=LIMD1 PE=1 SV=1
MDH1	2|2|1	1|1|0	0.47	Malate dehydrogenase, cytoplasmic OS=Homo sapiens OX=9606 GN=MDH1 PE=1 SV=4
RPL21	2|1|1	0|2|0	0.47	60S ribosomal protein L21 OS=Homo sapiens OX=9606 GN=RPL21 PE=1 SV=2
RPS12	2|1|0	1|0|0	0.47	40S ribosomal protein S12 OS=Homo sapiens OX=9606 GN=RPS12 PE=1 SV=3
SHMT2	1|0|2	0|0|0	0.47	Serine hydroxymethyltransferase, mitochondrial OS=Homo sapiens OX=9606 GN=SHMT2 PE=1 SV=3
ZW10	4|0|1	0|0|0	0.47	Centromere/kinetochore protein zw10 homolog OS=Homo sapiens OX=9606 GN=ZW10 PE=1 SV=3
ABCF3	2|1|0	0|0|0	0.46	ATP-binding cassette sub-family F member 3 OS=Homo sapiens OX=9606 GN=ABCF3 PE=1 SV=2
CAPN2	1|0|2	0|0|0	0.46	Calpain-2 catalytic subunit OS=Homo sapiens OX=9606 GN=CAPN2 PE=1 SV=6

prey Gene	Quant (SPC or Intensities)	User Controls (SPC or Intensities)	SP	Description of protein
EIF2S2	4|1|0	1|0|0	0.46	Eukaryotic translation initiation factor 2 subunit 2 OS=Homo sapiens OX=9606 GN=EIF2S2 PE=1 SV=2
HADHA	2|0|1	0|0|0	0.46	Trifunctional enzyme subunit alpha, mitochondrial OS=Homo sapiens OX=9606 GN=HADHA PE=1 SV=2
JUNB	5|3|6	2|1|2	0.46	Transcription factor jun-B OS=Homo sapiens OX=9606 GN=JUNB PE=1 SV=1
MAGEA4	4|2|4	2|2|0	0.46	Melanoma-associated antigen 4 OS=Homo sapiens OX=9606 GN=MAGEA4 PE=1 SV=2
RPSA	2|2|3	2|1|0	0.46	40S ribosomal protein SA OS=Homo sapiens OX=9606 GN=RPSA PE=1 SV=4
AP2A1	3|0|1	0|0|0	0.45	AP-2 complex subunit alpha-1 OS=Homo sapiens OX=9606 GN=AP2A1 PE=1 SV=3
AP2B1	3|0|1	0|0|0	0.45	AP-2 complex subunit beta OS=Homo sapiens OX=9606 GN=AP2B1 PE=1 SV=1
DOCK7	7|10|4	3|4|0	0.45	Dedicator of cytokinesis protein 7 OS=Homo sapiens OX=9606 GN=DOCK7 PE=1 SV=4
SPRR2E	3|0|3	3|0|0	0.45	Small proline-rich protein 2E OS=Homo sapiens OX=9606 GN=SPRR2E PE=2 SV=2
EXOC7	2|0|1	0|0|0	0.44	Exocyst complex component 7 OS=Homo sapiens OX=9606 GN=EXOC7 PE=1 SV=3
FKBP4	2|2|1	2|0|0	0.44	Peptidyl-prolyl cis-trans isomerase FKBP4 OS=Homo sapiens OX=9606 GN=FKBP4 PE=1 SV=3

prey Gene	Quant (SPC or Intensities)	User Controls (SPC or Intensities)	SP	Description of protein
GCN1	4|0|2	0|0|0	0.44	eIF-2-alpha kinase activator GCN1 OS=Homo sapiens OX=9606 GN=GCN1 PE=1 SV=6
MYH10	7|0|2	0|2|0	0.44	Myosin-10 OS=Homo sapiens OX=9606 GN=MYH10 PE=1 SV=3
NCOR2	2|4|0	0|0|0	0.44	Nuclear receptor corepressor 2 OS=Homo sapiens OX=9606 GN=NCOR2 PE=1 SV=3
NPEPPS	2|1|0	0|0|0	0.44	Puromycin-sensitive aminopeptidase OS=Homo sapiens OX=9606 GN=NPEPPS PE=1 SV=2
PFKP	3|0|1	0|0|0	0.44	ATP-dependent 6-phosphofructokinase, platelet type OS=Homo sapiens OX=9606 GN=PFKP PE=1 SV=2
DDX54	14|8|11	7|5|0	0.43	ATP-dependent RNA helicase DDX54 OS=Homo sapiens OX=9606 GN=DDX54 PE=1 SV=2
HNRNPUL2	2|0|1	0|0|0	0.43	Heterogeneous nuclear ribonucleoprotein U-like protein 2 OS=Homo sapiens OX=9606 GN=HNRNPUL2 PE=1 SV=1
IGHA1	1|3|0	0|1|0	0.43	Immunoglobulin heavy constant alpha 1 OS=Homo sapiens OX=9606 GN=IGHA1 PE=1 SV=2
NOM1	2|0|1	0|0|0	0.43	Nucleolar MIF4G domain-containing protein 1 OS=Homo sapiens OX=9606 GN=NOM1 PE=1 SV=1
TCF12	4|2|5	2|2|0	0.43	Transcription factor 12 OS=Homo sapiens OX=9606 GN=TCF12 PE=1 SV=1
CAPZA1	3|0|3	0|3|0	0.42	F-actin-capping protein subunit alpha-1 OS=Homo sapiens OX=9606 GN=CAPZA1 PE=1 SV=3

prey Gene	Quant (SPC or Intensities)	User Controls (SPC or Intensities)	SP	Description of protein
GATAD2B	4|0|1	0|1|0	0.42	Transcriptional repressor p66-beta OS=Homo sapiens OX=9606 GN=GATAD2B PE=1 SV=1
HADHB	2|2|1	1|1|0	0.42	Trifunctional enzyme subunit beta, mitochondrial OS=Homo sapiens OX=9606 GN=HADHB PE=1 SV=3
IARS	2|1|2	1|1|0	0.42	Isoleucine--tRNA ligase, cytoplasmic OS=Homo sapiens OX=9606 GN=IARS1 PE=1 SV=2
KMT2A	12|2|7	4|4|0	0.42	Histone-lysine N-methyltransferase 2A OS=Homo sapiens OX=9606 GN=KMT2A PE=1 SV=5
KRT6C	54|62|119	75|0|0	0.42	Keratin, type II cytoskeletal 6C OS=Homo sapiens OX=9606 GN=KRT6C PE=1 SV=3
KRT78	7|7|18	1|5|4	0.42	Keratin, type II cytoskeletal 78 OS=Homo sapiens OX=9606 GN=KRT78 PE=1 SV=2
LRCH3	1|0|2	0|0|0	0.42	DISP complex protein LRCH3 OS=Homo sapiens OX=9606 GN=LRCH3 PE=1 SV=2
PRKD2	1|0|2	0|0|0	0.42	Serine/threonine-protein kinase D2 OS=Homo sapiens OX=9606 GN=PRKD2 PE=1 SV=3
SFPQ	3|0|1	0|0|1	0.42	Splicing factor, proline- and glutamine-rich OS=Homo sapiens OX=9606 GN=SFPQ PE=1 SV=2
TCP1	19|9|15	6|7|0	0.42	T-complex protein 1 subunit alpha OS=Homo sapiens OX=9606 GN=TCP1 PE=1 SV=1
TOP1	3|0|3	0|1|1	0.42	DNA topoisomerase 1 OS=Homo sapiens OX=9606 GN=TOP1 PE=1 SV=2

prey Gene	Quant (SPC or Intensities)	User Controls (SPC or Intensities)	SP	Description of protein
WDFY1	2|1|0	0|1|0	0.42	WD repeat and FYVE domain-containing protein 1 OS=Homo sapiens OX=9606 GN=WDFY1 PE=1 SV=1
ARG1	3|2|4	1|3|0	0.41	Arginase-1 OS=Homo sapiens OX=9606 GN=ARG1 PE=1 SV=2
ETF1	1|2|0	0|1|0	0.41	Eukaryotic peptide chain release factor subunit 1 OS=Homo sapiens OX=9606 GN=ETF1 PE=1 SV=3
GNAS	3|0|2	2|0|0	0.41	Guanine nucleotide-binding protein G(s) subunit alpha isoforms XLas OS=Homo sapiens OX=9606 GN=GNAS PE=1 SV=2
ILF2	3|2|2	1|0|2	0.41	Interleukin enhancer-binding factor 2 OS=Homo sapiens OX=9606 GN=ILF2 PE=1 SV=2
ITGA3	2|1|0	0|0|0	0.41	Integrin alpha-3 OS=Homo sapiens OX=9606 GN=ITGA3 PE=1 SV=5
RRBP1	3|1|0	0|0|0	0.41	Ribosome-binding protein 1 OS=Homo sapiens OX=9606 GN=RRBP1 PE=1 SV=5
EPS15	0|1|2	1|0|0	0.4	Epidermal growth factor receptor substrate 15 OS=Homo sapiens OX=9606 GN=EPS15 PE=1 SV=2
NCKAP1	2|1|0	0|0|0	0.4	Nck-associated protein 1 OS=Homo sapiens OX=9606 GN=NCKAP1 PE=1 SV=1
PRDX2	5|0|6	0|5|0	0.4	Peroxiredoxin-2 OS=Homo sapiens OX=9606 GN=PRDX2 PE=1 SV=5
SHC1	3|1|1	1|1|0	0.4	SHC-transforming protein 1 OS=Homo sapiens OX=9606 GN=SHC1 PE=1 SV=4

prey Gene	Quant (SPC or Intensities)	User Controls (SPC or Intensities)	SP	Description of protein
FERMT2	5|2|4	1|2|1	0.39	Fermitin family homolog 2 OS=Homo sapiens OX=9606 GN=FERMT2 PE=1 SV=1
KRT17	19|26|52	12|9|12	0.39	Keratin, type I cytoskeletal 17 OS=Homo sapiens OX=9606 GN=KRT17 PE=1 SV=2
LRPPRC	3|1|0	0|0|0	0.39	Leucine-rich PPR motif-containing protein, mitochondrial OS=Homo sapiens OX=9606 GN=LRPPRC PE=1 SV=3
SBSN	2|2|3	1|2|0	0.39	Suprabasin OS=Homo sapiens OX=9606 GN=SBSN PE=1 SV=2
ATAD3B	1|1|2	0|2|0	0.38	ATPase family AAA domain-containing protein 3B OS=Homo sapiens OX=9606 GN=ATAD3B PE=1 SV=1
CEP55	1|0|2	1|0|0	0.38	Centrosomal protein of 55 kDa OS=Homo sapiens OX=9606 GN=CEP55 PE=1 SV=3
FAM120A	2|1|0	0|0|0	0.38	Constitutive coactivator of PPAR-gamma-like protein 1 OS=Homo sapiens OX=9606 GN=FAM120A PE=1 SV=2
H1FX	2|1|1	1|1|0	0.38	Histone H1.10 OS=Homo sapiens OX=9606 GN=H1-10 PE=1 SV=1
SNX2	2|0|1	1|0|0	0.38	Sorting nexin-2 OS=Homo sapiens OX=9606 GN=SNX2 PE=1 SV=2
TCF20	2|0|2	0|0|0	0.38	Transcription factor 20 OS=Homo sapiens OX=9606 GN=TCF20 PE=1 SV=3
ZNF185	2|0|1	1|0|0	0.38	Zinc finger protein 185 OS=Homo sapiens OX=9606 GN=ZNF185 PE=1 SV=3
MYL6	9|0|1	0|3|0	0.36	Myosin light polypeptide 6 OS=Homo sapiens OX=9606 GN=MYL6 PE=1 SV=2

prey Gene	Quant (SPC or Intensities)	User Controls (SPC or Intensities)	SP	Description of protein
POLR2B	3|0|1	1|0|0	0.36	DNA-directed RNA polymerase II subunit RPB2 OS=Homo sapiens OX=9606 GN=POLR2B PE=1 SV=1
RPL12	6|3|1	2|1|1	0.36	60S ribosomal protein L12 OS=Homo sapiens OX=9606 GN=RPL12 PE=1 SV=1
RUVBL2	1|2|1	1|1|0	0.36	RuvB-like 2 OS=Homo sapiens OX=9606 GN=RUVBL2 PE=1 SV=3
TFG	2|2|0	2|0|0	0.36	Protein TFG OS=Homo sapiens OX=9606 GN=TFG PE=1 SV=2
TUFM	4|4|3	3|1|1	0.36	Elongation factor Tu, mitochondrial OS=Homo sapiens OX=9606 GN=TUFM PE=1 SV=2
UTP20	1|2|4	1|1|0	0.36	Small subunit processome component 20 homolog OS=Homo sapiens OX=9606 GN=UTP20 PE=1 SV=3
CDSN	2|3|4	0|3|1	0.35	Corneodesmosin OS=Homo sapiens OX=9606 GN=CDSN PE=1 SV=3
TPR	5|1|0	0|0|0	0.35	Nucleoprotein TPR OS=Homo sapiens OX=9606 GN=TPR PE=1 SV=3
DDX19B	1|1|2	1|1|0	0.34	ATP-dependent RNA helicase DDX19B OS=Homo sapiens OX=9606 GN=DDX19B PE=1 SV=1
EDIL3	3|3|3	2|2|0	0.34	EGF-like repeat and discoidin I-like domain-containing protein 3 OS=Homo sapiens OX=9606 GN=EDIL3 PE=1 SV=1
USO1	2|0|1	1|0|0	0.34	General vesicular transport factor p115 OS=Homo sapiens OX=9606 GN=USO1 PE=1 SV=2

prey Gene	Quant (SPC or Intensities)	User Controls (SPC or Intensities)	SP	Description of protein
CTNNA2	23|0|0	0|0|0	0.33	Catenin alpha-2 OS=Homo sapiens OX=9606 GN=CTNNA2 PE=1 SV=5
KRT3	0|0|29	0|0|0	0.33	Keratin, type II cytoskeletal 3 OS=Homo sapiens OX=9606 GN=KRT3 PE=1 SV=3
KRT4	18|0|0	0|0|0	0.33	Keratin, type II cytoskeletal 4 OS=Homo sapiens OX=9606 GN=KRT4 PE=1 SV=5
KRT7	0|0|15	0|0|0	0.33	Keratin, type II cytoskeletal 7 OS=Homo sapiens OX=9606 GN=KRT7 PE=1 SV=5
LCN1	1|0|2	0|0|2	0.33	Lipocalin-1 OS=Homo sapiens OX=9606 GN=LCN1 PE=1 SV=1
TNS3	1|0|2	0|0|0	0.33	Tensin-3 OS=Homo sapiens OX=9606 GN=TNS3 PE=1 SV=2
AHDC1	2|0|1	0|0|0	0.32	AT-hook DNA-binding motif-containing protein 1 OS=Homo sapiens OX=9606 GN=AHDC1 PE=1 SV=1
EEF2	12|8|9	5|6|1	0.32	Elongation factor 2 OS=Homo sapiens OX=9606 GN=EEF2 PE=1 SV=4
EIF2S3	4|2|3	2|2|0	0.32	Eukaryotic translation initiation factor 2 subunit 3 OS=Homo sapiens OX=9606 GN=EIF2S3 PE=1 SV=3
GIGYF2	1|2|0	1|0|0	0.32	GRB10-interacting GYF protein 2 OS=Homo sapiens OX=9606 GN=GIGYF2 PE=1 SV=1
KRT15	12|0|0	0|0|0	0.32	Keratin, type I cytoskeletal 15 OS=Homo sapiens OX=9606 GN=KRT15 PE=1 SV=3
LGALS7; LGALS7B	1|3|2	1|1|1	0.32	Galectin-7 OS=Homo sapiens OX=9606 GN=LGALS7 PE=1 SV=2

prey Gene	Quant (SPC or Intensities)	User Controls (SPC or Intensities)	SP	Description of protein
NOP2	4|3|2	2|1|1	0.32	Probable 28S rRNA (cytosine(4447)-C(5))-methyltransferase OS=Homo sapiens OX=9606 GN=NOP2 PE=1 SV=2
SPRR2G	0|2|5	0|2|2	0.32	Small proline-rich protein 2G OS=Homo sapiens OX=9606 GN=SPRR2G PE=3 SV=1
TUBA1A	55|0|0	0|0|0	0.32	Tubulin alpha-1A chain OS=Homo sapiens OX=9606 GN=TUBA1A PE=1 SV=1
UQCRC2	2|4|4	3|2|0	0.32	Cytochrome b-c1 complex subunit 2, mitochondrial OS=Homo sapiens OX=9606 GN=UQCRC2 PE=1 SV=3
KRT12	0|0|5	0|0|0	0.31	Keratin, type I cytoskeletal 12 OS=Homo sapiens OX=9606 GN=KRT12 PE=1 SV=1
KRT72	8|0|0	0|0|0	0.31	Keratin, type II cytoskeletal 72 OS=Homo sapiens OX=9606 GN=KRT72 PE=1 SV=2
PGAM1	2|2|2	2|1|0	0.31	Phosphoglycerate mutase 1 OS=Homo sapiens OX=9606 GN=PGAM1 PE=1 SV=2
PPA1	6|0|0	0|0|0	0.31	Inorganic pyrophosphatase OS=Homo sapiens OX=9606 GN=PPA1 PE=1 SV=2
TOP2A	3|0|3	2|0|1	0.31	DNA topoisomerase 2-alpha OS=Homo sapiens OX=9606 GN=TOP2A PE=1 SV=3
TOP2B	0|1|2	0|1|0	0.31	DNA topoisomerase 2-beta OS=Homo sapiens OX=9606 GN=TOP2B PE=1 SV=3
YWHAH	6|0|0	0|0|0	0.31	14-3-3 protein eta OS=Homo sapiens OX=9606 GN=YWHAH PE=1 SV=4

prey Gene	Quant (SPC or Intensities)	User Controls (SPC or Intensities)	SP	Description of protein
YWHAZ	9|4|7	5|3|0	0.31	14-3-3 protein zeta/delta OS=Homo sapiens OX=9606 GN=YWHAZ PE=1 SV=1
CACYBP	2|1|0	1|1|0	0.3	Calcyclin-binding protein OS=Homo sapiens OX=9606 GN=CACYBP PE=1 SV=2
ITGB1	8|2|4	1|5|0	0.3	Integrin beta-1 OS=Homo sapiens OX=9606 GN=ITGB1 PE=1 SV=2
PRDX4	3|0|0	0|0|0	0.3	Peroxiredoxin-4 OS=Homo sapiens OX=9606 GN=PRDX4 PE=1 SV=1
RAB10	4|0|0	0|0|0	0.3	Ras-related protein Rab-10 OS=Homo sapiens OX=9606 GN=RAB10 PE=1 SV=1
RAB1A	4|6|6	7|0|0	0.3	Ras-related protein Rab-1A OS=Homo sapiens OX=9606 GN=RAB1A PE=1 SV=3
TCF7L1	0|4|0	0|0|0	0.3	Transcription factor 7-like 1 OS=Homo sapiens OX=9606 GN=TCF7L1 PE=2 SV=1
TENM3	5|0|1	0|0|0	0.3	Teneurin-3 OS=Homo sapiens OX=9606 GN=TENM3 PE=2 SV=3
8-Sep	3|0|0	0|0|0	0.29	Septin-8 OS=Homo sapiens OX=9606 GN=SEPTIN8 PE=1 SV=4
ASAP2	0|0|4	0|0|0	0.29	Arf-GAP with SH3 domain, ANK repeat and PH domain-containing protein 2 OS=Homo sapiens OX=9606 GN=ASAP2 PE=1 SV=3
CCT6A	11|5|4	4|3|1	0.29	T-complex protein 1 subunit zeta OS=Homo sapiens OX=9606 GN=CCT6A PE=1 SV=3
CCT6B	3|0|0	0|0|0	0.29	T-complex protein 1 subunit zeta-2 OS=Homo sapiens OX=9606 GN=CCT6B PE=1 SV=5

prey Gene	Quant (SPC or Intensities)	User Controls (SPC or Intensities)	SP	Description of protein
EWSR1	0|1|2	1|1|0	0.29	RNA-binding protein EWS OS=Homo sapiens OX=9606 GN=EWSR1 PE=1 SV=1
HIST1H1A	3|0|0	0|0|0	0.29	Histone H1.1 OS=Homo sapiens OX=9606 GN=H1-1 PE=1 SV=3
KRT31	3|0|0	0|0|0	0.29	Keratin, type I cuticular Ha1 OS=Homo sapiens OX=9606 GN=KRT31 PE=1 SV=3
LUZP1	4|5|1	4|1|0	0.29	Leucine zipper protein 1 OS=Homo sapiens OX=9606 GN=LUZP1 PE=1 SV=2
POF1B	0|0|3	0|0|0	0.29	Protein POF1B OS=Homo sapiens OX=9606 GN=POF1B PE=1 SV=3
PYCR1	2|0|0	0|0|0	0.29	Pyrroline-5-carboxylate reductase 1, mitochondrial OS=Homo sapiens OX=9606 GN=PYCR1 PE=1 SV=2
RAB3C	0|0|3	0|0|0	0.29	Ras-related protein Rab-3C OS=Homo sapiens OX=9606 GN=RAB3C PE=1 SV=1
RAB7A	4|0|0	0|0|0	0.29	Ras-related protein Rab-7a OS=Homo sapiens OX=9606 GN=RAB7A PE=1 SV=1
TFRC	4|0|0	1|0|0	0.29	Transferrin receptor protein 1 OS=Homo sapiens OX=9606 GN=TFRC PE=1 SV=2
TPM4	3|0|0	0|0|0	0.29	Tropomyosin alpha-4 chain OS=Homo sapiens OX=9606 GN=TPM4 PE=1 SV=3
ABLIM1	4|3|4	4|1|0	0.28	Actin-binding LIM protein 1 OS=Homo sapiens OX=9606 GN=ABLIM1 PE=1 SV=3
ANXA6	0|0|3	0|0|0	0.28	Annexin A6 OS=Homo sapiens OX=9606 GN=ANXA6 PE=1 SV=3

prey Gene	Quant (SPC or Intensities)	User Controls (SPC or Intensities)	SP	Description of protein
CLIC1	3|0|0	0|0|0	0.28	Chloride intracellular channel protein 1 OS=Homo sapiens OX=9606 GN=CLIC1 PE=1 SV=4
CRMP1	0|0|3	0|0|0	0.28	Dihydropyrimidinase-related protein 1 OS=Homo sapiens OX=9606 GN=CRMP1 PE=1 SV=1
DSC3	0|0|3	0|1|0	0.28	Desmocollin-3 OS=Homo sapiens OX=9606 GN=DSC3 PE=1 SV=3
NECAP2	2|0|0	0|0|0	0.28	Adaptin ear-binding coat-associated protein 2 OS=Homo sapiens OX=9606 GN=NECAP2 PE=1 SV=1
OR1B1	2|0|0	0|0|0	0.28	Olfactory receptor 1B1 OS=Homo sapiens OX=9606 GN=OR1B1 PE=3 SV=2
P0DPH8	48|41|34	30|23|0	0.28	Tubulin alpha-3D chain OS=Homo sapiens OX=9606 GN=TUBA3D PE=1 SV=1
RELL1	2|0|0	0|0|0	0.28	RELT-like protein 1 OS=Homo sapiens OX=9606 GN=RELL1 PE=1 SV=1
RPL27	4|2|5	1|2|2	0.28	60S ribosomal protein L27 OS=Homo sapiens OX=9606 GN=RPL27 PE=1 SV=2
SARNP	2|0|0	0|0|0	0.28	SAP domain-containing ribonucleoprotein OS=Homo sapiens OX=9606 GN=SARNP PE=1 SV=3
SDC1	2|0|0	0|0|0	0.28	Syndecan-1 OS=Homo sapiens OX=9606 GN=SDC1 PE=1 SV=3
TMEM263	0|0|3	0|0|0	0.28	Transmembrane protein 263 OS=Homo sapiens OX=9606 GN=TMEM263 PE=1 SV=1
ADD1	3|1|2	2|1|0	0.27	Alpha-adducin OS=Homo sapiens OX=9606 GN=ADD1 PE=1 SV=2

prey Gene	Quant (SPC or Intensities)	User Controls (SPC or Intensities)	SP	Description of protein
BZW2	2|0|0	0|0|0	0.27	Basic leucine zipper and W2 domain-containing protein 2 OS=Homo sapiens OX=9606 GN=BZW2 PE=1 SV=1
CYLD	10|2|2	4|2|0	0.27	Ubiquitin carboxyl-terminal hydrolase CYLD OS=Homo sapiens OX=9606 GN=CYLD PE=1 SV=1
DBN1	8|0|2	2|1|2	0.27	Drebrin OS=Homo sapiens OX=9606 GN=DBN1 PE=1 SV=4
DHX30	3|0|0	1|0|0	0.27	ATP-dependent RNA helicase DHX30 OS=Homo sapiens OX=9606 GN=DHX30 PE=1 SV=1
ECM1	0|0|2	0|0|0	0.27	Extracellular matrix protein 1 OS=Homo sapiens OX=9606 GN=ECM1 PE=1 SV=2
ETFA	2|0|0	0|0|0	0.27	Electron transfer flavoprotein subunit alpha, mitochondrial OS=Homo sapiens OX=9606 GN=ETFA PE=1 SV=1
FBLL1	0|0|2	0|0|0	0.27	rRNA/tRNA 2'-O-methyltransferase fibrillarin-like protein 1 OS=Homo sapiens OX=9606 GN=FBLL1 PE=3 SV=2
FEN1	2|0|0	0|0|0	0.27	Flap endonuclease 1 OS=Homo sapiens OX=9606 GN=FEN1 PE=1 SV=1
GNAI3	2|0|0	0|0|0	0.27	Guanine nucleotide-binding protein G(i) subunit alpha-3 OS=Homo sapiens OX=9606 GN=GNAI3 PE=1 SV=3
IGHG3	0|2|0	0|0|0	0.27	Immunoglobulin heavy constant gamma 3 OS=Homo sapiens OX=9606 GN=IGHG3 PE=1 SV=2
LCE3D	0|0|2	0|0|0	0.27	Late cornified envelope protein 3D OS=Homo sapiens OX=9606 GN=LCE3D PE=1 SV=1

prey Gene	Quant (SPC or Intensities)	User Controls (SPC or Intensities)	SP	Description of protein
PCBP3	0|3|2	4|0|0	0.27	Poly(rC)-binding protein 3 OS=Homo sapiens OX=9606 GN=PCBP3 PE=1 SV=2
RAB5B	2|0|0	0|0|0	0.27	Ras-related protein Rab-5B OS=Homo sapiens OX=9606 GN=RAB5B PE=1 SV=1
UGP2	2|0|0	0|0|0	0.27	UTP--glucose-1-phosphate uridylyltransferase OS=Homo sapiens OX=9606 GN=UGP2 PE=1 SV=5
ATP5C1	2|0|1	1|0|1	0.26	ATP synthase subunit gamma, mitochondrial OS=Homo sapiens OX=9606 GN=ATP5F1C PE=1 SV=1
DDB1	3|0|0	0|0|0	0.26	DNA damage-binding protein 1 OS=Homo sapiens OX=9606 GN=DDB1 PE=1 SV=1
GNL2	2|0|3	3|0|0	0.26	Nucleolar GTP-binding protein 2 OS=Homo sapiens OX=9606 GN=GNL2 PE=1 SV=1
MSN	0|0|2	0|0|0	0.26	Moesin OS=Homo sapiens OX=9606 GN=MSN PE=1 SV=3
PSMD4	2|0|0	0|0|0	0.26	26S proteasome non-ATPase regulatory subunit 4 OS=Homo sapiens OX=9606 GN=PSMD4 PE=1 SV=1
RAB5C	3|1|3	3|1|0	0.26	Ras-related protein Rab-5C OS=Homo sapiens OX=9606 GN=RAB5C PE=1 SV=2
SURF6	10|13|15	8|8|1	0.26	Surfeit locus protein 6 OS=Homo sapiens OX=9606 GN=SURF6 PE=1 SV=3
TUBA1C	40|0|0	29|0|0	0.26	Tubulin alpha-1C chain OS=Homo sapiens OX=9606 GN=TUBA1C PE=1 SV=1

prey Gene	Quant (SPC or Intensities)	User Controls (SPC or Intensities)	SP	Description of protein
TXNDC17	2|0|0	0|0|0	0.26	Thioredoxin domain-containing protein 17 OS=Homo sapiens OX=9606 GN=TXNDC17 PE=1 SV=1
UMPS	2|0|0	0|0|0	0.26	Uridine 5'-monophosphate synthase OS=Homo sapiens OX=9606 GN=UMPS PE=1 SV=1
WDR5	2|0|0	0|0|0	0.26	WD repeat-containing protein 5 OS=Homo sapiens OX=9606 GN=WDR5 PE=1 SV=1
ANXA11	2|0|0	0|0|0	0.25	Annexin A11 OS=Homo sapiens OX=9606 GN=ANXA11 PE=1 SV=1
ARHGAP23	4|0|0	0|0|0	0.25	Rho GTPase-activating protein 23 OS=Homo sapiens OX=9606 GN=ARHGAP23 PE=1 SV=2
BUB3	2|0|1	1|1|0	0.25	Mitotic checkpoint protein BUB3 OS=Homo sapiens OX=9606 GN=BUB3 PE=1 SV=1
DDX47	2|0|1	2|0|0	0.25	Probable ATP-dependent RNA helicase DDX47 OS=Homo sapiens OX=9606 GN=DDX47 PE=1 SV=1
DLAT	2|0|0	0|0|0	0.25	Dihydrolipoyllysine-residue acetyltransferase component of pyruvate dehydrogenase complex, mitochondrial OS=Homo sapiens OX=9606 GN=DLAT PE=1 SV=3
MRPL47	0|0|2	1|0|0	0.25	39S ribosomal protein L47, mitochondrial OS=Homo sapiens OX=9606 GN=MRPL47 PE=1 SV=2
MTHFD1L	0|2|0	0|0|0	0.25	Monofunctional C1-tetrahydrofolate synthase, mitochondrial OS=Homo sapiens OX=9606 GN=MTHFD1L PE=1 SV=1

prey Gene	Quant (SPC or Intensities)	User Controls (SPC or Intensities)	SP	Description of protein
PLK1	2|0|0	0|0|0	0.25	Serine/threonine-protein kinase PLK1 OS=Homo sapiens OX=9606 GN=PLK1 PE=1 SV=1
SYNCRIP	2|0|0	0|0|0	0.25	Heterogeneous nuclear ribonucleoprotein Q OS=Homo sapiens OX=9606 GN=SYNCRIP PE=1 SV=2
CAPRIN1	2|0|0	0|0|0	0.24	Caprin-1 OS=Homo sapiens OX=9606 GN=CAPRIN1 PE=1 SV=2
CAVIN1	6|2|4	2|2|2	0.24	Caveolae-associated protein 1 OS=Homo sapiens OX=9606 GN=CAVIN1 PE=1 SV=1
NECTIN3	2|0|0	0|0|0	0.24	Nectin-3 OS=Homo sapiens OX=9606 GN=NECTIN3 PE=1 SV=1
C1ORF198	2|0|0	0|1|0	0.23	Uncharacterized protein C1orf198 OS=Homo sapiens OX=9606 GN=C1orf198 PE=1 SV=1
CALR	2|0|0	0|0|1	0.23	Calreticulin OS=Homo sapiens OX=9606 GN=CALR PE=1 SV=1
DHX9	9|8|11	2|5|5	0.23	ATP-dependent RNA helicase A OS=Homo sapiens OX=9606 GN=DHX9 PE=1 SV=4
LRCH1	2|0|0	0|0|0	0.23	Leucine-rich repeat and calponin homology domain-containing protein 1 OS=Homo sapiens OX=9606 GN=LRCH1 PE=1 SV=3
MSH5	2|0|0	0|0|0	0.23	MutS protein homolog 5 OS=Homo sapiens OX=9606 GN=MSH5 PE=1 SV=1
MYH14	4|0|0	0|0|0	0.23	Myosin-14 OS=Homo sapiens OX=9606 GN=MYH14 PE=1 SV=2
MYH9	27|4|11	7|13|0	0.23	Myosin-9 OS=Homo sapiens OX=9606 GN=MYH9 PE=1 SV=4

prey Gene	Quant (SPC or Intensities)	User Controls (SPC or Intensities)	SP	Description of protein
NSF	2|0|0	0|0|0	0.23	Vesicle-fusing ATPase OS=Homo sapiens OX=9606 GN=NSF PE=1 SV=3
S100A9	11|14|16	2|8|5	0.23	Protein S100-A9 OS=Homo sapiens OX=9606 GN=S100A9 PE=1 SV=1
TMEM214	2|0|0	0|0|0	0.23	Transmembrane protein 214 OS=Homo sapiens OX=9606 GN=TMEM214 PE=1 SV=2
TTC27	2|0|0	0|0|0	0.23	Tetratricopeptide repeat protein 27 OS=Homo sapiens OX=9606 GN=TTC27 PE=1 SV=1
ABCF1	2|0|0	0|1|0	0.21	ATP-binding cassette sub-family F member 1 OS=Homo sapiens OX=9606 GN=ABCF1 PE=1 SV=2
EPHA2	2|0|0	0|0|0	0.21	Ephrin type-A receptor 2 OS=Homo sapiens OX=9606 GN=EPHA2 PE=1 SV=2
KRT77	20|16|44	14|0|28	0.21	Keratin, type II cytoskeletal 1b OS=Homo sapiens OX=9606 GN=KRT77 PE=1 SV=3
LATS2	2|0|0	0|0|0	0.21	Serine/threonine-protein kinase LATS2 OS=Homo sapiens OX=9606 GN=LATS2 PE=1 SV=2
PYGB	2|0|0	0|0|0	0.21	Glycogen phosphorylase, brain form OS=Homo sapiens OX=9606 GN=PYGB PE=1 SV=5
SLC25A6	3|2|4	2|3|0	0.21	ADP/ATP translocase 3 OS=Homo sapiens OX=9606 GN=SLC25A6 PE=1 SV=4
SRRM2	2|0|1	0|1|0	0.21	Serine/arginine repetitive matrix protein 2 OS=Homo sapiens OX=9606 GN=SRRM2 PE=1 SV=2

prey Gene	Quant (SPC or Intensities)	User Controls (SPC or Intensities)	SP	Description of protein
ZMIZ1	2|0|0	0|0|0	0.21	Zinc finger MIZ domain-containing protein 1 OS=Homo sapiens OX=9606 GN=ZMIZ1 PE=1 SV=3
CSPG4	3|0|0	0|0|0	0.2	Chondroitin sulfate proteoglycan 4 OS=Homo sapiens OX=9606 GN=CSPG4 PE=1 SV=2
FLG2	1|1|3	0|3|0	0.2	Filaggrin-2 OS=Homo sapiens OX=9606 GN=FLG2 PE=1 SV=1
PPME1	2|1|1	0|3|0	0.2	Protein phosphatase methylesterase 1 OS=Homo sapiens OX=9606 GN=PPME1 PE=1 SV=3
SEC24B	2|0|0	0|0|0	0.2	Protein transport protein Sec24B OS=Homo sapiens OX=9606 GN=SEC24B PE=1 SV=2
ANKRD50	2|0|0	0|0|0	0.19	Ankyrin repeat domain-containing protein 50 OS=Homo sapiens OX=9606 GN=ANKRD50 PE=1 SV=4
ATP2B4	2|0|0	0|0|0	0.19	Plasma membrane calcium-transporting ATPase 4 OS=Homo sapiens OX=9606 GN=ATP2B4 PE=1 SV=2
BAZ1B	2|0|0	0|0|0	0.19	Tyrosine-protein kinase BAZ1B OS=Homo sapiens OX=9606 GN=BAZ1B PE=1 SV=2
EIF3F	3|3|3	2|1|2	0.19	Eukaryotic translation initiation factor 3 subunit F OS=Homo sapiens OX=9606 GN=EIF3F PE=1 SV=1
EPB41L3	11|8|8	6|6|0	0.19	Band 4.1-like protein 3 OS=Homo sapiens OX=9606 GN=EPB41L3 PE=1 SV=2
GEMIN4	2|0|0	0|0|0	0.19	Gem-associated protein 4 OS=Homo sapiens OX=9606 GN=GEMIN4 PE=1 SV=2

prey Gene	Quant (SPC or Intensities)	User Controls (SPC or Intensities)	SP	Description of protein
RPS3A	5|5|4	2|3|2	0.19	40S ribosomal protein S3a OS=Homo sapiens OX=9606 GN=RPS3A PE=1 SV=2
UBE2O	2|0|0	0|0|0	0.19	(E3-independent) E2 ubiquitin-conjugating enzyme OS=Homo sapiens OX=9606 GN=UBE2O PE=1 SV=3
CHTOP	3|1|2	1|3|0	0.18	Chromatin target of PRMT1 protein OS=Homo sapiens OX=9606 GN=CHTOP PE=1 SV=2
CSTA	5|8|10	3|3|4	0.18	Cystatin-A OS=Homo sapiens OX=9606 GN=CSTA PE=1 SV=1
EHBP1	2|0|0	0|0|0	0.18	EH domain-binding protein 1 OS=Homo sapiens OX=9606 GN=EHBP1 PE=1 SV=3
GSTP1	11|11|5	2|9|4	0.18	Glutathione S-transferase P OS=Homo sapiens OX=9606 GN=GSTP1 PE=1 SV=2
NUMA1	7|0|2	2|1|3	0.18	Nuclear mitotic apparatus protein 1 OS=Homo sapiens OX=9606 GN=NUMA1 PE=1 SV=2
LDHB	14|11|10	8|3|4	0.17	L-lactate dehydrogenase B chain OS=Homo sapiens OX=9606 GN=LDHB PE=1 SV=2
NCL	10|4|3	1|1|9	0.17	Nucleolin OS=Homo sapiens OX=9606 GN=NCL PE=1 SV=3
SAFB	3|0|0	0|3|0	0.17	Scaffold attachment factor B1 OS=Homo sapiens OX=9606 GN=SAFB PE=1 SV=4
HRNR	2|2|2	0|3|0	0.16	Hornerin OS=Homo sapiens OX=9606 GN=HRNR PE=1 SV=2
KAT6A	0|0|2	0|0|0	0.16	Histone acetyltransferase KAT6A OS=Homo sapiens OX=9606 GN=KAT6A PE=1 SV=2

prey Gene	Quant (SPC or Intensities)	User Controls (SPC or Intensities)	SP	Description of protein
LARP4	2|0|0	1|1|0	0.16	La-related protein 4 OS=Homo sapiens OX=9606 GN=LARP4 PE=1 SV=3
LBR	2|1|2	1|1|1	0.16	Delta(14)-sterol reductase LBR OS=Homo sapiens OX=9606 GN=LBR PE=1 SV=2
QSER1	2|0|0	1|0|0	0.16	Glutamine and serine-rich protein 1 OS=Homo sapiens OX=9606 GN=QSER1 PE=1 SV=3
RPLP0	10|8|5	4|3|4	0.16	60S acidic ribosomal protein P0 OS=Homo sapiens OX=9606 GN=RPLP0 PE=1 SV=1
SLC25A1	1|1|2	2|0|1	0.16	Tricarboxylate transport protein, mitochondrial OS=Homo sapiens OX=9606 GN=SLC25A1 PE=1 SV=2
SRSF1	1|2|0	0|0|3	0.16	Serine/arginine-rich splicing factor 1 OS=Homo sapiens OX=9606 GN=SRSF1 PE=1 SV=2
CALD1	3|2|2	2|2|0	0.15	Caldesmon OS=Homo sapiens OX=9606 GN=CALD1 PE=1 SV=3
SNRPD3	2|1|1	1|1|1	0.15	Small nuclear ribonucleoprotein Sm D3 OS=Homo sapiens OX=9606 GN=SNRPD3 PE=1 SV=1
MAGI3	2|0|0	0|0|0	0.14	Membrane-associated guanylate kinase, WW and PDZ domain-containing protein 3 OS=Homo sapiens OX=9606 GN=MAGI3 PE=1 SV=3
STMN1	2|0|3	0|3|1	0.14	Stathmin OS=Homo sapiens OX=9606 GN=STMN1 PE=1 SV=3
APBB1	2|1|2	1|2|0	0.13	Amyloid-beta A4 precursor protein-binding family B member 1 OS=Homo sapiens OX=9606 GN=APBB1 PE=1 SV=2

prey Gene	Quant (SPC or Intensities)	User Controls (SPC or Intensities)	SP	Description of protein
MATR3	3|2|1	0|3|1	0.13	Matrin-3 OS=Homo sapiens OX=9606 GN=MATR3 PE=1 SV=2
MDH2	7|5|2	3|1|4	0.13	Malate dehydrogenase, mitochondrial OS=Homo sapiens OX=9606 GN=MDH2 PE=1 SV=3
RPLP2	6|1|1	4|2|1	0.13	60S acidic ribosomal protein P2 OS=Homo sapiens OX=9606 GN=RPLP2 PE=1 SV=1
TNRC6A	2|0|0	0|0|0	0.13	Trinucleotide repeat-containing gene 6A protein OS=Homo sapiens OX=9606 GN=TNRC6A PE=1 SV=2
ENO1	52|33|30	19|10|14	0.12	Alpha-enolase OS=Homo sapiens OX=9606 GN=ENO1 PE=1 SV=2
GFPT1	4|2|6	4|4|0	0.12	Glutamine--fructose-6-phosphate aminotransferase [isomerizing] 1 OS=Homo sapiens OX=9606 GN=GFPT1 PE=1 SV=3
PPIA	8|8|10	8|4|1	0.12	Peptidyl-prolyl cis-trans isomerase A OS=Homo sapiens OX=9606 GN=PPIA PE=1 SV=2
STIP1	1|1|3	2|2|0	0.12	Stress-induced-phosphoprotein 1 OS=Homo sapiens OX=9606 GN=STIP1 PE=1 SV=1
CYB5R3	9|5|3	3|5|1	0.11	NADH-cytochrome b5 reductase 3 OS=Homo sapiens OX=9606 GN=CYB5R3 PE=1 SV=3
NES	4|0|2	3|2|0	0.11	Nestin OS=Homo sapiens OX=9606 GN=NES PE=1 SV=2
SNRPD1	3|0|1	2|1|1	0.11	Small nuclear ribonucleoprotein Sm D1 OS=Homo sapiens OX=9606 GN=SNRPD1 PE=1 SV=1
TKT	6|4|5	4|2|2	0.11	Transketolase OS=Homo sapiens OX=9606 GN=TKT PE=1 SV=3

prey Gene	Quant (SPC or Intensities)	User Controls (SPC or Intensities)	SP	Description of protein
XP32	2|4|7	0|7|1	0.11	Skin-specific protein 32 OS=Homo sapiens OX=9606 GN=XP32 PE=1 SV=1
CCT3	9|6|7	6|4|1	0.1	T-complex protein 1 subunit gamma OS=Homo sapiens OX=9606 GN=CCT3 PE=1 SV=4
KRT18	4|0|0	2|1|2	0.1	Keratin, type I cytoskeletal 18 OS=Homo sapiens OX=9606 GN=KRT18 PE=1 SV=2
RPL22	5|5|4	5|3|0	0.1	60S ribosomal protein L22 OS=Homo sapiens OX=9606 GN=RPL22 PE=1 SV=2
RPS13	7|2|2	3|3|3	0.1	40S ribosomal protein S13 OS=Homo sapiens OX=9606 GN=RPS13 PE=1 SV=2
SNX1	3|0|2	2|2|0	0.1	Sorting nexin-1 OS=Homo sapiens OX=9606 GN=SNX1 PE=1 SV=3
SYNJ2	3|1|1	3|1|0	0.1	Synaptojanin-2 OS=Homo sapiens OX=9606 GN=SYNJ2 PE=1 SV=3
TNPO1	5|3|3	5|2|0	0.1	Transportin-1 OS=Homo sapiens OX=9606 GN=TNPO1 PE=1 SV=2
ARHGDIA	2|1|2	3|1|0	0.09	Rho GDP-dissociation inhibitor 1 OS=Homo sapiens OX=9606 GN=ARHGDIA PE=1 SV=3
RPS11	5|6|4	5|1|3	0.08	40S ribosomal protein S11 OS=Homo sapiens OX=9606 GN=RPS11 PE=1 SV=3
CLINT1	2|2|2	2|2|0	0.07	Clathrin interactor 1 OS=Homo sapiens OX=9606 GN=CLINT1 PE=1 SV=1
DNM1L	3|0|1	1|2|1	0.07	Dynamin-1-like protein OS=Homo sapiens OX=9606 GN=DNM1L PE=1 SV=2
EZR	8|6|3	2|8|1	0.07	Ezrin OS=Homo sapiens OX=9606 GN=EZR PE=1 SV=4

prey Gene	Quant (SPC or Intensities)	User Controls (SPC or Intensities)	SP	Description of protein
HSP90B1	7|4|0	3|3|3	0.07	Endoplasmin OS=Homo sapiens OX=9606 GN=HSP90B1 PE=1 SV=1
NACA	2|1|3	4|1|0	0.07	Nascent polypeptide-associated complex subunit alpha, muscle-specific form OS=Homo sapiens OX=9606 GN=NACA PE=1 SV=1
PRKDC	20|13|22	12|12|3	0.07	DNA-dependent protein kinase catalytic subunit OS=Homo sapiens OX=9606 GN=PRKDC PE=1 SV=3
CHMP4B	1|1|2	2|2|0	0.06	Charged multivesicular body protein 4b OS=Homo sapiens OX=9606 GN=CHMP4B PE=1 SV=1
EBNA1BP2	3|1|1	1|4|0	0.06	Probable rRNA-processing protein EBP2 OS=Homo sapiens OX=9606 GN=EBNA1BP2 PE=1 SV=2
HSPA9	8|3|6	5|3|3	0.06	Stress-70 protein, mitochondrial OS=Homo sapiens OX=9606 GN=HSPA9 PE=1 SV=2
NOP14	2|0|0	1|2|0	0.06	Nucleolar protein 14 OS=Homo sapiens OX=9606 GN=NOP14 PE=1 SV=3
PALLD	2|1|1	2|1|0	0.06	Palladin OS=Homo sapiens OX=9606 GN=PALLD PE=1 SV=3
SP110	1|2|3	3|2|0	0.06	Sp110 nuclear body protein OS=Homo sapiens OX=9606 GN=SP110 PE=1 SV=5
UTRN	0|0|2	0|0|0	0.06	Utrophin OS=Homo sapiens OX=9606 GN=UTRN PE=1 SV=2
ZNF281	3|2|0	1|4|0	0.06	Zinc finger protein 281 OS=Homo sapiens OX=9606 GN=ZNF281 PE=1 SV=1

prey Gene	Quant (SPC or Intensities)	User Controls (SPC or Intensities)	SP	Description of protein
CAPZB	2|0|1	1|3|0	0.05	F-actin-capping protein subunit beta OS=Homo sapiens OX=9606 GN=CAPZB PE=1 SV=4
DPYSL3	3|2|0	2|3|0	0.05	Dihydropyrimidinase-related protein 3 OS=Homo sapiens OX=9606 GN=DPYSL3 PE=1 SV=1
FLNC	27|25|23	16|18|4	0.05	Filamin-C OS=Homo sapiens OX=9606 GN=FLNC PE=1 SV=3
JUND	2|1|1	1|3|0	0.05	Transcription factor jun-D OS=Homo sapiens OX=9606 GN=JUND PE=1 SV=3
KRT16	38|24|87	47|27|36	0.05	Keratin, type I cytoskeletal 16 OS=Homo sapiens OX=9606 GN=KRT16 PE=1 SV=4
RPS24	8|5|3	4|5|2	0.05	40S ribosomal protein S24 OS=Homo sapiens OX=9606 GN=RPS24 PE=1 SV=1
DDX39B	3|3|2	3|2|1	0.04	Spliceosome RNA helicase DDX39B OS=Homo sapiens OX=9606 GN=DDX39B PE=1 SV=1
API5	3|0|1	1|3|1	0.03	Apoptosis inhibitor 5 OS=Homo sapiens OX=9606 GN=API5 PE=1 SV=3
ARCN1	2|1|1	2|1|1	0.03	Coatomer subunit delta OS=Homo sapiens OX=9606 GN=ARCN1 PE=1 SV=1
DHX15	4|2|1	2|4|0	0.03	Pre-mRNA-splicing factor ATP-dependent RNA helicase DHX15 OS=Homo sapiens OX=9606 GN=DHX15 PE=1 SV=2
PIP	4|6|8	6|2|4	0.03	Prolactin-inducible protein OS=Homo sapiens OX=9606 GN=PIP PE=1 SV=1

prey Gene	Quant (SPC or Intensities)	User Controls (SPC or Intensities)	SP	Description of protein
SUB1	2|2|0	2|2|1	0.03	Activated RNA polymerase II transcriptional coactivator p15 OS=Homo sapiens OX=9606 GN=SUB1 PE=1 SV=3
AHCYL2	2|0|2	2|2|0	0.02	Adenosylhomocysteinase 3 OS=Homo sapiens OX=9606 GN=AHCYL2 PE=1 SV=1
PFDN2	2|2|0	2|2|1	0.02	Prefoldin subunit 2 OS=Homo sapiens OX=9606 GN=PFDN2 PE=1 SV=1
TRIM28	1|1|3	2|3|1	0.02	Transcription intermediary factor 1-beta OS=Homo sapiens OX=9606 GN=TRIM28 PE=1 SV=5
BUB1B	2|0|0	2|2|0	0.01	Mitotic checkpoint serine/threonine-protein kinase BUB1 beta OS=Homo sapiens OX=9606 GN=BUB1B PE=1 SV=3
HNRNPM	4|3|4	4|1|3	0.01	Heterogeneous nuclear ribonucleoprotein M OS=Homo sapiens OX=9606 GN=HNRNPM PE=1 SV=3
HP1BP3	2|0|0	2|2|1	0.01	Heterochromatin protein 1-binding protein 3 OS=Homo sapiens OX=9606 GN=HP1BP3 PE=1 SV=1
KRT14	46|49|85	31|38|59	0.01	Keratin, type I cytoskeletal 14 OS=Homo sapiens OX=9606 GN=KRT14 PE=1 SV=4
NASP	3|0|0	2|4|0	0.01	Nuclear autoantigenic sperm protein OS=Homo sapiens OX=9606 GN=NASP PE=1 SV=2
NOC4L	2|1|1	1|3|1	0.01	Nucleolar complex protein 4 homolog OS=Homo sapiens OX=9606 GN=NOC4L PE=1 SV=1
NOL6	2|0|0	2|1|1	0.01	Nucleolar protein 6 OS=Homo sapiens OX=9606 GN=NOL6 PE=1 SV=2

prey Gene	Quant (SPC or Intensities)	User Controls (SPC or Intensities)	SP	Description of protein
P4HB	3|1|2	1|1|4	0.01	Protein disulfide-isomerase OS=Homo sapiens OX=9606 GN=P4HB PE=1 SV=3
PAK2	3|3|1	2|4|1	0.01	Serine/threonine-protein kinase PAK 2 OS=Homo sapiens OX=9606 GN=PAK2 PE=1 SV=3
PCBP2	4|0|0	0|5|3	0.01	Poly(rC)-binding protein 2 OS=Homo sapiens OX=9606 GN=PCBP2 PE=1 SV=1
RPL30	5|5|4	7|2|1	0.01	60S ribosomal protein L30 OS=Homo sapiens OX=9606 GN=RPL30 PE=1 SV=2
RPL5	6|5|5	3|5|2	0.01	60S ribosomal protein L5 OS=Homo sapiens OX=9606 GN=RPL5 PE=1 SV=3
RRP1B	2|1|2	2|3|1	0.01	Ribosomal RNA processing protein 1 homolog B OS=Homo sapiens OX=9606 GN=RRP1B PE=1 SV=3
SAR1A	2|2|2	3|2|1	0.01	GTP-binding protein SAR1a OS=Homo sapiens OX=9606 GN=SAR1A PE=1 SV=1
VARS	2|2|3	3|4|0	0.01	Valine--tRNA ligase OS=Homo sapiens OX=9606 GN=VARS1 PE=1 SV=4
ZFYVE16	2|0|0	2|2|0	0.01	Zinc finger FYVE domain-containing protein 16 OS=Homo sapiens OX=9606 GN=ZFYVE16 PE=1 SV=3
ZYX	2|1|1	3|1|1	0.01	Zyxin OS=Homo sapiens OX=9606 GN=ZYX PE=1 SV=1
AAK1	1|2|2	4|4|1	0	AP2-associated protein kinase 1 OS=Homo sapiens OX=9606 GN=AAK1 PE=1 SV=3

prey Gene	Quant (SPC or Intensities)	User Controls (SPC or Intensities)	SP	Description of protein
AARS	1|0|0	0|0|0	0	Alanine--tRNA ligase, cytoplasmic OS=Homo sapiens OX=9606 GN=AARS1 PE=1 SV=2
ABRAXAS2	1|0|0	1|1|0	0	BRISC complex subunit Abraxas 2 OS=Homo sapiens OX=9606 GN=ABRAXAS2 PE=1 SV=2
ABT1	1|0|1	1|1|0	0	Activator of basal transcription 1 OS=Homo sapiens OX=9606 GN=ABT1 PE=1 SV=1
ACAA2	0|0|1	0|0|0	0	3-ketoacyl-CoA thiolase, mitochondrial OS=Homo sapiens OX=9606 GN=ACAA2 PE=1 SV=2
ACACA	25|18|19	47|50|10	0	Acetyl-CoA carboxylase 1 OS=Homo sapiens OX=9606 GN=ACACA PE=1 SV=2
ACADVL	1|0|0	0|0|0	0	Very long-chain specific acyl-CoA dehydrogenase, mitochondrial OS=Homo sapiens OX=9606 GN=ACADVL PE=1 SV=1
ACAT1	0|0|1	0|0|0	0	Acetyl-CoA acetyltransferase, mitochondrial OS=Homo sapiens OX=9606 GN=ACAT1 PE=1 SV=1
ACLY	1|0|0	0|0|0	0	ATP-citrate synthase OS=Homo sapiens OX=9606 GN=ACLY PE=1 SV=3
ACO2	1|1|1	0|0|0	0	Aconitate hydratase, mitochondrial OS=Homo sapiens OX=9606 GN=ACO2 PE=1 SV=2
ACOT2	1|0|0	1|1|0	0	Acyl-coenzyme A thioesterase 2, mitochondrial OS=Homo sapiens OX=9606 GN=ACOT2 PE=1 SV=6
ACSL3	0|1|1	1|0|0	0	Long-chain-fatty-acid--CoA ligase 3 OS=Homo sapiens OX=9606 GN=ACSL3 PE=1 SV=3

prey Gene	Quant (SPC or Intensities)	User Controls (SPC or Intensities)	SP	Description of protein
ACTA2	25|21|21	21|26|22	0	Actin, aortic smooth muscle OS=Homo sapiens OX=9606 GN=ACTA2 PE=1 SV=1
ACTB	60|42|45	47|42|58	0	Actin, cytoplasmic 1 OS=Homo sapiens OX=9606 GN=ACTB PE=1 SV=1
ACTR2	1|0|0	0|0|0	0	Actin-related protein 2 OS=Homo sapiens OX=9606 GN=ACTR2 PE=1 SV=1
ADAM9	1|0|0	0|0|0	0	Disintegrin and metalloproteinase domain-containing protein 9 OS=Homo sapiens OX=9606 GN=ADAM9 PE=1 SV=1
ADNP	1|0|0	1|0|0	0	Activity-dependent neuroprotector homeobox protein OS=Homo sapiens OX=9606 GN=ADNP PE=1 SV=1
ADPRHL2	1|0|0	0|0|0	0	ADP-ribose glycohydrolase ARH3 OS=Homo sapiens OX=9606 GN=ADPRS PE=1 SV=1
ADSL	1|0|1	0|0|0	0	Adenylosuccinate lyase OS=Homo sapiens OX=9606 GN=ADSL PE=1 SV=2
AGFG1	5|4|4	15|11|8	0	Arf-GAP domain and FG repeat-containing protein 1 OS=Homo sapiens OX=9606 GN=AGFG1 PE=1 SV=2
AGK	1|1|0	0|1|0	0	Acylglycerol kinase, mitochondrial OS=Homo sapiens OX=9606 GN=AGK PE=1 SV=2
AHNAK	500|513|600	379|232|166	0	Neuroblast differentiation-associated protein AHNAK OS=Homo sapiens OX=9606 GN=AHNAK PE=1 SV=2

prey Gene	Quant (SPC or Intensities)	User Controls (SPC or Intensities)	SP	Description of protein
AHNAK2	17|16|17	20|12|3	0	Protein AHNAK2 OS=Homo sapiens OX=9606 GN=AHNAK2 PE=1 SV=2
AHSA1	1|0|1	0|2|0	0	Activator of 90 kDa heat shock protein ATPase homolog 1 OS=Homo sapiens OX=9606 GN=AHSA1 PE=1 SV=1
AK6	1|0|0	0|0|0	0	Adenylate kinase isoenzyme 6 OS=Homo sapiens OX=9606 GN=AK6 PE=1 SV=1
AKAP12	0|0|1	0|0|0	0	A-kinase anchor protein 12 OS=Homo sapiens OX=9606 GN=AKAP12 PE=1 SV=4
ALB	12|18|17	27|25|58	0	Albumin OS=Homo sapiens OX=9606 GN=ALB PE=1 SV=2
ALCAM	1|1|0	0|0|0	0	CD166 antigen OS=Homo sapiens OX=9606 GN=ALCAM PE=1 SV=2
ALDH1B1	1|0|0	0|0|0	0	Aldehyde dehydrogenase X, mitochondrial OS=Homo sapiens OX=9606 GN=ALDH1B1 PE=1 SV=3
ALDH7A1	1|0|0	0|0|0	0	Alpha-aminoadipic semialdehyde dehydrogenase OS=Homo sapiens OX=9606 GN=ALDH7A1 PE=1 SV=5
ALOXE3	0|0|1	0|0|0	0	Hydroperoxide isomerase ALOXE3 OS=Homo sapiens OX=9606 GN=ALOXE3 PE=1 SV=1
AMER1	1|1|0	0|0|0	0	APC membrane recruitment protein 1 OS=Homo sapiens OX=9606 GN=AMER1 PE=1 SV=2
AMOT	0|0|1	0|0|0	0	Angiomotin OS=Homo sapiens OX=9606 GN=AMOT PE=1 SV=1
AMPD2	0|0|1	1|0|0	0	AMP deaminase 2 OS=Homo sapiens OX=9606 GN=AMPD2 PE=1 SV=2

prey Gene	Quant (SPC or Intensities)	User Controls (SPC or Intensities)	SP	Description of protein
ANKRD26	1|0|0	0|0|0	0	Ankyrin repeat domain-containing protein 26 OS=Homo sapiens OX=9606 GN=ANKRD26 PE=1 SV=4
ANLN	1|1|1	1|1|0	0	Anillin OS=Homo sapiens OX=9606 GN=ANLN PE=1 SV=2
ANP32B	0|1|0	0|0|1	0	Acidic leucine-rich nuclear phosphoprotein 32 family member B OS=Homo sapiens OX=9606 GN=ANP32B PE=1 SV=1
ANP32E	1|1|1	0|0|0	0	Acidic leucine-rich nuclear phosphoprotein 32 family member E OS=Homo sapiens OX=9606 GN=ANP32E PE=1 SV=1
ANXA1	11|7|7	20|29|22	0	Annexin A1 OS=Homo sapiens OX=9606 GN=ANXA1 PE=1 SV=2
ANXA2	37|28|27	38|36|33	0	Annexin A2 OS=Homo sapiens OX=9606 GN=ANXA2 PE=1 SV=2
AOC2	1|0|0	0|0|0	0	Retina-specific copper amine oxidase OS=Homo sapiens OX=9606 GN=AOC2 PE=1 SV=2
AP1G1	1|0|1	0|0|0	0	AP-1 complex subunit gamma-1 OS=Homo sapiens OX=9606 GN=AP1G1 PE=1 SV=5
AP1S1	1|1|1	1|0|0	0	AP-1 complex subunit sigma-1A OS=Homo sapiens OX=9606 GN=AP1S1 PE=1 SV=1
AP3B1	0|1|0	0|0|0	0	AP-3 complex subunit beta-1 OS=Homo sapiens OX=9606 GN=AP3B1 PE=1 SV=3
AP3S1	1|0|0	0|0|0	0	AP-3 complex subunit sigma-1 OS=Homo sapiens OX=9606 GN=AP3S1 PE=1 SV=1
APEH	1|0|0	0|0|0	0	Acylamino-acid-releasing enzyme OS=Homo sapiens OX=9606 GN=APEH PE=1 SV=4

prey Gene	Quant (SPC or Intensities)	User Controls (SPC or Intensities)	SP	Description of protein
APMAP	1|0|1	0|1|0	0	Adipocyte plasma membrane-associated protein OS=Homo sapiens OX=9606 GN=APMAP PE=1 SV=2
APRT	1|0|1	0|0|0	0	Adenine phosphoribosyltransferase OS=Homo sapiens OX=9606 GN=APRT PE=1 SV=2
AQR	1|0|0	0|0|0	0	RNA helicase aquarius OS=Homo sapiens OX=9606 GN=AQR PE=1 SV=4
ARFGAP1	0|1|0	1|1|1	0	ADP-ribosylation factor GTPase-activating protein 1 OS=Homo sapiens OX=9606 GN=ARFGAP1 PE=1 SV=2
ARFGAP2	1|0|0	0|0|0	0	ADP-ribosylation factor GTPase-activating protein 2 OS=Homo sapiens OX=9606 GN=ARFGAP2 PE=1 SV=1
ARFGEF1	0|0|1	0|0|0	0	Brefeldin A-inhibited guanine nucleotide-exchange protein 1 OS=Homo sapiens OX=9606 GN=ARFGEF1 PE=1 SV=2
ARHGAP12	1|0|0	0|0|0	0	Rho GTPase-activating protein 12 OS=Homo sapiens OX=9606 GN=ARHGAP12 PE=1 SV=1
ARHGAP29	1|1|1	0|0|0	0	Rho GTPase-activating protein 29 OS=Homo sapiens OX=9606 GN=ARHGAP29 PE=1 SV=2
ARHGAP31	1|0|0	0|0|0	0	Rho GTPase-activating protein 31 OS=Homo sapiens OX=9606 GN=ARHGAP31 PE=1 SV=2

prey Gene	Quant (SPC or Intensities)	User Controls (SPC or Intensities)	SP	Description of protein
ARHGAP35	0|1|0	0|0|0	0	Rho GTPase-activating protein 35 OS=Homo sapiens OX=9606 GN=ARHGAP35 PE=1 SV=3
ARHGEF17	0|1|0	0|0|0	0	Rho guanine nucleotide exchange factor 17 OS=Homo sapiens OX=9606 GN=ARHGEF17 PE=1 SV=1
ARL1	1|1|1	0|0|0	0	ADP-ribosylation factor-like protein 1 OS=Homo sapiens OX=9606 GN=ARL1 PE=1 SV=1
ARL2	1|1|1	0|0|0	0	ADP-ribosylation factor-like protein 2 OS=Homo sapiens OX=9606 GN=ARL2 PE=1 SV=4
ASAH1	0|0|1	0|0|0	0	Acid ceramidase OS=Homo sapiens OX=9606 GN=ASAH1 PE=1 SV=5
ASF1A	0|0|1	0|0|0	0	Histone chaperone ASF1A OS=Homo sapiens OX=9606 GN=ASF1A PE=1 SV=1
ASPSCR1	1|0|0	0|0|0	0	Tether containing UBX domain for GLUT4 OS=Homo sapiens OX=9606 GN=ASPSCR1 PE=1 SV=1
ASRGL1	1|0|0	0|1|0	0	Isoaspartyl peptidase/L-asparaginase OS=Homo sapiens OX=9606 GN=ASRGL1 PE=1 SV=2
ATG2A	0|1|0	0|0|0	0	Autophagy-related protein 2 homolog A OS=Homo sapiens OX=9606 GN=ATG2A PE=1 SV=3
ATIC	0|0|1	0|0|0	0	Bifunctional purine biosynthesis protein ATIC OS=Homo sapiens OX=9606 GN=ATIC PE=1 SV=3
ATP1B1	1|0|0	0|0|0	0	Sodium/potassium-transporting ATPase subunit beta-1 OS=Homo sapiens OX=9606 GN=ATP1B1 PE=1 SV=1

prey Gene	Quant (SPC or Intensities)	User Controls (SPC or Intensities)	SP	Description of protein
ATP5A1	23|19|20	21|11|9	0	ATP synthase subunit alpha, mitochondrial OS=Homo sapiens OX=9606 GN=ATP5F1A PE=1 SV=1
ATP5B	19|10|11	12|4|18	0	ATP synthase subunit beta, mitochondrial OS=Homo sapiens OX=9606 GN=ATP5F1B PE=1 SV=3
ATP5J	1|0|1	0|0|0	0	ATP synthase-coupling factor 6, mitochondrial OS=Homo sapiens OX=9606 GN=ATP5PF PE=1 SV=1
ATP5L	1|0|1	0|1|0	0	ATP synthase subunit g, mitochondrial OS=Homo sapiens OX=9606 GN=ATP5MG PE=1 SV=3
ATP5O	1|0|0	0|0|0	0	ATP synthase subunit O, mitochondrial OS=Homo sapiens OX=9606 GN=ATP5PO PE=1 SV=1
ATP6V1B2	1|1|0	0|0|0	0	V-type proton ATPase subunit B, brain isoform OS=Homo sapiens OX=9606 GN=ATP6V1B2 PE=1 SV=3
ATP6V1H	1|1|0	0|0|0	0	V-type proton ATPase subunit H OS=Homo sapiens OX=9606 GN=ATP6V1H PE=1 SV=1
AVIL	1|0|0	0|0|0	0	Advillin OS=Homo sapiens OX=9606 GN=AVIL PE=1 SV=3
BAG2	1|0|0	1|0|0	0	BAG family molecular chaperone regulator 2 OS=Homo sapiens OX=9606 GN=BAG2 PE=1 SV=1
BAG3	1|0|0	0|1|0	0	BAG family molecular chaperone regulator 3 OS=Homo sapiens OX=9606 GN=BAG3 PE=1 SV=3
BAG6	1|0|0	0|0|0	0	Large proline-rich protein BAG6 OS=Homo sapiens OX=9606 GN=BAG6 PE=1 SV=2

prey Gene	Quant (SPC or Intensities)	User Controls (SPC or Intensities)	SP	Description of protein
BAP1	1|0|0	0|0|0	0	Ubiquitin carboxyl-terminal hydrolase BAP1 OS=Homo sapiens OX=9606 GN=BAP1 PE=1 SV=2
BCOR	1|0|0	0|0|0	0	BCL-6 corepressor OS=Homo sapiens OX=9606 GN=BCOR PE=1 SV=1
BLMH	0|0|1	0|0|1	0	Bleomycin hydrolase OS=Homo sapiens OX=9606 GN=BLMH PE=1 SV=1
BMS1	4|2|3	11|6|8	0	Ribosome biogenesis protein BMS1 homolog OS=Homo sapiens OX=9606 GN=BMS1 PE=1 SV=1
BOLA2; BOLA2B	0|0|1	0|0|0	0	BolA-like protein 2 OS=Homo sapiens OX=9606 GN=BOLA2 PE=1 SV=1
BOP1	1|0|0	0|0|0	0	Ribosome biogenesis protein BOP1 OS=Homo sapiens OX=9606 GN=BOP1 PE=1 SV=2
BPIFA2	0|1|0	0|0|0	0	BPI fold-containing family A member 2 OS=Homo sapiens OX=9606 GN=BPIFA2 PE=1 SV=2
BRCC3	3|0|1	9|7|2	0	Lys-63-specific deubiquitinase BRCC36 OS=Homo sapiens OX=9606 GN=BRCC3 PE=1 SV=2
BRIX1	0|0|1	0|0|0	0	Ribosome biogenesis protein BRX1 homolog OS=Homo sapiens OX=9606 GN=BRIX1 PE=1 SV=2
BZW1	1|0|1	1|0|0	0	Basic leucine zipper and W2 domain-containing protein 1 OS=Homo sapiens OX=9606 GN=BZW1 PE=1 SV=1
C11ORF98	2|2|2	6|2|1	0	Uncharacterized protein C11orf98 OS=Homo sapiens OX=9606 GN=C11orf98 PE=4 SV=2

prey Gene	Quant (SPC or Intensities)	User Controls (SPC or Intensities)	SP	Description of protein
C14ORF166	1|0|0	0|0|0	0	RNA transcription, translation and transport factor protein OS=Homo sapiens OX=9606 GN=RTRAF PE=1 SV=1
C1QBP	1|0|1	1|0|0	0	Complement component 1 Q subcomponent-binding protein, mitochondrial OS=Homo sapiens OX=9606 GN=C1QBP PE=1 SV=1
C2CD4C	1|0|0	0|0|0	0	C2 calcium-dependent domain-containing protein 4C OS=Homo sapiens OX=9606 GN=C2CD4C PE=1 SV=2
C6ORF47	1|1|1	0|0|0	0	Uncharacterized protein C6orf47 OS=Homo sapiens OX=9606 GN=C6orf47 PE=1 SV=2
CA2	1|0|0	0|0|0	0	Carbonic anhydrase 2 OS=Homo sapiens OX=9606 GN=CA2 PE=1 SV=2
CAMK2G	1|0|0	0|0|0	0	Calcium/calmodulin-dependent protein kinase type II subunit gamma OS=Homo sapiens OX=9606 GN=CAMK2G PE=1 SV=4
CAPN1	0|1|1	0|0|0	0	Calpain-1 catalytic subunit OS=Homo sapiens OX=9606 GN=CAPN1 PE=1 SV=1
CAPNS1	1|0|0	0|0|0	0	Calpain small subunit 1 OS=Homo sapiens OX=9606 GN=CAPNS1 PE=1 SV=1
CARD18	0|0|1	0|0|0	0	Caspase recruitment domain-containing protein 18 OS=Homo sapiens OX=9606 GN=CARD18 PE=1 SV=1
CAV1	1|1|0	0|0|0	0	Caveolin-1 OS=Homo sapiens OX=9606 GN=CAV1 PE=1 SV=4

prey Gene	Quant (SPC or Intensities)	User Controls (SPC or Intensities)	SP	Description of protein
CBR3	1|1|0	0|0|0	0	Carbonyl reductase [NADPH] 3 OS=Homo sapiens OX=9606 GN=CBR3 PE=1 SV=3
CBX1	0|1|0	0|0|0	0	Chromobox protein homolog 1 OS=Homo sapiens OX=9606 GN=CBX1 PE=1 SV=1
CBX3	1|0|0	0|0|2	0	Chromobox protein homolog 3 OS=Homo sapiens OX=9606 GN=CBX3 PE=1 SV=4
CCAR2	1|0|1	2|1|0	0	Cell cycle and apoptosis regulator protein 2 OS=Homo sapiens OX=9606 GN=CCAR2 PE=1 SV=2
CCDC138	1|1|0	0|0|0	0	Coiled-coil domain-containing protein 138 OS=Homo sapiens OX=9606 GN=CCDC138 PE=1 SV=1
CCDC39	1|0|0	0|0|0	0	Coiled-coil domain-containing protein 39 OS=Homo sapiens OX=9606 GN=CCDC39 PE=2 SV=3
CCDC86	0|0|1	0|0|0	0	Coiled-coil domain-containing protein 86 OS=Homo sapiens OX=9606 GN=CCDC86 PE=1 SV=1
CCDC88A	0|0|1	0|0|0	0	Girdin OS=Homo sapiens OX=9606 GN=CCDC88A PE=1 SV=2
CCNB1	1|1|1	1|1|0	0	G2/mitotic-specific cyclin-B1 OS=Homo sapiens OX=9606 GN=CCNB1 PE=1 SV=1
CCT4	8|6|8	8|6|2	0	T-complex protein 1 subunit delta OS=Homo sapiens OX=9606 GN=CCT4 PE=1 SV=4
CCT8	34|32|29	155|124|126	0	T-complex protein 1 subunit theta OS=Homo sapiens OX=9606 GN=CCT8 PE=1 SV=4

prey Gene	Quant (SPC or Intensities)	User Controls (SPC or Intensities)	SP	Description of protein
CD2AP	3|1|2	3|3|3	0	CD2-associated protein OS=Homo sapiens OX=9606 GN=CD2AP PE=1 SV=1
CDC16	1|0|0	0|0|0	0	Cell division cycle protein 16 homolog OS=Homo sapiens OX=9606 GN=CDC16 PE=1 SV=2
CDC42	1|0|0	0|0|0	0	Cell division control protein 42 homolog OS=Homo sapiens OX=9606 GN=CDC42 PE=1 SV=2
CDC42EP3	1|0|0	0|0|0	0	Cdc42 effector protein 3 OS=Homo sapiens OX=9606 GN=CDC42EP3 PE=1 SV=1
CDC5L	1|1|0	0|0|0	0	Cell division cycle 5-like protein OS=Homo sapiens OX=9606 GN=CDC5L PE=1 SV=2
CDCA3	1|0|0	0|0|0	0	Cell division cycle-associated protein 3 OS=Homo sapiens OX=9606 GN=CDCA3 PE=1 SV=1
CDV3	1|3|1	3|6|1	0	Protein CDV3 homolog OS=Homo sapiens OX=9606 GN=CDV3 PE=1 SV=1
CEBPZ	1|0|0	1|2|0	0	CCAAT/enhancer-binding protein zeta OS=Homo sapiens OX=9606 GN=CEBPZ PE=1 SV=3
CENPA	1|0|0	0|0|0	0	Histone H3-like centromeric protein A OS=Homo sapiens OX=9606 GN=CENPA PE=1 SV=1
CEP152	0|0|1	0|0|0	0	Centrosomal protein of 152 kDa OS=Homo sapiens OX=9606 GN=CEP152 PE=1 SV=4
CEP350	3|2|1	4|4|1	0	Centrosome-associated protein 350 OS=Homo sapiens OX=9606 GN=CEP350 PE=1 SV=1

prey Gene	Quant (SPC or Intensities)	User Controls (SPC or Intensities)	SP	Description of protein
CEP89	1|1|0	0|0|0	0	Centrosomal protein of 89 kDa OS=Homo sapiens OX=9606 GN=CEP89 PE=1 SV=3
CHD4	3|0|1	4|5|0	0	Chromodomain-helicase-DNA-binding protein 4 OS=Homo sapiens OX=9606 GN=CHD4 PE=1 SV=2
CHD5	0|1|0	0|0|0	0	Chromodomain-helicase-DNA-binding protein 5 OS=Homo sapiens OX=9606 GN=CHD5 PE=1 SV=1
CHERP	1|0|0	0|0|0	0	Calcium homeostasis endoplasmic reticulum protein OS=Homo sapiens OX=9606 GN=CHERP PE=1 SV=3
CHMP5	1|0|0	2|1|0	0	Charged multivesicular body protein 5 OS=Homo sapiens OX=9606 GN=CHMP5 PE=1 SV=1
CHORDC1	2|1|2	5|7|0	0	Cysteine and histidine-rich domain-containing protein 1 OS=Homo sapiens OX=9606 GN=CHORDC1 PE=1 SV=2
CKB	0|0|1	0|0|0	0	Creatine kinase B-type OS=Homo sapiens OX=9606 GN=CKB PE=1 SV=1
CKMT1A; CKMT1B	0|1|0	0|0|0	0	Creatine kinase U-type, mitochondrial OS=Homo sapiens OX=9606 GN=CKMT1A PE=1 SV=1
CLPX	1|0|0	0|0|0	0	ATP-dependent Clp protease ATP-binding subunit clpX-like, mitochondrial OS=Homo sapiens OX=9606 GN=CLPX PE=1 SV=2
CLU	0|0|1	0|0|0	0	Clusterin OS=Homo sapiens OX=9606 GN=CLU PE=1 SV=1

prey Gene	Quant (SPC or Intensities)	User Controls (SPC or Intensities)	SP	Description of protein
CLUH	1|0|0	0|0|0	0	Clustered mitochondria protein homolog OS=Homo sapiens OX=9606 GN=CLUH PE=1 SV=2
CNBP	1|0|0	0|0|0	0	Cellular nucleic acid-binding protein OS=Homo sapiens OX=9606 GN=CNBP PE=1 SV=1
CNDP2	1|0|0	0|0|0	0	Cytosolic non-specific dipeptidase OS=Homo sapiens OX=9606 GN=CNDP2 PE=1 SV=2
CNN2	1|0|0	1|2|0	0	Calponin-2 OS=Homo sapiens OX=9606 GN=CNN2 PE=1 SV=4
CNN3	1|0|1	0|1|1	0	Calponin-3 OS=Homo sapiens OX=9606 GN=CNN3 PE=1 SV=1
CNPY2	1|0|0	0|0|0	0	Protein canopy homolog 2 OS=Homo sapiens OX=9606 GN=CNPY2 PE=1 SV=1
COG1	1|0|0	0|0|0	0	Conserved oligomeric Golgi complex subunit 1 OS=Homo sapiens OX=9606 GN=COG1 PE=1 SV=1
COLGALT1	0|0|1	0|0|0	0	Procollagen galactosyltransferase 1 OS=Homo sapiens OX=9606 GN=COLGALT1 PE=1 SV=1
COMMD10	1|0|0	1|3|1	0	COMM domain-containing protein 10 OS=Homo sapiens OX=9606 GN=COMMD10 PE=1 SV=1
COMMD8	1|0|0	0|1|1	0	COMM domain-containing protein 8 OS=Homo sapiens OX=9606 GN=COMMD8 PE=1 SV=1
COPB1	1|0|1	0|0|0	0	Coatomer subunit beta OS=Homo sapiens OX=9606 GN=COPB1 PE=1 SV=3

prey Gene	Quant (SPC or Intensities)	User Controls (SPC or Intensities)	SP	Description of protein
COPE	0|1|0	0|0|0	0	Coatomer subunit epsilon OS=Homo sapiens OX=9606 GN=COPE PE=1 SV=3
COPS4	1|0|0	0|0|0	0	COP9 signalosome complex subunit 4 OS=Homo sapiens OX=9606 GN=COPS4 PE=1 SV=1
COPS8	1|0|0	1|1|0	0	COP9 signalosome complex subunit 8 OS=Homo sapiens OX=9606 GN=COPS8 PE=1 SV=1
CORO1C	0|1|0	2|2|1	0	Coronin-1C OS=Homo sapiens OX=9606 GN=CORO1C PE=1 SV=1
CORO7	1|0|1	3|5|2	0	Coronin-7 OS=Homo sapiens OX=9606 GN=CORO7 PE=1 SV=2
CPSF7	1|0|1	0|0|0	0	Cleavage and polyadenylation specificity factor subunit 7 OS=Homo sapiens OX=9606 GN=CPSF7 PE=1 SV=1
CRCP	1|0|0	0|3|0	0	DNA-directed RNA polymerase III subunit RPC9 OS=Homo sapiens OX=9606 GN=CRCP PE=1 SV=1
CRCT1	0|0|1	0|0|0	0	Cysteine-rich C-terminal protein 1 OS=Homo sapiens OX=9606 GN=CRCT1 PE=1 SV=1
CRIP2	1|0|1	1|1|0	0	Cysteine-rich protein 2 OS=Homo sapiens OX=9606 GN=CRIP2 PE=1 SV=1
CRKL	0|1|0	0|0|0	0	Crk-like protein OS=Homo sapiens OX=9606 GN=CRKL PE=1 SV=1
CRNKL1	0|1|0	0|0|0	0	Crooked neck-like protein 1 OS=Homo sapiens OX=9606 GN=CRNKL1 PE=1 SV=4
CRYBG3	1|1|2	2|3|0	0	Very large A-kinase anchor protein OS=Homo sapiens OX=9606 GN=CRYBG3 PE=1 SV=3

prey Gene	Quant (SPC or Intensities)	User Controls (SPC or Intensities)	SP	Description of protein
CSDE1	1|0|0	1|1|0	0	Cold shock domain-containing protein E1 OS=Homo sapiens OX=9606 GN=CSDE1 PE=1 SV=2
CSNK1A1	1|0|0	0|0|0	0	Casein kinase I isoform alpha OS=Homo sapiens OX=9606 GN=CSNK1A1 PE=1 SV=2
CSRP1	1|0|0	0|1|0	0	Cysteine and glycine-rich protein 1 OS=Homo sapiens OX=9606 GN=CSRP1 PE=1 SV=3
CST4	0|1|0	0|0|0	0	Cystatin-S OS=Homo sapiens OX=9606 GN=CST4 PE=1 SV=3
CSTF2T	1|1|1	0|0|0	0	Cleavage stimulation factor subunit 2 tau variant OS=Homo sapiens OX=9606 GN=CSTF2T PE=1 SV=1
CT45A6	1|0|0	1|0|0	0	Cancer/testis antigen family 45 member A6 OS=Homo sapiens OX=9606 GN=CT45A6 PE=2 SV=1
CTBP2	1|0|0	0|0|0	0	C-terminal-binding protein 2 OS=Homo sapiens OX=9606 GN=CTBP2 PE=1 SV=1
CTDSP2	1|1|1	0|0|0	0	Carboxy-terminal domain RNA polymerase II polypeptide A small phosphatase 2 OS=Homo sapiens OX=9606 GN=CTDSP2 PE=1 SV=2
CTDSPL2	1|0|1	0|1|0	0	CTD small phosphatase-like protein 2 OS=Homo sapiens OX=9606 GN=CTDSPL2 PE=1 SV=2
CTNND2	0|1|0	0|0|0	0	Catenin delta-2 OS=Homo sapiens OX=9606 GN=CTNND2 PE=1 SV=3
CTSA	1|0|1	0|0|0	0	Lysosomal protective protein OS=Homo sapiens OX=9606 GN=CTSA PE=1 SV=2

prey Gene	Quant (SPC or Intensities)	User Controls (SPC or Intensities)	SP	Description of protein
CTSV	0|1|1	0|0|0	0	Cathepsin L2 OS=Homo sapiens OX=9606 GN=CTSV PE=1 SV=2
CTTN	7|5|7	16|10|10	0	Src substrate cortactin OS=Homo sapiens OX=9606 GN=CTTN PE=1 SV=2
CUL4A	1|0|0	0|0|0	0	Cullin-4A OS=Homo sapiens OX=9606 GN=CUL4A PE=1 SV=3
CYCS	0|0|1	0|0|0	0	Cytochrome c OS=Homo sapiens OX=9606 GN=CYCS PE=1 SV=2
CYFIP1	1|0|0	0|0|0	0	Cytoplasmic FMR1-interacting protein 1 OS=Homo sapiens OX=9606 GN=CYFIP1 PE=1 SV=1
CYFIP2	0|1|1	0|0|0	0	Cytoplasmic FMR1-interacting protein 2 OS=Homo sapiens OX=9606 GN=CYFIP2 PE=1 SV=2
CYTH3	1|1|0	0|0|0	0	Cytohesin-3 OS=Homo sapiens OX=9606 GN=CYTH3 PE=1 SV=2
DAB2	1|1|0	0|0|0	0	Disabled homolog 2 OS=Homo sapiens OX=9606 GN=DAB2 PE=1 SV=3
DAP3	0|0|1	0|0|0	0	28S ribosomal protein S29, mitochondrial OS=Homo sapiens OX=9606 GN=DAP3 PE=1 SV=1
DBI	1|1|1	0|0|0	0	Acyl-CoA-binding protein OS=Homo sapiens OX=9606 GN=DBI PE=1 SV=2
DBNL	1|1|0	2|1|0	0	Drebrin-like protein OS=Homo sapiens OX=9606 GN=DBNL PE=1 SV=1
DCD	9|7|8	8|2|8	0	Dermcidin OS=Homo sapiens OX=9606 GN=DCD PE=1 SV=2

prey Gene	Quant (SPC or Intensities)	User Controls (SPC or Intensities)	SP	Description of protein
DCTN2	1|0|0	1|0|0	0	Dynactin subunit 2 OS=Homo sapiens OX=9606 GN=DCTN2 PE=1 SV=4
DDX1	1|1|1	0|0|0	0	ATP-dependent RNA helicase DDX1 OS=Homo sapiens OX=9606 GN=DDX1 PE=1 SV=2
DDX10	0|1|0	0|0|0	0	Probable ATP-dependent RNA helicase DDX10 OS=Homo sapiens OX=9606 GN=DDX10 PE=1 SV=2
DDX18	4|5|5	5|6|4	0	ATP-dependent RNA helicase DDX18 OS=Homo sapiens OX=9606 GN=DDX18 PE=1 SV=2
DDX3X	6|3|5	5|8|2	0	ATP-dependent RNA helicase DDX3X OS=Homo sapiens OX=9606 GN=DDX3X PE=1 SV=3
DDX42	1|0|0	3|4|1	0	ATP-dependent RNA helicase DDX42 OS=Homo sapiens OX=9606 GN=DDX42 PE=1 SV=1
DDX5	10|6|10	13|10|6	0	Probable ATP-dependent RNA helicase DDX5 OS=Homo sapiens OX=9606 GN=DDX5 PE=1 SV=1
DDX51	1|0|1	1|0|0	0	ATP-dependent RNA helicase DDX51 OS=Homo sapiens OX=9606 GN=DDX51 PE=1 SV=3
DERL2	0|0|1	0|0|0	0	Derlin-2 OS=Homo sapiens OX=9606 GN=DERL2 PE=1 SV=1
DHFR	1|1|0	0|0|0	0	Dihydrofolate reductase OS=Homo sapiens OX=9606 GN=DHFR PE=1 SV=2
DMBT1	1|1|1	0|0|0	0	Deleted in malignant brain tumors 1 protein OS=Homo sapiens OX=9606 GN=DMBT1 PE=1 SV=2

prey Gene	Quant (SPC or Intensities)	User Controls (SPC or Intensities)	SP	Description of protein
DNAAF4	0|1|0	0|0|0	0	Dynein axonemal assembly factor 4 OS=Homo sapiens OX=9606 GN=DNAAF4 PE=1 SV=2
DNAAF5	0|0|1	0|0|0	0	Dynein axonemal assembly factor 5 OS=Homo sapiens OX=9606 GN=DNAAF5 PE=1 SV=4
DNAJA1	1|1|1	0|0|0	0	DnaJ homolog subfamily A member 1 OS=Homo sapiens OX=9606 GN=DNAJA1 PE=1 SV=2
DNAJA2	1|0|0	0|0|0	0	DnaJ homolog subfamily A member 2 OS=Homo sapiens OX=9606 GN=DNAJA2 PE=1 SV=1
DNAJC13	1|0|0	0|0|0	0	DnaJ homolog subfamily C member 13 OS=Homo sapiens OX=9606 GN=DNAJC13 PE=1 SV=5
DNAJC19	1|1|1	0|0|0	0	Mitochondrial import inner membrane translocase subunit TIM14 OS=Homo sapiens OX=9606 GN=DNAJC19 PE=1 SV=3
DNAJC9	1|0|0	1|1|1	0	DnaJ homolog subfamily C member 9 OS=Homo sapiens OX=9606 GN=DNAJC9 PE=1 SV=1
DNM2	1|0|1	0|0|0	0	Dynamin-2 OS=Homo sapiens OX=9606 GN=DNM2 PE=1 SV=2
DNTTIP2	1|0|0	1|0|0	0	Deoxynucleotidyltransferase terminal-interacting protein 2 OS=Homo sapiens OX=9606 GN=DNTTIP2 PE=1 SV=2
DOCK1	1|0|0	0|0|0	0	Dedicator of cytokinesis protein 1 OS=Homo sapiens OX=9606 GN=DOCK1 PE=1 SV=2
DOCK2	0|0|1	0|0|0	0	Dedicator of cytokinesis protein 2 OS=Homo sapiens OX=9606 GN=DOCK2 PE=1 SV=2

prey Gene	Quant (SPC or Intensities)	User Controls (SPC or Intensities)	SP	Description of protein
DOK1	1|1|0	1|0|0	0	Docking protein 1 OS=Homo sapiens OX=9606 GN=DOK1 PE=1 SV=1
DPYSL2	5|3|3	9|4|1	0	Dihydropyrimidinase-related protein 2 OS=Homo sapiens OX=9606 GN=DPYSL2 PE=1 SV=1
DRG2	1|0|1	0|0|0	0	Developmentally-regulated GTP-binding protein 2 OS=Homo sapiens OX=9606 GN=DRG2 PE=1 SV=1
DSG1	10|11|20	10|13|21	0	Desmoglein-1 OS=Homo sapiens OX=9606 GN=DSG1 PE=1 SV=2
DST	1|0|1	0|0|0	0	Dystonin OS=Homo sapiens OX=9606 GN=DST PE=1 SV=4
DTD1	1|1|0	1|0|0	0	D-aminoacyl-tRNA deacylase 1 OS=Homo sapiens OX=9606 GN=DTD1 PE=1 SV=2
DVL2	1|0|1	0|1|0	0	Segment polarity protein dishevelled homolog DVL-2 OS=Homo sapiens OX=9606 GN=DVL2 PE=1 SV=1
DYSF	0|0|1	0|0|0	0	Dysferlin OS=Homo sapiens OX=9606 GN=DYSF PE=1 SV=1
ECHS1	1|0|0	0|0|0	0	Enoyl-CoA hydratase, mitochondrial OS=Homo sapiens OX=9606 GN=ECHS1 PE=1 SV=4
EDC3	5|2|3	10|11|8	0	Enhancer of mRNA-decapping protein 3 OS=Homo sapiens OX=9606 GN=EDC3 PE=1 SV=1
EEA1	1|0|0	0|0|0	0	Early endosome antigen 1 OS=Homo sapiens OX=9606 GN=EEA1 PE=1 SV=2
EEF1A1	43|30|32	24|22|24	0	Elongation factor 1-alpha 1 OS=Homo sapiens OX=9606 GN=EEF1A1 PE=1 SV=1

prey Gene	Quant (SPC or Intensities)	User Controls (SPC or Intensities)	SP	Description of protein
EEF1A2	20|0|20	20|12|0	0	Elongation factor 1-alpha 2 OS=Homo sapiens OX=9606 GN=EEF1A2 PE=1 SV=1
EEF1D	6|5|5	22|14|9	0	Elongation factor 1-delta OS=Homo sapiens OX=9606 GN=EEF1D PE=1 SV=5
EFHD2	3|1|2	9|6|2	0	EF-hand domain-containing protein D2 OS=Homo sapiens OX=9606 GN=EFHD2 PE=1 SV=1
EFR3A	1|0|0	0|0|0	0	Protein EFR3 homolog A OS=Homo sapiens OX=9606 GN=EFR3A PE=1 SV=2
EFTUD2	0|0|1	0|0|0	0	116 kDa U5 small nuclear ribonucleoprotein component OS=Homo sapiens OX=9606 GN=EFTUD2 PE=1 SV=1
EHD4	1|0|1	0|0|0	0	EH domain-containing protein 4 OS=Homo sapiens OX=9606 GN=EHD4 PE=1 SV=1
EIF1B	0|0|1	0|0|0	0	Eukaryotic translation initiation factor 1b OS=Homo sapiens OX=9606 GN=EIF1B PE=1 SV=2
EIF2A	6|2|2	13|13|4	0	Eukaryotic translation initiation factor 2A OS=Homo sapiens OX=9606 GN=EIF2A PE=1 SV=3
EIF2AK2	1|0|0	0|0|0	0	Interferon-induced, double-stranded RNA-activated protein kinase OS=Homo sapiens OX=9606 GN=EIF2AK2 PE=1 SV=2
EIF2B1	1|0|1	0|0|0	0	Translation initiation factor eIF-2B subunit alpha OS=Homo sapiens OX=9606 GN=EIF2B1 PE=1 SV=1

prey Gene	Quant (SPC or Intensities)	User Controls (SPC or Intensities)	SP	Description of protein
EIF2B3	1|0|1	0|0|0	0	Translation initiation factor eIF-2B subunit gamma OS=Homo sapiens OX=9606 GN=EIF2B3 PE=1 SV=1
EIF2S1	1|1|0	0|0|0	0	Eukaryotic translation initiation factor 2 subunit 1 OS=Homo sapiens OX=9606 GN=EIF2S1 PE=1 SV=3
EIF3D	1|0|0	1|0|0	0	Eukaryotic translation initiation factor 3 subunit D OS=Homo sapiens OX=9606 GN=EIF3D PE=1 SV=1
EIF3G	1|1|0	0|0|0	0	Eukaryotic translation initiation factor 3 subunit G OS=Homo sapiens OX=9606 GN=EIF3G PE=1 SV=2
EIF3H	0|0|1	0|0|0	0	Eukaryotic translation initiation factor 3 subunit H OS=Homo sapiens OX=9606 GN=EIF3H PE=1 SV=1
EIF3I	1|0|0	0|1|1	0	Eukaryotic translation initiation factor 3 subunit I OS=Homo sapiens OX=9606 GN=EIF3I PE=1 SV=1
EIF3M	1|1|1	0|0|0	0	Eukaryotic translation initiation factor 3 subunit M OS=Homo sapiens OX=9606 GN=EIF3M PE=1 SV=1
EIF4B	2|2|1	4|6|2	0	Eukaryotic translation initiation factor 4B OS=Homo sapiens OX=9606 GN=EIF4B PE=1 SV=2
EIF4G1	1|0|0	0|2|0	0	Eukaryotic translation initiation factor 4 gamma 1 OS=Homo sapiens OX=9606 GN=EIF4G1 PE=1 SV=4

prey Gene	Quant (SPC or Intensities)	User Controls (SPC or Intensities)	SP	Description of protein
EIF4G2	8|7|11	9|7|3	0	Eukaryotic translation initiation factor 4 gamma 2 OS=Homo sapiens OX=9606 GN=EIF4G2 PE=1 SV=1
EIF4H	0|1|0	1|1|0	0	Eukaryotic translation initiation factor 4H OS=Homo sapiens OX=9606 GN=EIF4H PE=1 SV=5
EIF5	1|1|0	1|0|0	0	Eukaryotic translation initiation factor 5 OS=Homo sapiens OX=9606 GN=EIF5 PE=1 SV=2
EIF5A	1|0|0	0|1|1	0	Eukaryotic translation initiation factor 5A-1 OS=Homo sapiens OX=9606 GN=EIF5A PE=1 SV=2
EIF5B	1|1|1	0|1|0	0	Eukaryotic translation initiation factor 5B OS=Homo sapiens OX=9606 GN=EIF5B PE=1 SV=4
ELAC2	1|0|0	0|0|0	0	Zinc phosphodiesterase ELAC protein 2 OS=Homo sapiens OX=9606 GN=ELAC2 PE=1 SV=2
ELOVL1	0|1|0	1|0|0	0	Elongation of very long chain fatty acids protein 1 OS=Homo sapiens OX=9606 GN=ELOVL1 PE=1 SV=1
ELP5	1|0|0	1|1|0	0	Elongator complex protein 5 OS=Homo sapiens OX=9606 GN=ELP5 PE=1 SV=2
EMC1	0|1|0	0|0|0	0	ER membrane protein complex subunit 1 OS=Homo sapiens OX=9606 GN=EMC1 PE=1 SV=1
EMC3	1|1|1	0|0|0	0	ER membrane protein complex subunit 3 OS=Homo sapiens OX=9606 GN=EMC3 PE=1 SV=3

prey Gene	Quant (SPC or Intensities)	User Controls (SPC or Intensities)	SP	Description of protein
EMD	1|1|0	3|2|1	0	Emerin OS=Homo sapiens OX=9606 GN=EMD PE=1 SV=1
EML4	1|0|0	1|1|0	0	Echinoderm microtubule-associated protein-like 4 OS=Homo sapiens OX=9606 GN=EML4 PE=1 SV=3
ENPP2	0|1|0	0|0|0	0	Ectonucleotide pyrophosphatase/phosphodiesterase family member 2 OS=Homo sapiens OX=9606 GN=ENPP2 PE=1 SV=3
ENSA	1|0|1	1|1|1	0	Alpha-endosulfine OS=Homo sapiens OX=9606 GN=ENSA PE=1 SV=1
EPB41L1	1|1|1	0|0|0	0	Band 4.1-like protein 1 OS=Homo sapiens OX=9606 GN=EPB41L1 PE=1 SV=2
EPN1	1|0|0	0|0|0	0	Epsin-1 OS=Homo sapiens OX=9606 GN=EPN1 PE=1 SV=2
EPS8	0|1|0	0|0|0	0	Epidermal growth factor receptor kinase substrate 8 OS=Homo sapiens OX=9606 GN=EPS8 PE=1 SV=1
ERAL1	1|0|0	0|0|0	0	GTPase Era, mitochondrial OS=Homo sapiens OX=9606 GN=ERAL1 PE=1 SV=2
ERC1	1|1|0	0|0|0	0	ELKS/Rab6-interacting/CAST family member 1 OS=Homo sapiens OX=9606 GN=ERC1 PE=1 SV=1
ERCC6L	1|0|0	0|2|0	0	DNA excision repair protein ERCC-6-like OS=Homo sapiens OX=9606 GN=ERCC6L PE=1 SV=1
ERLIN1	1|0|0	0|0|0	0	Erlin-1 OS=Homo sapiens OX=9606 GN=ERLIN1 PE=1 SV=2

prey Gene	Quant (SPC or Intensities)	User Controls (SPC or Intensities)	SP	Description of protein
ETFB	1|0|0	0|0|0	0	Electron transfer flavoprotein subunit beta OS=Homo sapiens OX=9606 GN=ETFB PE=1 SV=3
EXOC4	1|0|0	0|0|0	0	Exocyst complex component 4 OS=Homo sapiens OX=9606 GN=EXOC4 PE=1 SV=1
EXOSC9	1|1|1	2|0|0	0	Exosome complex component RRP45 OS=Homo sapiens OX=9606 GN=EXOSC9 PE=1 SV=3
FAF2	1|0|1	1|0|0	0	FAS-associated factor 2 OS=Homo sapiens OX=9606 GN=FAF2 PE=1 SV=2
FAM171A2	1|0|0	0|0|0	0	Protein FAM171A2 OS=Homo sapiens OX=9606 GN=FAM171A2 PE=1 SV=1
FAM83G	1|0|0	0|0|0	0	Protein FAM83G OS=Homo sapiens OX=9606 GN=FAM83G PE=1 SV=2
FAM98A	1|0|1	0|0|0	0	Protein FAM98A OS=Homo sapiens OX=9606 GN=FAM98A PE=1 SV=2
FANCD2	0|0|1	0|0|0	0	Fanconi anemia group D2 protein OS=Homo sapiens OX=9606 GN=FANCD2 PE=1 SV=2
FAR1	1|0|0	0|0|0	0	Fatty acyl-CoA reductase 1 OS=Homo sapiens OX=9606 GN=FAR1 PE=1 SV=1
FASN	12|8|11	31|27|7	0	Fatty acid synthase OS=Homo sapiens OX=9606 GN=FASN PE=1 SV=3
FASTKD2	0|1|0	0|0|0	0	FAST kinase domain-containing protein 2, mitochondrial OS=Homo sapiens OX=9606 GN=FASTKD2 PE=1 SV=1

prey Gene	Quant (SPC or Intensities)	User Controls (SPC or Intensities)	SP	Description of protein
FAU	0|1|0	5|1|2	0	40S ribosomal protein S30 OS=Homo sapiens OX=9606 GN=FAU PE=1 SV=1
FBRS	0|1|0	0|0|0	0	Probable fibrosin-1 OS=Homo sapiens OX=9606 GN=FBRS PE=1 SV=3
FBXL18	1|0|1	0|0|0	0	F-box/LRR-repeat protein 18 OS=Homo sapiens OX=9606 GN=FBXL18 PE=1 SV=2
FBXO22	1|0|0	0|0|0	0	F-box only protein 22 OS=Homo sapiens OX=9606 GN=FBXO22 PE=1 SV=1
FBXO28	1|0|0	0|0|0	0	F-box only protein 28 OS=Homo sapiens OX=9606 GN=FBXO28 PE=1 SV=1
FHL1	1|0|1	0|2|0	0	Four and a half LIM domains protein 1 OS=Homo sapiens OX=9606 GN=FHL1 PE=1 SV=4
FILIP1L	1|0|0	0|0|0	0	Filamin A-interacting protein 1-like OS=Homo sapiens OX=9606 GN=FILIP1L PE=1 SV=2
FIP1L1	1|0|1	0|1|0	0	Pre-mRNA 3'-end-processing factor FIP1 OS=Homo sapiens OX=9606 GN=FIP1L1 PE=1 SV=1
FKBP1A	0|0|1	0|0|0	0	Peptidyl-prolyl cis-trans isomerase FKBP1A OS=Homo sapiens OX=9606 GN=FKBP1A PE=1 SV=2
FLNA	62|46|40	147|103|63	0	Filamin-A OS=Homo sapiens OX=9606 GN=FLNA PE=1 SV=4
FN1	1|0|0	0|0|0	0	Fibronectin OS=Homo sapiens OX=9606 GN=FN1 PE=1 SV=5

prey Gene	Quant (SPC or Intensities)	User Controls (SPC or Intensities)	SP	Description of protein
FOSL2	1|1|0	1|1|0	0	Fos-related antigen 2 OS=Homo sapiens OX=9606 GN=FOSL2 PE=1 SV=1
FSIP2	0|1|0	0|0|0	0	Fibrous sheath-interacting protein 2 OS=Homo sapiens OX=9606 GN=FSIP2 PE=2 SV=4
FTSJ3	20|25|29	79|64|40	0	pre-rRNA 2'-O-ribose RNA methyltransferase FTSJ3 OS=Homo sapiens OX=9606 GN=FTSJ3 PE=1 SV=2
FXR1	0|0|1	0|0|0	0	Fragile X mental retardation syndrome-related protein 1 OS=Homo sapiens OX=9606 GN=FXR1 PE=1 SV=3
G3BP1	1|0|0	1|0|0	0	Ras GTPase-activating protein-binding protein 1 OS=Homo sapiens OX=9606 GN=G3BP1 PE=1 SV=1
G6PC	0|1|0	0|0|0	0	Glucose-6-phosphatase catalytic subunit 1 OS=Homo sapiens OX=9606 GN=G6PC1 PE=1 SV=2
G6PD	4|3|3	9|9|3	0	Glucose-6-phosphate 1-dehydrogenase OS=Homo sapiens OX=9606 GN=G6PD PE=1 SV=4
GAPDH	31|20|19	19|6|19	0	Glyceraldehyde-3-phosphate dehydrogenase OS=Homo sapiens OX=9606 GN=GAPDH PE=1 SV=3
GAPDHS	1|0|1	0|0|0	0	Glyceraldehyde-3-phosphate dehydrogenase, testis-specific OS=Homo sapiens OX=9606 GN=GAPDHS PE=1 SV=2
GATAD2A	1|0|0	0|0|0	0	Transcriptional repressor p66-alpha OS=Homo sapiens OX=9606 GN=GATAD2A PE=1 SV=1

prey Gene	Quant (SPC or Intensities)	User Controls (SPC or Intensities)	SP	Description of protein
GBE1	0|0|1	0|0|0	0	1,4-alpha-glucan-branching enzyme OS=Homo sapiens OX=9606 GN=GBE1 PE=1 SV=3
GC	1|0|0	0|0|1	0	Vitamin D-binding protein OS=Homo sapiens OX=9606 GN=GC PE=1 SV=2
GLI2	1|0|1	0|0|0	0	Zinc finger protein GLI2 OS=Homo sapiens OX=9606 GN=GLI2 PE=1 SV=4
GLO1	1|0|1	1|1|0	0	Lactoylglutathione lyase OS=Homo sapiens OX=9606 GN=GLO1 PE=1 SV=4
GLRX	1|0|1	0|0|0	0	Glutaredoxin-1 OS=Homo sapiens OX=9606 GN=GLRX PE=1 SV=2
GLRX3	0|0|1	0|0|0	0	Glutaredoxin-3 OS=Homo sapiens OX=9606 GN=GLRX3 PE=1 SV=2
GLUD1	1|0|1	0|0|0	0	Glutamate dehydrogenase 1, mitochondrial OS=Homo sapiens OX=9606 GN=GLUD1 PE=1 SV=2
GMPS	1|1|1	0|0|0	0	GMP synthase [glutamine-hydrolyzing] OS=Homo sapiens OX=9606 GN=GMPS PE=1 SV=1
GNL3	2|0|4	4|8|1	0	Guanine nucleotide-binding protein-like 3 OS=Homo sapiens OX=9606 GN=GNL3 PE=1 SV=2
GOT1	0|1|0	0|0|0	0	Aspartate aminotransferase, cytoplasmic OS=Homo sapiens OX=9606 GN=GOT1 PE=1 SV=3
GPHN	1|0|0	0|0|0	0	Gephyrin OS=Homo sapiens OX=9606 GN=GPHN PE=1 SV=1
GRB2	1|0|0	0|0|0	0	Growth factor receptor-bound protein 2 OS=Homo sapiens OX=9606 GN=GRB2 PE=1 SV=1

prey Gene	Quant (SPC or Intensities)	User Controls (SPC or Intensities)	SP	Description of protein
GRIA1	1|0|0	0|0|0	0	Glutamate receptor 1 OS=Homo sapiens OX=9606 GN=GRIA1 PE=1 SV=2
GSE1	1|0|0	0|0|0	0	Genetic suppressor element 1 OS=Homo sapiens OX=9606 GN=GSE1 PE=1 SV=3
GSN	0|1|1	0|0|0	0	Gelsolin OS=Homo sapiens OX=9606 GN=GSN PE=1 SV=1
GSPT1	0|3|2	17|9|4	0	Eukaryotic peptide chain release factor GTP-binding subunit ERF3A OS=Homo sapiens OX=9606 GN=GSPT1 PE=1 SV=1
GSPT2	2|0|2	15|6|2	0	Eukaryotic peptide chain release factor GTP-binding subunit ERF3B OS=Homo sapiens OX=9606 GN=GSPT2 PE=1 SV=2
GSS	1|0|0	0|0|0	0	Glutathione synthetase OS=Homo sapiens OX=9606 GN=GSS PE=1 SV=1
GSTM3	1|1|0	0|0|0	0	Glutathione S-transferase Mu 3 OS=Homo sapiens OX=9606 GN=GSTM3 PE=1 SV=3
GSTM4	0|0|1	0|0|0	0	Glutathione S-transferase Mu 4 OS=Homo sapiens OX=9606 GN=GSTM4 PE=1 SV=3
GSTO1	0|0|1	0|0|0	0	Glutathione S-transferase omega-1 OS=Homo sapiens OX=9606 GN=GSTO1 PE=1 SV=2
GTF2A1	1|0|0	2|3|1	0	Transcription initiation factor IIA subunit 1 OS=Homo sapiens OX=9606 GN=GTF2A1 PE=1 SV=1
GTSE1	1|0|0	0|0|0	0	G2 and S phase-expressed protein 1 OS=Homo sapiens OX=9606 GN=GTSE1 PE=1 SV=3

prey Gene	Quant (SPC or Intensities)	User Controls (SPC or Intensities)	SP	Description of protein
H1F0	1|0|0	0|0|0	0	Histone H1.0 OS=Homo sapiens OX=9606 GN=H1-0 PE=1 SV=3
H2AFX	6|7|5	11|6|17	0	Histone H2AX OS=Homo sapiens OX=9606 GN=H2AX PE=1 SV=2
H2AFY	1|1|1	1|1|1	0	Core histone macro-H2A.1 OS=Homo sapiens OX=9606 GN=MACROH2A1 PE=1 SV=4
H2AFZ	6|6|5	14|5|18	0	Histone H2A.Z OS=Homo sapiens OX=9606 GN=H2AZ1 PE=1 SV=2
HBA2; HBA1	4|6|6	3|4|92	0	Hemoglobin subunit alpha OS=Homo sapiens OX=9606 GN=HBA1 PE=1 SV=2
HBB	5|8|9	13|10|168	0	Hemoglobin subunit beta OS=Homo sapiens OX=9606 GN=HBB PE=1 SV=2
HCFC1	3|0|0	5|3|0	0	Host cell factor 1 OS=Homo sapiens OX=9606 GN=HCFC1 PE=1 SV=2
HEBP1	1|0|0	0|0|0	0	Heme-binding protein 1 OS=Homo sapiens OX=9606 GN=HEBP1 PE=1 SV=1
HELLS	2|0|2	17|17|7	0	Lymphoid-specific helicase OS=Homo sapiens OX=9606 GN=HELLS PE=1 SV=1
HEPH	1|0|0	0|0|0	0	Hephaestin OS=Homo sapiens OX=9606 GN=HEPH PE=1 SV=3
HIST1H1D	9|5|4	8|6|5	0	Histone H1.3 OS=Homo sapiens OX=9606 GN=H1-3 PE=1 SV=2
HIST1H2AE; HIST1H2AB	6|7|6	12|6|36	0	Histone H2A type 1-B/E OS=Homo sapiens OX=9606 GN=H2AC4 PE=1 SV=2
HIST1H2BJ	20|14|26	30|14|63	0	Histone H2B type 1-J OS=Homo sapiens OX=9606 GN=H2BC11 PE=1 SV=3

prey Gene	Quant (SPC or Intensities)	User Controls (SPC or Intensities)	SP	Description of protein
HIST1H2BK	22|17|30	33|17|71	0	Histone H2B type 1-K OS=Homo sapiens OX=9606 GN=H2BC12 PE=1 SV=3
HIST1H3G; HIST1H3C;HI...	4|4|7	10|8|2	0	Histone H3.1 OS=Homo sapiens OX=9606 GN=H3C1 PE=1 SV=2
HIST1H4L;HIST1H4K;HI...	102|61|73	70|72|133	0	Histone H4 OS=Homo sapiens OX=9606 GN=H4C1 PE=1 SV=2
HLTF	1|0|1	0|0|0	0	Helicase-like transcription factor OS=Homo sapiens OX=9606 GN=HLTF PE=1 SV=2
HM13	1|0|0	0|0|0	0	Minor histocompatibility antigen H13 OS=Homo sapiens OX=9606 GN=HM13 PE=1 SV=1
HMGA1	1|1|1	2|2|0	0	High mobility group protein HMG-I/HMG-Y OS=Homo sapiens OX=9606 GN=HMGA1 PE=1 SV=3
HMGCS1	0|0|1	0|0|0	0	Hydroxymethylglutaryl$-CoA synthase, cytoplasmic OS=Homo sapiens OX=9606 GN=HMGCS1 PE=1 SV=2
HNRNPA0	4|0|0	12|11|2	0	Heterogeneous nuclear ribonucleoprotein A0 OS=Homo sapiens OX=9606 GN=HNRNPA0 PE=1 SV=1
HNRNPA1	5|4|4	20|25|21	0	Heterogeneous nuclear ribonucleoprotein A1 OS=Homo sapiens OX=9606 GN=HNRNPA1 PE=1 SV=5
HNRNPA2B1	4|2|3	16|15|11	0	Heterogeneous nuclear ribonucleoproteins A2/B1 OS=Homo sapiens OX=9606 GN=HNRNPA2B1 PE=1 SV=2
HNRNPA3	3|2|3	12|14|2	0	Heterogeneous nuclear ribonucleoprotein A3 OS=Homo sapiens OX=9606 GN=HNRNPA3 PE=1 SV=2

prey Gene	Quant (SPC or Intensities)	User Controls (SPC or Intensities)	SP	Description of protein
HNRNPC	4|2|2	1|1|10	0	Heterogeneous nuclear ribonucleoproteins C1/C2 OS=Homo sapiens OX=9606 GN=HNRNPC PE=1 SV=4
HNRNPD	3|1|1	2|1|4	0	Heterogeneous nuclear ribonucleoprotein D0 OS=Homo sapiens OX=9606 GN=HNRNPD PE=1 SV=1
HNRNPF	2|3|4	10|5|10	0	Heterogeneous nuclear ribonucleoprotein F OS=Homo sapiens OX=9606 GN=HNRNPF PE=1 SV=3
HNRNPH1	5|3|3	4|2|6	0	Heterogeneous nuclear ribonucleoprotein H OS=Homo sapiens OX=9606 GN=HNRNPH1 PE=1 SV=4
HNRNPH3	1|2|2	2|2|4	0	Heterogeneous nuclear ribonucleoprotein H3 OS=Homo sapiens OX=9606 GN=HNRNPH3 PE=1 SV=2
HNRNPK	11|5|6	20|19|28	0	Heterogeneous nuclear ribonucleoprotein K OS=Homo sapiens OX=9606 GN=HNRNPK PE=1 SV=1
HNRNPL	1|0|1	0|0|1	0	Heterogeneous nuclear ribonucleoprotein L OS=Homo sapiens OX=9606 GN=HNRNPL PE=1 SV=2
HNRNPR	0|1|1	1|0|1	0	Heterogeneous nuclear ribonucleoprotein R OS=Homo sapiens OX=9606 GN=HNRNPR PE=1 SV=1
HNRNPU	9|5|7	10|9|7	0	Heterogeneous nuclear ribonucleoprotein U OS=Homo sapiens OX=9606 GN=HNRNPU PE=1 SV=6

prey Gene	Quant (SPC or Intensities)	User Controls (SPC or Intensities)	SP	Description of protein
HNRNPUL1	1|1|1	0|2|0	0	Heterogeneous nuclear ribonucleoprotein U-like protein 1 OS=Homo sapiens OX=9606 GN=HNRNPUL1 PE=1 SV=2
HPRT1	0|0|1	0|0|0	0	Hypoxanthine-guanine phosphoribosyltransferase OS=Homo sapiens OX=9606 GN=HPRT1 PE=1 SV=2
HSDL2	1|0|0	0|0|0	0	Hydroxysteroid dehydrogenase-like protein 2 OS=Homo sapiens OX=9606 GN=HSDL2 PE=1 SV=1
HSP90AA1	15|15|13	18|6|0	0	Heat shock protein HSP 90-alpha OS=Homo sapiens OX=9606 GN=HSP90AA1 PE=1 SV=5
HSP90AB1	28|23|23	28|14|8	0	Heat shock protein HSP 90-beta OS=Homo sapiens OX=9606 GN=HSP90AB1 PE=1 SV=4
HSPA1B	14|11|12	19|12|5	0	Heat shock 70 kDa protein 1B OS=Homo sapiens OX=9606 GN=HSPA1B PE=1 SV=1
HSPA5	23|18|12	32|15|22	0	Endoplasmic reticulum chaperone BiP OS=Homo sapiens OX=9606 GN=HSPA5 PE=1 SV=2
HSPA8	37|28|23	48|32|19	0	Heat shock cognate 71 kDa protein OS=Homo sapiens OX=9606 GN=HSPA8 PE=1 SV=1
HSPB1	8|7|7	9|4|4	0	Heat shock protein beta-1 OS=Homo sapiens OX=9606 GN=HSPB1 PE=1 SV=2
HSPD1	22|16|14	9|5|24	0	60 kDa heat shock protein, mitochondrial OS=Homo sapiens OX=9606 GN=HSPD1 PE=1 SV=2
HSPE1	3|1|1	1|2|9	0	10 kDa heat shock protein, mitochondrial OS=Homo sapiens OX=9606 GN=HSPE1 PE=1 SV=2

prey Gene	Quant (SPC or Intensities)	User Controls (SPC or Intensities)	SP	Description of protein
HSPH1	4|1|3	3|3|2	0	Heat shock protein 105 kDa OS=Homo sapiens OX=9606 GN=HSPH1 PE=1 SV=1
HUWE1	1|1|1	1|0|0	0	E3 ubiquitin-protein ligase HUWE1 OS=Homo sapiens OX=9606 GN=HUWE1 PE=1 SV=3
HYOU1	0|1|1	1|0|0	0	Hypoxia up-regulated protein 1 OS=Homo sapiens OX=9606 GN=HYOU1 PE=1 SV=1
IARS2	1|0|0	0|0|0	0	Isoleucine--tRNA ligase, mitochondrial OS=Homo sapiens OX=9606 GN=IARS2 PE=1 SV=2
IDE	0|0|1	0|0|0	0	Insulin-degrading enzyme OS=Homo sapiens OX=9606 GN=IDE PE=1 SV=4
IDH3A	1|1|0	0|0|0	0	Isocitrate dehydrogenase [NAD] subunit alpha, mitochondrial OS=Homo sapiens OX=9606 GN=IDH3A PE=1 SV=1
IFI16	49|42|46	239|166|143	0	Gamma-interferon-inducible protein 16 OS=Homo sapiens OX=9606 GN=IFI16 PE=1 SV=3
IGBP1	4|3|3	10|5|1	0	Immunoglobulin-binding protein 1 OS=Homo sapiens OX=9606 GN=IGBP1 PE=1 SV=1
IGF2BP2	1|0|0	0|0|0	0	Insulin-like growth factor 2 mRNA-binding protein 2 OS=Homo sapiens OX=9606 GN=IGF2BP2 PE=1 SV=2
IL36G	0|1|1	0|0|0	0	Interleukin-36 gamma OS=Homo sapiens OX=9606 GN=IL36G PE=1 SV=1
ILDR2	1|0|1	0|0|0	0	Immunoglobulin-like domain-containing receptor 2 OS=Homo sapiens OX=9606 GN=ILDR2 PE=2 SV=1

prey Gene	Quant (SPC or Intensities)	User Controls (SPC or Intensities)	SP	Description of protein
ILKAP	1|0|1	2|1|2	0	Integrin-linked kinase-associated serine/threonine phosphatase 2C OS=Homo sapiens OX=9606 GN=ILKAP PE=1 SV=1
IMMT	1|0|0	0|0|0	0	MICOS complex subunit MIC60 OS=Homo sapiens OX=9606 GN=IMMT PE=1 SV=1
IMPA2	0|0|1	0|0|0	0	Inositol monophosphatase 2 OS=Homo sapiens OX=9606 GN=IMPA2 PE=1 SV=1
INCENP	1|0|1	1|1|0	0	Inner centromere protein OS=Homo sapiens OX=9606 GN=INCENP PE=1 SV=3
IPO7	3|0|0	4|3|0	0	Importin-7 OS=Homo sapiens OX=9606 GN=IPO7 PE=1 SV=1
IPO8	1|0|0	0|0|0	0	Importin-8 OS=Homo sapiens OX=9606 GN=IPO8 PE=1 SV=2
IQCA1L	1|0|0	0|0|0	0	IQ and AAA domain-containing protein 1-like OS=Homo sapiens OX=9606 GN=IQCA1L PE=3 SV=3
IRS1	0|0|1	0|0|0	0	Insulin receptor substrate 1 OS=Homo sapiens OX=9606 GN=IRS1 PE=1 SV=1
ITGAV	1|0|0	0|0|0	0	Integrin alpha-V OS=Homo sapiens OX=9606 GN=ITGAV PE=1 SV=2
JPT2	4|2|3	5|6|3	0	Jupiter microtubule associated homolog 2 OS=Homo sapiens OX=9606 GN=JPT2 PE=1 SV=1
JUN	1|1|0	0|0|0	0	Transcription factor AP-1 OS=Homo sapiens OX=9606 GN=JUN PE=1 SV=2

prey Gene	Quant (SPC or Intensities)	User Controls (SPC or Intensities)	SP	Description of protein
KANK1	1|0|0	0|0|0	0	KN motif and ankyrin repeat domain-containing protein 1 OS=Homo sapiens OX=9606 GN=KANK1 PE=1 SV=3
KANK2	0|1|1	1|1|0	0	KN motif and ankyrin repeat domain-containing protein 2 OS=Homo sapiens OX=9606 GN=KANK2 PE=1 SV=1
KHSRP	2|1|1	4|2|0	0	Far upstream element-binding protein 2 OS=Homo sapiens OX=9606 GN=KHSRP PE=1 SV=4
KIAA0895	0|0|1	0|0|0	0	Uncharacterized protein KIAA0895 OS=Homo sapiens OX=9606 GN=KIAA0895 PE=2 SV=4
KIAA1671	1|0|0	0|0|0	0	Uncharacterized protein KIAA1671 OS=Homo sapiens OX=9606 GN=KIAA1671 PE=1 SV=2
KIF22	1|0|0	1|1|0	0	Kinesin-like protein KIF22 OS=Homo sapiens OX=9606 GN=KIF22 PE=1 SV=5
KIF23	0|1|0	2|1|1	0	Kinesin-like protein KIF23 OS=Homo sapiens OX=9606 GN=KIF23 PE=1 SV=3
KIF2A	1|0|0	0|0|0	0	Kinesin-like protein KIF2A OS=Homo sapiens OX=9606 GN=KIF2A PE=1 SV=3
KLC4	1|0|0	1|0|0	0	Kinesin light chain 4 OS=Homo sapiens OX=9606 GN=KLC4 PE=1 SV=3
KLK10	0|1|1	0|0|0	0	Kallikrein-10 OS=Homo sapiens OX=9606 GN=KLK10 PE=1 SV=3
KLK7	0|0|1	0|0|0	0	Kallikrein-7 OS=Homo sapiens OX=9606 GN=KLK7 PE=1 SV=1
KLK8	0|0|1	0|0|0	0	Kallikrein-8 OS=Homo sapiens OX=9606 GN=KLK8 PE=1 SV=1

prey Gene	Quant (SPC or Intensities)	User Controls (SPC or Intensities)	SP	Description of protein
KPNA3	1|0|0	2|0|2	0	Importin subunit alpha-4 OS=Homo sapiens OX=9606 GN=KPNA3 PE=1 SV=2
KPNA6	1|0|0	1|0|0	0	Importin subunit alpha-7 OS=Homo sapiens OX=9606 GN=KPNA6 PE=1 SV=1
KPNB1	0|0|1	0|0|0	0	Importin subunit beta-1 OS=Homo sapiens OX=9606 GN=KPNB1 PE=1 SV=2
KPRP	8|12|13	7|13|5	0	Keratinocyte proline-rich protein OS=Homo sapiens OX=9606 GN=KPRP PE=1 SV=1
KRR1	1|0|1	0|0|0	0	KRR1 small subunit processome component homolog OS=Homo sapiens OX=9606 GN=KRR1 PE=1 SV=4
KRT1	204|217|338	236|222|401	0	Keratin, type II cytoskeletal 1 OS=Homo sapiens OX=9606 GN=KRT1 PE=1 SV=6
KRT10	131|122|219	135|149|209	0	Keratin, type I cytoskeletal 10 OS=Homo sapiens OX=9606 GN=KRT10 PE=1 SV=6
KRT2	130|116|212	120|184|181	0	Keratin, type II cytoskeletal 2 epidermal OS=Homo sapiens OX=9606 GN=KRT2 PE=1 SV=2
KRT33B	1|0|0	0|0|0	0	Keratin, type I cuticular Ha3-II OS=Homo sapiens OX=9606 GN=KRT33B PE=1 SV=3
KRT5	56|73|108	59|75|78	0	Keratin, type II cytoskeletal 5 OS=Homo sapiens OX=9606 GN=KRT5 PE=1 SV=3
KRT6A	54|61|109	76|71|72	0	Keratin, type II cytoskeletal 6A OS=Homo sapiens OX=9606 GN=KRT6A PE=1 SV=3

prey Gene	Quant (SPC or Intensities)	User Controls (SPC or Intensities)	SP	Description of protein
KRT6B	60|68|120	82|74|76	0	Keratin, type II cytoskeletal 6B OS=Homo sapiens OX=9606 GN=KRT6B PE=1 SV=5
KRT8	23|23|23	0|25|21	0	Keratin, type II cytoskeletal 8 OS=Homo sapiens OX=9606 GN=KRT8 PE=1 SV=7
KRT82	1|0|0	0|0|0	0	Keratin, type II cuticular Hb2 OS=Homo sapiens OX=9606 GN=KRT82 PE=1 SV=3
KRT9	207|214|253	100|205|217	0	Keratin, type I cytoskeletal 9 OS=Homo sapiens OX=9606 GN=KRT9 PE=1 SV=3
KTN1	1|0|0	0|0|0	0	Kinectin OS=Homo sapiens OX=9606 GN=KTN1 PE=1 SV=1
LAP3	1|0|0	0|0|0	0	Cytosol aminopeptidase OS=Homo sapiens OX=9606 GN=LAP3 PE=1 SV=3
LAS1L	1|1|0	1|0|0	0	Ribosomal biogenesis protein LAS1L OS=Homo sapiens OX=9606 GN=LAS1L PE=1 SV=2
LASP1	3|4|3	5|3|1	0	LIM and SH3 domain protein 1 OS=Homo sapiens OX=9606 GN=LASP1 PE=1 SV=2
LCN2	0|1|1	0|0|0	0	Neutrophil gelatinase-associated lipocalin OS=Homo sapiens OX=9606 GN=LCN2 PE=1 SV=2
LDB1	1|0|1	0|0|0	0	LIM domain-binding protein 1 OS=Homo sapiens OX=9606 GN=LDB1 PE=1 SV=2
LEKR1	0|1|0	0|0|0	0	Leucine-, glutamate- and lysine-rich protein 1 OS=Homo sapiens OX=9606 GN=LEKR1 PE=2 SV=2

prey Gene	Quant (SPC or Intensities)	User Controls (SPC or Intensities)	SP	Description of protein
LETMD1	1|1|1	0|0|0	0	LETM1 domain-containing protein 1 OS=Homo sapiens OX=9606 GN=LETMD1 PE=1 SV=1
LGALSL	1|0|0	0|0|0	0	Galectin-related protein OS=Homo sapiens OX=9606 GN=LGALSL PE=1 SV=2
LIMCH1	1|0|0	5|2|0	0	LIM and calponin homology domains-containing protein 1 OS=Homo sapiens OX=9606 GN=LIMCH1 PE=1 SV=4
LIMS1	1|0|0	0|0|0	0	LIM and senescent cell antigen-like-containing domain protein 1 OS=Homo sapiens OX=9606 GN=LIMS1 PE=1 SV=4
LLGL1	0|0|1	0|0|0	0	Lethal(2) giant larvae protein homolog 1 OS=Homo sapiens OX=9606 GN=LLGL1 PE=1 SV=3
LLPH	1|0|1	0|0|0	0	Protein LLP homolog OS=Homo sapiens OX=9606 GN=LLPH PE=1 SV=1
LRRC40	1|0|1	0|0|0	0	Leucine-rich repeat-containing protein 40 OS=Homo sapiens OX=9606 GN=LRRC40 PE=1 SV=1
LRRC59	0|1|0	0|0|0	0	Leucine-rich repeat-containing protein 59 OS=Homo sapiens OX=9606 GN=LRRC59 PE=1 SV=1
LSG1	1|0|0	0|0|0	0	Large subunit GTPase 1 homolog OS=Homo sapiens OX=9606 GN=LSG1 PE=1 SV=2
LSM12	1|0|0	1|0|0	0	Protein LSM12 homolog OS=Homo sapiens OX=9606 GN=LSM12 PE=1 SV=2

prey Gene	Quant (SPC or Intensities)	User Controls (SPC or Intensities)	SP	Description of protein
LTA4H	1|0|0	0|0|0	0	Leukotriene A-4 hydrolase OS=Homo sapiens OX=9606 GN=LTA4H PE=1 SV=2
LUC7L	1|0|0	0|0|0	0	Putative RNA-binding protein Luc7-like 1 OS=Homo sapiens OX=9606 GN=LUC7L PE=1 SV=1
LY6G6C	0|1|0	0|0|0	0	Lymphocyte antigen 6 complex locus protein G6c OS=Homo sapiens OX=9606 GN=LY6G6C PE=1 SV=1
LYPD3	0|1|1	0|0|0	0	Ly6/PLAUR domain-containing protein 3 OS=Homo sapiens OX=9606 GN=LYPD3 PE=1 SV=2
MAGED2	7|7|8	19|11|9	0	Melanoma-associated antigen D2 OS=Homo sapiens OX=9606 GN=MAGED2 PE=1 SV=2
MAMLD1	0|1|1	0|0|0	0	Mastermind-like domain-containing protein 1 OS=Homo sapiens OX=9606 GN=MAMLD1 PE=1 SV=2
MANF	1|0|1	0|0|0	0	Mesencephalic astrocyte-derived neurotrophic factor OS=Homo sapiens OX=9606 GN=MANF PE=1 SV=3
MAP1B	2|1|1	15|14|2	0	Microtubule-associated protein 1B OS=Homo sapiens OX=9606 GN=MAP1B PE=1 SV=2
MAP2K3	1|0|0	0|0|0	0	Dual specificity mitogen-activated protein kinase kinase 3 OS=Homo sapiens OX=9606 GN=MAP2K3 PE=1 SV=2
MAP4	10|11|9	64|53|54	0	Microtubule-associated protein 4 OS=Homo sapiens OX=9606 GN=MAP4 PE=1 SV=3

prey Gene	Quant (SPC or Intensities)	User Controls (SPC or Intensities)	SP	Description of protein
MAP7D1	5|3|5	8|9|3	0	MAP7 domain-containing protein 1 OS=Homo sapiens OX=9606 GN=MAP7D1 PE=1 SV=1
MAP7D3	1|1|0	0|0|0	0	MAP7 domain-containing protein 3 OS=Homo sapiens OX=9606 GN=MAP7D3 PE=1 SV=2
MARCKSL1	1|0|0	0|0|0	0	MARCKS-related protein OS=Homo sapiens OX=9606 GN=MARCKSL1 PE=1 SV=2
MARK1	1|0|0	0|0|0	0	Serine/threonine-protein kinase MARK1 OS=Homo sapiens OX=9606 GN=MARK1 PE=1 SV=2
MAST4	0|1|0	0|0|0	0	Microtubule-associated serine/threonine-protein kinase 4 OS=Homo sapiens OX=9606 GN=MAST4 PE=1 SV=4
MAT2A	1|0|1	0|0|0	0	S-adenosylmethionine synthase isoform type-2 OS=Homo sapiens OX=9606 GN=MAT2A PE=1 SV=1
MBD2	1|0|0	1|0|0	0	Methyl-CpG-binding domain protein 2 OS=Homo sapiens OX=9606 GN=MBD2 PE=1 SV=1
MBD6	1|0|0	0|0|0	0	Methyl-CpG-binding domain protein 6 OS=Homo sapiens OX=9606 GN=MBD6 PE=1 SV=2
MCCC1	35|32|33	58|42|10	0	Methylcrotonoyl-CoA carboxylase subunit alpha, mitochondrial OS=Homo sapiens OX=9606 GN=MCCC1 PE=1 SV=3
MCM3	1|0|1	0|0|0	0	DNA replication licensing factor MCM3 OS=Homo sapiens OX=9606 GN=MCM3 PE=1 SV=3
MCM4	1|0|0	0|0|0	0	DNA replication licensing factor MCM4 OS=Homo sapiens OX=9606 GN=MCM4 PE=1 SV=5

prey Gene	Quant (SPC or Intensities)	User Controls (SPC or Intensities)	SP	Description of protein
MDC1	1|0|0	1|4|0	0	Mediator of DNA damage checkpoint protein 1 OS=Homo sapiens OX=9606 GN=MDC1 PE=1 SV=3
MDN1	0|0|1	0|0|0	0	Midasin OS=Homo sapiens OX=9606 GN=MDN1 PE=1 SV=2
ME2	1|1|1	0|0|0	0	NAD-dependent malic enzyme, mitochondrial OS=Homo sapiens OX=9606 GN=ME2 PE=1 SV=1
MEI1	0|1|0	0|0|0	0	Meiosis inhibitor protein 1 OS=Homo sapiens OX=9606 GN=MEI1 PE=2 SV=2
MEMO1	0|0|1	0|0|0	0	Protein MEMO1 OS=Homo sapiens OX=9606 GN=MEMO1 PE=1 SV=1
METTL13	0|0|1	0|0|0	0	eEF1A lysine and N-terminal methyltransferase OS=Homo sapiens OX=9606 GN=EEF1AKNMT PE=1 SV=1
MICAL3	0|0|1	0|0|0	0	[F-actin]-monooxygenase MICAL3 OS=Homo sapiens OX=9606 GN=MICAL3 PE=1 SV=2
MICALL2	1|0|1	0|0|0	0	MICAL-like protein 2 OS=Homo sapiens OX=9606 GN=MICALL2 PE=1 SV=1
MKI67	4|2|2	9|9|1	0	Proliferation marker protein Ki-67 OS=Homo sapiens OX=9606 GN=MKI67 PE=1 SV=2
MME	0|1|0	0|0|0	0	Neprilysin OS=Homo sapiens OX=9606 GN=MME PE=1 SV=2
MOB1B	1|0|1	0|1|0	0	MOB kinase activator 1B OS=Homo sapiens OX=9606 GN=MOB1B PE=1 SV=3

prey Gene	Quant (SPC or Intensities)	User Controls (SPC or Intensities)	SP	Description of protein
MPC2	0|0|1	0|0|0	0	Mitochondrial pyruvate carrier 2 OS=Homo sapiens OX=9606 GN=MPC2 PE=1 SV=1
MPP6	0|0|1	0|0|0	0	Protein PALS2 OS=Homo sapiens OX=9606 GN=PALS2 PE=1 SV=2
MPRIP	1|0|0	0|0|1	0	Myosin phosphatase Rho-interacting protein OS=Homo sapiens OX=9606 GN=MPRIP PE=1 SV=3
MPZL1	1|0|0	0|0|0	0	Myelin protein zero-like protein 1 OS=Homo sapiens OX=9606 GN=MPZL1 PE=1 SV=1
MRE11	2|2|1	9|5|2	0	Double-strand break repair protein MRE11 OS=Homo sapiens OX=9606 GN=MRE11 PE=1 SV=3
MRPL21	1|0|0	0|0|0	0	39S ribosomal protein L21, mitochondrial OS=Homo sapiens OX=9606 GN=MRPL21 PE=1 SV=2
MRPL23	0|0|1	0|0|0	0	39S ribosomal protein L23, mitochondrial OS=Homo sapiens OX=9606 GN=MRPL23 PE=1 SV=1
MRPL35	1|1|1	0|1|0	0	39S ribosomal protein L35, mitochondrial OS=Homo sapiens OX=9606 GN=MRPL35 PE=1 SV=3
MRPL37	1|0|1	0|0|0	0	39S ribosomal protein L37, mitochondrial OS=Homo sapiens OX=9606 GN=MRPL37 PE=1 SV=2
MRPL41	1|0|0	0|0|0	0	39S ribosomal protein L41, mitochondrial OS=Homo sapiens OX=9606 GN=MRPL41 PE=1 SV=1
MRPL42	0|0|1	0|0|0	0	39S ribosomal protein L42, mitochondrial OS=Homo sapiens OX=9606 GN=MRPL42 PE=1 SV=1
MRPS31	0|1|0	0|0|0	0	28S ribosomal protein S31, mitochondrial OS=Homo sapiens OX=9606 GN=MRPS31 PE=1 SV=3

prey Gene	Quant (SPC or Intensities)	User Controls (SPC or Intensities)	SP	Description of protein
MST1R	0|0|1	0|0|0	0	Macrophage-stimulating protein receptor OS=Homo sapiens OX=9606 GN=MST1R PE=1 SV=3
MT-CO2	0|0|1	0|0|0	0	Cytochrome c oxidase subunit 2 OS=Homo sapiens OX=9606 GN=MT-CO2 PE=1 SV=1
MTA2	3|2|2	5|4|8	0	Metastasis-associated protein MTA2 OS=Homo sapiens OX=9606 GN=MTA2 PE=1 SV=1
MTDH	1|0|0	0|1|0	0	Protein LYRIC OS=Homo sapiens OX=9606 GN=MTDH PE=1 SV=2
MTHFD2	1|0|0	0|0|0	0	Bifunctional methylenetetrahydrofolate dehydrogenase/cyclohydrolase, mitochondrial OS=Homo sapiens OX=9606 GN=MTHFD2 PE=1 SV=2
MTPN	1|1|1	0|0|0	0	Myotrophin OS=Homo sapiens OX=9606 GN=MTPN PE=1 SV=2
MTRR	1|0|0	1|1|0	0	Methionine synthase reductase OS=Homo sapiens OX=9606 GN=MTRR PE=1 SV=4
MTUS1	0|0|1	0|0|0	0	Microtubule-associated tumor suppressor 1 OS=Homo sapiens OX=9606 GN=MTUS1 PE=1 SV=2
MUC19	0|1|0	0|0|0	0	Mucin-19 OS=Homo sapiens OX=9606 GN=MUC19 PE=1 SV=3
MUCL1	1|0|1	0|0|0	0	Mucin-like protein 1 OS=Homo sapiens OX=9606 GN=MUCL1 PE=1 SV=1
MVD	1|0|0	0|0|0	0	Diphosphomevalonate decarboxylase OS=Homo sapiens OX=9606 GN=MVD PE=1 SV=1
MVP	1|0|0	0|0|0	0	Major vault protein OS=Homo sapiens OX=9606 GN=MVP PE=1 SV=4

prey Gene	Quant (SPC or Intensities)	User Controls (SPC or Intensities)	SP	Description of protein
MYBBP1A	10|4|7	12|9|13	0	Myb-binding protein 1A OS=Homo sapiens OX=9606 GN=MYBBP1A PE=1 SV=2
MYL12B	1|0|1	0|0|0	0	Myosin regulatory light chain 12B OS=Homo sapiens OX=9606 GN=MYL12B PE=1 SV=2
NAA50	1|0|0	0|0|0	0	N-alpha-acetyltransferase 50 OS=Homo sapiens OX=9606 GN=NAA50 PE=1 SV=1
NAB1	0|1|0	1|1|1	0	NGFI-A-binding protein 1 OS=Homo sapiens OX=9606 GN=NAB1 PE=1 SV=2
NAMPT	1|0|0	0|0|0	0	Nicotinamide phosphoribosyltransferase OS=Homo sapiens OX=9606 GN=NAMPT PE=1 SV=1
NAP1L1	1|0|1	0|0|0	0	Nucleosome assembly protein 1-like 1 OS=Homo sapiens OX=9606 GN=NAP1L1 PE=1 SV=1
NARS	1|0|0	0|0|0	0	Asparagine--tRNA ligase, cytoplasmic OS=Homo sapiens OX=9606 GN=NARS1 PE=1 SV=1
NAT10	0|0|1	1|1|0	0	RNA cytidine acetyltransferase OS=Homo sapiens OX=9606 GN=NAT10 PE=1 SV=2
NCAPD2	1|1|1	1|0|0	0	Condensin complex subunit 1 OS=Homo sapiens OX=9606 GN=NCAPD2 PE=1 SV=3
NCAPG	1|1|1	1|1|0	0	Condensin complex subunit 3 OS=Homo sapiens OX=9606 GN=NCAPG PE=1 SV=1
NCBP1	0|0|1	0|0|0	0	Nuclear cap-binding protein subunit 1 OS=Homo sapiens OX=9606 GN=NCBP1 PE=1 SV=1

prey Gene	Quant (SPC or Intensities)	User Controls (SPC or Intensities)	SP	Description of protein
NCBP2-AS2	2|4|4	8|3|2	0	Protein NCBP2AS2 OS=Homo sapiens OX=9606 GN=NCBP2AS2 PE=1 SV=1
NCLN	1|1|1	0|0|0	0	Nicalin OS=Homo sapiens OX=9606 GN=NCLN PE=1 SV=2
NDRG3	1|0|1	0|0|0	0	Protein NDRG3 OS=Homo sapiens OX=9606 GN=NDRG3 PE=1 SV=2
NDUFA4	1|1|0	1|0|0	0	Cytochrome c oxidase subunit NDUFA4 OS=Homo sapiens OX=9606 GN=NDUFA4 PE=1 SV=1
NDUFA9	0|1|1	0|1|0	0	NADH dehydrogenase [ubiquinone] 1 alpha subcomplex subunit 9, mitochondrial OS=Homo sapiens OX=9606 GN=NDUFA9 PE=1 SV=2
NDUFV2	1|0|0	0|0|0	0	NADH dehydrogenase [ubiquinone] flavoprotein 2, mitochondrial OS=Homo sapiens OX=9606 GN=NDUFV2 PE=1 SV=2
NEB	0|1|0	0|0|0	0	Nebulin OS=Homo sapiens OX=9606 GN=NEB PE=1 SV=5
NEK7	1|0|0	0|0|0	0	Serine/threonine-protein kinase Nek7 OS=Homo sapiens OX=9606 GN=NEK7 PE=1 SV=1
NFATC2	0|1|0	0|0|0	0	Nuclear factor of activated T-cells, cytoplasmic 2 OS=Homo sapiens OX=9606 GN=NFATC2 PE=1 SV=2
NFIA	1|0|1	0|0|0	0	Nuclear factor 1 A-type OS=Homo sapiens OX=9606 GN=NFIA PE=1 SV=2
NIFK	1|0|0	0|0|0	0	MKI67 FHA domain-interacting nucleolar phosphoprotein OS=Homo sapiens OX=9606 GN=NIFK PE=1 SV=1

prey Gene	Quant (SPC or Intensities)	User Controls (SPC or Intensities)	SP	Description of protein
NLN	1|0|0	0|0|0	0	Neurolysin, mitochondrial OS=Homo sapiens OX=9606 GN=NLN PE=1 SV=1
NME4	0|0|1	0|0|0	0	Nucleoside diphosphate kinase, mitochondrial OS=Homo sapiens OX=9606 GN=NME4 PE=1 SV=1
NNMT	0|1|0	0|1|0	0	Nicotinamide N-methyltransferase OS=Homo sapiens OX=9606 GN=NNMT PE=1 SV=1
NNT	1|1|0	0|0|0	0	NAD(P) transhydrogenase, mitochondrial OS=Homo sapiens OX=9606 GN=NNT PE=1 SV=3
NOC2L	1|1|1	0|0|0	0	Nucleolar complex protein 2 homolog OS=Homo sapiens OX=9606 GN=NOC2L PE=1 SV=4
NOC3L	6|2|4	10|10|9	0	Nucleolar complex protein 3 homolog OS=Homo sapiens OX=9606 GN=NOC3L PE=1 SV=1
NOL7	0|0|1	0|0|0	0	Nucleolar protein 7 OS=Homo sapiens OX=9606 GN=NOL7 PE=1 SV=2
NONO	2|2|2	2|3|2	0	Non-POU domain-containing octamer-binding protein OS=Homo sapiens OX=9606 GN=NONO PE=1 SV=4
NOP56	4|3|6	5|8|7	0	Nucleolar protein 56 OS=Homo sapiens OX=9606 GN=NOP56 PE=1 SV=4
NOSTRIN	0|1|0	0|0|0	0	Nostrin OS=Homo sapiens OX=9606 GN=NOSTRIN PE=1 SV=2
NPM1	5|4|3	5|4|15	0	Nucleophosmin OS=Homo sapiens OX=9606 GN=NPM1 PE=1 SV=2
NSA2	1|0|1	0|1|2	0	Ribosome biogenesis protein NSA2 homolog OS=Homo sapiens OX=9606 GN=NSA2 PE=1 SV=1

prey Gene	Quant (SPC or Intensities)	User Controls (SPC or Intensities)	SP	Description of protein
NUDC	1|1|1	6|3|3	0	Nuclear migration protein nudC4 OS=Homo sapiens OX=9606 GN=NUDC PE=1 SV=1
NUDT1	1|0|1	0|0|0	0	7,8-dihydro-8-oxoguanine triphosphatase OS=Homo sapiens OX=9606 GN=NUDT1 PE=1 SV=3
NUDT12	1|0|0	0|0|0	0	NAD-capped RNA hydrolase NUDT12 OS=Homo sapiens OX=9606 GN=NUDT12 PE=1 SV=1
NUDT21	1|0|0	0|2|0	0	Cleavage and polyadenylation specificity factor subunit 5 OS=Homo sapiens OX=9606 GN=NUDT21 PE=1 SV=1
NUDT5	1|0|1	4|2|7	0	ADP-sugar pyrophosphatase OS=Homo sapiens OX=9606 GN=NUDT5 PE=1 SV=1
NUMB	1|0|0	1|0|0	0	Protein numb homolog OS=Homo sapiens OX=9606 GN=NUMB PE=1 SV=2
NUP107	1|0|1	0|0|0	0	Nuclear pore complex protein Nup107 OS=Homo sapiens OX=9606 GN=NUP107 PE=1 SV=1
NUP188	1|0|1	0|0|0	0	Nucleoporin NUP188 OS=Homo sapiens OX=9606 GN=NUP188 PE=1 SV=1
NUP214	0|0|1	3|0|0	0	Nuclear pore complex protein Nup214 OS=Homo sapiens OX=9606 GN=NUP214 PE=1 SV=2
NUP43	0|0|1	0|0|0	0	Nucleoporin Nup43 OS=Homo sapiens OX=9606 GN=NUP43 PE=1 SV=1
NUP93	1|0|0	0|0|0	0	Nuclear pore complex protein Nup93 OS=Homo sapiens OX=9606 GN=NUP93 PE=1 SV=2

prey Gene	Quant (SPC or Intensities)	User Controls (SPC or Intensities)	SP	Description of protein
NUP98	1|1|1	1|1|0	0	Nuclear pore complex protein Nup98-Nup96 OS=Homo sapiens OX=9606 GN=NUP98 PE=1 SV=4
NWD2	0|0|1	0|0|0	0	NACHT and WD repeat domain-containing protein 2 OS=Homo sapiens OX=9606 GN=NWD2 PE=2 SV=3
OCLN	1|1|1	1|0|0	0	Occludin OS=Homo sapiens OX=9606 GN=OCLN PE=1 SV=1
OCRL	1|1|0	0|0|0	0	Inositol polyphosphate 5-phosphatase OCRL OS=Homo sapiens OX=9606 GN=OCRL PE=1 SV=3
OPA1	1|0|0	0|0|0	0	Dynamin-like 120 kDa protein, mitochondrial OS=Homo sapiens OX=9606 GN=OPA1 PE=1 SV=3
ORC3	0|0|1	0|0|0	0	Origin recognition complex subunit 3 OS=Homo sapiens OX=9606 GN=ORC3 PE=1 SV=1
OSBPL3	1|0|0	0|0|0	0	Oxysterol-binding protein-related protein 3 OS=Homo sapiens OX=9606 GN=OSBPL3 PE=1 SV=1
OTOS	0|0|1	0|0|0	0	Otospiralin OS=Homo sapiens OX=9606 GN=OTOS PE=1 SV=1
OTUB1	1|1|0	0|0|0	0	Ubiquitin thioesterase OTUB1 OS=Homo sapiens OX=9606 GN=OTUB1 PE=1 SV=2
OTUD6B	1|0|0	0|0|0	0	Deubiquitinase OTUD6B OS=Homo sapiens OX=9606 GN=OTUD6B PE=1 SV=1
OTUD7B	0|1|0	0|0|0	0	OTU domain-containing protein 7B OS=Homo sapiens OX=9606 GN=OTUD7B PE=1 SV=1

prey Gene	Quant (SPC or Intensities)	User Controls (SPC or Intensities)	SP	Description of protein
PABPN1	1|0|1	0|0|0	0	Polyadenylate-binding protein 2 OS=Homo sapiens OX=9606 GN=PABPN1 PE=1 SV=3
PAFAH1B3	1|0|0	0|0|0	0	Platelet-activating factor acetylhydrolase IB subunit alpha1 OS=Homo sapiens OX=9606 GN=PAFAH1B3 PE=1 SV=1
PAICS	3|4|3	15|9|3	0	Multifunctional protein ADE2 OS=Homo sapiens OX=9606 GN=PAICS PE=1 SV=3
PAK4	0|1|1	0|0|0	0	Serine/threonine-protein kinase PAK 4 OS=Homo sapiens OX=9606 GN=PAK4 PE=1 SV=1
PARD3B	1|1|1	0|0|0	0	Partitioning defective 3 homolog B OS=Homo sapiens OX=9606 GN=PARD3B PE=1 SV=2
PATL1	1|0|0	0|0|0	0	Protein PAT1 homolog 1 OS=Homo sapiens OX=9606 GN=PATL1 PE=1 SV=2
PC	113|80|69	136|147|58	0	Pyruvate carboxylase, mitochondrial OS=Homo sapiens OX=9606 GN=PC PE=1 SV=2
PCBP1	5|4|3	13|6|8	0	Poly(rC)-binding protein 1 OS=Homo sapiens OX=9606 GN=PCBP1 PE=1 SV=2
PCCA	66|56|53	80|63|22	0	Propionyl-CoA carboxylase alpha chain, mitochondrial OS=Homo sapiens OX=9606 GN=PCCA PE=1 SV=4
PCCB	28|24|22	44|36|12	0	Propionyl-CoA carboxylase beta chain, mitochondrial OS=Homo sapiens OX=9606 GN=PCCB PE=1 SV=3
PCNA	0|1|1	1|0|0	0	Proliferating cell nuclear antigen OS=Homo sapiens OX=9606 GN=PCNA PE=1 SV=1

prey Gene	Quant (SPC or Intensities)	User Controls (SPC or Intensities)	SP	Description of protein
PDAP1	1|0|2	4|2|1	0	28 kDa heat- and acid-stable phosphoprotein OS=Homo sapiens OX=9606 GN=PDAP1 PE=1 SV=1
PDCD11	1|1|0	0|0|0	0	Protein RRP5 homolog OS=Homo sapiens OX=9606 GN=PDCD11 PE=1 SV=3
PDCD5	0|0|1	0|0|0	0	Programmed cell death protein 5 OS=Homo sapiens OX=9606 GN=PDCD5 PE=1 SV=3
PDCL3	1|0|0	2|2|0	0	Phosducin-like protein 3 OS=Homo sapiens OX=9606 GN=PDCL3 PE=1 SV=1
PDE6C	1|0|0	0|0|0	0	Cone cGMP-specific 3',5'-cyclic phosphodiesterase subunit alpha' OS=Homo sapiens OX=9606 GN=PDE6C PE=1 SV=2
PDHB	0|1|0	0|0|0	0	Pyruvate dehydrogenase E1 component subunit beta, mitochondrial OS=Homo sapiens OX=9606 GN=PDHB PE=1 SV=3
PDIA4	1|0|0	0|0|0	0	Protein disulfide-isomerase A4 OS=Homo sapiens OX=9606 GN=PDIA4 PE=1 SV=2
PDLIM4	1|1|1	0|2|0	0	PDZ and LIM domain protein 4 OS=Homo sapiens OX=9606 GN=PDLIM4 PE=1 SV=2
PDLIM5	1|1|0	0|0|0	0	PDZ and LIM domain protein 5 OS=Homo sapiens OX=9606 GN=PDLIM5 PE=1 SV=5
PDLIM7	1|1|1	0|0|0	0	PDZ and LIM domain protein 7 OS=Homo sapiens OX=9606 GN=PDLIM7 PE=1 SV=1
PDS5A	1|0|0	0|0|0	0	Sister chromatid cohesion protein PDS5 homolog A OS=Homo sapiens OX=9606 GN=PDS5A PE=1 SV=1

prey Gene	Quant (SPC or Intensities)	User Controls (SPC or Intensities)	SP	Description of protein
PFDN1	0|1|0	0|0|0	0	Prefoldin subunit 1 OS=Homo sapiens OX=9606 GN=PFDN1 PE=1 SV=2
PFDN4	1|1|1	0|0|0	0	Prefoldin subunit 4 OS=Homo sapiens OX=9606 GN=PFDN4 PE=1 SV=1
PFDN5	1|1|0	0|0|0	0	Prefoldin subunit 5 OS=Homo sapiens OX=9606 GN=PFDN5 PE=1 SV=2
PFN2	1|1|0	0|0|0	0	Profilin-2 OS=Homo sapiens OX=9606 GN=PFN2 PE=1 SV=3
PGC	1|0|0	0|0|0	0	Gastricsin OS=Homo sapiens OX=9606 GN=PGC PE=1 SV=1
PHLDB2	1|0|0	0|0|0	0	Pleckstrin homology-like domain family B member 2 OS=Homo sapiens OX=9606 GN=PHLDB2 PE=1 SV=2
PHRF1	0|0|1	0|0|0	0	PHD and RING finger domain-containing protein 1 OS=Homo sapiens OX=9606 GN=PHRF1 PE=1 SV=3
PIAS1	1|1|1	1|1|1	0	E3 SUMO-protein ligase PIAS1 OS=Homo sapiens OX=9606 GN=PIAS1 PE=1 SV=2
PKM	52|38|42	41|36|31	0	Pyruvate kinase PKM OS=Homo sapiens OX=9606 GN=PKM PE=1 SV=4
PKN2	1|0|0	0|0|0	0	Serine/threonine-protein kinase N2 OS=Homo sapiens OX=9606 GN=PKN2 PE=1 SV=1
PKP2	0|1|0	0|0|0	0	Plakophilin-2 OS=Homo sapiens OX=9606 GN=PKP2 PE=1 SV=2
PLAA	3|3|2	7|4|4	0	Phospholipase A-2-activating protein OS=Homo sapiens OX=9606 GN=PLAA PE=1 SV=2

prey Gene	Quant (SPC or Intensities)	User Controls (SPC or Intensities)	SP	Description of protein
PLBD1	0|0|1	0|0|0	0	Phospholipase B-like 1 OS=Homo sapiens OX=9606 GN=PLBD1 PE=1 SV=2
PLCB3	1|0|1	0|0|0	0	1-phosphatidylinositol 4,5-bisphosphate phosphodiesterase beta-3 OS=Homo sapiens OX=9606 GN=PLCB3 PE=1 SV=2
PLCD3	0|0|1	1|0|0	0	1-phosphatidylinositol 4,5-bisphosphate phosphodiesterase delta-3 OS=Homo sapiens OX=9606 GN=PLCD3 PE=1 SV=3
PLIN3	3|3|2	11|6|2	0	Perilipin-3 OS=Homo sapiens OX=9606 GN=PLIN3 PE=1 SV=3
PMPCB	1|1|0	0|0|0	0	Mitochondrial-processing peptidase subunit beta OS=Homo sapiens OX=9606 GN=PMPCB PE=1 SV=2
PNP	0|0|1	0|0|0	0	Purine nucleoside phosphorylase OS=Homo sapiens OX=9606 GN=PNP PE=1 SV=2
POLD1	1|0|0	0|0|0	0	DNA polymerase delta catalytic subunit OS=Homo sapiens OX=9606 GN=POLD1 PE=1 SV=2
POLD3	1|0|0	0|0|0	0	DNA polymerase delta subunit 3 OS=Homo sapiens OX=9606 GN=POLD3 PE=1 SV=2
POLR2A	1|0|1	0|0|0	0	DNA-directed RNA polymerase II subunit RPB1 OS=Homo sapiens OX=9606 GN=POLR2A PE=1 SV=2
POM121	1|0|1	2|0|0	0	Nuclear envelope pore membrane protein POM 121 OS=Homo sapiens OX=9606 GN=POM121 PE=1 SV=2

prey Gene	Quant (SPC or Intensities)	User Controls (SPC or Intensities)	SP	Description of protein
PPAN	0|0|1	0|0|0	0	Suppressor of SWI4 1 homolog OS=Homo sapiens OX=9606 GN=PPAN PE=2 SV=1
PPIB	1|1|1	3|0|0	0	Peptidyl-prolyl cis-trans isomerase B OS=Homo sapiens OX=9606 GN=PPIB PE=1 SV=2
PPP1CA	0|1|1	1|0|0	0	Serine/threonine-protein phosphatase PP1-alpha catalytic subunit OS=Homo sapiens OX=9606 GN=PPP1CA PE=1 SV=1
PPP1R12A	0|1|0	1|0|0	0	Protein phosphatase 1 regulatory subunit 12A OS=Homo sapiens OX=9606 GN=PPP1R12A PE=1 SV=1
PPP2CB	1|0|0	0|0|0	0	Serine/threonine-protein phosphatase 2A catalytic subunit beta isoform OS=Homo sapiens OX=9606 GN=PPP2CB PE=1 SV=1
PPP6R3	1|1|1	2|3|0	0	Serine/threonine-protein phosphatase 6 regulatory subunit 3 OS=Homo sapiens OX=9606 GN=PPP6R3 PE=1 SV=2
PPT1	0|1|0	0|0|0	0	Palmitoyl-protein thioesterase 1 OS=Homo sapiens OX=9606 GN=PPT1 PE=1 SV=1
PRDX1	13|9|11	13|11|12	0	Peroxiredoxin-1 OS=Homo sapiens OX=9606 GN=PRDX1 PE=1 SV=1
PRICKLE1	1|0|0	0|0|0	0	Prickle-like protein 1 OS=Homo sapiens OX=9606 GN=PRICKLE1 PE=1 SV=2
PRIM2	1|0|0	0|1|0	0	DNA primase large subunit OS=Homo sapiens OX=9606 GN=PRIM2 PE=1 SV=2
PRKCI	1|1|1	0|0|0	0	Protein kinase C iota type OS=Homo sapiens OX=9606 GN=PRKCI PE=1 SV=2

prey Gene	Quant (SPC or Intensities)	User Controls (SPC or Intensities)	SP	Description of protein
PRKD3	1|0|0	0|0|0	0	Serine/threonine-protein kinase D3 OS=Homo sapiens OX=9606 GN=PRKD3 PE=1 SV=1
PRPF19	1|0|0	0|0|0	0	Pre-mRNA-processing factor 19 OS=Homo sapiens OX=9606 GN=PRPF19 PE=1 SV=1
PRPF40A	1|0|1	0|1|0	0	Pre-mRNA-processing factor 40 homolog A OS=Homo sapiens OX=9606 GN=PRPF40A PE=1 SV=2
PRPF6	1|0|1	0|0|0	0	Pre-mRNA-processing factor 6 OS=Homo sapiens OX=9606 GN=PRPF6 PE=1 SV=1
PRPF8	1|1|0	0|0|0	0	Pre-mRNA-processing-splicing factor 8 OS=Homo sapiens OX=9606 GN=PRPF8 PE=1 SV=2
PRR11	3|6|8	8|5|4	0	Proline-rich protein 11 OS=Homo sapiens OX=9606 GN=PRR11 PE=1 SV=1
PRRC2C	1|0|0	1|1|0	0	Protein PRRC2C OS=Homo sapiens OX=9606 GN=PRRC2C PE=1 SV=4
PRSS1	11|14|12	6|19|17	0	Trypsin-1 OS=Homo sapiens OX=9606 GN=PRSS1 PE=1 SV=1
PRSS3	2|2|2	3|2|4	0	Trypsin-3 OS=Homo sapiens OX=9606 GN=PRSS3 PE=1 SV=2
PSMA2	0|0|1	0|0|0	0	Proteasome subunit alpha type-2 OS=Homo sapiens OX=9606 GN=PSMA2 PE=1 SV=2
PSMA3	0|1|1	0|0|0	0	Proteasome subunit alpha type-3 OS=Homo sapiens OX=9606 GN=PSMA3 PE=1 SV=2
PSMA4	1|1|1	0|1|0	0	Proteasome subunit alpha type-4 OS=Homo sapiens OX=9606 GN=PSMA4 PE=1 SV=1

prey Gene	Quant (SPC or Intensities)	User Controls (SPC or Intensities)	SP	Description of protein
PSMB1	0|0|1	0|0|0	0	Proteasome subunit beta type-1 OS=Homo sapiens OX=9606 GN=PSMB1 PE=1 SV=2
PSMB2	1|0|1	0|0|0	0	Proteasome subunit beta type-2 OS=Homo sapiens OX=9606 GN=PSMB2 PE=1 SV=1
PSMB4	1|1|1	0|0|0	0	Proteasome subunit beta type-4 OS=Homo sapiens OX=9606 GN=PSMB4 PE=1 SV=4
PSMB6	1|0|0	0|0|0	0	Proteasome subunit beta type-6 OS=Homo sapiens OX=9606 GN=PSMB6 PE=1 SV=4
PSMC3	1|1|1	1|0|0	0	26S proteasome regulatory subunit 6A OS=Homo sapiens OX=9606 GN=PSMC3 PE=1 SV=3
PSMD1	1|0|1	0|0|0	0	26S proteasome non-ATPase regulatory subunit 1 OS=Homo sapiens OX=9606 GN=PSMD1 PE=1 SV=2
PSMD14	1|1|1	1|1|0	0	26S proteasome non-ATPase regulatory subunit 14 OS=Homo sapiens OX=9606 GN=PSMD14 PE=1 SV=1
PSME3	0|0|1	2|2|0	0	Proteasome activator complex subunit 3 OS=Homo sapiens OX=9606 GN=PSME3 PE=1 SV=1
PTBP1	2|2|4	2|3|4	0	Polypyrimidine tract-binding protein 1 OS=Homo sapiens OX=9606 GN=PTBP1 PE=1 SV=1
PTGES3	1|1|0	0|0|0	0	Prostaglandin E synthase 3 OS=Homo sapiens OX=9606 GN=PTGES3 PE=1 SV=1
PTK2	1|0|0	0|0|0	0	Focal adhesion kinase 1 OS=Homo sapiens OX=9606 GN=PTK2 PE=1 SV=2

prey Gene	Quant (SPC or Intensities)	User Controls (SPC or Intensities)	SP	Description of protein
PTPN11	1|0|0	0|0|0	0	Tyrosine-protein phosphatase non-receptor type 11 OS=Homo sapiens OX=9606 GN=PTPN11 PE=1 SV=3
PUF60	2|1|1	13|7|2	0	Poly(U)-binding-splicing factor PUF60 OS=Homo sapiens OX=9606 GN=PUF60 PE=1 SV=1
PYCR2	1|0|1	0|0|0	0	Pyrroline-5-carboxylate reductase 2 OS=Homo sapiens OX=9606 GN=PYCR2 PE=1 SV=1
PYGO2	1|0|0	0|0|0	0	Pygopus homolog 2 OS=Homo sapiens OX=9606 GN=PYGO2 PE=1 SV=2
PZP	1|1|1	0|0|0	0	Pregnancy zone protein OS=Homo sapiens OX=9606 GN=PZP PE=1 SV=4
RAB11B	1|1|0	0|0|0	0	Ras-related protein Rab-11B OS=Homo sapiens OX=9606 GN=RAB11B PE=1 SV=4
RAB11FIP5	1|1|1	1|2|0	0	Rab11 family-interacting protein 5 OS=Homo sapiens OX=9606 GN=RAB11FIP5 PE=1 SV=1
RAB19	1|0|0	0|0|0	0	Ras-related protein Rab-19 OS=Homo sapiens OX=9606 GN=RAB19 PE=1 SV=2
RAB23	0|1|0	0|0|0	0	Ras-related protein Rab-23 OS=Homo sapiens OX=9606 GN=RAB23 PE=1 SV=1
RAB34	1|1|1	0|0|0	0	Ras-related protein Rab-34 OS=Homo sapiens OX=9606 GN=RAB34 PE=1 SV=1
RAB44	1|0|0	0|0|0	0	Ras-related protein Rab-44 OS=Homo sapiens OX=9606 GN=RAB44 PE=1 SV=4

prey Gene	Quant (SPC or Intensities)	User Controls (SPC or Intensities)	SP	Description of protein
RACK1	14|12|10	14|9|3	0	Receptor of activated protein C kinase 1 OS=Homo sapiens OX=9606 GN=RACK1 PE=1 SV=3
RAE1	0|0|1	0|0|0	0	mRNA export factor OS=Homo sapiens OX=9606 GN=RAE1 PE=1 SV=1
RALGAPA2	0|0|1	0|0|0	0	Ral GTPase-activating protein subunit alpha-2 OS=Homo sapiens OX=9606 GN=RALGAPA2 PE=1 SV=2
RAN	11|10|12	17|9|3	0	GTP-binding nuclear protein Ran OS=Homo sapiens OX=9606 GN=RAN PE=1 SV=3
RANBP2	2|0|0	6|6|0	0	E3 SUMO-protein ligase RanBP2 OS=Homo sapiens OX=9606 GN=RANBP2 PE=1 SV=2
RANGAP1	1|0|1	0|0|0	0	Ran GTPase-activating protein 1 OS=Homo sapiens OX=9606 GN=RANGAP1 PE=1 SV=1
RAP1B	1|0|1	0|0|0	0	Ras-related protein Rap-1b OS=Homo sapiens OX=9606 GN=RAP1B PE=1 SV=1
RASSF8	1|0|0	0|0|0	0	Ras association domain-containing protein 8 OS=Homo sapiens OX=9606 GN=RASSF8 PE=1 SV=2
RAVER1	1|0|1	0|0|0	0	Ribonucleoprotein PTB-binding 1 OS=Homo sapiens OX=9606 GN=RAVER1 PE=1 SV=1
RBBP4	0|0|1	0|0|0	0	Histone-binding protein RBBP4 OS=Homo sapiens OX=9606 GN=RBBP4 PE=1 SV=3
RBM12	1|0|0	0|0|0	0	RNA-binding protein 12 OS=Homo sapiens OX=9606 GN=RBM12 PE=1 SV=1

prey Gene	Quant (SPC or Intensities)	User Controls (SPC or Intensities)	SP	Description of protein
RBM14	8|5|5	9|7|1	0	RNA-binding protein 14 OS=Homo sapiens OX=9606 GN=RBM14 PE=1 SV=2
RBM25	1|0|0	2|1|0	0	RNA-binding protein 25 OS=Homo sapiens OX=9606 GN=RBM25 PE=1 SV=3
RBM39	1|0|0	0|1|0	0	RNA-binding protein 39 OS=Homo sapiens OX=9606 GN=RBM39 PE=1 SV=2
RBM4	1|0|0	0|0|0	0	RNA-binding protein 4 OS=Homo sapiens OX=9606 GN=RBM4 PE=1 SV=1
RBM8A	0|1|0	1|1|0	0	RNA-binding protein 8A OS=Homo sapiens OX=9606 GN=RBM8A PE=1 SV=1
RBMX	1|1|1	0|0|3	0	RNA-binding motif protein, X chromosome OS=Homo sapiens OX=9606 GN=RBMX PE=1 SV=3
RCN1	1|1|1	0|1|0	0	Reticulocalbin-1 OS=Homo sapiens OX=9606 GN=RCN1 PE=1 SV=1
REPIN1	0|1|1	0|0|0	0	Replication initiator 1 OS=Homo sapiens OX=9606 GN=REPIN1 PE=1 SV=1
RFC1	1|0|1	0|0|0	0	Replication factor C subunit 1 OS=Homo sapiens OX=9606 GN=RFC1 PE=1 SV=4
RFC2	0|0|1	0|0|0	0	Replication factor C subunit 2 OS=Homo sapiens OX=9606 GN=RFC2 PE=1 SV=3
RHEB	1|0|0	0|0|0	0	GTP-binding protein Rheb OS=Homo sapiens OX=9606 GN=RHEB PE=1 SV=1
RHOC	1|0|0	0|0|0	0	Rho-related GTP-binding protein RhoC OS=Homo sapiens OX=9606 GN=RHOC PE=1 SV=1

prey Gene	Quant (SPC or Intensities)	User Controls (SPC or Intensities)	SP	Description of protein
RHOG	1|0|0	0|0|0	0	Rho-related GTP-binding protein RhoG OS=Homo sapiens OX=9606 GN=RHOG PE=1 SV=1
RHOT2	0|0|1	0|0|0	0	Mitochondrial Rho GTPase 2 OS=Homo sapiens OX=9606 GN=RHOT2 PE=1 SV=2
RING1	1|0|1	0|0|0	0	E3 ubiquitin-protein ligase RING1 OS=Homo sapiens OX=9606 GN=RING1 PE=1 SV=2
RIOX1	1|0|0	0|0|0	0	Ribosomal oxygenase 1 OS=Homo sapiens OX=9606 GN=RIOX1 PE=1 SV=2
RPAP3	1|1|0	5|5|1	0	RNA polymerase II-associated protein 3 OS=Homo sapiens OX=9606 GN=RPAP3 PE=1 SV=2
RPGRIP1L	0|1|0	0|0|0	0	Protein fantom OS=Homo sapiens OX=9606 GN=RPGRIP1L PE=1 SV=2
RPL10	10|8|5	13|11|11	0	60S ribosomal protein L10 OS=Homo sapiens OX=9606 GN=RPL10 PE=1 SV=4
RPL10A	0|0|1	0|0|0	0	60S ribosomal protein L10a OS=Homo sapiens OX=9606 GN=RPL10A PE=1 SV=2
RPL11	3|2|3	6|2|3	0	60S ribosomal protein L11 OS=Homo sapiens OX=9606 GN=RPL11 PE=1 SV=2
RPL13	19|13|16	39|21|64	0	60S ribosomal protein L13 OS=Homo sapiens OX=9606 GN=RPL13 PE=1 SV=4
RPL13A	17|12|13	40|31|39	0	60S ribosomal protein L13a OS=Homo sapiens OX=9606 GN=RPL13A PE=1 SV=2
RPL14	4|3|4	6|8|12	0	60S ribosomal protein L14 OS=Homo sapiens OX=9606 GN=RPL14 PE=1 SV=4

prey Gene	Quant (SPC or Intensities)	User Controls (SPC or Intensities)	SP	Description of protein
RPL15	5|8|5	9|6|6	0	60S ribosomal protein L15 OS=Homo sapiens OX=9606 GN=RPL15 PE=1 SV=2
RPL17	11|6|7	8|8|7	0	60S ribosomal protein L17 OS=Homo sapiens OX=9606 GN=RPL17 PE=1 SV=3
RPL18	45|45|38	100|68|58	0	60S ribosomal protein L18 OS=Homo sapiens OX=9606 GN=RPL18 PE=1 SV=2
RPL18A	5|6|5	5|4|9	0	60S ribosomal protein L18a OS=Homo sapiens OX=9606 GN=RPL18A PE=1 SV=2
RPL19	28|16|16	48|24|20	0	60S ribosomal protein L19 OS=Homo sapiens OX=9606 GN=RPL19 PE=1 SV=1
RPL23A	3|1|2	5|3|4	0	60S ribosomal protein L23a OS=Homo sapiens OX=9606 GN=RPL23A PE=1 SV=1
RPL24	4|6|5	9|6|15	0	60S ribosomal protein L24 OS=Homo sapiens OX=9606 GN=RPL24 PE=1 SV=1
RPL27A	9|8|8	14|9|19	0	60S ribosomal protein L27a OS=Homo sapiens OX=9606 GN=RPL27A PE=1 SV=2
RPL28	2|3|3	4|5|0	0	60S ribosomal protein L28 OS=Homo sapiens OX=9606 GN=RPL28 PE=1 SV=3
RPL29	4|2|3	8|6|8	0	60S ribosomal protein L29 OS=Homo sapiens OX=9606 GN=RPL29 PE=1 SV=2
RPL3	11|5|7	14|18|14	0	60S ribosomal protein L3 OS=Homo sapiens OX=9606 GN=RPL3 PE=1 SV=2
RPL32	16|8|11	34|50|32	0	60S ribosomal protein L32 OS=Homo sapiens OX=9606 GN=RPL32 PE=1 SV=2

prey Gene	Quant (SPC or Intensities)	User Controls (SPC or Intensities)	SP	Description of protein
RPL34	5|5|4	3|11|7	0	60S ribosomal protein L34 OS=Homo sapiens OX=9606 GN=RPL34 PE=1 SV=3
RPL35	12|3|5	8|13|10	0	60S ribosomal protein L35 OS=Homo sapiens OX=9606 GN=RPL35 PE=1 SV=2
RPL36	25|22|24	35|30|26	0	60S ribosomal protein L36 OS=Homo sapiens OX=9606 GN=RPL36 PE=1 SV=3
RPL37A	2|2|1	3|3|4	0	60S ribosomal protein L37a OS=Homo sapiens OX=9606 GN=RPL37A PE=1 SV=2
RPL4	66|61|78	55|41|37	0	60S ribosomal protein L4 OS=Homo sapiens OX=9606 GN=RPL4 PE=1 SV=5
RPL6	21|16|17	23|37|19	0	60S ribosomal protein L6 OS=Homo sapiens OX=9606 GN=RPL6 PE=1 SV=3
RPL7	35|26|32	73|45|74	0	60S ribosomal protein L7 OS=Homo sapiens OX=9606 GN=RPL7 PE=1 SV=1
RPL7A	11|8|11	10|16|17	0	60S ribosomal protein L7a OS=Homo sapiens OX=9606 GN=RPL7A PE=1 SV=2
RPL7L1	6|6|4	12|7|10	0	60S ribosomal protein L7-like 1 OS=Homo sapiens OX=9606 GN=RPL7L1 PE=1 SV=2
RPL8	10|8|7	19|15|15	0	60S ribosomal protein L8 OS=Homo sapiens OX=9606 GN=RPL8 PE=1 SV=2
RPL9P8;RPL9;RPL9P7;R...	8|3|4	4|7|10	0	60S ribosomal protein L9 OS=Homo sapiens OX=9606 GN=RPL9 PE=1 SV=1

prey Gene	Quant (SPC or Intensities)	User Controls (SPC or Intensities)	SP	Description of protein
RPRD1B	1|0|0	0|0|0	0	Regulation of nuclear pre-mRNA domain-containing protein 1B OS=Homo sapiens OX=9606 GN=RPRD1B PE=1 SV=1
RPS10P5	1|1|0	0|0|0	0	Putative 40S ribosomal protein S10-like OS=Homo sapiens OX=9606 GN=RPS10P5 PE=5 SV=1
RPS17	7|5|8	10|6|7	0	40S ribosomal protein S17 OS=Homo sapiens OX=9606 GN=RPS17 PE=1 SV=2
RPS23	3|2|3	4|5|4	0	40S ribosomal protein S23 OS=Homo sapiens OX=9606 GN=RPS23 PE=1 SV=3
RPS26	3|1|3	6|2|1	0	40S ribosomal protein S26 OS=Homo sapiens OX=9606 GN=RPS26 PE=1 SV=3
RPS27A	13|6|15	8|6|8	0	Ubiquitin-40S ribosomal protein S27a OS=Homo sapiens OX=9606 GN=RPS27A PE=1 SV=2
RPS28	0|0|1	0|0|0	0	40S ribosomal protein S28 OS=Homo sapiens OX=9606 GN=RPS28 PE=1 SV=1
RPS3	20|21|17	20|13|7	0	40S ribosomal protein S3 OS=Homo sapiens OX=9606 GN=RPS3 PE=1 SV=2
RPS5	8|6|12	15|8|8	0	40S ribosomal protein S5 OS=Homo sapiens OX=9606 GN=RPS5 PE=1 SV=4
RPS6	12|8|11	30|25|22	0	40S ribosomal protein S6 OS=Homo sapiens OX=9606 GN=RPS6 PE=1 SV=1
RPS7	1|0|1	0|1|0	0	40S ribosomal protein S7 OS=Homo sapiens OX=9606 GN=RPS7 PE=1 SV=1

prey Gene	Quant (SPC or Intensities)	User Controls (SPC or Intensities)	SP	Description of protein
RPS8	9|11|14	27|19|17	0	40S ribosomal protein S8 OS=Homo sapiens OX=9606 GN=RPS8 PE=1 SV=2
RPS9	15|15|18	47|39|72	0	40S ribosomal protein S9 OS=Homo sapiens OX=9606 GN=RPS9 PE=1 SV=3
RRM1	1|0|0	0|0|0	0	Ribonucleoside-diphosphate reductase large subunit OS=Homo sapiens OX=9606 GN=RRM1 PE=1 SV=1
RRM2	1|1|1	3|3|1	0	Ribonucleoside-diphosphate reductase subunit M2 OS=Homo sapiens OX=9606 GN=RRM2 PE=1 SV=1
RRP12	14|5|11	14|12|4	0	RRP12-like protein OS=Homo sapiens OX=9606 GN=RRP12 PE=1 SV=2
RRS1	0|1|0	0|0|0	0	Ribosome biogenesis regulatory protein homolog OS=Homo sapiens OX=9606 GN=RRS1 PE=1 SV=2
RSL1D1	14|11|12	36|22|35	0	Ribosomal L1 domain-containing protein 1 OS=Homo sapiens OX=9606 GN=RSL1D1 PE=1 SV=3
RTCB	1|0|1	0|0|0	0	RNA-splicing ligase RtcB homolog OS=Homo sapiens OX=9606 GN=RTCB PE=1 SV=1
RUSC2	1|0|1	0|0|0	0	Iporin OS=Homo sapiens OX=9606 GN=RUSC2 PE=1 SV=3
S100A2	0|1|0	0|0|0	0	Protein S100-A2 OS=Homo sapiens OX=9606 GN=S100A2 PE=1 SV=3
S100A7	4|5|4	7|6|10	0	Protein S100-A7 OS=Homo sapiens OX=9606 GN=S100A7 PE=1 SV=4
S100A8	8|10|6	7|8|8	0	Protein S100-A8 OS=Homo sapiens OX=9606 GN=S100A8 PE=1 SV=1

prey Gene	Quant (SPC or Intensities)	User Controls (SPC or Intensities)	SP	Description of protein
S100P	0|1|1	0|0|0	0	Protein S100-P OS=Homo sapiens OX=9606 GN=S100P PE=1 SV=2
SAFB2	0|1|1	2|3|1	0	Scaffold attachment factor B2 OS=Homo sapiens OX=9606 GN=SAFB2 PE=1 SV=1
SARS	1|0|0	0|0|0	0	Serine--tRNA ligase, cytoplasmic OS=Homo sapiens OX=9606 GN=SARS1 PE=1 SV=3
SART1	0|0|1	11|10|0	0	U4/U6.U5 tri-snRNP-associated protein 1 OS=Homo sapiens OX=9606 GN=SART1 PE=1 SV=1
SAV1	1|0|0	0|0|0	0	Protein salvador homolog 1 OS=Homo sapiens OX=9606 GN=SAV1 PE=1 SV=2
SCAMP3	1|0|0	0|0|0	0	Secretory carrier-associated membrane protein 3 OS=Homo sapiens OX=9606 GN=SCAMP3 PE=1 SV=3
SCFD1	0|1|0	0|0|0	0	Sec1 family domain-containing protein 1 OS=Homo sapiens OX=9606 GN=SCFD1 PE=1 SV=4
SCGB1D2	0|1|1	0|0|0	0	Secretoglobin family 1D member 2 OS=Homo sapiens OX=9606 GN=SCGB1D2 PE=2 SV=1
SCGB2A1	0|0|1	0|0|0	0	Mammaglobin-B OS=Homo sapiens OX=9606 GN=SCGB2A1 PE=1 SV=1
SDAD1	0|0|1	0|1|0	0	Protein SDA1 homolog OS=Homo sapiens OX=9606 GN=SDAD1 PE=1 SV=3
SEC11A	1|1|0	0|0|0	0	Signal peptidase complex catalytic subunit SEC11A OS=Homo sapiens OX=9606 GN=SEC11A PE=1 SV=1

prey Gene	Quant (SPC or Intensities)	User Controls (SPC or Intensities)	SP	Description of protein
SEC22B	2|1|2	8|2|4	0	Vesicle-trafficking protein SEC22b OS=Homo sapiens OX=9606 GN=SEC22B PE=1 SV=4
SEC23B	1|0|0	0|0|0	0	Protein transport protein Sec23B OS=Homo sapiens OX=9606 GN=SEC23B PE=1 SV=2
SERBP1	0|0|1	1|1|1	0	Plasminogen activator inhibitor 1 RNA-binding protein OS=Homo sapiens OX=9606 GN=SERBP1 PE=1 SV=2
SERPINA12	0|1|1	0|0|0	0	Serpin A12 OS=Homo sapiens OX=9606 GN=SERPINA12 PE=1 SV=1
SERPINB5	0|1|0	0|0|0	0	Serpin B5 OS=Homo sapiens OX=9606 GN=SERPINB5 PE=1 SV=2
SERPINB7	0|0|1	0|0|0	0	Serpin B7 OS=Homo sapiens OX=9606 GN=SERPINB7 PE=1 SV=1
SF3A1	1|1|1	2|0|0	0	Splicing factor 3A subunit 1 OS=Homo sapiens OX=9606 GN=SF3A1 PE=1 SV=1
SF3B1	3|1|3	9|9|2	0	Splicing factor 3B subunit 1 OS=Homo sapiens OX=9606 GN=SF3B1 PE=1 SV=3
SF3B2	1|0|0	1|2|0	0	Splicing factor 3B subunit 2 OS=Homo sapiens OX=9606 GN=SF3B2 PE=1 SV=2
SF3B3	5|2|4	22|14|5	0	Splicing factor 3B subunit 3 OS=Homo sapiens OX=9606 GN=SF3B3 PE=1 SV=4
SFXN1	1|1|1	1|0|0	0	Sideroflexin-1 OS=Homo sapiens OX=9606 GN=SFXN1 PE=1 SV=4
SGPL1	1|0|1	0|0|0	0	Sphingosine-1-phosphate lyase 1 OS=Homo sapiens OX=9606 GN=SGPL1 PE=1 SV=3

prey Gene	Quant (SPC or Intensities)	User Controls (SPC or Intensities)	SP	Description of protein
SH3GL1	1|0|0	0|0|0	0	Endophilin-A2 OS=Homo sapiens OX=9606 GN=SH3GL1 PE=1 SV=1
SH3KBP1	1|0|0	0|0|0	0	SH3 domain-containing kinase-binding protein 1 OS=Homo sapiens OX=9606 GN=SH3KBP1 PE=1 SV=2
SHB	1|0|0	0|0|0	0	SH2 domain-containing adapter protein B OS=Homo sapiens OX=9606 GN=SHB PE=1 SV=2
SHROOM2	1|1|0	0|0|0	0	Protein Shroom2 OS=Homo sapiens OX=9606 GN=SHROOM2 PE=1 SV=1
SLAIN2	4|1|4	4|5|1	0	SLAIN motif-containing protein 2 OS=Homo sapiens OX=9606 GN=SLAIN2 PE=1 SV=2
SLC16A4	1|0|0	0|0|0	0	Monocarboxylate transporter 5 OS=Homo sapiens OX=9606 GN=SLC16A4 PE=1 SV=1
SLC1A5	0|0|1	0|0|0	0	Neutral amino acid transporter B(0) OS=Homo sapiens OX=9606 GN=SLC1A5 PE=1 SV=2
SLC25A11	1|1|1	0|0|0	0	Mitochondrial 2-oxoglutarate/malate carrier protein OS=Homo sapiens OX=9606 GN=SLC25A11 PE=1 SV=3
SLC25A3	1|0|0	0|0|0	0	Phosphate carrier protein, mitochondrial OS=Homo sapiens OX=9606 GN=SLC25A3 PE=1 SV=2
SLC25A5	6|8|7	8|4|7	0	ADP/ATP translocase 2 OS=Homo sapiens OX=9606 GN=SLC25A5 PE=1 SV=7
SLC2A1	1|0|0	0|0|0	0	Solute carrier family 2, facilitated glucose transporter member 1 OS=Homo sapiens OX=9606 GN=SLC2A1 PE=1 SV=2

prey Gene	Quant (SPC or Intensities)	User Controls (SPC or Intensities)	SP	Description of protein
SLC38A1	1|0|1	0|0|0	0	Sodium-coupled neutral amino acid transporter 1 OS=Homo sapiens OX=9606 GN=SLC38A1 PE=1 SV=1
SLC39A10	1|0|0	0|0|0	0	Zinc transporter ZIP10 OS=Homo sapiens OX=9606 GN=SLC39A10 PE=1 SV=2
SLC6A9	0|0|1	0|0|0	0	Sodium- and chloride-dependent glycine transporter 1 OS=Homo sapiens OX=9606 GN=SLC6A9 PE=1 SV=3
SLC7A5	0|1|1	0|0|0	0	Large neutral amino acids transporter small subunit 1 OS=Homo sapiens OX=9606 GN=SLC7A5 PE=1 SV=2
SLC9A3R1	1|0|1	0|1|1	0	Na(+)/H(+) exchange regulatory cofactor NHE-RF1 OS=Homo sapiens OX=9606 GN=SLC9A3R1 PE=1 SV=4
SLK	1|1|1	1|0|0	0	STE20-like serine/threonine-protein kinase OS=Homo sapiens OX=9606 GN=SLK PE=1 SV=1
SLURP1	0|1|1	0|1|0	0	Secreted Ly-6/uPAR-related protein 1 OS=Homo sapiens OX=9606 GN=SLURP1 PE=1 SV=2
SMARCA4	1|1|0	0|0|0	0	Transcription activator BRG1 OS=Homo sapiens OX=9606 GN=SMARCA4 PE=1 SV=2
SMARCA5	1|1|0	1|0|0	0	SWI/SNF-related matrix-associated actin-dependent regulator of chromatin subfamily A member 5 OS=Homo sapiens OX=9606 GN=SMARCA5 PE=1 SV=1

prey Gene	Quant (SPC or Intensities)	User Controls (SPC or Intensities)	SP	Description of protein
SMARCB1	1|0|0	0|0|0	0	SWI/SNF-related matrix-associated actin-dependent regulator of chromatin subfamily B member 1 OS=Homo sapiens OX=9606 GN=SMARCB1 PE=1 SV=2
SMARCC1	1|0|0	0|0|0	0	SWI/SNF complex subunit SMARCC1 OS=Homo sapiens OX=9606 GN=SMARCC1 PE=1 SV=3
SMARCC2	0|0|1	0|0|0	0	SWI/SNF complex subunit SMARCC2 OS=Homo sapiens OX=9606 GN=SMARCC2 PE=1 SV=1
SMC2	1|0|1	1|0|0	0	Structural maintenance of chromosomes protein 2 OS=Homo sapiens OX=9606 GN=SMC2 PE=1 SV=2
SMPDL3B	0|1|0	0|0|0	0	Acid sphingomyelinase-like phosphodiesterase 3b OS=Homo sapiens OX=9606 GN=SMPDL3B PE=1 SV=2
SMR3B	1|0|1	1|0|0	0	Submaxillary gland androgen-regulated protein 3B OS=Homo sapiens OX=9606 GN=SMR3B PE=1 SV=2
SNAP29	0|1|1	2|0|0	0	Synaptosomal-associated protein 29 OS=Homo sapiens OX=9606 GN=SNAP29 PE=1 SV=1
SNAP91	1|0|0	0|1|0	0	Clathrin coat assembly protein AP180 OS=Homo sapiens OX=9606 GN=SNAP91 PE=1 SV=2
SNCA	2|0|0	2|4|0	0	Alpha-synuclein OS=Homo sapiens OX=9606 GN=SNCA PE=1 SV=1
SNRNP200	1|0|2	2|2|1	0	U5 small nuclear ribonucleoprotein 200 kDa helicase OS=Homo sapiens OX=9606 GN=SNRNP200 PE=1 SV=2

prey Gene	Quant (SPC or Intensities)	User Controls (SPC or Intensities)	SP	Description of protein
SNRNP70	1|0|0	0|0|0	0	U1 small nuclear ribonucleoprotein 70 kDa OS=Homo sapiens OX=9606 GN=SNRNP70 PE=1 SV=2
SNRPA1	1|0|0	1|1|0	0	U2 small nuclear ribonucleoprotein A' OS=Homo sapiens OX=9606 GN=SNRPA1 PE=1 SV=2
SNRPB	1|0|1	3|2|0	0	Small nuclear ribonucleoprotein-associated proteins B and B' OS=Homo sapiens OX=9606 GN=SNRPB PE=1 SV=2
SNRPC	1|0|0	0|0|0	0	U1 small nuclear ribonucleoprotein C OS=Homo sapiens OX=9606 GN=SNRPC PE=1 SV=1
SNRPD2	1|0|1	4|5|3	0	Small nuclear ribonucleoprotein Sm D2 OS=Homo sapiens OX=9606 GN=SNRPD2 PE=1 SV=1
SNU13	1|0|1	0|0|0	0	NHP2-like protein 1 OS=Homo sapiens OX=9606 GN=SNU13 PE=1 SV=3
SNW1	1|0|0	3|2|0	0	SNW domain-containing protein 1 OS=Homo sapiens OX=9606 GN=SNW1 PE=1 SV=1
SON	1|1|0	1|3|0	0	Protein SON OS=Homo sapiens OX=9606 GN=SON PE=1 SV=4
SORBS1	0|0|1	0|0|0	0	Sorbin and SH3 domain-containing protein 1 OS=Homo sapiens OX=9606 GN=SORBS1 PE=1 SV=3
SPG20	1|0|4	5|3|2	0	Spartin OS=Homo sapiens OX=9606 GN=SPART PE=1 SV=1
SPTBN4	0|1|1	0|0|0	0	Spectrin beta chain, non-erythrocytic 4 OS=Homo sapiens OX=9606 GN=SPTBN4 PE=1 SV=2

prey Gene	Quant (SPC or Intensities)	User Controls (SPC or Intensities)	SP	Description of protein
SPTLC1	1|1|1	0|0|0	0	Serine palmitoyltransferase 1 OS=Homo sapiens OX=9606 GN=SPTLC1 PE=1 SV=1
SRM	1|0|0	0|0|0	0	Spermidine synthase OS=Homo sapiens OX=9606 GN=SRM PE=1 SV=1
SRP9	1|1|1	0|0|0	0	Signal recognition particle 9 kDa protein OS=Homo sapiens OX=9606 GN=SRP9 PE=1 SV=2
SRPRB	1|0|0	1|0|0	0	Signal recognition particle receptor subunit beta OS=Homo sapiens OX=9606 GN=SRPRB PE=1 SV=3
SRRT	1|1|0	0|0|0	0	Serrate RNA effector molecule homolog OS=Homo sapiens OX=9606 GN=SRRT PE=1 SV=1
SRSF7	1|0|0	1|0|1	0	Serine/arginine-rich splicing factor 7 OS=Homo sapiens OX=9606 GN=SRSF7 PE=1 SV=1
SSBP3	1|0|0	0|0|0	0	Single-stranded DNA-binding protein 3 OS=Homo sapiens OX=9606 GN=SSBP3 PE=1 SV=1
SSH1	0|1|0	0|0|0	0	Protein phosphatase Slingshot homolog 1 OS=Homo sapiens OX=9606 GN=SSH1 PE=1 SV=2
SSR1	1|1|0	0|0|1	0	Translocon-associated protein subunit alpha OS=Homo sapiens OX=9606 GN=SSR1 PE=1 SV=3
SSR3	1|1|1	0|0|0	0	Translocon-associated protein subunit gamma OS=Homo sapiens OX=9606 GN=SSR3 PE=1 SV=1

prey Gene	Quant (SPC or Intensities)	User Controls (SPC or Intensities)	SP	Description of protein
ST13	1|0|1	0|0|0	0	Hsc70-interacting protein OS=Homo sapiens OX=9606 GN=ST13 PE=1 SV=2
STAT3	2|1|2	2|4|1	0	Signal transducer and activator of transcription 3 OS=Homo sapiens OX=9606 GN=STAT3 PE=1 SV=2
STAU1	2|0|1	3|3|0	0	Double-stranded RNA-binding protein Staufen homolog 1 OS=Homo sapiens OX=9606 GN=STAU1 PE=1 SV=2
STAU2	0|0|1	0|0|0	0	Double-stranded RNA-binding protein Staufen homolog 2 OS=Homo sapiens OX=9606 GN=STAU2 PE=1 SV=2
STMN2	0|1|0	0|0|0	0	Stathmin-2 OS=Homo sapiens OX=9606 GN=STMN2 PE=1 SV=3
STOM	1|1|1	0|0|0	0	Stomatin OS=Homo sapiens OX=9606 GN=STOM PE=1 SV=3
STON1	1|0|0	0|0|0	0	Stonin-1 OS=Homo sapiens OX=9606 GN=STON1 PE=1 SV=2
STON2	0|1|0	0|0|0	0	Stonin-2 OS=Homo sapiens OX=9606 GN=STON2 PE=1 SV=1
STXBP3	1|0|0	0|0|0	0	Syntaxin-binding protein 3 OS=Homo sapiens OX=9606 GN=STXBP3 PE=1 SV=2
SUGP2	1|0|0	4|5|1	0	SURP and G-patch domain-containing protein 2 OS=Homo sapiens OX=9606 GN=SUGP2 PE=1 SV=2
SYMPK	1|0|0	6|9|1	0	Symplekin OS=Homo sapiens OX=9606 GN=SYMPK PE=1 SV=2
SYNRG	11|5|9	31|20|8	0	Synergin gamma OS=Homo sapiens OX=9606 GN=SYNRG PE=1 SV=2

prey Gene	Quant (SPC or Intensities)	User Controls (SPC or Intensities)	SP	Description of protein
SYTL4	18|21|19	21|27|13	0	Synaptotagmin-like protein 4 OS=Homo sapiens OX=9606 GN=SYTL4 PE=1 SV=2
TACC3	1|0|1	1|0|0	0	Transforming acidic coiled-coil-containing protein 3 OS=Homo sapiens OX=9606 GN=TACC3 PE=1 SV=1
TAGLN	1|0|0	1|1|1	0	Transgelin OS=Homo sapiens OX=9606 GN=TAGLN PE=1 SV=4
TAGLN2	13|12|8	24|26|24	0	Transgelin-2 OS=Homo sapiens OX=9606 GN=TAGLN2 PE=1 SV=3
TANK	1|1|0	1|1|0	0	TRAF family member-associated NF-kappa-B activator OS=Homo sapiens OX=9606 GN=TANK PE=1 SV=2
TARDBP	1|1|0	2|3|1	0	TAR DNA-binding protein 43 OS=Homo sapiens OX=9606 GN=TARDBP PE=1 SV=1
TARS	1|1|1	0|0|0	0	Threonine--tRNA ligase 1, cytoplasmic OS=Homo sapiens OX=9606 GN=TARS1 PE=1 SV=3
TAX1BP3	1|1|1	0|0|0	0	Tax1-binding protein 3 OS=Homo sapiens OX=9606 GN=TAX1BP3 PE=1 SV=2
TBCA	1|1|0	0|0|0	0	Tubulin-specific chaperone A OS=Homo sapiens OX=9606 GN=TBCA PE=1 SV=3
TBK1	1|0|0	0|0|0	0	Serine/threonine-protein kinase TBK1 OS=Homo sapiens OX=9606 GN=TBK1 PE=1 SV=1
TBL2	1|0|1	0|0|0	0	Transducin beta-like protein 2 OS=Homo sapiens OX=9606 GN=TBL2 PE=1 SV=1
TCHP	1|0|0	0|0|0	0	Trichoplein keratin filament-binding protein OS=Homo sapiens OX=9606 GN=TCHP PE=1 SV=1

prey Gene	Quant (SPC or Intensities)	User Controls (SPC or Intensities)	SP	Description of protein
TCOF1	1|0|0	1|2|0	0	Treacle protein OS=Homo sapiens OX=9606 GN=TCOF1 PE=1 SV=3
TCTEX1D1	1|0|0	0|0|0	0	Dynein light chain Tctex-type 5 OS=Homo sapiens OX=9606 GN=DYNLT5 PE=1 SV=2
TDP2	1|0|0	3|4|0	0	Tyrosyl-DNA phosphodiesterase 2 OS=Homo sapiens OX=9606 GN=TDP2 PE=1 SV=1
TELO2	0|0|1	0|0|0	0	Telomere length regulation protein TEL2 homolog OS=Homo sapiens OX=9606 GN=TELO2 PE=1 SV=2
TET2	0|0|1	0|0|0	0	Methylcytosine dioxygenase TET2 OS=Homo sapiens OX=9606 GN=TET2 PE=1 SV=3
THSD7B	1|0|0	0|0|0	0	Thrombospondin type-1 domain-containing protein 7B OS=Homo sapiens OX=9606 GN=THSD7B PE=2 SV=3
TIGAR	1|1|1	0|0|0	0	Fructose-2,6-bisphosphatase TIGAR OS=Homo sapiens OX=9606 GN=TIGAR PE=1 SV=1
TIMM23	0|0|1	0|0|0	0	Mitochondrial import inner membrane translocase subunit Tim23 OS=Homo sapiens OX=9606 GN=TIMM23 PE=1 SV=1
TLN1	23|8|8	32|26|4	0	Talin-1 OS=Homo sapiens OX=9606 GN=TLN1 PE=1 SV=3
TMEM109	1|1|1	0|0|0	0	Transmembrane protein 109 OS=Homo sapiens OX=9606 GN=TMEM109 PE=1 SV=1
TMEM126A	1|0|0	0|0|0	0	Transmembrane protein 126A OS=Homo sapiens OX=9606 GN=TMEM126A PE=1 SV=1

prey Gene	Quant (SPC or Intensities)	User Controls (SPC or Intensities)	SP	Description of protein
TMEM132A	0|0|1	0|0|0	0	Transmembrane protein 132A OS=Homo sapiens OX=9606 GN=TMEM132A PE=1 SV=1
TMEM2	1|1|0	0|0|0	0	Cell surface hyaluronidase OS=Homo sapiens OX=9606 GN=CEMIP2 PE=1 SV=1
TMPO	1|1|1	6|0|3	0	Lamina-associated polypeptide 2, isoform alpha OS=Homo sapiens OX=9606 GN=TMPO PE=1 SV=2
TNPO3	1|0|1	0|0|0	0	Transportin-3 OS=Homo sapiens OX=9606 GN=TNPO3 PE=1 SV=3
TNS1	1|0|1	0|0|0	0	Tensin-1 OS=Homo sapiens OX=9606 GN=TNS1 PE=1 SV=2
TOMM34	1|0|0	0|0|0	0	Mitochondrial import receptor subunit TOM34 OS=Homo sapiens OX=9606 GN=TOMM34 PE=1 SV=2
TOMM40	1|0|1	0|0|0	0	Mitochondrial import receptor subunit TOM40 homolog OS=Homo sapiens OX=9606 GN=TOMM40 PE=1 SV=1
TOMM70	0|1|0	0|0|0	0	Mitochondrial import receptor subunit TOM70 OS=Homo sapiens OX=9606 GN=TOMM70 PE=1 SV=1
TPGS1	0|0|1	0|0|0	0	Tubulin polyglutamylase complex subunit 1 OS=Homo sapiens OX=9606 GN=TPGS1 PE=1 SV=2
TRA2B	1|0|0	0|0|0	0	Transformer-2 protein homolog beta OS=Homo sapiens OX=9606 GN=TRA2B PE=1 SV=1
TRAP1	3|1|2	7|1|0	0	Heat shock protein 75 kDa, mitochondrial OS=Homo sapiens OX=9606 GN=TRAP1 PE=1 SV=3

prey Gene	Quant (SPC or Intensities)	User Controls (SPC or Intensities)	SP	Description of protein
TRIM24	1|0|0	0|0|0	0	Transcription intermediary factor 1-alpha OS=Homo sapiens OX=9606 GN=TRIM24 PE=1 SV=3
TRIM25	2|0|1	3|3|1	0	E3 ubiquitin/ISG15 ligase TRIM25 OS=Homo sapiens OX=9606 GN=TRIM25 PE=1 SV=2
TRIM33	1|1|1	0|0|0	0	E3 ubiquitin-protein ligase TRIM33 OS=Homo sapiens OX=9606 GN=TRIM33 PE=1 SV=3
TRIP10	0|0|1	1|0|0	0	Cdc42-interacting protein 4 OS=Homo sapiens OX=9606 GN=TRIP10 PE=1 SV=3
TRIP13	1|0|0	1|0|0	0	Pachytene checkpoint protein 2 homolog OS=Homo sapiens OX=9606 GN=TRIP13 PE=1 SV=2
TRMT112	1|0|0	0|0|0	0	Multifunctional methyltransferase subunit TRM112-like protein OS=Homo sapiens OX=9606 GN=TRMT112 PE=1 SV=1
TRMT5	1|0|0	1|0|0	0	tRNA (guanine(37)-N1)-methyltransferase OS=Homo sapiens OX=9606 GN=TRMT5 PE=1 SV=2
TSN	1|0|1	1|1|0	0	Translin OS=Homo sapiens OX=9606 GN=TSN PE=1 SV=1
TSPYL5	1|0|0	0|0|0	0	Testis-specific Y-encoded-like protein 5 OS=Homo sapiens OX=9606 GN=TSPYL5 PE=1 SV=2
TSTA3	1|0|0	0|0|0	0	GDP-L-fucose synthase OS=Homo sapiens OX=9606 GN=GFUS PE=1 SV=1
TSTD2	1|0|0	3|5|0	0	Thiosulfate sulfurtransferase/rhodanese-like domain-containing protein 2 OS=Homo sapiens OX=9606 GN=TSTD2 PE=1 SV=1

prey Gene	Quant (SPC or Intensities)	User Controls (SPC or Intensities)	SP	Description of protein
TTI1	0|0|1	1|0|0	0	TELO2-interacting protein 1 homolog OS=Homo sapiens OX=9606 GN=TTI1 PE=1 SV=3
TTK	1|1|1	1|0|0	0	Dual specificity protein kinase TTK OS=Homo sapiens OX=9606 GN=TTK PE=1 SV=2
TUBA1B	0|48|48	38|29|29	0	Tubulin alpha-1B chain OS=Homo sapiens OX=9606 GN=TUBA1B PE=1 SV=1
TUBB	65|52|64	46|40|25	0	Tubulin beta chain OS=Homo sapiens OX=9606 GN=TUBB PE=1 SV=2
TUBB3	35|34|36	31|21|0	0	Tubulin beta-3 chain OS=Homo sapiens OX=9606 GN=TUBB3 PE=1 SV=2
TWF1	1|0|0	0|0|0	0	Twinfilin-1 OS=Homo sapiens OX=9606 GN=TWF1 PE=1 SV=3
TWF2	2|2|2	4|5|1	0	Twinfilin-2 OS=Homo sapiens OX=9606 GN=TWF2 PE=1 SV=2
TXN	4|2|2	10|7|8	0	Thioredoxin OS=Homo sapiens OX=9606 GN=TXN PE=1 SV=3
U2AF2	1|0|0	0|1|0	0	Splicing factor U2AF 65 kDa subunit OS=Homo sapiens OX=9606 GN=U2AF2 PE=1 SV=4
UACA	1|0|1	0|1|0	0	Uveal autoantigen with coiled-coil domains and ankyrin repeats OS=Homo sapiens OX=9606 GN=UACA PE=1 SV=2
UBA6	1|0|0	0|0|0	0	Ubiquitin-like modifier-activating enzyme 6 OS=Homo sapiens OX=9606 GN=UBA6 PE=1 SV=1
UBAP2	1|1|1	3|2|1	0	Ubiquitin-associated protein 2 OS=Homo sapiens OX=9606 GN=UBAP2 PE=1 SV=1

prey Gene	Quant (SPC or Intensities)	User Controls (SPC or Intensities)	SP	Description of protein
UBAP2L	2|1|0	8|4|2	0	Ubiquitin-associated protein 2-like OS=Homo sapiens OX=9606 GN=UBAP2L PE=1 SV=2
UBE2D3	1|0|0	0|0|0	0	Ubiquitin-conjugating enzyme E2 D3 OS=Homo sapiens OX=9606 GN=UBE2D3 PE=1 SV=1
UBE2E1	1|0|0	0|0|0	0	Ubiquitin-conjugating enzyme E2 E1 OS=Homo sapiens OX=9606 GN=UBE2E1 PE=1 SV=1
UBE2L3	1|0|0	0|0|0	0	Ubiquitin-conjugating enzyme E2 L3 OS=Homo sapiens OX=9606 GN=UBE2L3 PE=1 SV=1
UBE3A	1|0|1	0|0|0	0	Ubiquitin-protein ligase E3A OS=Homo sapiens OX=9606 GN=UBE3A PE=1 SV=4
UFD1	0|1|1	0|0|0	0	Ubiquitin recognition factor in ER-associated degradation protein 1 OS=Homo sapiens OX=9606 GN=UFD1 PE=1 SV=3
UGGT1	1|0|0	0|0|0	0	UDP-glucose:glycoprotein glucosyltransferase 1 OS=Homo sapiens OX=9606 GN=UGGT1 PE=1 SV=3
UNC13A	1|0|0	0|0|0	0	Protein unc-13 homolog A OS=Homo sapiens OX=9606 GN=UNC13A PE=2 SV=4
UNC45A	1|1|0	0|0|0	0	Protein unc-45 homolog A OS=Homo sapiens OX=9606 GN=UNC45A PE=1 SV=1
UPF1	1|0|2	2|8|2	0	Regulator of nonsense transcripts 1 OS=Homo sapiens OX=9606 GN=UPF1 PE=1 SV=2
UQCR10	0|0|1	0|0|0	0	Cytochrome b-c1 complex subunit 9 OS=Homo sapiens OX=9606 GN=UQCR10 PE=1 SV=3

prey Gene	Quant (SPC or Intensities)	User Controls (SPC or Intensities)	SP	Description of protein
UQCRC1	1|0|0	0|0|0	0	Cytochrome b-c1 complex subunit 1, mitochondrial OS=Homo sapiens OX=9606 GN=UQCRC1 PE=1 SV=3
UQCRFS1	1|0|0	0|0|0	0	Cytochrome b-c1 complex subunit Rieske, mitochondrial OS=Homo sapiens OX=9606 GN=UQCRFS1 PE=1 SV=2
USP15	0|1|0	0|0|0	0	Ubiquitin carboxyl-terminal hydrolase 15 OS=Homo sapiens OX=9606 GN=USP15 PE=1 SV=3
USP17L23	0|1|0	0|0|0	0	Putative ubiquitin carboxyl-terminal hydrolase 17-like protein 23 OS=Homo sapiens OX=9606 GN=USP17L23 PE=5 SV=1
USP24	1|0|0	0|0|0	0	Ubiquitin carboxyl-terminal hydrolase 24 OS=Homo sapiens OX=9606 GN=USP24 PE=1 SV=3
USP47	1|0|0	0|0|0	0	Ubiquitin carboxyl-terminal hydrolase 47 OS=Homo sapiens OX=9606 GN=USP47 PE=1 SV=3
USP5	1|0|0	2|3|1	0	Ubiquitin carboxyl-terminal hydrolase 5 OS=Homo sapiens OX=9606 GN=USP5 PE=1 SV=2
USP7	0|0|1	1|3|0	0	Ubiquitin carboxyl-terminal hydrolase 7 OS=Homo sapiens OX=9606 GN=USP7 PE=1 SV=2
UTP18	0|0|1	0|0|0	0	U3 small nucleolar RNA-associated protein 18 homolog OS=Homo sapiens OX=9606 GN=UTP18 PE=1 SV=3
UVRAG	1|0|0	0|0|0	0	UV radiation resistance-associated gene protein OS=Homo sapiens OX=9606 GN=UVRAG PE=1 SV=1

prey Gene	Quant (SPC or Intensities)	User Controls (SPC or Intensities)	SP	Description of protein
VAMP2	0|1|0	0|0|0	0	Vesicle-associated membrane protein 2 OS=Homo sapiens OX=9606 GN=VAMP2 PE=1 SV=3
VANGL1	1|1|1	0|0|0	0	Vang-like protein 1 OS=Homo sapiens OX=9606 GN=VANGL1 PE=1 SV=1
VAPA	1|1|1	0|2|0	0	Vesicle-associated membrane protein-associated protein A OS=Homo sapiens OX=9606 GN=VAPA PE=1 SV=3
VAPB	1|0|0	0|0|0	0	Vesicle-associated membrane protein-associated protein B/C OS=Homo sapiens OX=9606 GN=VAPB PE=1 SV=3
VAT1	1|0|0	0|0|0	0	Synaptic vesicle membrane protein VAT-1 homolog OS=Homo sapiens OX=9606 GN=VAT1 PE=1 SV=2
VBP1	1|0|0	0|1|0	0	Prefoldin subunit 3 OS=Homo sapiens OX=9606 GN=VBP1 PE=1 SV=4
VDAC2	6|4|3	5|3|2	0	Voltage-dependent anion-selective channel protein 2 OS=Homo sapiens OX=9606 GN=VDAC2 PE=1 SV=2
VIM	39|25|28	50|26|91	0	Vimentin OS=Homo sapiens OX=9606 GN=VIM PE=1 SV=4
VPS35	0|0|1	0|0|0	0	Vacuolar protein sorting-associated protein 35 OS=Homo sapiens OX=9606 GN=VPS35 PE=1 SV=2
WDR1	1|1|1	0|0|0	0	WD repeat-containing protein 1 OS=Homo sapiens OX=9606 GN=WDR1 PE=1 SV=4

prey Gene	Quant (SPC or Intensities)	User Controls (SPC or Intensities)	SP	Description of protein
WDR36	1|0|0	1|1|0	0	WD repeat-containing protein 36 OS=Homo sapiens OX=9606 GN=WDR36 PE=1 SV=1
WDR77	1|0|0	0|0|0	0	Methylosome protein 50 OS=Homo sapiens OX=9606 GN=WDR77 PE=1 SV=1
WNK1	1|1|0	0|0|0	0	Serine/threonine-protein kinase WNK1 OS=Homo sapiens OX=9606 GN=WNK1 PE=1 SV=2
XAB2	1|1|0	13|22|5	0	Pre-mRNA-splicing factor SYF1 OS=Homo sapiens OX=9606 GN=XAB2 PE=1 SV=2
XPO7	1|1|1	0|0|0	0	Exportin-7 OS=Homo sapiens OX=9606 GN=XPO7 PE=1 SV=3
XRN2	1|0|0	0|0|0	0	5'-3' exoribonuclease 2 OS=Homo sapiens OX=9606 GN=XRN2 PE=1 SV=1
YAP1	7|4|6	7|7|1	0	Transcriptional coactivator YAP1 OS=Homo sapiens OX=9606 GN=YAP1 PE=1 SV=2
YARS	1|0|1	0|0|0	0	Tyrosine--tRNA ligase, cytoplasmic OS=Homo sapiens OX=9606 GN=YARS1 PE=1 SV=4
YOD1	0|0|1	0|0|0	0	Ubiquitin thioesterase OTU1 OS=Homo sapiens OX=9606 GN=YOD1 PE=1 SV=1
YTHDF1	1|0|0	0|1|0	0	YTH domain-containing family protein 1 OS=Homo sapiens OX=9606 GN=YTHDF1 PE=1 SV=1
ZBTB11	0|1|1	0|0|0	0	Zinc finger and BTB domain-containing protein 11 OS=Homo sapiens OX=9606 GN=ZBTB11 PE=1 SV=2

prey Gene	Quant (SPC or Intensities)	User Controls (SPC or Intensities)	SP	Description of protein
ZCCHC10	0|0|1	0|0|0	0	Zinc finger CCHC domain-containing protein 10 OS=Homo sapiens OX=9606 GN=ZCCHC10 PE=1 SV=1
ZDHHC22	1|0|0	0|0|0	0	Palmitoyltransferase ZDHHC22 OS=Homo sapiens OX=9606 GN=ZDHHC22 PE=1 SV=2
ZFP91	1|0|0	3|1|1	0	E3 ubiquitin-protein ligase ZFP91 OS=Homo sapiens OX=9606 GN=ZFP91 PE=1 SV=1
ZFR	0|0|1	0|1|0	0	Zinc finger RNA-binding protein OS=Homo sapiens OX=9606 GN=ZFR PE=1 SV=2
ZNF148	1|0|0	2|4|0	0	Zinc finger protein 148 OS=Homo sapiens OX=9606 GN=ZNF148 PE=1 SV=2
ZNF207	1|0|1	0|0|0	0	BUB3-interacting and GLEBS motif-containing protein ZNF207 OS=Homo sapiens OX=9606 GN=ZNF207 PE=1 SV=1
ZNF384	1|0|0	1|1|0	0	Zinc finger protein 384 OS=Homo sapiens OX=9606 GN=ZNF384 PE=1 SV=2
ZNF512	1|0|1	0|0|0	0	Zinc finger protein 512 OS=Homo sapiens OX=9606 GN=ZNF512 PE=1 SV=2
ZNF579	0|0|1	0|0|0	0	Zinc finger protein 579 OS=Homo sapiens OX=9606 GN=ZNF579 PE=1 SV=2
ZNF595	1|0|0	0|0|1	0	Zinc finger protein 595 OS=Homo sapiens OX=9606 GN=ZNF595 PE=1 SV=2
ZNF598	1|0|0	0|0|0	0	E3 ubiquitin-protein ligase ZNF598 OS=Homo sapiens OX=9606 GN=ZNF598 PE=1 SV=1

prey Gene	Quant (SPC or Intensities)	User Controls (SPC or Intensities)	SP	Description of protein
ZNF774	1|0|0	0|0|0	0	Zinc finger protein 774 OS=Homo sapiens OX=9606 GN=ZNF774 PE=1 SV=2

Supplementary Table 4. Full list of differentially expressed proteins from SW480 cells treated with MAM4-141 compound and subjected to Mass spectrometry. Analysed using Peaks software. n=3.

Gene name	Description	Treated log2 mean (3 d.p)	Control log2 mean (3 d.p.)	log2fold (3 d.p.)	P value (3 d.p.)
DCTN5	Dynactin subunit 5 OS=Homo sapiens OX=9606 GN=DCTN5 PE=1 SV=1	-2.798	-5.556	2.758	8.666E-07
RIN1	Ras and Rab interactor 1 OS=Homo sapiens OX=9606 GN=RIN1 PE=1 SV=4	-6.286	-4.962	-1.324	2.847E-04
C2	Ashwin OS=Homo sapiens OX=9606 GN=C2orf49 PE=1 SV=1	-4.939	-3.490	-1.449	0.002
GMFB	Glia maturation factor beta OS=Homo sapiens OX=9606 GN=GMFB PE=1 SV=2	0.216	-1.737	1.953	0.002
NDUFA12	NADH dehydrogenase [ubiquinone] 1 alpha subcomplex subunit 12 OS=Homo sapiens OX=9606 GN=NDUFA12 PE=1 SV=1	-0.648	-2.263	1.615	0.002
GFM2	Ribosome-releasing factor 2 mitochondrial OS=Homo sapiens OX=9606 GN=GFM2 PE=1 SV=1	-1.675	-2.679	1.004	0.003
ORC2	Origin recognition complex subunit 2 OS=Homo sapiens OX=9606 GN=ORC2 PE=1 SV=2	-1.347	-2.562	1.216	0.004
FIS1	Mitochondrial fission 1 protein OS=Homo sapiens OX=9606 GN=FIS1 PE=1 SV=2	2.124	0.361	1.762	0.005

Gene name	Description	Treated log2 mean (3 d.p)	Control log2 mean (3 d.p.)	log2fold (3 d.p.)	P value (3 d.p.)
UBE2G2	Ubiquitin-conjugating enzyme E2 G2 OS=Homo sapiens OX=9606 GN=UBE2G2 PE=1 SV=1	-0.455	-1.484	1.027	0.006
STK4	Serine/threonine-protein kinase 4 OS=Homo sapiens OX=9606 GN=STK4 PE=1 SV=2	-2.787	-4.518	1.732	0.010
HOOK3	Protein Hook homolog 3 OS=Homo sapiens OX=9606 GN=HOOK3 PE=1 SV=2	-5.141	-3.372	-1.769	0.010
ADGRE2	Adhesion G protein-coupled receptor E2 OS=Homo sapiens OX=9606 GN=ADGRE2 PE=1 SV=2	-3.697	-4.886	1.189	0.010
ACTG1	Actin cytoplasmic 2 OS=Homo sapiens OX=9606 GN=ACTG1 PE=1 SV=1	4.570	3.541	1.029	0.011
RAB13	Ras-related protein Rab-13 OS=Homo sapiens OX=9606 GN=RAB13 PE=1 SV=1	-3.668	-4.724	1.056	0.013
HYPK	Huntingtin-interacting protein K OS=Homo sapiens OX=9606 GN=HYPK PE=1 SV=2	-2.817	-4.066	1.248	0.014
FASTKD5	FAST kinase domain-containing protein 5 mitochondrial OS=Homo sapiens OX=9606 GN=FASTKD5 PE=1 SV=1	-1.567	-0.539	-1.029	0.014

Gene name	Description	Treated log2 mean (3 d.p)	Control log2 mean (3 d.p.)	log2fold (3 d.p.)	P value (3 d.p.)
VAV2	Guanine nucleotide exchange factor VAV2 OS=Homo sapiens OX=9606 GN=VAV2 PE=1 SV=2	-2.117	-1.008	-1.108	0.015
GOLT1B	Vesicle transport protein GOT1B OS=Homo sapiens OX=9606 GN=GOLT1B PE=1 SV=1	1.011	-0.948	1.959	0.015
TDRKH	Tudor and KH domain-containing protein OS=Homo sapiens OX=9606 GN=TDRKH PE=1 SV=2	-2.799	-3.936	1.137	0.015
SARDH	Sarcosine dehydrogenase mitochondrial OS=Homo sapiens OX=9606 GN=SARDH PE=1 SV=1	-2.091	-3.293	1.202	0.016
TMTC3	Protein O-mannosyl-transferase TMTC3 OS=Homo sapiens OX=9606 GN=TMTC3 PE=1 SV=2	-2.215	-4.697	2.482	0.017
KCNAB2	Voltage-gated potassium channel subunit beta-2 OS=Homo sapiens OX=9606 GN=KCNAB2 PE=1 SV=2	-5.021	-3.767	-1.255	0.018
CD8B	T-cell surface glycoprotein CD8 beta chain OS=Homo sapiens OX=9606 GN=CD8B PE=1 SV=1	-2.967	-4.533	1.566	0.019

Gene name	Description	Treated log2 mean (3 d.p)	Control log2 mean (3 d.p.)	log2fold (3 d.p.)	P value (3 d.p.)
CD8B2	T-cell surface glycoprotein CD8 beta-2 chain OS=Homo sapiens OX=9606 GN=CD8B2 PE=3 SV=3	-2.967	-4.533	1.566	0.019
NDUFB5	NADH dehydrogenase [ubiquinone] 1 beta subcomplex subunit 5 mitochondrial OS=Homo sapiens OX=9606 GN=NDUFB5 PE=1 SV=1	-0.477	-1.541	1.064	0.020
RIF1	Telomere-associated protein RIF1 OS=Homo sapiens OX=9606 GN=RIF1 PE=1 SV=2	0.312	-0.706	1.018	0.022
ITGA3	Integrin alpha-3 OS=Homo sapiens OX=9606 GN=ITGA3 PE=1 SV=5	-3.443	-4.805	1.362	0.024
RBM7	RNA-binding protein 7 OS=Homo sapiens OX=9606 GN=RBM7 PE=1 SV=1	-4.383	-2.558	-1.825	0.025
COX20	Cytochrome c oxidase assembly protein COX20 mitochondrial OS=Homo sapiens OX=9606 GN=COX20 PE=1 SV=2	0.271	-1.189	1.460	0.026
LONP2	Lon protease homolog 2 peroxisomal OS=Homo sapiens OX=9606 GN=LONP2 PE=1 SV=1	-3.584	-7.033	3.449	0.031

Gene name	Description	Treated log2 mean (3 d.p)	Control log2 mean (3 d.p.)	log2fold (3 d.p.)	P value (3 d.p.)
NOL8	Nucleolar protein 8 OS=Homo sapiens OX=9606 GN=NOL8 PE=1 SV=1	-1.660	-2.746	1.086	0.038
CAPG	Macrophage-capping protein OS=Homo sapiens OX=9606 GN=CAPG PE=1 SV=2	0.139	1.539	-1.400	0.039
ACOX3	Peroxisomal acyl-coenzyme A oxidase 3 OS=Homo sapiens OX=9606 GN=ACOX3 PE=1 SV=2	-5.183	-4.145	-1.038	0.042
CKAP2	Cytoskeleton-associated protein 2 OS=Homo sapiens OX=9606 GN=CKAP2 PE=1 SV=1	-3.242	-4.353	1.112	0.042
DNAAF2	Protein kintoun OS=Homo sapiens OX=9606 GN=DNAAF2 PE=1 SV=2	-3.521	-2.024	-1.497	0.044
POP4	Ribonuclease P protein subunit p29 OS=Homo sapiens OX=9606 GN=POP4 PE=1 SV=2	-3.768	-2.678	-1.090	0.045
GPATCH2	G patch domain-containing protein 2 OS=Homo sapiens OX=9606 GN=GPATCH2 PE=1 SV=1	-5.734	-4.438	-1.296	0.048

Supplementary Table 5. Full list of proteins from U2OS MiniTurbo CTNNB1 with MAM4-141 treatment. SAINT analysis complete. For analysis SP>0.5 was selected. n=3.

prey Gene	Quant (SPC or Intensities)	User Controls (SPC or Intensities)	SP
KCTD3	4|4|4	0|0|0	0.96
TCF7L1	9|9|9	0|4|0	0.88
LZTS2	5|5|5	1|1|1	0.64
DVL2	0|4|4	0|0|0	0.62
LDB1	5|5|0	1|0|1	0.58
C2CD4C	2|2|2	1|0|0	0.52
NFIC	2|2|0	0|0|0	0.47
CTNNBIP1	0|5|5	0|0|0	0.46
AMOTL1	0|4|4	1|1|0	0.42
RELL1	0|3|3	2|0|0	0.41
SHKBP1	15|15|15	4|4|4	0.34
NCOA3	6|6|6	2|2|2	0.34
POTEE	20|0|0	0|0|0	0.32
SORBS1	2|2|2	0|0|1	0.32
KRT79	0|0|21	0|0|0	0.31
ACTBL2	0|0|23	0|0|0	0.28
ARID1B	0|2|2	0|0|0	0.26
ANP32B	0|0|6	0|0|0	0.26
CDH4	0|4|0	0|0|0	0.25
HLA-A	0|0|3	0|0|0	0.24
SRCIN1	46|46|46	11|11|11	0.24
TLN2	0|5|0	0|0|0	0.24
ARF5	0|0|7	0|0|0	0.23
EP300	7|7|0	2|2|2	0.23
CCT6B	0|0|5	3|0|0	0.23
PDLIM5	0|4|0	1|1|0	0.22
DECR1	0|0|2	0|0|0	0.21
KAZN	0|2|0	0|0|0	0.21
PFKL	0|0|2	0|0|0	0.2
KDM1B	2|2|2	1|0|1	0.2
NECTIN3	0|2|2	2|0|0	0.2
CALCOCO1	0|2|0	0|0|0	0.2
FRMD4A	0|5|0	1|1|1	0.2
RHOC	0|0|2	1|0|0	0.19
KRT15	0|0|14	12|0|0	0.19
G6PC	2|0|0	0|1|0	0.19
PSMA8	2|0|0	0|0|0	0.19
RAC2	0|0|2	0|0|0	0.18
ERBB2	0|2|0	0|0|0	0.17
CAPNS1	0|0|2	1|0|0	0.17

prey Gene	Quant (SPC or Intensities)	User Controls (SPC or Intensities)	SP
SPRR2E	0|0|3	0|0|0	0.17
C15ORF39	0|2|0	0|0|0	0.17
FSIP2	0|0|3	0|1|0	0.16
USP31	0|2|0	0|0|0	0.16
MICALL2	0|3|0	1|0|1	0.16
FBRS	0|2|0	0|1|0	0.16
CRMP1	0|3|0	0|0|3	0.14
C1ORF106	8|8|8	3|3|3	0.12
EPS8	0|0|2	0|1|0	0.11
MUCL1	0|0|2	1|0|1	0.11
PPP1R13B	16|16|16	5|5|5	0.11
JAM3	2|2|2	1|1|1	0.11
SHROOM2	2|2|2	1|1|0	0.1
ARHGAP31	0|2|0	1|0|0	0.1
MBD6	0|2|0	1|0|0	0.09
FARSB	0|0|2	1|0|1	0.09
TENM3	0|4|0	1|0|1	0.09
CTNND2	0|2|0	0|1|0	0.09
LZTS3	2|2|2	1|1|1	0.08
CCDC120	4|4|4	2|2|2	0.05
PKP3	4|4|4	2|2|2	0.05
ELFN1	4|4|0	2|2|2	0.04
NHSL2	4|4|4	2|2|2	0.04
CSTF2T	0|2|0	1|1|1	0.04
NECTIN2	14|14|14	6|6|6	0.03
ARHGAP32	4|4|4	2|2|2	0.02
KMT2D	0|2|0	0|0|0	0.02
HDAC1	2|2|0	2|0|2	0.02
PRKD2	0|0|2	2|0|2	0.01
FAM171A2	0|1|1	1|0|0	0
SNRPGP15	0|0|1	0|0|0	0
CXORF49B; CXORF49	4|4|4	5|5|5	0
ARVCF	7|7|7	6|6|6	0
AGRN	0|0|1	0|0|0	0
CTDSP2	1|1|0	1|1|1	0
CASK	0|1|0	0|0|0	0
TRIM24	0|1|1	1|0|0	0
AXIN1	4|4|4	4|4|4	0
SPTLC1	0|1|1	1|1|1	0
DNPH1	0|0|1	0|0|0	0
SIPA1L3	10|10|10	10|10|10	0
COX7A2P2	1|0|0	0|0|0	0

prey Gene	Quant (SPC or Intensities)	User Controls (SPC or Intensities)	SP
ATP8B3	1|1|0	0|0|0	0
TRIM13	0|1|0	0|0|0	0
DNAJA2	0|1|0	1|0|0	0
SH3BGRL	0|0|1	0|0|0	0
HSBP1	0|0|1	0|0|0	0
TAF5L	0|0|1	0|0|0	0
OFD1	0|0|1	0|0|0	0
CAPN15	0|1|0	0|0|0	0
POP7	0|0|1	0|0|0	0
FLOT1	2|2|2	5|5|5	0
CDKL5	0|1|0	0|0|0	0
FARP2	0|1|0	0|0|0	0
ABLIM3	0|1|0	0|0|0	0
SNUPN	0|0|1	0|0|0	0
LYPD3	0|0|1	0|1|1	0
MPZL1	0|1|1	1|0|0	0
LATS1	1|0|0	1|1|1	0
CLPTM1	0|1|0	0|0|0	0
PAK4	0|1|1	0|1|1	0
BCHE	0|0|1	0|0|0	0
SP1	0|0|1	0|0|0	0
STS	1|0|0	0|0|0	0
TROVE2	0|0|1	0|0|0	0
RLBP1	0|1|0	0|0|0	0
NCAM1	0|1|0	0|0|0	0
POU2F1	0|0|1	0|0|0	0
PPP3CB	0|0|1	0|0|0	0
NAGA	0|0|1	0|0|0	0
CEBPB	0|1|0	0|0|0	0
CDH2	34|34|34	18|18|18	0
MAG	0|0|1	0|0|0	0
NEB	0|1|0	0|1|0	0
ATP6V1C1	0|1|0	0|0|0	0
APC	83|83|83	53|53|53	0
ITGA3	0|0|1	1|1|0	0
DNMT1	0|0|1	0|0|0	0
TACR3	0|0|1	0|0|0	0
PPIF	0|0|1	0|0|0	0
HOXC13	0|1|0	0|0|0	0
CTNNA1	57|57|57	45|45|45	0
RFC5	0|1|0	0|0|0	0
TMPO	0|0|1	0|0|0	0
MAGEA10	1|0|0	0|0|0	0

prey Gene	Quant (SPC or Intensities)	User Controls (SPC or Intensities)	SP
SOX9	0|1|0	0|0|0	0
CSNK1A1	0|1|0	1|0|0	0
CASP4	1|0|0	0|0|0	0
KLK7	0|0|1	0|0|1	0
BLVRA	0|1|0	0|0|0	0
RRP1	0|0|1	0|0|0	0
PAFAH1B2	0|0|1	0|0|0	0
CRB1	0|1|0	0|0|0	0
TFAM	0|0|1	0|0|0	0
HMGCS1	0|0|1	0|0|1	0
MECOM	0|0|1	0|0|0	0
CAV1	0|0|1	1|1|0	0
NOTCH2	1|1|0	2|2|2	0
SRSF4	0|0|1	0|0|0	0
ARHGAP5	0|1|0	0|0|0	0
MAD2L1	0|0|1	0|0|0	0
PTK7	0|1|1	0|0|0	0
SNTB2	0|1|0	0|0|0	0
GAB1	0|1|0	0|0|0	0
CBFB	0|0|1	0|0|0	0
DSG2	4|4|4	7|7|7	0
GALE	0|1|0	0|0|0	0
NFIX	1|0|0	0|0|0	0
WDR43	0|0|1	0|0|0	0
LLGL1	0|1|0	0|0|1	0
RSU1	0|0|1	0|0|0	0
SHB	1|0|1	1|0|0	0
EFNB3	0|1|0	0|0|0	0
NCOA1	3|3|3	3|3|3	0
NEDD8	0|0|1	0|0|0	0
OCLN	1|1|0	0|0|0	0
COL24A1	0|1|0	0|0|0	0
AMOT	1|1|0	0|0|1	0
PDZD11	17|17|17	9|9|9	0
SH3D19	0|1|0	0|0|0	0
AMER1	0|1|1	1|1|0	0
ELFN2	1|0|1	2|2|2	0
NHSL1	0|0|1	0|0|0	0
KIAA1217	66|66|66	30|30|30	0
MAGI3	1|0|1	2|0|0	0
PLEKHA7	14|14|14	15|15|15	0
CC2D1A	1|1|1	2|2|2	0
NHS	2|2|2	7|7|7	0

prey Gene	Quant (SPC or Intensities)	User Controls (SPC or Intensities)	SP
CCDC171	0|1|0	0|0|0	0
BCOR	1|1|1	1|0|0	0
HSDL2	0|1|0	1|0|0	0
USP54	12|12|12	9|9|9	0
ASXL2	6|6|6	5|5|5	0
GLRX5	0|0|1	0|0|0	0
BCL9L	7|7|7	4|4|4	0
SERPINA9	0|1|0	0|0|0	0
LSR	0|0|1	0|0|0	0
MAP7D3	0|1|0	1|1|0	0
SULF2	0|0|1	0|0|0	0
RUSC2	1|1|1	1|0|1	0
MINK1	2|2|2	4|4|4	0
MREG	1|0|0	0|0|0	0
ARFGAP2	0|0|1	1|0|0	0
NGDN	0|0|1	0|0|0	0
NAV1	0|0|1	0|0|0	0
KDM2B	0|1|0	0|0|0	0
RASSF8	0|1|0	1|0|0	0
PATJ	1|1|0	0|0|0	0
DLG5	2|2|2	13|13|13	0
NEK7	1|0|0	1|0|0	0
SNX29	0|0|1	0|0|0	0
PARD3B	1|1|1	1|1|1	0
NUDCD2	1|1|0	0|0|0	0
MUC16	1|0|0	0|0|0	0
BAP1	0|1|0	1|0|0	0
USP6NL	0|1|0	2|2|2	0
DLG3	1|1|1	1|1|1	0
STMN2	1|0|0	0|1|0	0
SMARCE1	0|0|1	0|0|0	0
RSPRY1	0|0|1	0|0|0	0
ZNF503	0|1|1	0|0|0	0
RSRC1	0|0|1	0|0|0	0
BTF3L4	0|0|1	0|0|0	0
CCDC138	0|1|0	1|1|0	0
PRICKLE1	0|1|0	1|0|0	0
TOX2	0|1|0	0|0|0	0
MCEE	1|0|0	0|0|0	0
GFM1	0|0|1	0|0|0	0
CEP89	0|1|0	1|1|0	0
PKP4	14|14|14	9|9|9	0
CDCA3	0|0|1	1|0|0	0

prey Gene	Quant (SPC or Intensities)	User Controls (SPC or Intensities)	SP
DOK1	1|1|1	0|0|0	0
PKP2	1|1|0	0|1|0	0
PAIP2	0|0|1	0|0|0	0
BUD13	0|0|1	0|0|0	0
SSBP3	0|1|1	1|0|0	0
BCL2L13	0|0|1	0|0|0	0
MAK16	0|1|0	0|0|0	0
ITPA	0|0|1	0|0|0	0
MRPL4	0|0|1	0|0|0	0
YTHDF1	0|1|0	0|0|0	0
RHOBTB2	1|0|0	0|0|0	0
UACA	0|1|1	0|0|0	0
ZDHHC5	1|1|1	3|3|3	0
ARHGAP39	0|0|1	0|0|0	0
LAT2	1|1|1	1|0|1	0
SAP130	0|1|0	0|0|0	0
VPS33B	0|1|0	0|0|0	0
EHD1	1|1|1	2|0|2	0
PEAK1	1|0|0	0|0|0	0
PARVG	0|0|1	0|0|0	0
NOD2	0|1|0	0|0|0	0
TANC2	6|6|6	4|4|4	0
HHATL	0|1|0	0|0|0	0
CELSR2	0|1|0	0|0|0	0
KIF13B	0|0|1	0|0|0	0
EIF2B3	0|1|0	1|0|1	0
CHRAC1	0|0|1	0|0|0	0
LATS2	0|0|1	2|0|0	0
OSTC	0|0|1	0|0|0	0
TENM2	0|2|0	3|0|3	0
ARGLU1	0|0|1	0|0|0	0
NHP2	0|0|1	0|0|0	0
IMPAD1	0|0|1	0|0|0	0
PSD3	0|1|1	0|0|0	0
MARK1	0|0|1	1|0|0	0
KIAA1522	0|1|1	0|0|0	0
PAK5	0|1|0	0|0|0	0
CRNN	0|1|0	0|0|0	0
TJP2	2|2|2	2|2|2	0
LIMD1	1|1|1	1|0|1	0
SEC63	0|1|0	0|0|0	0
TMEM2	1|0|0	1|1|0	0
IPO11	0|1|0	0|0|0	0

prey Gene	Quant (SPC or Intensities)	User Controls (SPC or Intensities)	SP
PLXNA1	0|1|0	0|0|0	0
AKAP11	0|1|0	0|0|0	0
FBXW11	7|0|0	7|7|7	0
ACAD8	0|0|1	0|0|0	0
DNPEP	0|0|1	0|0|0	0
ZDHHC8	1|1|1	1|1|1	0
ZMIZ1	1|0|0	2|0|0	0
ANKRD50	0|1|0	2|0|0	0
SSR3	0|0|1	1|1|1	0
ANKRD26	0|1|0	1|0|0	0
BTRC	6|6|6	7|7|7	0
PLEKHA6	1|1|1	1|1|1	0
AXIN2	1|1|1	1|1|0	0
COQ6	0|1|0	0|0|0	0
AK6	0|0|1	1|0|0	0
HSPB11	0|0|1	0|0|0	0
BZW2	0|0|1	2|0|0	0

List of References

1. Kusserow A, Pang K, Sturm C, Hrouda M, Lentfer J, Schmidt HA, et al. Unexpected complexity of the Wnt gene family in a sea anemone. Nature. 2005;433(7022):156-60.

2. Rijsewijk F, Schuermann M, Wagenaar E, Parren P, Weigel D, Nusse R. The Drosophila homolog of the mouse mammary oncogene int-1 is identical to the segment polarity gene wingless. Cell. 1987;50(4):649-57.

3. Nüsslein-Volhard C, Wieschaus E. Mutations affecting segment number and polarity in Drosophila. Nature. 1980;287(5785):795-801.

4. Sharma RP, Chopra VL. Effect of the Wingless (wg1) mutation on wing and haltere development in Drosophila melanogaster. Dev Biol. 1976;48(2):461-5.

5. McCrea PD, Turck CW, Gumbiner B. A homolog of the armadillo protein in Drosophila (plakoglobin) associated with E-cadherin. Science. 1991;254(5036):1359-61.

6. McMahon AP, Moon RT. Ectopic expression of the proto-oncogene int-1 in Xenopus embryos leads to duplication of the embryonic axis. Cell. 1989;58(6):1075-84.

7. Nusse R, Brown A, Papkoff J, Scambler P, Shackleford G, McMahon A, et al. A new nomenclature for int-1 and related genes: the Wnt gene family. Cell. 1991;64(2):231.

8. Thomas KR, Capecchi MR. Targeted disruption of the murine int-1 proto-oncogene resulting in severe abnormalities in midbrain and cerebellar development. Nature. 1990;346(6287):847-50.

9. Tsukamoto AS, Grosschedl R, Guzman RC, Parslow T, Varmus HE. Expression of the int-1 gene in transgenic mice is associated with mammary gland hyperplasia and adenocarcinomas in male and female mice. Cell. 1988;55(4):619-25.

10. Fearon ER, Vogelstein B. A genetic model for colorectal tumorigenesis. Cell. 1990;61(5):759-67.

11. Groden J, Thliveris A, Samowitz W, Carlson M, Gelbert L, Albertsen H, et al. Identification and characterization of the familial adenomatous polyposis coli gene. Cell. 1991;66(3):589-600.

12. Kinzler KW, Nilbert MC, Vogelstein B, Bryan TM, Levy DB, Smith KJ, et al. Identification of a gene located at chromosome 5q21 that is mutated in colorectal cancers. Science. 1991;251(4999):1366-70.

13. Nishisho I, Nakamura Y, Miyoshi Y, Miki Y, Ando H, Horii A, et al. Mutations of chromosome 5q21 genes in FAP and colorectal cancer patients. Science. 1991;253(5020):665-9.

14. Rubinfeld B, Souza B, Albert I, Müller O, Chamberlain SH, Masiarz FR, et al. Association of the APC gene product with beta-catenin. Science. 1993;262(5140):1731-4.

15. Su LK, Vogelstein B, Kinzler KW. Association of the APC tumor suppressor protein with catenins. Science. 1993;262(5140):1734-7.

16. Kinzler KW, Vogelstein B. Lessons from hereditary colorectal cancer. Cell. 1996;87(2):159-70.

17. Korinek V, Barker N, Morin PJ, van Wichen D, de Weger R, Kinzler KW, et al. Constitutive transcriptional activation by a beta-catenin-Tcf complex in APC-/- colon carcinoma. Science. 1997;275(5307):1784-7.
18. Morin PJ, Sparks AB, Korinek V, Barker N, Clevers H, Vogelstein B, et al. Activation of beta-catenin-Tcf signaling in colon cancer by mutations in beta-catenin or APC. Science. 1997;275(5307):1787-90.
19. Munemitsu S, Albert I, Souza B, Rubinfeld B, Polakis P. Regulation of intracellular beta-catenin levels by the adenomatous polyposis coli (APC) tumor-suppressor protein. Proc Natl Acad Sci U S A. 1995;92(7):3046-50.
20. Nusse R, Varmus HE. Many tumors induced by the mouse mammary tumor virus contain a provirus integrated in the same region of the host genome. Cell. 1982;31(1):99-109.
21. Ozawa M, Baribault H, Kemler R. The cytoplasmic domain of the cell adhesion molecule uvomorulin associates with three independent proteins structurally related in different species. Embo j. 1989;8(6):1711-7.
22. Siegfried E, Chou TB, Perrimon N. wingless signaling acts through zeste-white 3, the Drosophila homolog of glycogen synthase kinase-3, to regulate engrailed and establish cell fate. Cell. 1992;71(7):1167-79.
23. Behrens J, von Kries JP, Kühl M, Bruhn L, Wedlich D, Grosschedl R, et al. Functional interaction of beta-catenin with the transcription factor LEF-1. Nature. 1996;382(6592):638-42.
24. Bhanot P, Brink M, Samos CH, Hsieh JC, Wang Y, Macke JP, et al. A new member of the frizzled family from Drosophila functions as a Wingless receptor. Nature. 1996;382(6588):225-30.
25. Yang-Snyder J, Miller JR, Brown JD, Lai CJ, Moon RT. A frizzled homolog functions in a vertebrate Wnt signaling pathway. Curr Biol. 1996;6(10):1302-6.
26. Behrens J, Jerchow BA, Würtele M, Grimm J, Asbrand C, Wirtz R, et al. Functional interaction of an axin homolog, conductin, with beta-catenin, APC, and GSK3beta. Science. 1998;280(5363):596-9.
27. Graham TA, Weaver C, Mao F, Kimelman D, Xu W. Crystal structure of a beta-catenin/Tcf complex. Cell. 2000;103(6):885-96.
28. Pinson KI, Brennan J, Monkley S, Avery BJ, Skarnes WC. An LDL-receptor-related protein mediates Wnt signalling in mice. Nature. 2000;407(6803):535-8.
29. Tamai K, Semenov M, Kato Y, Spokony R, Liu C, Katsuyama Y, et al. LDL-receptor-related proteins in Wnt signal transduction. Nature. 2000;407(6803):530-5.
30. Oishi I, Suzuki H, Onishi N, Takada R, Kani S, Ohkawara B, et al. The receptor tyrosine kinase Ror2 is involved in non-canonical Wnt5a/JNK signalling pathway. Genes Cells. 2003;8(7):645-54.
31. Yoshikawa S, McKinnon RD, Kokel M, Thomas JB. Wnt-mediated axon guidance via the Drosophila Derailed receptor. Nature. 2003;422(6932):583-8.

32. van Amerongen R, Mikels A, Nusse R. Alternative wnt signaling is initiated by distinct receptors. Sci Signal. 2008;1(35):re9.

33. Chen B, Dodge ME, Tang W, Lu J, Ma Z, Fan CW, et al. Small molecule-mediated disruption of Wnt-dependent signaling in tissue regeneration and cancer. Nat Chem Biol. 2009;5(2):100-7.

34. Goldstein B, Takeshita H, Mizumoto K, Sawa H. Wnt signals can function as positional cues in establishing cell polarity. Dev Cell. 2006;10(3):391-6.

35. Huang YL, Niehrs C. Polarized Wnt signaling regulates ectodermal cell fate in Xenopus. Dev Cell. 2014;29(2):250-7.

36. Schneider J, Arraf AA, Grinstein M, Yelin R, Schultheiss TM. Wnt signaling orients the proximal-distal axis of chick kidney nephrons. Development. 2015;142(15):2686-95.

37. Kitajima K, Oki S, Ohkawa Y, Sumi T, Meno C. Wnt signaling regulates left-right axis formation in the node of mouse embryos. Dev Biol. 2013;380(2):222-32.

38. Loh KM, van Amerongen R, Nusse R. Generating Cellular Diversity and Spatial Form: Wnt Signaling and the Evolution of Multicellular Animals. Dev Cell. 2016;38(6):643-55.

39. Clevers H, Nusse R. Wnt/β-catenin signaling and disease. Cell. 2012;149(6):1192-205.

40. Clevers H, Loh KM, Nusse R. Stem cell signaling. An integral program for tissue renewal and regeneration: Wnt signaling and stem cell control. Science. 2014;346(6205):1248012.

41. Klaus A, Birchmeier W. Wnt signalling and its impact on development and cancer. Nat Rev Cancer. 2008;8(5):387-98.

42. Niehrs C, Acebron SP. Mitotic and mitogenic Wnt signalling. Embo j. 2012;31(12):2705-13.

43. Rios-Esteves J, Resh MD. Stearoyl CoA desaturase is required to produce active, lipid-modified Wnt proteins. Cell Rep. 2013;4(6):1072-81.

44. Willert K, Brown JD, Danenberg E, Duncan AW, Weissman IL, Reya T, et al. Wnt proteins are lipid-modified and can act as stem cell growth factors. Nature. 2003;423(6938):448-52.

45. Janda CY, Waghray D, Levin AM, Thomas C, Garcia KC. Structural basis of Wnt recognition by Frizzled. Science. 2012;337(6090):59-64.

46. Bartscherer K, Pelte N, Ingelfinger D, Boutros M. Secretion of Wnt ligands requires Evi, a conserved transmembrane protein. Cell. 2006;125(3):523-33.

47. Kimelman D, Xu W. beta-catenin destruction complex: insights and questions from a structural perspective. Oncogene. 2006;25(57):7482-91.

48. Amit S, Hatzubai A, Birman Y, Andersen JS, Ben-Shushan E, Mann M, et al. Axin-mediated CKI phosphorylation of beta-catenin at Ser 45: a molecular switch for the Wnt pathway. Genes Dev. 2002;16(9):1066-76.

49. Liu C, Li Y, Semenov M, Han C, Baeg GH, Tan Y, et al. Control of beta-catenin phosphorylation/degradation by a dual-kinase mechanism. Cell. 2002;108(6):837-47.

50. Kitagawa M, Hatakeyama S, Shirane M, Matsumoto M, Ishida N, Hattori K, et al. An F-box protein, FWD1, mediates ubiquitin-dependent proteolysis of beta-catenin. Embo j. 1999;18(9):2401-10.
51. Aberle H, Bauer A, Stappert J, Kispert A, Kemler R. beta-catenin is a target for the ubiquitin-proteasome pathway. Embo j. 1997;16(13):3797-804.
52. Wong HC, Bourdelas A, Krauss A, Lee HJ, Shao Y, Wu D, et al. Direct binding of the PDZ domain of Dishevelled to a conserved internal sequence in the C-terminal region of Frizzled. Mol Cell. 2003;12(5):1251-60.
53. Schwarz-Romond T, Metcalfe C, Bienz M. Dynamic recruitment of axin by Dishevelled protein assemblies. J Cell Sci. 2007;120(Pt 14):2402-12.
54. Cliffe A, Hamada F, Bienz M. A role of Dishevelled in relocating Axin to the plasma membrane during wingless signaling. Curr Biol. 2003;13(11):960-6.
55. Chen G, Courey AJ. Groucho/TLE family proteins and transcriptional repression. Gene. 2000;249(1-2):1-16.
56. Kramps T, Peter O, Brunner E, Nellen D, Froesch B, Chatterjee S, et al. Wnt/wingless signaling requires BCL9/legless-mediated recruitment of pygopus to the nuclear beta-catenin-TCF complex. Cell. 2002;109(1):47-60.
57. Städeli R, Basler K. Dissecting nuclear Wingless signalling: recruitment of the transcriptional co-activator Pygopus by a chain of adaptor proteins. Mech Dev. 2005;122(11):1171-82.
58. Thompson B, Townsley F, Rosin-Arbesfeld R, Musisi H, Bienz M. A new nuclear component of the Wnt signalling pathway. Nat Cell Biol. 2002;4(5):367-73.
59. Bannister AJ, Kouzarides T. The CBP co-activator is a histone acetyltransferase. Nature. 1996;384(6610):641-3.
60. Ogryzko VV, Schiltz RL, Russanova V, Howard BH, Nakatani Y. The transcriptional coactivators p300 and CBP are histone acetyltransferases. Cell. 1996;87(5):953-9.
61. Leung JY, Kolligs FT, Wu R, Zhai Y, Kuick R, Hanash S, et al. Activation of AXIN2 expression by beta-catenin-T cell factor. A feedback repressor pathway regulating Wnt signaling. J Biol Chem. 2002;277(24):21657-65.
62. Shtutman M, Zhurinsky J, Simcha I, Albanese C, D'Amico M, Pestell R, et al. The cyclin D1 gene is a target of the beta-catenin/LEF-1 pathway. Proc Natl Acad Sci U S A. 1999;96(10):5522-7.
63. He TC, Sparks AB, Rago C, Hermeking H, Zawel L, da Costa LT, et al. Identification of c-MYC as a target of the APC pathway. Science. 1998;281(5382):1509-12.
64. Lin SY, Xia W, Wang JC, Kwong KY, Spohn B, Wen Y, et al. Beta-catenin, a novel prognostic marker for breast cancer: its roles in cyclin D1 expression and cancer progression. Proc Natl Acad Sci U S A. 2000;97(8):4262-6.

65. Kielman MF, Rindapää M, Gaspar C, van Poppel N, Breukel C, van Leeuwen S, et al. Apc modulates embryonic stem-cell differentiation by controlling the dosage of β-catenin signaling. Nature Genetics. 2002;32(4):594-605.

66. Sedgwick AE, D'Souza-Schorey C. Wnt Signaling in Cell Motility and Invasion: Drawing Parallels between Development and Cancer. Cancers (Basel). 2016;8(9).

67. Hao HX, Xie Y, Zhang Y, Charlat O, Oster E, Avello M, et al. ZNRF3 promotes Wnt receptor turnover in an R-spondin-sensitive manner. Nature. 2012;485(7397):195-200.

68. Koo BK, Spit M, Jordens I, Low TY, Stange DE, van de Wetering M, et al. Tumour suppressor RNF43 is a stem-cell E3 ligase that induces endocytosis of Wnt receptors. Nature. 2012;488(7413):665-9.

69. Glinka A, Wu W, Delius H, Monaghan AP, Blumenstock C, Niehrs C. Dickkopf-1 is a member of a new family of secreted proteins and functions in head induction. Nature. 1998;391(6665):357-62.

70. Kohler EM, Chandra SH, Behrens J, Schneikert J. Beta-catenin degradation mediated by the CID domain of APC provides a model for the selection of APC mutations in colorectal, desmoid and duodenal tumours. Hum Mol Genet. 2009;18(2):213-26.

71. Roberts DM, Pronobis MI, Poulton JS, Waldmann JD, Stephenson EM, Hanna S, et al. Deconstructing the ßcatenin destruction complex: mechanistic roles for the tumor suppressor APC in regulating Wnt signaling. Mol Biol Cell. 2011;22(11):1845-63.

72. Tago K, Nakamura T, Nishita M, Hyodo J, Nagai S, Murata Y, et al. Inhibition of Wnt signaling by ICAT, a novel beta-catenin-interacting protein. Genes Dev. 2000;14(14):1741-9.

73. Sparks AB, Morin PJ, Vogelstein B, Kinzler KW. Mutational analysis of the APC/beta-catenin/Tcf pathway in colorectal cancer. Cancer Res. 1998;58(6):1130-4.

74. Giannakis M, Hodis E, Jasmine Mu X, Yamauchi M, Rosenbluh J, Cibulskis K, et al. RNF43 is frequently mutated in colorectal and endometrial cancers. Nat Genet. 2014;46(12):1264-6.

75. Gruszka AM, Valli D, Alcalay M. Wnt Signalling in Acute Myeloid Leukaemia. Cells. 2019;8(11).

76. Spranger S, Bao R, Gajewski TF. Melanoma-intrinsic β-catenin signalling prevents anti-tumour immunity. Nature. 2015;523(7559):231-5.

77. Kageshita T, Hamby CV, Ishihara T, Matsumoto K, Saida T, Ono T. Loss of beta-catenin expression associated with disease progression in malignant melanoma. Br J Dermatol. 2001;145(2):210-6.

78. Maelandsmo GM, Holm R, Nesland JM, Fodstad Ø, Flørenes VA. Reduced beta-catenin expression in the cytoplasm of advanced-stage superficial spreading malignant melanoma. Clin Cancer Res. 2003;9(9):3383-8.

79. Demunter A, Libbrecht L, Degreef H, De Wolf-Peeters C, van den Oord JJ. Loss of membranous expression of beta-catenin is associated with tumor progression in cutaneous melanoma and rarely caused by exon 3 mutations. Mod Pathol. 2002;15(4):454-61.
80. Xu X, Zhang M, Xu F, Jiang S. Wnt signaling in breast cancer: biological mechanisms, challenges and opportunities. Molecular Cancer. 2020;19(1):165.
81. Prasad S, Ramachandran S, Gupta N, Kaushik I, Srivastava SK. Cancer cells stemness: A doorstep to targeted therapy. Biochim Biophys Acta Mol Basis Dis. 2020;1866(4):165424.
82. Zhao H, Ming T, Tang S, Ren S, Yang H, Liu M, et al. Wnt signaling in colorectal cancer: pathogenic role and therapeutic target. Mol Cancer. 2022;21(1):144.
83. Zhu Z, Khan MA, Weiler M, Blaes J, Jestaedt L, Geibert M, et al. Targeting self-renewal in high-grade brain tumors leads to loss of brain tumor stem cells and prolonged survival. Cell Stem Cell. 2014;15(2):185-98.
84. de Sousa e Melo F, Kurtova AV, Harnoss JM, Kljavin N, Hoeck JD, Hung J, et al. A distinct role for Lgr5(+) stem cells in primary and metastatic colon cancer. Nature. 2017;543(7647):676-80.
85. Yang J, Mani SA, Donaher JL, Ramaswamy S, Itzykson RA, Come C, et al. Twist, a master regulator of morphogenesis, plays an essential role in tumor metastasis. Cell. 2004;117(7):927-39.
86. Kahlert C, Kalluri R. Exosomes in tumor microenvironment influence cancer progression and metastasis. J Mol Med (Berl). 2013;91(4):431-7.
87. Baccelli I, Schneeweiss A, Riethdorf S, Stenzinger A, Schillert A, Vogel V, et al. Identification of a population of blood circulating tumor cells from breast cancer patients that initiates metastasis in a xenograft assay. Nat Biotechnol. 2013;31(6):539-44.
88. Comprehensive molecular characterization of human colon and rectal cancer. Nature. 2012;487(7407):330-7.
89. Kim S, Jeong S. Mutation Hotspots in the β-Catenin Gene: Lessons from the Human Cancer Genome Databases. Mol Cells. 2019;42(1):8-16.
90. Liu J, Xing Y, Hinds TR, Zheng J, Xu W. The third 20 amino acid repeat is the tightest binding site of APC for beta-catenin. J Mol Biol. 2006;360(1):133-44.
91. Zhan T, Rindtorff N, Boutros M. Wnt signaling in cancer. Oncogene. 2017;36(11):1461-73.
92. Huber AH, Weis WI. The structure of the beta-catenin/E-cadherin complex and the molecular basis of diverse ligand recognition by beta-catenin. Cell. 2001;105(3):391-402.
93. Pokutta S, Weis WI. Structure of the dimerization and beta-catenin-binding region of alpha-catenin. Mol Cell. 2000;5(3):533-43.
94. Rimm DL, Koslov ER, Kebriaei P, Cianci CD, Morrow JS. Alpha 1(E)-catenin is an actin-binding and -bundling protein mediating the attachment of F-actin to the membrane adhesion complex. Proc Natl Acad Sci U S A. 1995;92(19):8813-7.
95. Jiang J, Struhl G. Regulation of the Hedgehog and Wingless signalling pathways by the F-box/WD40-repeat protein Slimb. Nature. 1998;391(6666):493-6.

96. Megy S, Bertho G, Gharbi-Benarous J, Evrard-Todeschi N, Coadou G, Ségéral E, et al. STD and TRNOESY NMR studies on the conformation of the oncogenic protein beta-catenin containing the phosphorylated motif DpSGXXpS bound to the beta-TrCP protein. J Biol Chem. 2005;280(32):29107-16.

97. Huber AH, Nelson WJ, Weis WI. Three-dimensional structure of the armadillo repeat region of beta-catenin. Cell. 1997;90(5):871-82.

98. Hülsken J, Birchmeier W, Behrens J. E-cadherin and APC compete for the interaction with beta-catenin and the cytoskeleton. J Cell Biol. 1994;127(6 Pt 2):2061-9.

99. Choi HJ, Huber AH, Weis WI. Thermodynamics of beta-catenin-ligand interactions: the roles of the N- and C-terminal tails in modulating binding affinity. J Biol Chem. 2006;281(2):1027-38.

100. Xing Y, Takemaru K, Liu J, Berndt JD, Zheng JJ, Moon RT, et al. Crystal structure of a full-length beta-catenin. Structure. 2008;16(3):478-87.

101. Xu W, Kimelman D. Mechanistic insights from structural studies of beta-catenin and its binding partners. J Cell Sci. 2007;120(Pt 19):3337-44.

102. Knapp S, Zamai M, Volpi D, Nardese V, Avanzi N, Breton J, et al. Thermodynamics of the high-affinity interaction of TCF4 with beta-catenin. J Mol Biol. 2001;306(5):1179-89.

103. Kikuchi A, Kishida S, Yamamoto H. Regulation of Wnt signaling by protein-protein interaction and post-translational modifications. Exp Mol Med. 2006;38(1):1-10.

104. Dajani R, Fraser E, Roe SM, Yeo M, Good VM, Thompson V, et al. Structural basis for recruitment of glycogen synthase kinase 3beta to the axin-APC scaffold complex. Embo j. 2003;22(3):494-501.

105. Eklof Spink K, Fridman SG, Weis WI. Molecular mechanisms of beta-catenin recognition by adenomatous polyposis coli revealed by the structure of an APC-beta-catenin complex. Embo j. 2001;20(22):6203-12.

106. Xing Y, Clements WK, Kimelman D, Xu W. Crystal structure of a beta-catenin/axin complex suggests a mechanism for the beta-catenin destruction complex. Genes Dev. 2003;17(22):2753-64.

107. Ha NC, Tonozuka T, Stamos JL, Choi HJ, Weis WI. Mechanism of phosphorylation-dependent binding of APC to beta-catenin and its role in beta-catenin degradation. Mol Cell. 2004;15(4):511-21.

108. Willert K, Jones KA. Wnt signaling: is the party in the nucleus? Genes Dev. 2006;20(11):1394-404.

109. Sampietro J, Dahlberg CL, Cho US, Hinds TR, Kimelman D, Xu W. Crystal structure of a beta-catenin/BCL9/Tcf4 complex. Mol Cell. 2006;24(2):293-300.

110. Fasolini M, Wu X, Flocco M, Trosset JY, Oppermann U, Knapp S. Hot spots in Tcf4 for the interaction with beta-catenin. J Biol Chem. 2003;278(23):21092-8.

111. Nusse R, Clevers H. Wnt/β-Catenin Signaling, Disease, and Emerging Therapeutic Modalities. Cell. 2017;169(6):985-99.
112. Tran FH, Zheng JJ. Modulating the wnt signaling pathway with small molecules. Protein Sci. 2017;26(4):650-61.
113. Kahn M. Can we safely target the WNT pathway? Nat Rev Drug Discov. 2014;13(7):513-32.
114. Anastas JN, Moon RT. WNT signalling pathways as therapeutic targets in cancer. Nat Rev Cancer. 2013;13(1):11-26.
115. Bastakoty D, Young PP. Wnt/β-catenin pathway in tissue injury: roles in pathology and therapeutic opportunities for regeneration. Faseb j. 2016;30(10):3271-84.
116. Hoeppner LH, Secreto FJ, Westendorf JJ. Wnt signaling as a therapeutic target for bone diseases. Expert Opin Ther Targets. 2009;13(4):485-96.
117. Huang SM, Mishina YM, Liu S, Cheung A, Stegmeier F, Michaud GA, et al. Tankyrase inhibition stabilizes axin and antagonizes Wnt signalling. Nature. 2009;461(7264):614-20.
118. Thorne CA, Hanson AJ, Schneider J, Tahinci E, Orton D, Cselenyi CS, et al. Small-molecule inhibition of Wnt signaling through activation of casein kinase 1α. Nat Chem Biol. 2010;6(11):829-36.
119. Emami KH, Nguyen C, Ma H, Kim DH, Jeong KW, Eguchi M, et al. A small molecule inhibitor of beta-catenin/CREB-binding protein transcription [corrected]. Proc Natl Acad Sci U S A. 2004;101(34):12682-7.
120. de la Roche M, Rutherford TJ, Gupta D, Veprintsev DB, Saxty B, Freund SM, et al. An intrinsically labile α-helix abutting the BCL9-binding site of β-catenin is required for its inhibition by carnosic acid. Nat Commun. 2012;3:680.
121. Sang P, Zhang M, Shi Y, Li C, Abdulkadir S, Li Q, et al. Inhibition of β-catenin/B cell lymphoma 9 protein-protein interaction using α-helix-mimicking sulfono-γ-AApeptide inhibitors. Proc Natl Acad Sci U S A. 2019;116(22):10757-62.
122. Grossmann TN, Yeh JT, Bowman BR, Chu Q, Moellering RE, Verdine GL. Inhibition of oncogenic Wnt signaling through direct targeting of β-catenin. Proc Natl Acad Sci U S A. 2012;109(44):17942-7.
123. Dietrich L, Rathmer B, Ewan K, Bange T, Heinrichs S, Dale TC, et al. Cell Permeable Stapled Peptide Inhibitor of Wnt Signaling that Targets β-Catenin Protein-Protein Interactions. Cell Chem Biol. 2017;24(8):958-68.e5.
124. Sukhdeo K, Mani M, Zhang Y, Dutta J, Yasui H, Rooney MD, et al. Targeting the beta-catenin/TCF transcriptional complex in the treatment of multiple myeloma. Proc Natl Acad Sci U S A. 2007;104(18):7516-21.
125. Lepourcelet M, Chen YN, France DS, Wang H, Crews P, Petersen F, et al. Small-molecule antagonists of the oncogenic Tcf/beta-catenin protein complex. Cancer Cell. 2004;5(1):91-102.

126. Chen HJ, Hsu LS, Shia YT, Lin MW, Lin CM. The β-catenin/TCF complex as a novel target of resveratrol in the Wnt/β-catenin signaling pathway. Biochem Pharmacol. 2012;84(9):1143-53.

127. Shin SH, Lim DY, Reddy K, Malakhova M, Liu F, Wang T, et al. A Small Molecule Inhibitor of the β-Catenin-TCF4 Interaction Suppresses Colorectal Cancer Growth In Vitro and In Vivo. EBioMedicine. 2017;25:22-31.

128. Sakamoto KM, Kim KB, Kumagai A, Mercurio F, Crews CM, Deshaies RJ. Protacs: chimeric molecules that target proteins to the Skp1-Cullin-F box complex for ubiquitination and degradation. Proc Natl Acad Sci U S A. 2001;98(15):8554-9.

129. Simonetta KR, Taygerly J, Boyle K, Basham SE, Padovani C, Lou Y, et al. Prospective discovery of small molecule enhancers of an E3 ligase-substrate interaction. Nat Commun. 2019;10(1):1402.

130. Hwang SY, Deng X, Byun S, Lee C, Lee SJ, Suh H, et al. Direct Targeting of β-Catenin by a Small Molecule Stimulates Proteasomal Degradation and Suppresses Oncogenic Wnt/β-Catenin Signaling. Cell Rep. 2016;16(1):28-36.

131. McCoy MA, Spicer D, Wells N, Hoogewijs K, Fiedler M, Baud MGJ. Biophysical Survey of Small-Molecule β-Catenin Inhibitors: A Cautionary Tale. J Med Chem. 2022;65(10):7246-61.

132. Lenz HJ, Kahn M. Safely targeting cancer stem cells via selective catenin coactivator antagonism. Cancer Sci. 2014;105(9):1087-92.

133. Yamada K, Hori Y, Inoue S, Yamamoto Y, Iso K, Kamiyama H, et al. E7386, a Selective Inhibitor of the Interaction between β-Catenin and CBP, Exerts Antitumor Activity in Tumor Models with Activated Canonical Wnt Signaling. Cancer Res. 2021;81(4):1052-62.

134. Fiskus W, Sharma S, Saha S, Shah B, Devaraj SGT, Sun B, et al. Pre-clinical efficacy of combined therapy with novel β-catenin antagonist BC2059 and histone deacetylase inhibitor against AML cells. Leukemia. 2015;29(6):1267-78.

135. Li J, Wang CY. TBL1-TBLR1 and beta-catenin recruit each other to Wnt target-gene promoter for transcription activation and oncogenesis. Nat Cell Biol. 2008;10(2):160-9.

136. Cranmer LD, Razak ARA, Ratan R, Choy E, George S, Liebner DA, et al. Results of a phase I dose escalation and expansion study of tegavivint (BC2059), a first-in-class TBL1 inhibitor for patients with progressive, unresectable desmoid tumor. Journal of Clinical Oncology. 2022;40(16_suppl):11523-.

137. Neiheisel A, Kaur M, Ma N, Havard P, Shenoy AK. Wnt pathway modulators in cancer therapeutics: An update on completed and ongoing clinical trials. Int J Cancer. 2022;150(5):727-40.

138. Alwine JC, Kemp DJ, Stark GR. Method for detection of specific RNAs in agarose gels by transfer to diazobenzyloxymethyl-paper and hybridization with DNA probes. Proc Natl Acad Sci U S A. 1977;74(12):5350-4.

139. Tan SC, Yiap BC. DNA, RNA, and protein extraction: the past and the present. J Biomed Biotechnol. 2009;2009:574398.
140. Saiki RK, Scharf S, Faloona F, Mullis KB, Horn GT, Erlich HA, et al. Enzymatic Amplification of β-Globin Genomic Sequences and Restriction Site Analysis for Diagnosis of Sickle Cell Anemia. Science. 1985;230(4732):1350-4.
141. Absher M. CHAPTER 1 - Hemocytometer Counting. In: Kruse PF, Patterson MK, editors. Tissue Culture: Academic Press; 1973. p. 395-7.
142. Liang C-C, Park AY, Guan J-L. In vitro scratch assay: a convenient and inexpensive method for analysis of cell migration in vitro. Nature Protocols. 2007;2(2):329-33.
143. Puck TT, Marcus PI, Cieciura SJ. Clonal growth of mammalian cells in vitro; growth characteristics of colonies from single HeLa cells with and without a feeder layer. J Exp Med. 1956;103(2):273-83.
144. Franken NA, Rodermond HM, Stap J, Haveman J, van Bree C. Clonogenic assay of cells in vitro. Nat Protoc. 2006;1(5):2315-9.
145. Macpherson I, Montagnier L. Agar suspension culture for the selective assay of cells transformed by polyoma virus. Virology. 1964;23(2):291-4.
146. Shin SI, Freedman VH, Risser R, Pollack R. Tumorigenicity of virus-transformed cells in nude mice is correlated specifically with anchorage independent growth in vitro. Proc Natl Acad Sci U S A. 1975;72(11):4435-9.
147. Coons AH, Creech HJ, Jones RN. Immunological Properties of an Antibody Containing a Fluorescent Group. Proceedings of the Society for Experimental Biology and Medicine. 1941;47(2):200-2.
148. Blobel G, Potter VR. Nuclei from Rat Liver: Isolation Method That Combines Purity with High Yield. Science. 1966;154(3757):1662-5.
149. Aaij C, Borst P. The gel electrophoresis of DNA. Biochim Biophys Acta. 1972;269(2):192-200.
150. Zhang Y, Werling U, Edelmann W. Seamless Ligation Cloning Extract (SLiCE) cloning method. Methods Mol Biol. 2014;1116:235-44.
151. Dawson MH, Sia RH. IN VITRO TRANSFORMATION OF PNEUMOCOCCAL TYPES : I. A TECHNIQUE FOR INDUCING TRANSFORMATION OF PNEUMOCOCCAL TYPES IN VITRO. J Exp Med. 1931;54(5):681-99.
152. Liu X, Salokas K, Weldatsadik RG, Gawriyski L, Varjosalo M. Combined proximity labeling and affinity purification−mass spectrometry workflow for mapping and visualizing protein interaction networks. Nature Protocols. 2020;15(10):3182-211.
153. Branon TC, Bosch JA, Sanchez AD, Udeshi ND, Svinkina T, Carr SA, et al. Efficient proximity labeling in living cells and organisms with TurboID. Nat Biotechnol. 2018;36(9):880-7.
154. Jinek M, Chylinski K, Fonfara I, Hauer M, Doudna JA, Charpentier E. A programmable dual-RNA-guided DNA endonuclease in adaptive bacterial immunity. Science. 2012;337(6096):816-21.

155. Sanjana NE, Shalem O, Zhang F. Improved vectors and genome-wide libraries for CRISPR screening. Nat Methods. 2014;11(8):783-4.

156. Naldini L, Blömer U, Gallay P, Ory D, Mulligan R, Gage FH, et al. In Vivo Gene Delivery and Stable Transduction of Nondividing Cells by a Lentiviral Vector. Science. 1996;272(5259):263-7.

157. Choi H, Larsen B, Lin ZY, Breitkreutz A, Mellacheruvu D, Fermin D, et al. SAINT: probabilistic scoring of affinity purification-mass spectrometry data. Nat Methods. 2011;8(1):70-3.

158. Frank AM. A Ranking-Based Scoring Function for Peptide−Spectrum Matches. Journal of Proteome Research. 2009;8(5):2241-52.

159. Szklarczyk D, Kirsch R, Koutrouli M, Nastou K, Mehryary F, Hachilif R, et al. The STRING database in 2023: protein-protein association networks and functional enrichment analyses for any sequenced genome of interest. Nucleic Acids Res. 2023;51(D1):D638-d46.

160. Mellacheruvu D, Wright Z, Couzens AL, Lambert JP, St-Denis NA, Li T, et al. The CRAPome: a contaminant repository for affinity purification-mass spectrometry data. Nat Methods. 2013;10(8):730-6.

161. Wu X, Kriz AJ, Sharp PA. Target specificity of the CRISPR-Cas9 system. Quant Biol. 2014;2(2):59-70.

162. Cheon SS, Wei Q, Gurung A, Youn A, Bright T, Poon R, et al. Beta-catenin regulates wound size and mediates the effect of TGF-beta in cutaneous healing. Faseb j. 2006;20(6):692-701.

163. Fathke C, Wilson L, Shah K, Kim B, Hocking A, Moon R, et al. Wnt signaling induces epithelial differentiation during cutaneous wound healing. BMC Cell Biol. 2006;7:4.

164. Salomon A, Keramidas M, Maisin C, Thomas M. Loss of β-catenin in adrenocortical cancer cells causes growth inhibition and reversal of epithelial-to-mesenchymal transition. Oncotarget. 2015;6(13):11421-33.

165. Buechel D, Sugiyama N, Rubinstein N, Saxena M, Kalathur RKR, Lüönd F, et al. Parsing β-catenin's cell adhesion and Wnt signaling functions in malignant mammary tumor progression. Proceedings of the National Academy of Sciences. 2021;118(34):e2020227118.

166. Grossmann AH, Yoo JH, Clancy J, Sorensen LK, Sedgwick A, Tong Z, et al. The small GTPase ARF6 stimulates β-catenin transcriptional activity during WNT5A-mediated melanoma invasion and metastasis. Sci Signal. 2013;6(265):ra14.

167. Douarre C, Sourbier C, Dalla Rosa I, Brata Das B, Redon CE, Zhang H, et al. Mitochondrial topoisomerase I is critical for mitochondrial integrity and cellular energy metabolism. PLoS One. 2012;7(7):e41094.

168. Zong WX, Rabinowitz JD, White E. Mitochondria and Cancer. Mol Cell. 2016;61(5):667-76.

169. Vasan K, Werner M, Chandel NS. Mitochondrial Metabolism as a Target for Cancer Therapy. Cell Metabolism. 2020;32(3):341-52.

170. Kessler SW. Rapid isolation of antigens from cells with a staphylococcal protein A-antibody adsorbent: parameters of the interaction of antibody-antigen complexes with protein A. J Immunol. 1975;115(6):1617-24.

171. Free RB, Hazelwood LA, Sibley DR. Identifying novel protein-protein interactions using co-immunoprecipitation and mass spectroscopy. Curr Protoc Neurosci. 2009;Chapter 5:Unit 5.28.

172. Ewing RM, Chu P, Elisma F, Li H, Taylor P, Climie S, et al. Large-scale mapping of human protein-protein interactions by mass spectrometry. Mol Syst Biol. 2007;3:89.

173. Li P, Meng Y, Wang L, Di LJ. BioID: A Proximity-Dependent Labeling Approach in Proteomics Study. Methods Mol Biol. 2019;1871:143-51.

174. Roux KJ, Kim DI, Raida M, Burke B. A promiscuous biotin ligase fusion protein identifies proximal and interacting proteins in mammalian cells. Journal of Cell Biology. 2012;196(6):801-10.

175. Lam SS, Martell JD, Kamer KJ, Deerinck TJ, Ellisman MH, Mootha VK, et al. Directed evolution of APEX2 for electron microscopy and proximity labeling. Nat Methods. 2015;12(1):51-4.

176. Johansen K, Svensson L. Immunoprecipitation. Methods Mol Med. 1998;13:15-28.

177. Gnanasekaran P, Pappu HR. Affinity Purification-Mass Spectroscopy (AP-MS) and Co-Immunoprecipitation (Co-IP) Technique to Study Protein-Protein Interactions. Methods Mol Biol. 2023;2690:81-5.

178. Samavarchi-Tehrani P, Samson R, Gingras AC. Proximity Dependent Biotinylation: Key Enzymes and Adaptation to Proteomics Approaches. Mol Cell Proteomics. 2020;19(5):757-73.

179. Go CD, Knight JDR, Rajasekharan A, Rathod B, Hesketh GG, Abe KT, et al. A proximity-dependent biotinylation map of a human cell. Nature. 2021;595(7865):120-4.

180. Singh V, Singh A, Liu AJ, Fuchs SY, Sharma AK, Spiegelman VS. RNA Binding Proteins as Potential Therapeutic Targets in Colorectal Cancer. Cancers. 2024;16(20):3502.

181. Narita T, Weinert BT, Choudhary C. Functions and mechanisms of non-histone protein acetylation. Nature Reviews Molecular Cell Biology. 2019;20(3):156-74.

182. Wolf D, Rodova M, Miska EA, Calvet JP, Kouzarides T. Acetylation of β-Catenin by CREB-binding Protein (CBP) *. Journal of Biological Chemistry. 2002;277(28):25562-7.

183. Loussouarn M, Krieger-Liszkay A, Svilar L, Bily A, Birtić S, Havaux M. Carnosic Acid and Carnosol, Two Major Antioxidants of Rosemary, Act through Different Mechanisms. Plant Physiol. 2017;175(3):1381-94.

184. [Internet]. [Human Protein Atlas]. Available from: https://www.proteinatlas.org/ENSG00000174791-RIN1/pathology

185. Senda K, Goi T, Hirono Y, Katayama K, Yamaguchi A. Analysis of RIN1 gene expression in colorectal cancer. Oncol Rep. 2007;17(5):1171-5.

186. UniProt: a worldwide hub of protein knowledge. Nucleic Acids Res. 2019;47(D1):D506-d15.

187. Magraner-Pardo L, Gobelli D, de la Fuente MA, Pons T, Simarro M. Systematic Analysis of FASTK Gene Family Alterations in Cancer. Int J Mol Sci. 2021;22(21).

188. Li W, Chen J, Xiong Z, Zhou H, Huang S, Ren J, et al. Dynactin 2 acts as an oncogene in hepatocellular carcinoma through promoting cell cycle progression. Liver Research. 2022;6(3):155-66.

189. Lin SR, Mokgautsi N, Liu YN. Ras and Wnt Interaction Contribute in Prostate Cancer Bone Metastasis. Molecules. 2020;25(10).

190. Parri M, Chiarugi P. Rac and Rho GTPases in cancer cell motility control. Cell Communication and Signaling. 2010;8(1):23.

191. Ewing RM, Song J, Gokulrangan G, Bai S, Bowler EH, Bolton R, et al. Multiproteomic and Transcriptomic Analysis of Oncogenic β-Catenin Molecular Networks. J Proteome Res. 2018;17(6):2216-25.

192. Hanswillemenke A, Hofacker DT, Sorgenfrei M, Fruhner C, Franz-Wachtel M, Schwarzer D, et al. Profiling the interactome of oligonucleotide drugs by proximity biotinylation. Nature Chemical Biology. 2024;20(5):555-65.